

Alma Mater Studiorum – Università di Bologna

DOTTORATO DI RICERCA IN
Scienze Mediche Veterinarie

Ciclo 36°

Settore Concorsuale: 07/H2 – PATOLOGIA VETERINARIA E ISPEZIONE DEGLI ALIMENTI
DI ORIGINE ANIMALE

Settore Scientifico Disciplinare: VET/03 – PATOLOGIA GENERALE E ANATOMIA
PATOLOGICA VETERINARIA

**Microenvironment and therapeutic modulation
of myelofibrosis in an experimental mouse model**

Presentata da: Francesca Gobbo

Coordinatore Dottorato

Carolina Castagnetti

Supervisore

Giuseppe Sarli

Co-Supervisore

Anna Rita Migliaccio

Esame finale anno 2024

Summary

Chapter I. Literature review	3
1. <i>Primary myelofibrosis in humans</i>	3
1.1. Genetic mutations in PMF	4
1.2. Pathogenesis of PMF	6
1.3. The role of Megakaryocytes in the pathogenesis of PMF	7
1.4. Histological features of Myelofibrosis	10
1.5. Treatments strategies	14
2. <i>Murine models of myelofibrosis</i>	15
2.1. JAK2 ^{V617F}	17
2.2. MPL Mutation (W515L and W515W)	17
2.3. CALR	18
2.4. TPO Overexpression	18
2.5. Trisomy 21 mouse	19
2.6. Abi-1 knockout mouse	19
3. <i>Gata1^{low} Mouse model of myelofibrosis</i>	19
3.1. GATA family transcriptional factors	19
3.2. GATA1 in hematopoiesis and disease	21
3.3. <i>Gata1^{low}</i> mouse model of PMF	21
3.4. Pharmacologic molecules tested in <i>Gata1^{low}</i> mice	24
4. <i>References</i>	26
Chapter II. Experimental section	43
Abstract	43
1. <i>Introduction</i>	43
1.1 References	45
2. <i>Results</i>	49
2.1. Resident Self-Tissue of Proinflammatory Cytokines Rather Than Their Systemic Levels Correlates with Development of Myelofibrosis in <i>Gata1^{low}</i> Mice	50
1. Introduction	51
2. Materials and Methods	52
3. Results	56
4. Discussion	72

5. References	76
6. Supplementary Figures	84
2.2. The CXCR1/CXCR2 Inhibitor Reparixin Alters the Development of Myelofibrosis in the <i>Gatal</i> ^{low} Mice	87
1. Introduction	88
2. Materials and methods	90
3. Results	93
4. Discussion	105
5. References	109
6. Supplementary Figures	115
2.3. Preclinical studies on the use of a P-selectin-blocking monoclonal antibody to halt progression of myelofibrosis in the <i>Gatal</i> ^{low} mouse model	116
1. Introduction	117
2. Materials and methods	118
3. Results	122
4. Discussion	138
5. References	142
6. Supplementary Figures	148
3. <i>General discussion and conclusions</i>	158
4. <i>References</i>	165
<u>List of acronyms</u>	171

Chapter I. Literature review

1. Primary myelofibrosis in humans

Myelofibrosis (MF) is a chronic Philadelphia-chromosome (BCR-ABL1) -negative myeloproliferative neoplasms (MPNs), characterized by bone marrow fibrosis, ineffective hematopoiesis, extramedullary hematopoiesis, splenomegaly and shortened survival. MF can be primary (termed “primary myelofibrosis” [PMF]; or “idiopathic MF,” or “myeloid metaplasia with MF”) or secondary, developing from a pre-fibrotic phase of polycythemia vera (PV) or essential thrombocythemia (ET) that inevitably transform to a fibrotic phase referred to “post PV/ET MF” (Gangat & Tefferi, 2020; Garmezzy et al., 2021).

MF, characterized by pre-fibrotic and fibrotic variants, is the result of an hematopoietic stem cell defect that causes abnormal proliferation of megakaryocytes (MKs) and myeloid cells. The result is an aberrant deposition of reticulin and collagen in the bone marrow with osteosclerosis, and overproduction of pro-inflammatory cytokines (Arber et al., 2022; Barbui et al., 2019; Pettit & Odenike, 2017).

MPNs are rare with an annual incidence estimate of 0.47-1.98 per 100,000, and a prevalence of 1.76-4.05 per 100,000 (Barbui et al., 2011; Barosi, 2014). Incidence data indicate that the diseases are more common in males than in females. Male dominance seems to hold true for both PMF and MF evolving from a pre-existing PV. However, data suggests that more females are diagnosed with ET (Mehta et al., 2014). One study showed that females under 34 years-old developed PMF more frequently than males of the same age, and blacks aged 35 to 49 had a higher rate of PMF diagnoses than whites. The authors speculated that this may be related to a delayed diagnosis of ET in these groups (Deadmond & Smith-Gagen, 2015). PMF may be slightly more common among white and non-Hispanic patients, although it seems unlikely that these differences are clinically significant. The rate of PMF diagnosis increases with age, with the highest incidence among those over 75 but the majority of cases fall in the 50-74 age group (Deadmond & Smith-Gagen, 2015; Srour et al., 2016).

Symptoms include fever, night sweats, itching and weight loss and are believed to be due to abnormal cytokine production. Both hepatomegaly and splenomegaly are considered characteristic of MF and are largely, though not exclusively, due to extramedullary hematopoiesis. In fact, palpable splenomegaly has been observed in over 80% of MF patients and can lead to a series of physical complaints, including generalized abdominal discomfort, left upper quadrant/subcostal pain, and early satiety (Mughal et al., 2014). Progressive bone marrow fibrosis leads to a "myelotic" phenotype with worsening cytopenias, particularly thrombocytopenia and anemia. The latter results in fatigue, weakness, palpitations, compensatory tachycardia, bone pain, and dyspnea and may lead to tissue hypoxia in patients with vasculopathy. Anemia also can negatively affect pulmonary function parameters in patients with pre-existing lung diseases (Bacigalupo, 2017; Mughal et al., 2014;

Ouellette, 2005). Thrombocytopenia, which can lead to hemorrhage, can be aggravated by acquired platelet dysfunction and sometimes by a state of low-grade disseminated intravascular coagulation, which occasionally causes thrombosis (Prentice, 1985). Hepatomegaly has been observed in 39%–65% of patients with MF and can cause abnormal liver function tests and coagulopathy. In MF, can also occur the thrombosis of the splanchnic veins (portal, mesenteric or splenic). Interestingly, although the hyperplasia of Kupffer cells were detected in MF, neither hepatic stellate cell activation nor liver parenchymal fibrosis are characteristic of this disease (Mughal et al., 2014). Moreover, extramedullary hematopoiesis can result in a range of different complications depending on the specific organ involved. It can affect the central nervous system which can lead to intracranial hypertension with symptoms such as chronic headache, delirium, and photophobia. It can affect the paraspinal site, with compression of the spinal cord. Involvement of lymph nodes causing generalized lymphadenopathy. Extramedullary haematopoiesis in the gastrointestinal tract can manifest as an exacerbation of already existing abdominal and/or intestinal pain lumen obstruction. Obstructive uropathy, gastric outlet obstruction, bile duct obstruction, acalculous cholecystitis, arthritis and renal colic can rarely occur (Koch et al., 2003; Nadrous et al., 2004). Cutaneous manifestations of extramedullary hematopoiesis are quite rare and may include nodules, ulcers, erythematous plaques, bullae, myeloid leukemic-like infiltrates and even neutrophilic dermatosis (Sweet's syndrome) (Altomare et al., 1996). Moreover, the risk of leukemic transformation appears to increase with time (Mesa et al., 2005).

1.1. Genetic mutations in PMF

Primary myelofibrosis is characterized by driver genetic mutations. In fact, the majority of patients with myelofibrosis (more than 90%) carry mutations that alter JAK-STAT signaling; 60% of patients with myelofibrosis harbor the $JAK2^{V617F}$ mutation (Vannucchi et al., 2013), approximately 30% carry a calreticulin mutation (CALR) (Imai et al., 2017), and 13.6% carry a myeloproliferative leukemia virus oncogene (MPL) mutation (Song et al., 2017).

JAK2 is a tyrosine kinase within the JAK-STAT pathway that regulates the cell cycle, apoptosis, and proteasomal degradation. JAK2 also activates the PI3K/Akt and MAPK signaling pathways (Zahr et al., 2016). Mutation of CALR represents the second most common mutation found in patients with PMF after $JAK2^{V617F}$ (Imai et al., 2017). CALR is a chaperone of the endoplasmic reticulum (ER) involved in protein folding and calcium storage. Mutant CALR protein interfaces with thrombopoietin receptor, MPL, to cause constitutive activation of JAK-STAT signaling (Garmezzy et al., 2021; Imai et al., 2017). The thrombopoietin receptor, MPL, is an important signaling protein upstream to JAK2. MPL is required for $JAK2^{V617F}$ signaling activation and transformation of hematopoietic cells. Mutations in the transmembrane region of *MPL* (e.g., MPL^{W515L}) lead to

constitutive activation of JAK-STAT signaling as well as increased activation of JAK-STAT through the ERK/MAPK and PI3K/AKT pathways (Lu et al., 2005).

In addition to mutations affecting the JAK-STAT signaling pathway, other alterations have also been identified that can further contribute to MF initiation or progression and may explain some of the variability in the disease phenotype. These mutations can involve cellular pathways such as DNA methylation (i.e. TET2, DNMT3A mutations), histone modification (ASXL1, EZH2 mutations), RNA splicing (U2AF1, SF3B1, SRSF2 mutations), and signaling through other pathways (RAS/RAF/MEK/ERK, PI3K/AKT/mTOR, LNK) (Grinfeld et al., 2017; Vainchenker & Kralovics, 2017). Among those patients who do not have a mutation in JAK2, MPL, or CALR, there is a small subset of patients without identifiable mutations, recently termed “triple negative” and associated with a worse prognosis (Gangat & Tefferi, 2020; Grinfeld et al., 2017; Vainchenker & Kralovics, 2017). The most common mutations described in PMF are shown in **Figure 1**.

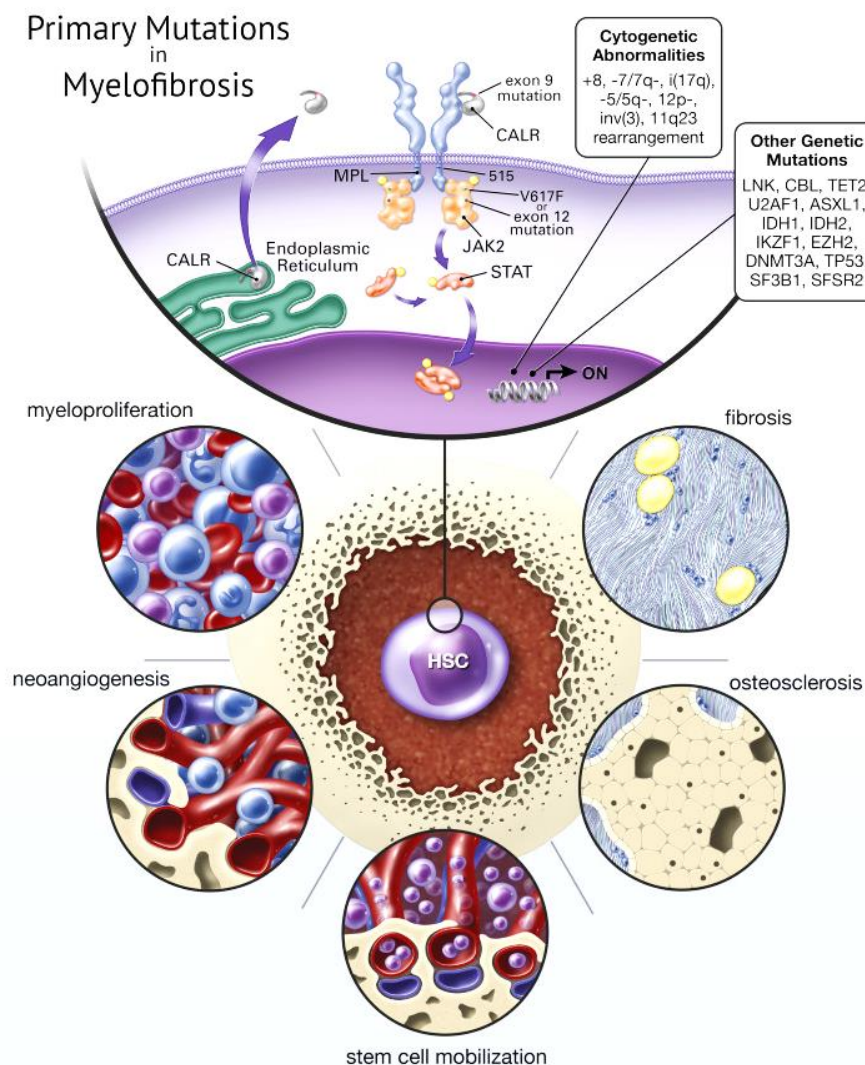


Figure 1. Primary Mutations in Myelofibrosis. This figure highlights the mutations, cytogenetic abnormalities, and their relationship with the crucial JAK-STAT signaling pathway in MF. Abbreviation: MPL, myeloproliferative leukaemia virus oncogene (thrombopoietin receptor); JAK2, Janus kinase 2; STAT, signal transducer and activation of transcription; CALR, calreticulin; HSC, hematopoietic stem cell (Garmezy et al., 2021).

1.2. Pathogenesis of PMF

The exact cause of PMF is unknown, but, along with the other chronic myeloproliferative disorders, is considered to arise from a single somatic mutation of hematopoietic stem cell (HSC). The expansion of the mutated clone is accompanied by hyperplasia of a single phenotype-defining lineage and abnormal deposition of collagen fibers that leads to the destruction of the healthy marrow (Garmezy et al., 2021).

Normally, hematopoiesis is polyclonal. In fact, none of the hematopoietic progenitors have a competitive advantage to expand over others. However, patients with PMF have a monoclonal increase of myeloid, lymphoid, and erythroid lineages, suggesting that a mutant clone with a possible stem cell origin initiates the disease (Reeder et al., 2003).

To understand the pathogenesis of myelofibrosis, it is important to analyse the constituent of the stem cell niche, which is composed of adipocytes, osteoblasts, smooth muscle cells, endothelial and hematopoietic stem cells. HSC reside in the stem cell niche, that commonly refers to the pairing of hematopoietic and mesenchymal cell populations that regulate HSC self-renewal, differentiation, and proliferation (Yin, 2006). Of note, disrupted interaction within these closely connected niches is frequent in MF (Varricchio et al., 2009). For example, hematopoietic stem cells carrying the JAK2 mutation secrete IL-1 β , which promotes their expansion. However, this cytokine causes apoptosis of mesenchymal cells, thus affecting the survival of normal HSCs. In addition, aberrant mutant megakaryocytes release fibrotic cytokines of various types causing fibrosis (Bock et al., 2008; Lin et al., 2016). JAK2 mutation was also found in endothelial cells, thus, they also contribute to promoting the malignant proliferation of HSCs (Lin et al., 2016).

Cytokines released in the microenvironment by the cellular compartment of BM appear to be necessary (but not sufficient) for fibrosis to occur. These are produced mainly by the malignant clone throughout its various stages of aberrant differentiation (megakaryocytes, monocytes or both). In particular, megakaryocytes are the major contributor to the excessive extracellular matrix deposition by production of proinflammatory cytokines such as IL-1 β , VEGF, TGF- β , β -FGF and PDGF (Abbonante et al., 2016).

Based on the above synopsis, the biology of myelofibrosis remains elusive. Current theories are multi-faceted, favoring contributions from aberrant megakaryocytes with constitutive activation of JAK/STAT and other signaling pathways, together with epigenetic dysregulation and excessive pro-inflammatory cytokine production resulting in fibrosis. These complex interactions between MKs and non-malignant hematopoietic marrow elements are depicted in **Figure 2**.

Pathogenesis of myelofibrosis

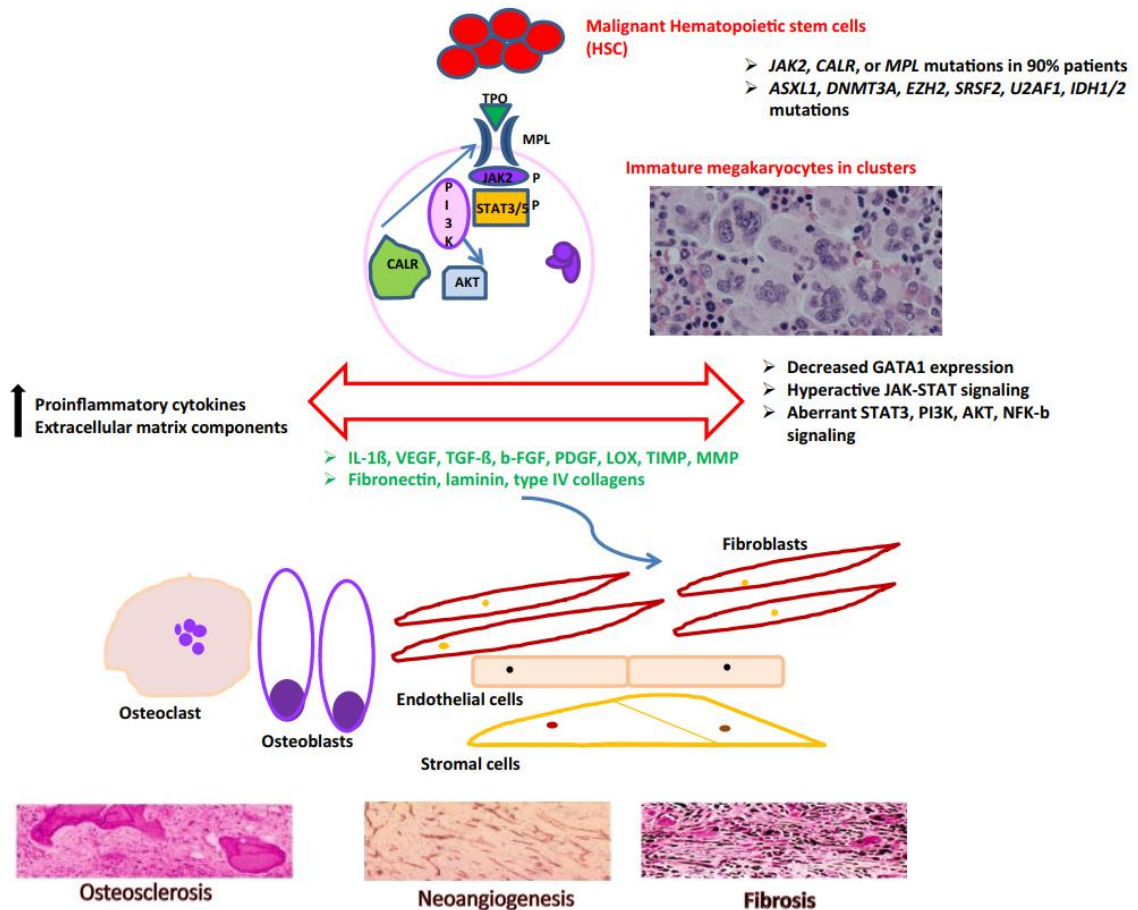


Figure 2. Pathogenesis of myelofibrosis. Malignant HSCs give rise to immature megakaryocytes with reduced expression of GATA1, hyperactive JAK-STAT signaling that secrete pro-inflammatory cytokines and excessive extracellular matrix. These aberrant mutant megakaryocytes secrete IL-1 β , VEGF, TGF- β , b-FGF, PDGF, LOX, TIMP, and MMP, which affect vascularization, extracellular matrix stability, and mesenchymal stromal cells, causing osteosclerosis, neoangiogenesis, and fibrosis. Abbreviations: TPO, thrombopoietin; MPL, myeloproliferative leukaemia virus oncogene (thrombopoietin receptor); JAK2, Janus kinase 2; STAT, signal transducer and activation of transcription; PI3K, phosphoinositol kinase 3; CALR, calreticulin; ASXL1, additional sex comb-like; DNMT3A, DNA methyl transferase 3; EZH2, enhancer of zeste homolog 2; SRSF2, serine arginine splicing factor 2; U2AF1, U2 small nuclear RNA auxiliary factor 1; IDH1/2, isocitrate dehydrogenase 1/2; IL-1 β , interleukin 1 β ; VEGF, vascular endothelial growth factor; TGF- β , transforming growth factor β ; b-FGF, basic fibroblast growth factor; PDGF, platelet derived growth factor; LOX, lysyl oxidase; TIMP, tissue inhibitors of matrix metalloproteinase; MMP, matrix metalloproteinase (Gangat & Tefferi, 2020).

1.3. The role of Megakaryocytes in the pathogenesis of PMF

Bone marrow fibrosis in primary myelofibrosis results from the abnormal excessive deposition of collagen derived from fibroblast. The major components of bone marrow fibrosis are collagen types I, III, IV, and V, laminin, and glycoproteins, which in healthy bone marrow provide support for the reticular matrix but are abundantly present during myelofibrosis (Agarwal et al., 2016; Castro-Malaspina & Jhanwar, 1984). Collagen-producing fibroblast are functional and physically similar to normal fibroblast, but they are stimulated to proliferate and overproduce collagen by growth factor secreted by the neighboring megakaryocytes (Castro-Malaspina et al., 1981; Garmezzy et al., 2021).

Aberrant immature MKs are a dominant feature of the disease, occurring in clusters and releasing pro-inflammatory cytokines, causing fibrosis (**Figure 3**). Unlike normal megakaryocytes, they express cell adhesion molecules P-selectin on their intracytoplasmic vacuoles and demarcation membrane system rather than on the α -granule membrane, the normal location (Schmitt et al., 2000). This altered expression allows P-selectin to mediate emperipolesis, and stimulate the release of cytokines by the altered MKs. The activated cytokine pathways lead to fibrosis, neoangiogenesis, and osteosclerosis, main features of PMF (Tefferi, 2005).

Transforming growth factor beta (TGF- β) is the main driver of fibrosis in many organs (Meng et al., 2016). It is synthesized by the monocyte-macrophage system, endothelial cells, and also by megakaryocytes that seems to be the main source (Melo-Cardenas et al., 2021; Terui et al., 1990). TGF- β directly stimulates the production and secretion of extracellular matrix proteins from fibroblast (Agarwal et al., 2016). Furthermore, TGF- β decreases extracellular matrix degradation through down-regulation of matrix metalloproteinase 3 (MMP3) and upregulation of tissue inhibitor of metalloproteinase 1 (TIMP-1). The result is a reduction in proteolysis of collagen and other ECM components (Wang, 2005). Currently, a TGF- β inhibitor (AVID200) is tested in a clinical trial in PMF (NCT03895112).

Interleukin 8 (IL-8) is a member of the family of chemokines related by a CXC motif. It binds with high affinity to two 7-transmembrane-domain CXC chemokine receptor 1 (CXCR1) and 2 (CXCR2) that belong to the superfamily of G protein-coupled receptors (Emadi et al., 2005). It acts as a chemoattractive and proinflammatory agent as well as a neutrophil activator. It is normally produced by monocytes and macrophages, but also by endothelial cells in response to pro-inflammatory stimuli (Waugh & Wilson, 2008). *In vitro* studies have also shown that it can also be produced by other cell types, including fibroblasts, endothelial cells, neutrophils, mast cells, and megakaryocytes (Hashimoto et al., 1996; Kaplanski et al., 1994; Matsushima & Oppenheim, 1989; Takeuchi et al., 1999). Elevated IL-8 serum levels are responsible for the abnormal growth and differentiation of MKs observed in patients with PMF. Furthermore, the addition of IL-8 receptor inhibitory antibodies (against CXCR1 and CXCR2, the two receptors of IL-8) to MKs isolated from the peripheral blood of myelofibrosis patients *in vitro*, increases the differentiation and proliferation of MK and restores their polyploidization (Emadi et al., 2005).

CXCL4, also known as platelet factor 4 (PF4), has been implicated in fibrotic diseases in the liver and in systemic sclerosis (Van Bon et al., 2014; Zaldivar et al., 2010). It drives a broad spectrum of immune-modulatory effects in hematopoiesis and angiogenesis and has also been implicated in the pathology of a variety of inflammatory diseases (Affandi et al., 2018; Aivado et al., 2007; Pitsilos et al., 2003; Vrij et al., 2000). Studies in MPN models showed that CXCL4 derived from megakaryocytes is a key in promoting bone marrow fibrosis by inducing myofibroblastic differentiation of stromal cells (Schneider et al., 2017).

Thrombopoietin (TPO) is the major physiologic humoral regulator of megakaryopoiesis and platelet production. It binds to its receptor, MPL, and induces activation of JAK/STAT, MAPK/ERK and PI3K/AKT in HSCs, which are critical for the regulation of megakaryopoiesis (De Sauvage et al., 1994). MPL expression on megakaryocytes and platelets is essential to prevent myeloproliferation and expansion of megakaryocytes by limiting TPO availability from HSCs and progenitors. Several studies have shown the role of the TPO-MPL signaling in MPNs. Normal or elevated levels of serum TPO have been found in patients with ET and PV (Griesshammer et al., 1998; Wang et al., 1998). By contrast, patients with MF have elevated levels of thrombopoietin (Wang et al., 1997). More recent studies have found heterogeneous expression of MPL in bone marrow cells of patients with MPNs, in which megakaryocytes and platelets express low levels of MPL (Melo-Cardenas et al., 2021). Studies in mice show that overexpression of TPO in bone marrow induces fibrosis (Villevall et al., 1997).

Osteoprotegerin (OPG) is a member of the TNF receptor family but it is secreted and acts like a cytokine and it is produced by osteoblasts and bone marrow stromal cells (Riches et al., 2009). Bone remodelling results from the equilibrium of two cell types activity: the osteoblasts (the bone-forming cells) and the osteoclasts (the bone-resorbing cells). Osteoblasts derive from mesenchymal progenitors via different regulatory processes including the action of several growth factors such as TGF- β 1, which could exert stimulatory or inhibitory effects. Osteoclasts are of haematopoietic origin; they derive from monocytic cells and require macrophage-stimulating factor (M-CSF) for proliferation and RANK-L, via its binding to the receptor RANK expressed at the surface of osteoclast progenitors, for differentiation and maturation (Chagraoui et al., 2006). Osteoprotegerin is a decoy secreted receptor that prevents RANK-L binding to its receptor RANK, thus inhibiting osteoclastogenesis (Simonet et al., 1997). The critical role of the trio OPG/RANK/RANK-L in bone homeostasis has been elegantly demonstrated in genetically manipulated mice. Specifically, OPG overexpression in transgenic mice and RANK or RANK-L knock-out mice led to impaired osteoclastogenesis and severe osteosclerosis, whereas administration of soluble RANK-L or OPG in knockout mice resulted in enhanced osteoclastogenesis and osteoporosis (Hofbauer, 1999). Furthermore, using the *Gata1*^{low} mouse model of MF, the idea that MK-osteoblast contact is a prerequisite for increased bone formation, perhaps mediated by interactions between osteoblasts and mutant megakaryocytes, was supported (Kacena et al., 2004).

Inflammation is one of the key features in MPNs. A great number of inflammatory cytokines are elevated in the serum of MPN patients (Mondet et al., 2015; Tefferi et al., 2011). IL-8 and TGF- β have been shown to induce the proliferation of the aberrant MKs in samples from MF patients (Badaluco et al., 2013; Emadi et al., 2005). Furthermore, inflammatory signaling has been shown to promote megakaryopoiesis by increasing the protein expression of megakaryocytic genes that induce the activation of the proliferation of stem-like megakaryocyte-committed progenitors (Haas et al., 2015). MPNs are chronic diseases that are more common in the elderly indicating that age related

changes might have a prominent role in the initiation and maintenance of the disease. Further studies on the effect of inflammation and aging in megakaryopoiesis in MPNs will improve our understanding of the disease.

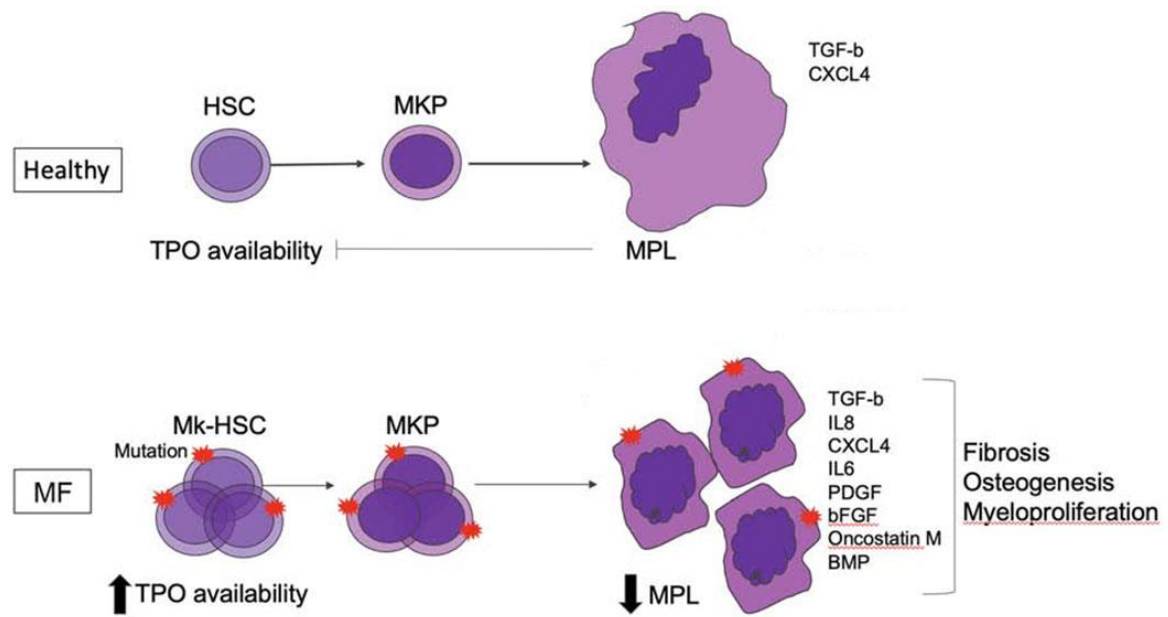


Figure 3. Schematic representation of megakaryocyte contributions to MPN pathogenesis. Upon acquisition of an MPN driver mutation, megakaryocytes in MF display impaired differentiation, decreased GATA1 expression and enhanced cytokine/chemokine secretion. A number of these secreted factors promote fibrosis, osteogenesis and myeloproliferation (Melo-Cardenas et al., 2021). Abbreviations: HSC, hematopoietic stem cell; MPK, megakaryocyte progenitors; TPO, thrombopoietin; MPL, myeloproliferative leukaemia virus oncogene; TGF- β , transforming growth factor β ; IL-8, interleukin-8; CXCL4, chemokine (C-X-C motif) ligand 4; IL-6, interleukin-6; PDGF, platelet derived growth factor; BMP, bone morphogenetic proteins.

1.4. Histological features of Myelofibrosis

The presence of stromal fibers in the bone marrow, can be associated with a variety of both benign and malignant disorders. These fibers are composed primarily of reticulin fibers, but may also include collagen fibers (Bain et al., 2001). Reticulin fibrosis, characterized by an increase in reticulin fibers, and collagen fibrosis, an increase in collagen fibers, may involve very different clinical manifestations. Reticulin fibrosis, shows a low correlation with cell blood counts (CBC) and disease severity, in contrast, the presence of collagen fibrosis is associated with abnormal CBC and disease severity. In addition, the increase in reticular fibers is reversible, and responds to drug treatment, whereas collagen fibrosis is less likely to be so (Bain et al., 2001; Hann et al., 1978; O'Malley et al., 2005; Thiele et al., 1991; Thiele & Kvasnicka, 2006). Although reticulin is composed in part of collagen, the terms "reticulin fibrosis" and "collagen fibrosis" are used to distinguish between the histochemical, biochemical, and clinical features associated with these two different types of bone marrow stromal fibers (Kuter et al., 2007).

The bone marrow microenvironment includes cells and stroma, this latter composed of structural fibrils and extracellular matrix ("ground substance"). The cellular components includes macrophages, fibroblasts, adipocytes and endothelial cells, and other less well characterized cells (Kuter et al., 2007). The most prevalent structural fibrils in the bone marrow are collagen (type I and III), reticulin, laminin and fibronectin (Agarwal et al., 2016; Castro-Malaspina & Jhanwar, 1984). The ground substance includes water, salts, glycosaminoglycans, and glycoproteins (Clark & Keating, 1995). These elements provide a physical and biochemical support for hematopoietic progenitor cells. In addition, bone marrow components, especially its cellular compartment, play an important role in hematopoiesis. They provide humoral factors and interactions that support the proliferation and maintenance of hematopoietic cells (Bain et al., 2001).

1.4.1 Changes in bone marrow fibrotic tissue

Routine histological stains, such as haematoxylin and eosin stain, do not show the bone marrow connective tissue structure that usually requires histochemical stains. These are for example Mallory's trichrome stain, van Gieson stain or Masson's trichrome stain (Bain et al., 2001; Bancroft & Gamble, 2002) that highlighted the collagen fibers in blue. Instead, histochemical stains such as silver impregnation are used for the identification of reticular fibers. These are the Gomori stain and the Gordon Sweet stain (Gömöri, 1937; Puchtler & Waldrop, 1978), in which reticulin fibers appear stained black.

Ideally, both stains identifying mature collagen and reticular fibers should be used to evaluate bone marrow fibrosis; and both type and amount of fibrosis should be investigated using a clearly defined grading scale.

Two slightly different classification scales of bone marrow fibrosis using the interpretation of these stains have been created (Bauermeister, 1971; Thiele et al., 2005). The original Bauermeister scheme (Bauermeister, 1971) used six different grades, but was later simplified to a five-grade system (**Figure 4**) (Bain et al., 2001; Manoharan et al., 1979). The more recent Thiele scale includes only four categories (Thiele et al., 2005) (**Figure 5**). Both classification scales take into account both the type of fibers observed (reticulin or collagen) and the overall amount of fibrosis (**Table 1**).

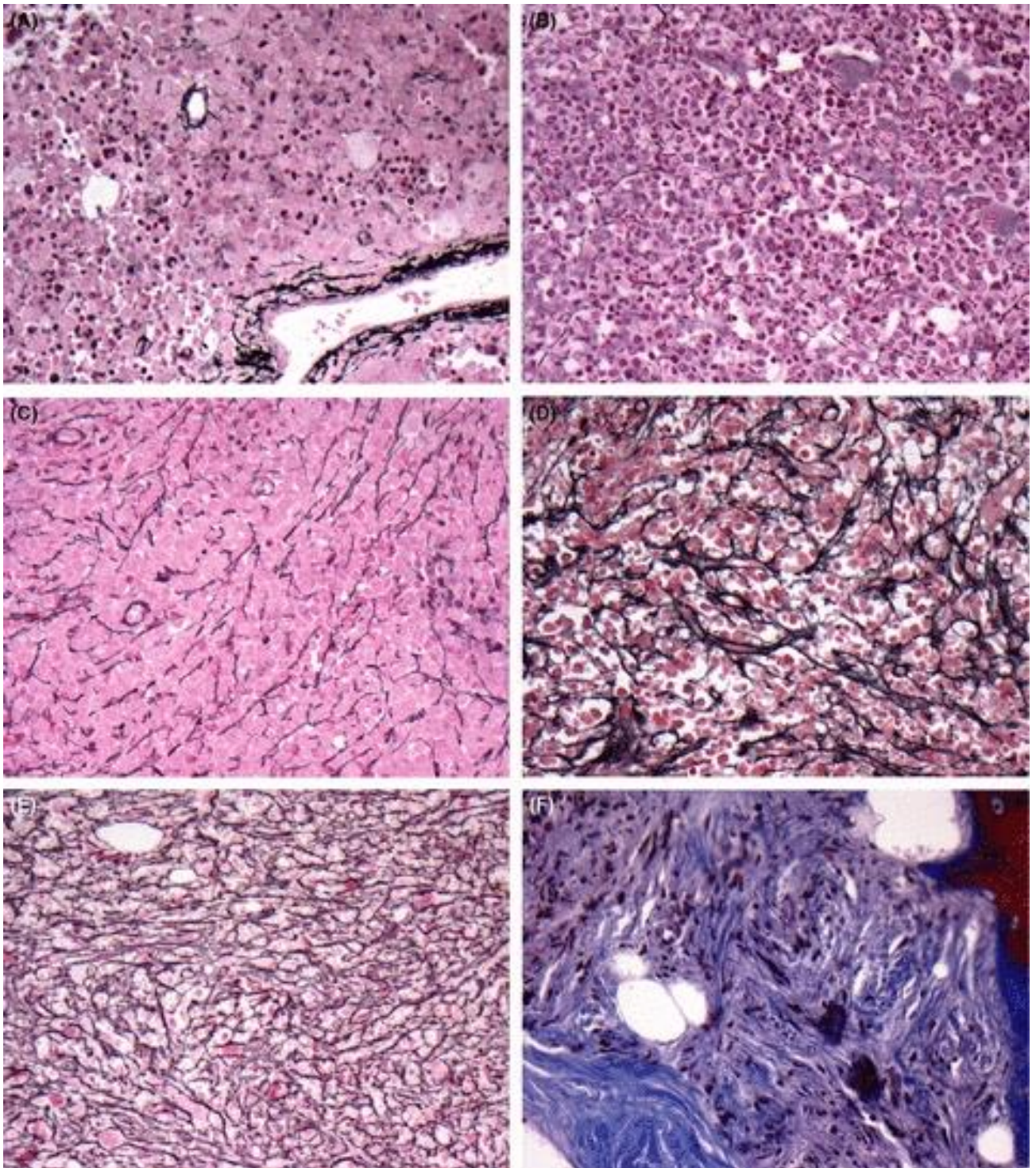


Figure 4. Examples of reticulin staining grades (modified Bauermeister scale (Bauermeister, 1971)) and collagen fibrosis in bone marrow trephine biopsies. **(A)** Grade 0. No reticulin fiber demonstrable. **(B)** Grade 1. Short, thin reticulin fibers are found in the bone marrow, but they do not form a network. **(C)** Grade 2. Thin reticulin fibers with numerous fiber intersections are observed. **(D)** Grade 3. There is a network of reticulin fibers including thick and reduplicated fibers. **(E)** Grade 4. A dense network of thick reticulin fibers are found throughout the bone marrow. **(F)** Trichrome stain, demonstrating collagen fibrosis which stains blue. (Original magnification: 200 \times . A–E: Gordon-Sweet (Reticulin) stain, F: Masson's trichrome stain) (Kuter et al., 2007).

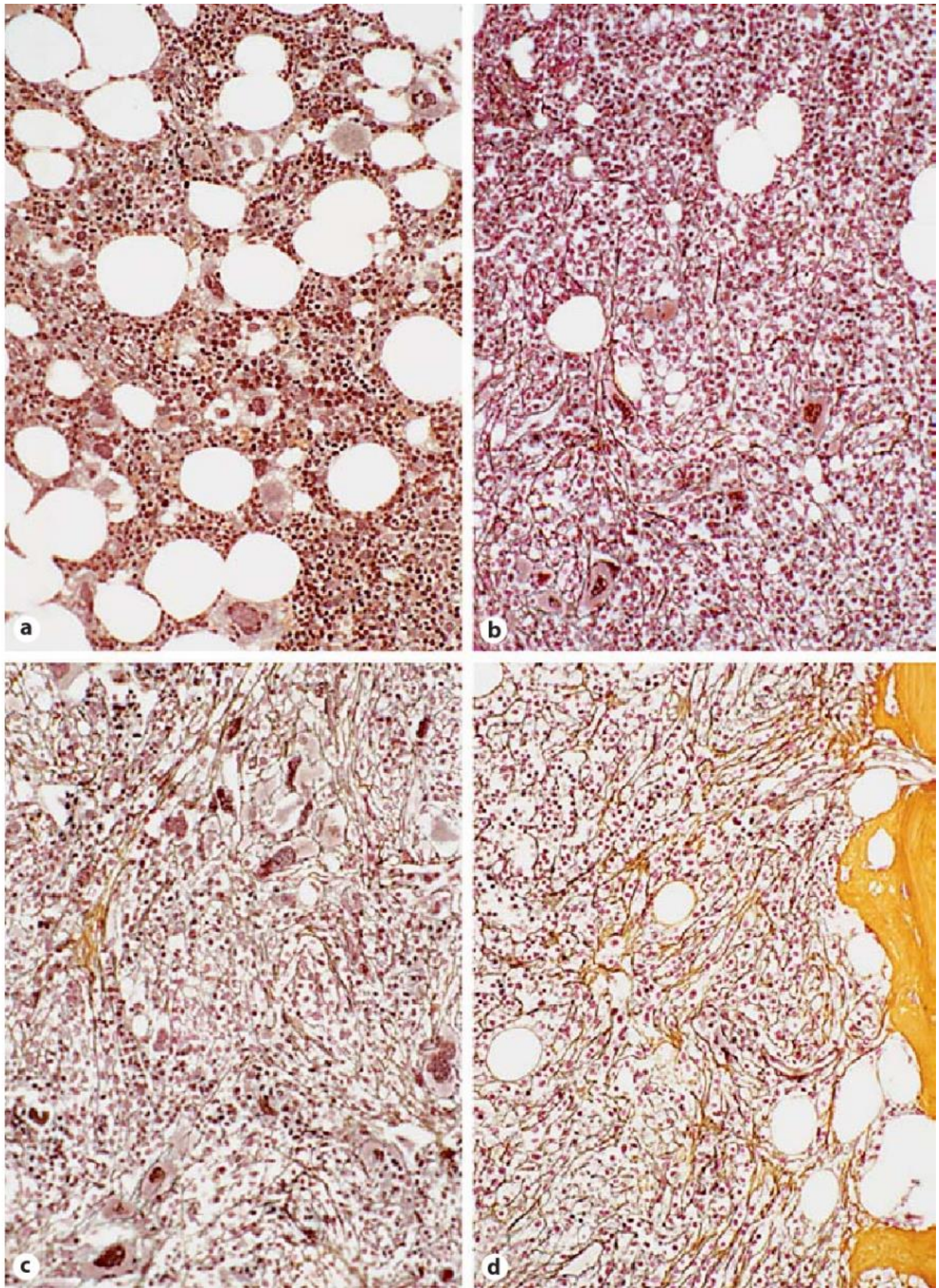


Figure 5. Grading of MF according to a consensus scoring system (Thiele et al., 2005; Thiele & Kvasnicka, 2006). **a)** Grade 0: very few scattered linear reticulin fibers corresponding with the normal appearance. **b)** Grade 1: loose network of finely dispersed reticulin. **c)** Grade 2: diffuse increase in reticulin with focal (mostly perivascular) bundles of collagen. **d)** Dense increase in reticulin and coarse bundles of collagen associated with osteosclerosis (left margin). (Original Magnification a–d 180X, Gomori's silver impregnation).

Table 1. Grading scales for the quantification of bone marrow reticulin and collagen

A) Quantification of bone marrow reticulin and collagen (modified Bauermeister) (Bain et al., 2001; Bauermeister, 1971)	
0	No reticulin fibers demonstrable
1	Occasional fine individual fibers and foci of a fine fiber network
2	Fine fiber network throughout most of the section; no coarse fibers
3	Diffuse fiber network with scattered thick coarse fibers but no mature collagen (negative trichrome staining)
4	Diffuse, often coarse fiber network with areas of collagenization (positive trichrome staining)
(B) European consensus on the grading of bone marrow fibrosis (Thiele et al., 2005)	
0	Scattered linear reticulin with no intersection (cross-overs) corresponding to normal bone marrow
1	Loose network of reticulin with many intersections, especially in perivascular areas
2	Diffuse and dense increase in reticulin with extensive intersections, occasionally with only focal bundles of collagen and/or focal osteosclerosis
3	Diffuse and dense increase in reticulin with extensive intersections with coarse bundles of collagen, often associated with significant osteosclerosis

However, these scores have several limitations including the interobserver variability, inconsistency of use and possible confusion for the clinician as to which system was used to classify the neoplasm of an individual patient. This is further hampered by the lack of studies which attempt to validate the data of proposed histomorphological features, or by rare reports demonstrating the inability of experienced reviewers to ensure the reproducibility of morphological criteria for making the diagnosis (Wilkins et al., 2008).

Digital imaging is an emerging technology, with great promise for numerous applications throughout the field of pathology. In fact, many studies have moved towards using a numerical (computer-assisted) assessment of reticulin fibrosis and osteosclerosis. These methods should provide a reproducible and accurate way of following patients over time and would help standardize assessment of fibrosis between pathologists and hematologists (Teman et al., 2010).

1.5. Treatments strategies

There are currently few options for patients with PMF. The only treatment capable of prolonging survival in PMF is allogeneic hematopoietic stem cell transplant, but, unfortunately, it is associated with at least 50% rate of treatment-related mortality or severe morbidity (Ballen et al., 2010; Vannucchi et al., 2015). Other treatment options are aimed to reducing symptoms and improving blood

counts, with little effects on disease natural history or prolong survival. Specifically, JAK2 inhibitors did not show to reverse bone marrow fibrosis or induce complete or partial remissions, instead its value is limited to symptoms relief and reduction in spleen size (Tefferi, 2021).

The only FDA approved agent for PMF patients is Ruxolitinib, a JAK1/2 inhibitor, that demonstrated clinical benefit including spleen volume reduction, improvement in quality of the patients' life, and improvement or stabilization of bone marrow fibrosis, but the challenge still remain. First, Ruxolitinib has no antitumor activity and has not been shown to reverse bone marrow fibrosis or induce cytogenetic or molecular remission. Second, anemia and thrombocytopenia limit the use and/or achievement of the therapeutic dose of ruxolitinib in some populations (Pettit & Odenike, 2017; Tefferi, 2021). A number of other agents have been used to improve cytopenia or to reduce splenomegaly with variable success, including erythropoietin stimulating agents, androgens (i.e. danazol), immunomodulators (i.e. thalidomide), and hydroxyurea (Pettit & Odenike, 2017).

2. Murine models of myelofibrosis

Clinical manifestations of PMF are anemia, neutrophilia, thrombocytosis, splenomegaly, presence of immature granulocytes and megakaryocytes, increased number of CD34⁺ (HSC) cells, presence of nucleated red blood cells, teardrop-shaped red blood cells (dacrocytes), bone marrow fibrosis and often osteosclerosis. MPNs arises from the hyperproliferation of mutant clones of hematopoietic cells harboring the so-called "driver mutation" in genes important for normal myeloproliferation: Janus kinase 2 (*JAK2*) and thrombopoietin receptor (*MPL*), or in ET and PMF, mutated calreticulin gene (*CALR*) (Skoda et al., 2015; Vainchenker & Kralovics, 2017). Over time, patients may change their mutational profiles and microenvironmental characteristics, which induce a change in the disease phenotype. This mechanism supports the idea that MPNs are not distinct biological entities but rather a continuum where ET transforms into PV, or chronic phase PV and ET shift to PMF and all three transform into acute leukemia (Grinfeld et al., 2017).

Several experimental models have been used to identify the mechanisms and dynamics underlying myelofibrosis. These include *in vitro* experiments with cell lines that simulate the impact of known alterations on hematopoietic signaling pathways, and *in vivo* experiments employing animal models that allow studying the interaction between molecular alteration of the hematopoietic line and microenvironment in a physiological context, such as zebrafish and mouse models (Lanikova et al., 2019).

In hematologic studies, one technique of *in vivo* experiments is bone marrow transplantation in immunocompromised mice of BM cells transduced with retrovirus that delivers the target mutated gene (Nguyen et al., 2016) (**Figure 6A**). The disadvantage of this technique is that viral vectors integrate randomly into the genome and the expression of the target gene is non-physiologic. Other studies also use primary patient-derived cells (PDX) as donor cells in bone marrow transplantation models (**Figure 6B**). This technique has multiple advantages, those cells are the best source of pathological cells, but they are different between samples, they are difficult to store, and immunocompromised mice have an altered environment. Transgenic mouse models are constructed by integrating the target gene into the genome at a non-endogenous site and this provides a consistent genetic model where regulation of the gene is under the same context (**Figure 6C**) (Lamprecht Tratar et al., 2018). Furthermore, knock-in mouse models use recombination or targeted gene editing to express the mutant gene at the endogenous locus, under the control of the native promoter, and thus, more closely modeling physiological expression levels (**Figure 6D**). (Chen & Shih, 2021; Lamprecht Tratar et al., 2018).

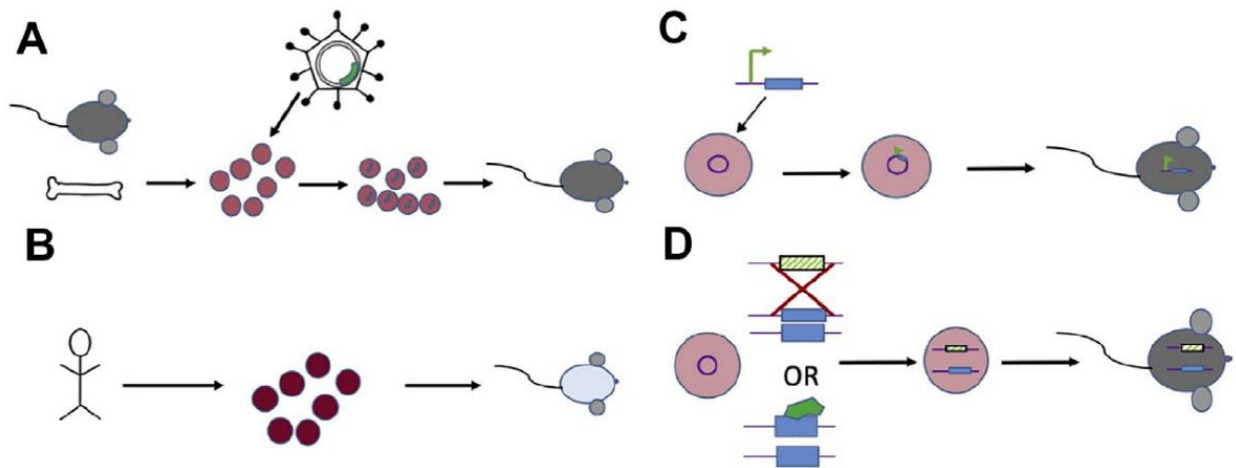


Figure 6. Mouse models of myeloproliferative neoplasms. **(A)** Retroviral-BMT model. Murine bone marrow cells are transduced with a virus that encodes a target gene. These cells are then reimplanted into a recipient mice. **(B)** Patient-derived cells model. Cells from MPN affected patients are isolated and injected into an immune-compromised mice. **(C)** Transgenic model. Embryonic stem (ES) cells are targeted with a transgene that integrates into the genome. Mice are then derived from these modified ES cells. **(D)** Knock-in model. ES cells are targeted by recombination methods or gene editing methods to modify a specific endogenous locus of the target gene. Mice are then derived from these modified ES cells (Chen & Shih, 2021).

Several mouse models have been created to study PMF. These include retroviral bone marrow transplant models, transgenic and knock-in mice. The most used mouse models of PMF are those harboring in the hematopoietic lineage the most common mutations in MPNs: JAK2, CALR, MPL. Other mouse models, that have helped to understand many of the pathways involved in these diseases and to find new targets for the treatment of MPNs, are: TPO overexpressing mouse, Trisomy 21 mouse, Abi-1 knock out mouse, and *Gata1*^{low} mouse.

2.1. *JAK2*^{V617F}

JAK2 is a non-receptor tyrosine kinase that plays a key role as an effector of intracellular signaling of the superfamily of the hematopoietic receptors, including the receptors for erythropoietin (EPO), thrombopoietin (TPO), and granulocyte-colony stimulating factor (G-CSF) and that controls the proliferation of normal hematopoietic cells of many lineages (Vainchenker et al., 2016).

A gain-of-function *JAK2*^{V617F} mutation was first identified in 2005 and is found in the 95% of patients with polycythemia vera (PV) and in 50% to 60% of those with essential thrombocythemia (ET) or idiopathic myelofibrosis (PMF) (Baxter et al., 2005; Kralovics et al., 2005; Levine et al., 2005). After the discovery of this mutation in MPN patients, retroviral models were generated to study the phenotypic effects of this mutation *in vivo* (Bumm et al., 2006; Lacout et al., 2006; Wernig et al., 2006; Zaleskas et al., 2006).

Mice transplanted with *JAK2*^{V617F} expressing donor bone marrow cells, developed a phenotype resembling PV, but in two studies was described also myelofibrosis (Lacout et al., 2006; Wernig et al., 2006). In these two studies, at early stages, features such as high hemoglobin, leukocytosis and megakaryocyte hyperplasia were observed and splenomegaly was identified at endpoints, consistent with PV progressing to MF (Lacout et al., 2006; Wernig et al., 2006). Similarly, mice transplanted with *JAK2*^{V617F} - transduced bone marrow cells presents a PV-phenotype at early stage, with an increased hematocrit, splenomegaly, leukocytosis and neutrophilia; subsequently they develop myelofibrosis (Chen & Shih, 2021). In order to closely recapitulate physiological level expression, genetically engineered mouse models of *JAK2*^{V617F} were also developed. Knock-in mouse models were published over the years in which murine *JAK2*^{V617F} was expressed in different manners (Akada et al., 2010; Li et al., 2010; Marty et al., 2010; Mullally et al., 2010). In all these models, erythrocytosis, leukocytosis, extramedullary hematopoiesis, and MF development (in a minority of mice after 26 weeks) were observed.

2.2. *MPL* Mutation (*W515L* and *W515W*)

In 2006, a somatic point mutation in *MPL*, *MPL*^{W515L/K}, was found in 5% and 1% of patients with PMF and ET, respectively (A. D. Pardanani et al., 2006). To better understand the features of this mutation *in vivo*, a mouse model has been developed where *MPL*^{W515L} was expressed retrovirally in hematopoietic stem cell progenitors (Kleppe et al., 2015; Pikman et al., 2006). This model recapitulated phenotypic features of human myelofibrosis such as MKs hyperplasia, splenomegaly, extra medullary hematopoiesis, and thrombocytosis. *MPL*^{W515L} -mutant HSPC were the largest source of IL-6; however, mutant and wild-type cells secreted tumor necrosis factor (TNF), IL-10, and C-C motif chemokine 2 (CCL2) (Kleppe et al., 2015). These data show that cytokine production by both populations is an important feature of MF, and suggest an interaction between malignant and non-malignant cells (Koppikar et al., 2010; Wernig et al., 2012).

2.3. CALR

CALR is a molecular chaperone protein localized in the endoplasmic reticulum that aids the quality control of newly synthesized proteins. More than 50 mutations in this gene are now described, but the most prevalent are two that account for approximately 80% of all identified CALR mutations in MPN: a 52-base deletion (del52) (type 1: c.1092_1143del) and a 5-base insertion bases (ins5) (type 2: c.1154_1155insTTGTC) (Pietra et al., 2016; Vainchenker & Kralovics, 2017). All mutations described are located in exon 9 inducing a +1 (-1+2) base-pair frameshift that generates a mutant-specific 36 amino acid sequence in the CALR-R C-terminus. The mutations leading to this +1 frameshift are known to be central to the pathogenesis of the disease (Klampfl et al., 2013; Nangalia et al., 2013). These mutations lead to the activation of the JAK/STAT signaling pathway by a pathogenic interaction with the thrombopoietin receptor MPL to induce MPNs (Araki et al., 2016; Chachoua et al., 2016; Elf et al., 2016; Imai et al., 2017; Pietra et al., 2016).

Retroviral (Marty et al., 2016), transgenic (Shide et al., 2017), and knock-in (Li et al., 2018) mutant CALR mouse models generate a MPN phenotype that closely recapitulates the human disease. In 2016, Marty *et al.* showed that CALR^{del52} retroviral-expressed in mouse lineage-negative bone marrow (BM) cells induce MPN, with fibrosis in the bone marrow, amplification of the MKs lineage, rapidly develop splenomegaly and thrombocytosis and osteosclerosis (Marty et al., 2016). Shide et al. developed transgenic mice expressing a human CALR mutation with a 52 bp deletion that developed ET, with an increase in platelet count, but not hemoglobin level or white blood cell count, in association with an increase in mature MKs (Shide et al., 2017). In 2018, Li et al., demonstrated that type I mutant del52 CALR knock-in mice developed ET-like disease with proliferation of morphologically abnormal MK associated with thrombocytosis, leukocytosis, reduced hematocrit, splenomegaly and increased bone marrow reticulin fibrosis and number of HSCs; particularly when the mutant gene was homozygous (Li et al., 2018).

2.4. TPO Overexpression

Thrombopoietin is important in megakaryopoiesis and plays a role as a survival/proliferation factor for HSC progenitors (Chagraoui et al., 2006). Overexpression of TPO in the BM was not found in patients with MF, but serum levels of TPO in these patients were elevated (Wang et al., 1997). In addition, in two different studies, retroviral expression of TPO in mouse bone marrow cells induced the development of myelofibrosis (Villeval et al., 1997; Yan et al., 1995). In both models, forced expression of TPO in transplanted bone marrow cells leads to a fatal MPN with MF and osteosclerosis. At 10 weeks after transplantation, mice showed megakaryocytosis and granulocytosis in both spleen and bone marrow with erythroblastic hypoplasia. Subsequently, the mice displayed pancytopenia, decreased hematopoietic progenitors, osteosclerosis and fibrosis in the spleen and bone marrow. Another study generated murine TPO transgenic mice (TPO Tg) driven by the IgH promoter

(Kakumitsu et al., 2005). In this model, mice exhibited thrombocytosis, neutrophilia. Anemia was also observed in TPO Tg mice, while erythrocyte progenitors were increased. This suggests a shift of erythroid differentiation toward megakaryocytic/platelet differentiation. At 9 months, with progression to 12 months, TPO Tg mice developed myelofibrosis and osteosclerosis, associated with extramedullary hematopoiesis (Kakumitsu et al., 2005).

2.5. Trisomy 21 mouse

Trisomy 21 is often found as a somatic aberration in myeloid neoplasms. It is a relatively common acquired aneuploidy observed in myeloid leukemia blasts. Children with Down syndrome (DS) have macrocytosis, thrombocytosis and a 500-fold increased risk of developing megakaryocytic leukemia; however, the specific effects of trisomy 21 on hematopoiesis remain poorly defined (Gurbuxani et al., 2004; Roizen & Amarose, 1993). Kirsammer et al. observed a highly penetrant MPN with modest MF in Ts65Dn mice (Kirsammer et al., 2008). These mice are trisomic for 104 orthologs of mouse chromosome 21 (Hsa21) and are the most widely used mouse model for DS. They demonstrated that Ts65Dn mice display persistent macrocytosis and develop a myeloproliferative disease characterized by profound thrombocytosis, megakaryocyte hyperplasia, dysplastic megakaryocyte morphology, and myelofibrosis. In addition, these animals bear distorted hematopoietic stem and myeloid progenitor cell compartments compared with euploid control littermates.

2.6. Abi-1 knockout mouse

Chorzalska et al. recently demonstrated that Abelson's Interactor 1 (Abi-1), a negative regulator of ABL, is downregulated in CD34⁺ cells from patients with PMF. Downregulation of Abi-1 gene expression was observed in granulocytes from patients with PMF and patients with MF secondary to PV, but not in ET, PV or MF secondary to ET. Therefore, Chorzalska et al. induced conditional deletion of Abi-1 in mice using the Mx1Cre system (Chorzalska et al., 2018). Abi-1 deletion in the bone marrow of mice resulted in a PMF phenotype characterized by leukocytosis, thrombocytosis, anemia, splenomegaly, megakaryocytosis, and fibrosis. Transduction of heterozygous Abi-1 knockout mice with MPL^{W515L} accelerated the development of the MPN phenotype, demonstrating that loss of Abi-1 cooperates with mutant Mpl to induce MPN. Therefore, Abi-1-deficient mice represent an interesting new model to interrogate Src, Stat3 and NF-K β signaling in MF.

3. Gata1^{low} Mouse model of myelofibrosis

3.1. GATA family transcriptional factors

GATA transcription factors are zinc finger DNA binding protein that regulate transcription during the embryonic development and differentiation (Gao et al., 2015). Human, and mammalian

genomes encode six structurally related members of the GATA family. Three of them, are involved in distinct and overlapping aspects of hematopoiesis, GATA1, GATA2 and GATA3 (Chlon & Crispino, 2012).

GATA1 is essential in the development of particular hematopoietic cell lineages, in particular it is required for the erythroid and megakaryocytic commitment during hematopoiesis (Iwasaki et al., 2003; S.-F. Tsai et al., 1989). The interaction of GATA1 with N terminal zinc finger cofactors such as FOG-1 (Friend of GATA) is essential for megakaryocyte or erythroid development (Gao et al., 2015). GATA2 is required for the proliferation and survival of early hematopoietic cells, but dispensable for the erythroid and myeloid terminal differentiation, and is also involved in lineage specific transcriptional regulation as GATA2 gene is one of the target genes that GATA1 regulates (Suzuki et al., 2013; F. Y. Tsai & Orkin, 1997). GATA3 plays an essential role in T lymphoid cell development and immune regulation as it is required for producing early T-lineage progenitor cells (Gao et al., 2015) (**Figure 7**). The others three members of the GATA family, GATA4, GATA5, and GATA6 are involved in heart formation as they are predominantly expressed during embryonic heart development (Singh et al., 2010).

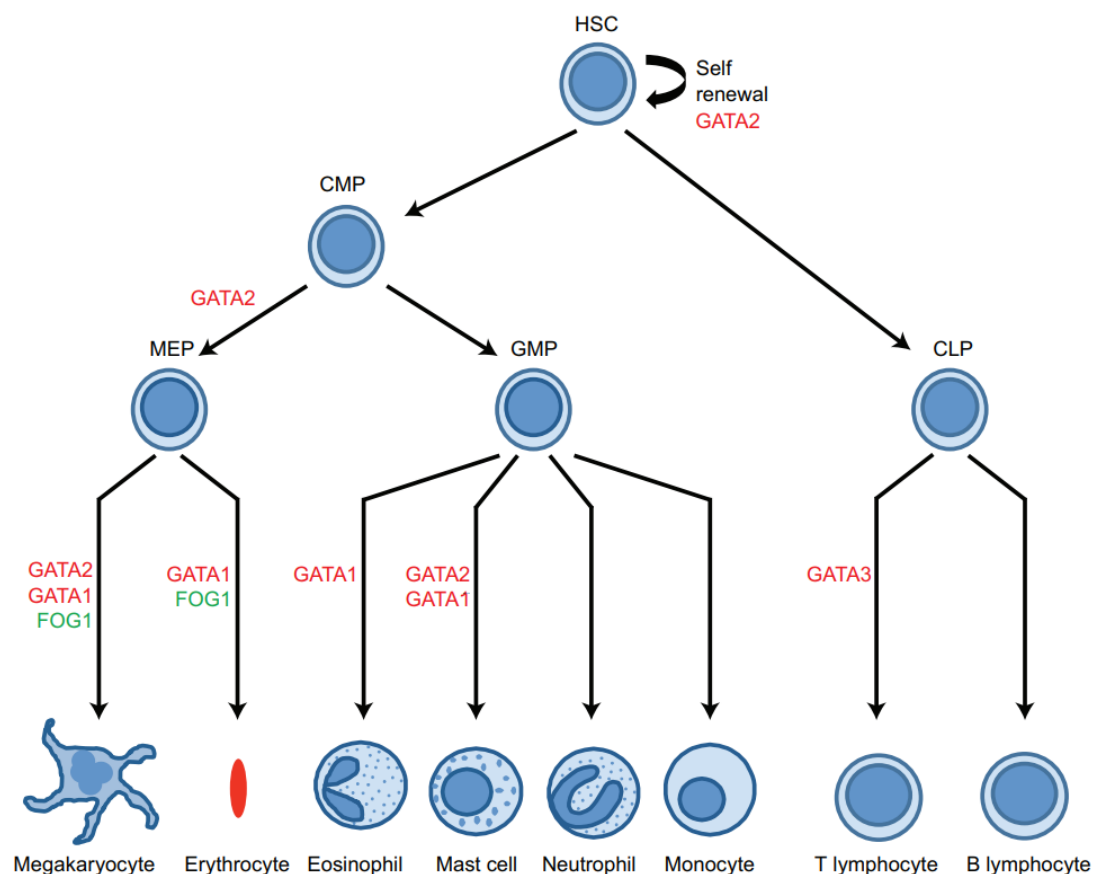


Figure 7. Control of mammalian hematopoiesis by GATA and FOG factors. A classical representation of mammalian hematopoiesis is depicted, and the roles of GATA and FOG proteins at each step are indicated. Abbreviations: HSC, hematopoietic stem cell; CMP, common myeloid progenitor; MEP, megakaryocyte/erythrocyte progenitor; GMP, granulocyte/macrophage progenitor; CLP, common lymphoid progenitor (Chlon & Crispino, 2012).

3.2. *GATA1 in hematopoiesis and disease*

GATA1 is a transcription factor that regulates the maturation of erythroid cells. It binds the consensus sequence GATA (hence their name) present in the regulatory regions of all the erythroid-specific genes including the erythropoietin (EPO), receptor (EPO-R) and *Gata1* itself (Crispino & Horwitz, 2017).

GATA1 expression is both necessary and sufficient for terminal maturation of erythroid cells and megakaryocytes (Ling et al., 2018). It is expressed, although at very low levels, in hematopoietic stem cells (Migliaccio et al., 1996). Its expression then increases during the transition from stem cells to the common myeloid progenitor cells (CMP). Lineage restriction is associated with a further increase in GATA1 expression in megakaryocyte-erythroid progenitor cells (MEP) and by a decrease in expression in granulomonocytic progenitor cells (GMP). Among differentiated cells, high levels of GATA1 expression are detected in erythroblasts and megakaryocytes (Lee et al., 2017) while the expression of this mRNA is low in eosinophils (Yu et al., 2002), mast cells (Campos & Chiesi, 1985; Migliaccio et al., 2003) and dendritic cells (Auerbach, 1992; Kozma et al., 2010). Of note, T and B cells do not express GATA1 mRNA. Among non-hematopoietic cells, GATA1 expression is restricted to the Sertoli cells of the testis (Lee et al., 2017; Shivdasani et al., 1997).

3.3. *Gata1^{low} mouse model of PMF*

The hypomorphic *Gata1^{low}* mutation, which specifically deletes the first hypersensitive site upstream to the gene (HS1, also known as HS-3.5 and G1H2), was developed in 1997 in the Stuart Orkin laboratory (Mcdevitt et al., 1997). The mutation totally abolished GATA1 expression in megakaryocytes and strongly reduced it in erythroid (McDevitt et al., 1997) and mast cells (Migliaccio et al., 2003).

Since GATA1 is encoded by an X-linked gene, both in mice and men (Crispino & Horwitz, 2017), *Gata1^{low}* male die of profound anemia at birth, by contrast heterozygote female survive to adulthood, but eventually develop hematopoietic neoplasms (Shimizu et al., 2004). This mutation was originally established in the C57BL/6 background, where it induces high perinatal mortality due to severe anemia (Mcdevitt et al., 1997). On the contrary, in the CD1 mouse strain, this mutation is not lethal (Vannucchi et al., 2001), because in a few weeks they developed extramedullary hematopoiesis in the spleen and express normal hematocrit levels from 1 to 18 months of age, with an apparently normal life span (Vannucchi et al., 2001). Almost all circulating red blood cells of *Gata1^{low}* mice are generated from the hematopoietic site located in the spleen of these mice. Proof of this statement is provided by the observation that splenectomy induces the death of mice from profound anemia within 2 weeks (Migliaccio et al., 2009).

Megakaryocytes from PMF patients are noted to be significantly deficient in GATA1 expression, with almost half megakaryocytes not stained by immunohistochemistry for GATA1

(Vannucchi et al., 2005). Conversely, they show a normal expression level of GATA1 mRNA, but this is explained by the finding that they express an abnormal ribosomal signature (RSP14 signature), which may contribute to reduced GATA1 expression in MKs by impaired mRNA translation (Vannucchi et al., 2005; Zingariello et al., 2017).

The transcription factor GATA1 regulates MK development, including platelet biogenesis; in fact, megakaryocytes from *Gata1*^{low} mice express an abnormal phenotype that includes increased proliferation and delayed maturation, features similar to those found in PMF (Centurione et al., 2004; Vyas et al., 1999; Zucker-Franklin D, 1974). Such abnormalities are also associated with the development of myelofibrosis with age, with high levels of collagen fibers in the bone marrow (Eliades et al., 2011; Vannucchi et al., 2002).

Similarities between PMF patients and *Gata1*^{low} mice, including molecular (reduced GATA1 content) and biological (increased proliferation with reduced maturation of MKs) behavior, led researchers to investigate nearly 20 years ago whether *Gata1*^{low} mice would develop myelofibrosis. It was determined that *Gata1*^{low} mice were one of the first animal models suitable for the study this human disease (Vannucchi et al., 2002). Young (1 to 8 months-old) *Gata1*^{low} mice display traits associated with the pre-fibrotic stage of primary myelofibrosis such as splenomegaly, extramedullary hematopoiesis, increased rates of thrombosis, and osteosclerosis. Adult mice (8 to 12 months-old), display myelofibrotic traits including fibrosis and neo-angiogenesis, and from 12 months of age until their natural death, express also a late myelofibrotic phenotype that includes increased trafficking of stem/progenitor cells and extramedullary hematopoiesis in the liver (Vannucchi et al., 2002). This disease progression clearly mimics the evolution from a pre-fibrotic stage (Pre-PMF) to overt primary myelofibrosis (PMF) (Arber et al., 2016).

Because the reduced level of GATA1 in megakaryocytes impairs MK maturation, the bone marrow and spleen of *Gata1*^{low} mice can contain twice as many MKs as those present in Wild-type mice. These MKs are located in clusters and have a predominantly immature morphology, characterized by a large, hyperchromatic nucleus and scanty cytoplasm, and the blocking of their maturation also includes failure to properly organize α -granules (Centurione et al., 2004).

Gata1^{low} mice remain thrombocytopenic for life, with circulating platelets on average 50% larger but still homogeneous in size compared with normal cells (Vyas et al., 1999). *Gata1*^{low} platelet α -granules are reduced in number and electron density, an indication of low protein content (Centurione et al., 2004). They contain low levels of Von Willebrand factor, and although they contain normal levels of P-selectin that is abnormally accumulated on the demarcation membrane system (DMS) of megakaryocytes (Zingariello et al., 2010). These abnormalities indicate that the *Gata1*^{low} mutation impairs terminal maturation of megakaryocytes into platelets (Ling et al., 2018).

Numerous morphological data, support the hypothesis that the development of myelofibrosis is associated with megakaryocyte abnormalities. These abnormalities, as previously discussed, include

hyperproliferation of MKs with delayed maturation (Zucker-Franklin D, 1974), high TGF- β content (Schmitt et al., 2002; Zingariello et al., 2013b) and are embedded by high numbers of neutrophils entrapped in their cytoplasm by a process of pathological emperipolesis (Centurione et al., 2004; Schmitt et al., 2000).

TGF- β 1 is a factor involved in both fibrosis and cancer progression. Specifically, it induces growth arrest of several cell types, suggesting that activation of TGF- β 1 signaling may induce quiescent cancer cells to proliferate and thus advance into the early stages of cancer (Massagué, 2008). In addition, TGF- β 1, by activating the expression of both components of the extracellular matrix (type I collagen and fibronectin), may also promote interactions between cancer cells and the microenvironment, promoting cancer progression to the metastatic stage (Massagué, 2008). It is also involved in fibrosis since it is among the growth factors responsible for the epithelial-mesenchymal transition, which induces the formation of activated fibrocytes, believed to be responsible for fibrosis (Dongre & Weinberg, 2019).

As mentioned above, megakaryocytes from *Gata1*^{low} mice also remain immature, localized in clusters in the spleen, and express high levels of TGF- β and P-selectin. In addition, abnormal emperipoletic interactions with neutrophils are frequently observed as in human disease (Spangrude et al., 2016; Vannucchi et al., 2002; Zingariello et al., 2013b). Emperipolesis is a transient interaction between neutrophils and MKs, which alters neither the neutrophil nor the megakaryocyte, observed in 0.8 percent of MKs in the healthy bone marrow. This mechanism is used by neutrophils to move rapidly from one site to another in the microenvironment using the DMS of MKs as a shortcut. In the bone marrow, and spleen of *Gata1*^{low} mice, however, the process involves up to 30% of the MKs present. Moreover, this process occurs abnormally, inasmuch as neutrophils become trapped within the MKs, fuse their plasma membrane with the DMS by releasing the proteolytic contents of their α -granules (such as metalloproteinase 9, MPP9) within the cytoplasm of the megakaryocytes and leading to the death of both cells by paraptosis, an immune-mediated cell death process that, unlike apoptosis, involves a high level of chromatin condensation within the nuclei, and proteolytic leakage from the cytoplasm (Centurione et al., 2014). All these abnormalities should be considered as cellular hallmarks of the disease, as they have been observed in the MKs of patients with PMF (Alvarez-Larrán et al., 2008; Schmitt et al., 2000, 2002; Thiele et al., 1997). These observations led to the pathobiological model of myelofibrosis, which hypothesizes that the disease is underpinned by a progressive accumulation of TGF- β in the microenvironment triggered by a pathological P-selectin-dependent emperipolesis between MKs and neutrophils (Zingariello et al., 2019) (**Figure 8**).

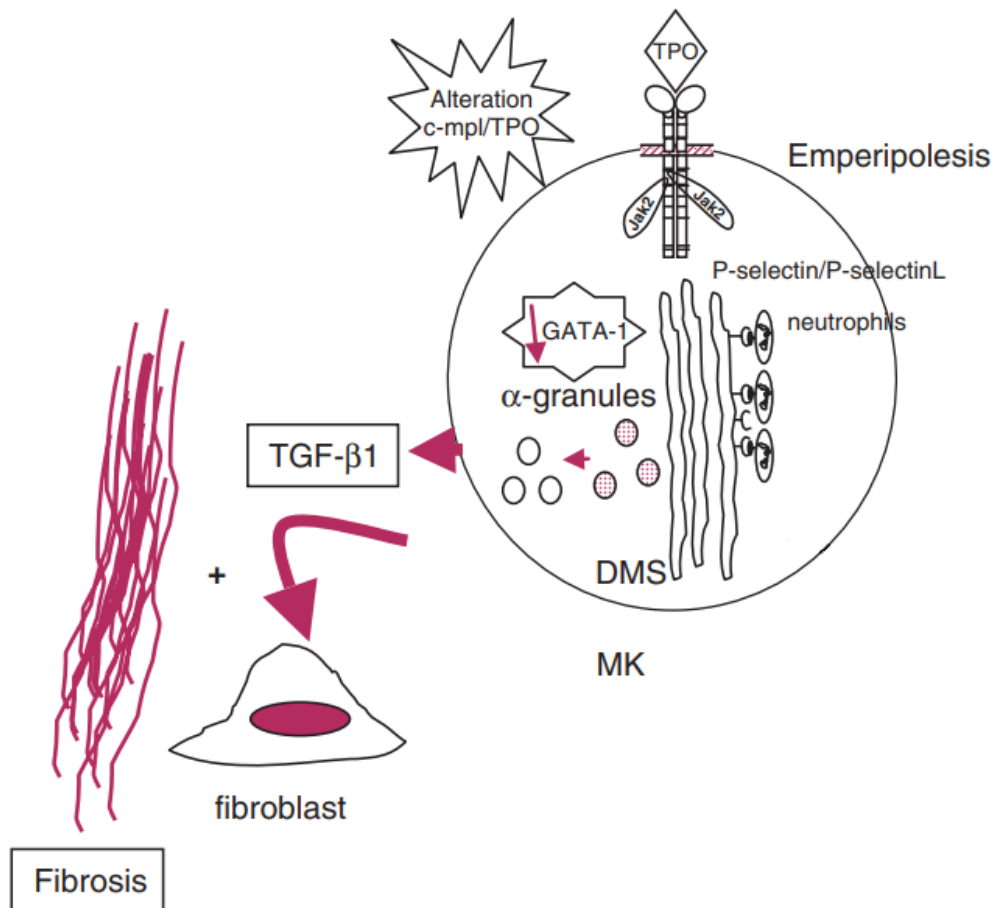


Figure 8. Pathophysiological model of myelofibrosis. Thrombopoietin (TP)-overexpressing or *Gata1*^{low} mice displayed reduced GATA-1 content in megakaryocytes (MK). These resulted in the same defects (e.g. abnormal P-selectin localization on the DMS and increased neutrophil emperipolesis), which triggered increased release of transforming growth factor beta 1 (TGF- β 1) in the extracellular fluids of the bone marrow and spleen responsible for the activated fibroblast-mediated fibrosis. Adapted from: (Chagraoui et al., 2006).

3.4. Pharmacologic molecules tested in *Gata1*^{low} mice

During decade long studies on the pathogenetic mechanisms leading to the establishment of the myelofibrotic phenotype in *Gata1*^{low} mice, investigators have identified several abnormalities expressed by the megakaryocytes from these mice that are similar to those identified in the megakaryocytes of patients with myelofibrosis and that may represent possible targets to cure the human disease (Vannucchi et al., 2002; Zingariello et al., 2019). The malignant megakaryocytes present in the bone marrow of the patients with myelofibrosis and of the murine models of the disease, contain great levels of TGF- β (Zingariello et al., 2013b, 2015), of the adhesion protein P-Selectin (Spangrude et al., 2016) and of lysyl oxidase (Abbonante et al., 2017; Eliades et al., 2011). In addition, the malignant stem/progenitor cells from the mouse models express low levels of p27kip1, a protein that regulates stem/progenitor cell fate decisions, with low levels favoring proliferation and high levels promoting differentiation (Cheng et al., 2000; Messina et al., 2005).

Inhibitors of these pathways are available and were tested for their effectiveness in rescuing the myelofibrosis traits of *Gata1*^{low} mice.

Two different studies tested compound that inhibit Lysyl oxidase (LOX) in the *Gata1*^{low} mouse model of PMF. Lysyl oxidase (LOX), an enzyme vital for collagen cross-linking and extracellular matrix stiffening, has been found to be up-regulated in PMF. The first study tested β -aminopropionitrile (a LOX inhibitor). The treatment significantly improved the bone marrow fibrotic phenotype, and MK number in the spleen (Eliades et al., 2011). The second one tested two LOX inhibitors, PXS-LOX_1 and PXS-LOX_2. Both inhibitors were effective in reducing bone marrow fibrosis. The number of Mks was reduced in PXS-LOX_1 treated mice (Leiva et al., 2019).

Corey et al (2018), tested captopril, an inhibitor of angiotensin-converting enzyme that blocks the production of angiotensin II that has a role in fibrotic remodelling of the lung, heart, kidney, skin and liver. The treatment of *Gata1*^{low} mice with captopril administered in the drinking water was associated with normalization of the bone marrow cellularity; reduced reticulin fibers, splenomegaly and megakaryocytosis; and decreased collagen expression (Corey et al., 2018)

Migliaccio's group tested Aplidin (a cyclic depsipeptide that activates p27kip1 in several cancer cells) developed by Pharma Mar (Verrucci et al., 2010) and two TGF- β inhibitors (SB431542, a small compound which inhibits ALK5 the first element of the signal transduction of TGF- β receptor commercially available (Zingariello et al., 2013), and the TGF- β trap AVID200) developed by Forbius (Varricchio et al., 2021).

Treatment with Aplidin increased platelet counts, marrow cellularity, and reduced microvessel density and expression of TGF- β , vascular endothelial growth factor and thrombopoietin in *Gata1*^{low} mice (Verrucci et al., 2010). This study led to a clinical trial that tested the efficacy of Aplidin in a total of 11 patients with PMF, post-PV MF or post-ET MF. The drug was well tolerated with limited toxicity but the study was interrupted because only one patient had some response (anemia improvement) (A. Pardanani et al., 2015).

Treatment with the TGF- β signaling inhibitor SB431542 restores haematopoiesis and megakaryocyte development in the bone marrow, increasing blood platelets, and reducing TGF- β content and fibrosis in the bone marrow of *Gata1*^{low} mice (Zingariello et al., 2013). It also reduces extramedullary haematopoiesis in the spleen. This drug was not tested in patients due to difficulties in obtaining Galunisertib, a drug with a chemical structure similar to that of SB431542 from Lilly (Herbertz et al., 2015). The group tested then the effects of targeting TGF- β by treating *Gata1*^{low} mice with AVID200, a potent TGF- β 1/TGF- β 3 protein trap, developed specifically for clinical studies (Verrucci et al., 2010). Treatment with AVID200 reduced TGF- β content and fibrosis while increasing cellularity and restoring haematopoiesis and stem cell frequency in the bone marrow. These data supported a clinical trial that tested AVID200 in a limited number of patients with advanced myelofibrosis which is just completed (NCT03895112) (Mascarenhas et al., 2021). Although

ineffective in preventing disease progression, treatment with AVID200 increased platelet counts at least in some of the patients recruited in the study.

All these treatments were effective in rescuing at least some of the myelofibrosis traits expressed by *Gatal*^{low} mice, but none of them rescued completely the MF phenotype in this mouse model of PMF.

4. References

Abbonante, V., Chitalia, V., Rosti, V., Leiva, O., Matsuura, S., Balduini, A., Ravid, K. (2017). Upregulation of lysyl oxidase and adhesion to collagen of human megakaryocytes and platelets in primary myelofibrosis. *Blood*, 130(6), 829–831. <https://doi.org/10.1182/blood-2017-04-777417>.

Abbonante, V., Di Buduo, C. A., Gruppi, C., Malara, A., Gianelli, U., Celesti, G., Anselmo, A., Laghi, L., Vercellino, M., Visai, L., Iurlo, A., Moratti, R., Barosi, G., Rosti, V., Balduini, A. (2016). Thrombopoietin/TGF- β 1 loop regulates megakaryocyte extracellular matrix component synthesis. *Stem Cells*, 34(4), 1123–1133. <https://doi.org/10.1002/stem.2285>.

Affandi, A.J., Silva-Cardoso, S.C., Garcia, S., Leijten, E.F.A., Van Kempen, T.S., Marut, W., Van Roon, J.A.G., Radstake, T.R.D.J. (2018). CXCL4 is a novel inducer of human Th17 cells and correlates with IL-17 and IL-22 in psoriatic arthritis. *European Journal of Immunology*, 48(3), 522–531. <https://doi.org/10.1002/eji.201747195>.

Agarwal, A., Morrone, K., Bartenstein, M., Zhao, Z.J., Verma, A., Goel, S. (2016). Bone marrow fibrosis in primary myelofibrosis: pathogenic mechanisms and the role of TGF- β . *Stem Cell Investigation*, 3, 5. <https://doi.org/10.3978/j.issn.2306-9759.2016.02.03>.

Aivado, M., Spentzos, D., Germing, U., Alterovitz, G., Meng, X.-Y., Grall, F., Giagounidis, A.A.N., Klement, G., Steidl, U., Otu, H.H., Czibere, A., Prall, W.C., Iking-Konert, C., Shayne, M., Ramoni, M.F., Gattermann, N., Haas, R., Mitsiades, C.S., Fung, E.T., Libermann, T.A. (2007). Serum proteome profiling detects myelodysplastic syndromes and identifies CXC chemokine ligands 4 and 7 as markers for advanced disease. *Proceedings of the National Academy of Sciences of the United States of America*, 104(4), 1307–1312. <https://doi.org/10.1073/pnas.0610330104>.

Akada, H., Yan, D., Zou, H., Fiering, S., Hutchison, R.E., Mohi, M.G. (2010). Conditional expression of heterozygous or homozygous *Jak2*^{V617F} from its endogenous promoter induces a polycythemia vera-like disease. *Blood*, 115(17), 3589–3597. <https://doi.org/10.1182/blood-2009-04-215848>.

Altomare, G., Capella, G. L., Frigerio, E. (1996). Sweet's syndrome in a patient with idiopathic myelofibrosis and thymoma-myasthenia gravis-immunodeficiency complex: efficacy of treatment with etretinate. *Haematologica*, 81(1), 54–58.

Alvarez-Larrán, A., Arellano-Rodrigo, E., Reverter, J. C., Domingo, A., Villamor, N., Colomer, D., Cervantes, F. (2008). Increased platelet, leukocyte, and coagulation activation in primary myelofibrosis. *Annals of Hematology*, 87, 269–276. <https://doi.org/10.1007/s00277-007-0386-3>.

Araki, M., Yang, Y., Masubuchi, N., Hironaka, Y., Takei, H., Morishita, S., Mizukami, Y., Kan, S., Shirane, S., Eda Hiro, Y., Sunami, Y., Ohsaka, A., Komatsu, N. (2016). Activation of the thrombopoietin receptor by mutant calreticulin in CALR-mutant myeloproliferative neoplasms. *Blood*, 127(10), 1307–1316. <https://doi.org/10.1182/blood-2015-09-671172>.

Arber, D. A., Orazi, A., Hasserjian, R. P., Borowitz, M. J., Calvo, K. R., Kvasnicka, H.-M., Wang, S. A., Bagg, A., Barbui, T., Branford, S., Bueso-Ramos, C. E., Cortes, J. E., Dal Cin, P., DiNardo, C. D., Dombret, H., Duncavage, E. J., Ebert, B. L., Estey, E. H., Facchetti, F., Foucar, K., Gangat, N., Gianelli, U., Godley, L.A., Gökbuget, N., Gotlib, J., Hellström-Lindberg, E., Hobbs, G.S., Hoffman, R., Jabbour, E.J., Kiladjan, J.J., Larson, R.A., Le Beau, M.M., Loh, M.L., Löwenberg, B., Macintyre, E., Malcovati, L., Mullighan, C.G., Niemeyer, C., Odenike, O.M., Ogawa, S., Orfao, A., Papaemmanuil, E., Passamonti, F., Porkka, K., Pui, C.H., Radich, J.P., Reiter, A., Rozman, M., Rudelius, M., Savona, M.R., Schiffer, C.A., Schmitt-Graeff, A., Shimamura, A., Sierra, J., Stock, W.A., Stone, R.M., Tallman, M.S., Thiele, J., Tien, H.F., Tzankov, A., Vannucchi, A.M., Vyas, P., Wei, A.H., Weinberg, O.K., Wierzbowska, A., Cazzola, M., Döhner, H., Tefferi, A. (2022). International consensus classification of myeloid neoplasms and acute leukemias: integrating morphologic, clinical, and genomic data. *Blood*, 140(11), 1200–1228. <https://doi.org/10.1182/blood.2022015850>.

Arber, D. A., Orazi, A., Hasserjian, R., Thiele, J., Borowitz, M. J., Le Beau, M. M., Bloomfield, C. D., Cazzola, M., Vardiman, J. W. (2016). The 2016 revision to the World Health Organization classification of myeloid neoplasms and acute leukemia. *Blood*, 127(20), 2391–2405. <https://doi.org/10.1182/blood-2016-03-643544>.

Auerbach, A. (1992). Kinetic behavior of cloned mouse acetylcholine receptors. A semi-autonomous, stepwise model of gating. *Biophysical Journal*, 62(1), 72–73. [https://doi.org/10.1016/S0006-3495\(92\)81783-6](https://doi.org/10.1016/S0006-3495(92)81783-6).

Bacigalupo, A. (2017). How I treat acquired aplastic anemia. *Blood*, 129(11), 1428–1436. <https://doi.org/10.1182/blood-2016-08-693481>.

Badalucco, S., Di Buduo, C.A., Campanelli, R., Pallotta, I., Catarsi, P., Rosti, V., Kaplan, D. L., Barosi, G., Massa, M., Balduini, A. (2013). Involvement of TGFβ-1 in autocrine regulation of proplatelet formation in healthy subjects and patients with primary myelofibrosis. *Haematologica*, 98(4), 514–517. <https://doi.org/10.3324/haematol.2012.076752>.

Bain, B.J., Clark, D.M., Lampert, I.A., Wilkins, B.S. (2001). *Bone marrow pathology*. (2nd ed.). Blackwell Science Ltd.

Ballen, K.K., Shrestha, S., Sobocinski, K.A., Zhang, M.J., Bashey, A., Bolwell, B.J., Cervantes, F., Devine, S.M., Gale, R.P., Gupta, V., Hahn, T.E., Hogan, W.J., Kröger, N., Litzow, M.R., Marks, D.I., Maziarz, R.T., McCarthy, P.L., Schiller, G., Schouten, H.C., Roy, V., Wiernik, P.H., Horowitz, M.M., Giral, S.A., Arora, M. (2010). Outcome of transplantation for myelofibrosis. *Biology of Blood and Marrow Transplantation: Journal of the American Society for Blood and Marrow Transplantation*, 16(3), 358–367. <https://doi.org/10.1016/j.bbmt.2009.10.025>.

Bancroft, J.D., Gamble, M. (2002). *Theory and practice of histological techniques*. Ed. 3. Churchill-Livingstone.

Barbui, T., Thiele, J., Gisslinger, H., Orazi, A., Vannucchi, A. M., Gianelli, U., Beham-Schmid, C., Tefferi, A. (2019). Comments on pre-fibrotic myelofibrosis and how should it be managed. *British Journal of Haematology*, 186(2), 358–360. <https://doi.org/10.1111/bjh.15840>.

Barbui, T., Thiele, J., Passamonti, F., Rumi, E., Boveri, E., Ruggeri, M., Rodeghiero, F., d'Amore, E.S.G., Randi, M.L., Bertozzi, I., Marino, F., Vannucchi, A.M., Antonioli, E., Carrai, V., Gisslinger, H., Buxhofer-Ausch, V., Müllauer, L., Carobbio, A., Gianatti, A., Gangat, N., Hanson, C.A., Tefferi, A. (2011). Survival and disease progression in essential thrombocythemia are significantly influenced by accurate morphologic diagnosis: an international study. *Journal of Clinical Oncology*, 29(23), 3179–3184. <https://doi.org/10.1200/JCO.2010.34.5298>.

Barosi, G. (2014). Essential thrombocythemia vs. early/prefibrotic myelofibrosis: why does it matter. *Best Practice & Research. Clinical Haematology*, 27(2), 129–140. <https://doi.org/10.1016/j.beha.2014.07.004>.

Bauermeister, D.E. (1971). Quantitation of bone marrow reticulin - a normal range. *American Journal of Clinical Pathology*, 56(1), 24–31. <https://doi.org/10.1093/ajcp/56.1.24>.

Baxter, E.J., Scott, L.M., Campbell, P.J., East, C., Fourouclas, N., Swanton, S., Vassiliou, G. S., Bench, A.J., Boyd, E.M., Curtin, N., Scott, M.A., Erber, W.N., Green, A.R., Cancer Genome Project. (n.d.). (2005). Acquired mutation of the tyrosine kinase JAK2 in human myeloproliferative disorders. *Lancet (London, England)*, 365(9464), 1054–1061. [https://doi.org/10.1016/S0140-6736\(05\)71142-9](https://doi.org/10.1016/S0140-6736(05)71142-9).

Bock, O., Höftmann, J., Theophile, K., Hussein, K., Wiese, B., Schlué, J., Kreipe, H. (2008). Bone morphogenetic proteins are overexpressed in the bone marrow of primary myelofibrosis and are apparently induced by fibrogenic cytokines. *The American Journal of Pathology*, 172(4), 951–960. <https://doi.org/10.2353/ajpath.2008.071030>.

Bumm, T.G.P., Elsea, C., Corbin, A.S., Loriaux, M., Sherbenou, D., Wood, L., Deininger, J., Silver, R.T., Druker, B. J., Deininger, M.W.N. (2006). Characterization of murine JAK2^{V617F}-Positive myeloproliferative disease. *Cancer Research*, 66(23), 11156–11165. <https://doi.org/10.1158/0008-5472.CAN-06-2210>.

Campos, E.C., Chiesi, C. (1985). Critical analysis of visual function evaluating techniques in newborn babies. *International Ophthalmology*, 8(1), 25–31. <https://doi.org/10.1007/BF00136458>.

Castro-Malaspina, H., Jhanwar, S. (1984). Properties of myelofibrosis-derived fibroblasts. *Progress in clinical and biological research*, 154, 307–322.

Castro-Malaspina, H., Rabellino, E.M., Yen, A., Nachman, R.L., Moore, M.A. (1981). Human megakaryocyte stimulation of proliferation of bone marrow fibroblasts. *Blood*, 57(4), 781–787.

Centurione, L., Di Baldassarre, A., Zingariello, M., Bosco, D., Gatta, V., Rana, R.A., Langella, V., Di Virgilio, A., Vannucchi, A.M., Migliaccio, A.R. (2004). Increased and pathologic emperipolesis of neutrophils within megakaryocytes associated with marrow fibrosis in *Gatal*^{low} mice. *Blood*, 104(12), 3573–3580. <https://doi.org/10.1182/blood-2004-01-0193>.

Chachoua, I., Pecquet, C., El-Khoury, M., Nivarthi, H., Albu, R.I., Marty, C., Gryshkova, V., Defour, J.P., Vertenoil, G., Ngo, A., Koay, A., Raslova, H., Courtoy, P.J., Choong, M.L., Plo, I., Vainchenker, W.,

Kralovics, R., Constantinescu, S.N. (2016). Thrombopoietin receptor activation by myeloproliferative neoplasm associated calreticulin mutants. *Blood*, 127(10), 1325–1335. <https://doi.org/10.1182/blood-2015-11-681932>.

Chagraoui, H., Wendling, F., Vainchenker, W. (2006). Pathogenesis of myelofibrosis with myeloid metaplasia: Insight from mouse models. *Best Practice & Research Clinical Haematology*, 19(3), 399–412. <https://doi.org/10.1016/j.beha.2005.07.002>.

Chen, K., & Shih, A. H. (2021). Murine modeling of myeloproliferative neoplasms. *Hematology/Oncology Clinics of North America*, 35(2), 253–265. <https://doi.org/10.1016/j.hoc.2020.11.007>.

Cheng, T., Rodrigues, N., Dombkowski, D., Stier, S., Scadden, D.T. (2000). Stem cell repopulation efficiency but not pool size is governed by p27kip1. *Nature Medicine*, 6(11), 1235–1240. <https://doi.org/10.1038/81335>.

Chlon, T.M., Crispino, J.D. (2012). Combinatorial regulation of tissue specification by GATA and FOG factors. *Development*, 139(21), 3905–3916. <https://doi.org/10.1242/dev.080440>.

Chorzalska, A., Morgan, J., Ahsan, N., Treaba, D. O., Olszewski, A. J., Petersen, M., Kingston, N., Cheng, Y., Lombardo, K., Schorl, C., Yu, X., Zini, R., Pacilli, A., Tepper, A., Coburn, J., Hryniewicz-Jankowska, A., Zhao, T. C., Oancea, E., Reagan, J. L., Liang, O., Kotula, L., Quesenberry, P.J., Gruppuso, P.A., Manfredini, R., Vannucchi, A.M., Dubielecka, P.M. (2018). Bone marrow-specific loss of ABI-1 induces myeloproliferative neoplasm with features resembling human myelofibrosis. *Blood*, 132(19), 2053–2066. <https://doi.org/10.1182/blood-2018-05-848408>.

Clark, B. R., Keating, A. (1995). Biology of bone marrow stroma. *Annals of the New York Academy of Sciences*, 770(1 Bone Marrow T), 70–78. <https://doi.org/10.1111/j.1749-6632.1995.tb31044.x>.

Corey, S.J., Jha, J., McCart, E.A., Rittase, W.B., George, J., Mattapallil, J.J., Mehta, H., Ognoon, M., Bylicky, M.A., Summers, T.A., Day, R.M. (2018). Captopril mitigates splenomegaly and myelofibrosis in the *Gata1*^{low} murine model of myelofibrosis. *Journal of Cellular and Molecular Medicine*, 22(9), 4274–4282. <https://doi.org/10.1111/jcmm.13710>.

Crispino, J.D., Horwitz, M.S. (2017). GATA factor mutations in hematologic disease. *Blood*, 129(15), 2103–2110. <https://doi.org/10.1182/blood-2016-09-687889>.

De Sauvage, F.J., Hass, P.E., Spencer, S.D., Malloy, B.E., Gurney, A.L., Spencer, S.A., Darbonne, W.C., Henzel, W.J., Wong, S.C., Kuang, W.J. (1994). Stimulation of megakaryocytopoiesis and thrombopoiesis by the c-Mpl ligand. *Nature*, 369(6481), 533–538. <https://doi.org/10.1038/369533a0>.

Deadmond, M.A., Smith-Gagen, J.A. (2015). Changing incidence of myeloproliferative neoplasms: trends and subgroup risk profiles in the USA, 1973-2011. *Journal of Cancer Research and Clinical Oncology*, 141(12), 2131–2138. <https://doi.org/10.1007/s00432-015-1983-5>.

Dongre, A., Weinberg, R.A. (2019). New insights into the mechanisms of epithelial–mesenchymal transition and implications for cancer. *Nature Reviews Molecular Cell Biology*, 20(2), 69–84. <https://doi.org/10.1038/s41580-018-0080-4>.

Elf, S., Abdelfattah, N.S., Chen, E., Perales-Patón, J., Rosen, E. A., Ko, A., Peisker, F., Florescu, N., Giannini, S., Wolach, O., Morgan, E.A., Tothova, Z., Losman, J.A., Schneider, R.K., Al-Shahrour, F., Mullally, A. (2016). Mutant calreticulin requires both its mutant c-terminus and the thrombopoietin receptor for oncogenic transformation. *Cancer Discovery*, 6(4), 368–381. <https://doi.org/10.1158/2159-8290.CD-15-1434>.

Eliades, A., Papadantonakis, N., Bhupatiraju, A., Burridge, K.A., Johnston-Cox, H.A., Migliaccio, A.R., Crispino, J.D., Lucero, H.A., Trackman, P.C., Ravid, K. (2011). Control of megakaryocyte expansion and bone marrow fibrosis by lysyl oxidase. *Journal of Biological Chemistry*, 286(31), 27630–27638. <https://doi.org/10.1074/jbc.M111.243113>.

Emadi, S., Clay, D., Desterke, C., Guerton, B., Maquarre, E., Jasmin, C. (2005). IL-8 and its CXCR1 and CXCR2 receptors participate in the control of megakaryocytic proliferation, differentiation, and ploidy in myeloid metaplasia with myelofibrosis. *Blood*, 105(2), 464–473. <https://doi.org/10.1182/blood-2003-12-4415>.

Gangat, N., Tefferi, A. (2020). Myelofibrosis biology and contemporary management. *British Journal of Haematology*. <https://doi.org/10.1111/bjh.16576>.

Gao, J., Chen, Y.H., Peterson, L.A.C. (2015). GATA family transcriptional factors: Emerging suspects in hematologic disorders. In *Experimental Hematology and Oncology* (Vol. 4, Issue 1). BioMed Central Ltd. <https://doi.org/10.1186/s40164-015-0024-z>.

Garmezzy, B., Schaefer, J.K., Mercer, J., Talpaz, M. (2021). A provider’s guide to primary myelofibrosis: pathophysiology, diagnosis, and management. *Blood Reviews*, 45, 100691. <https://doi.org/10.1016/j.blre.2020.100691>.

Gömöri, G. (1937). Silver impregnation of reticulum in paraffin sections. *The American Journal of Pathology*, 13(6), 993-1002.5.

Griesshammer, M., Hornkohl, A., Nichol, J. L., Hecht, T., Raghavachar, A., Heimpel, H., Schrezenmeier, H. (1998). High levels of thrombopoietin in sera of patients with essential thrombocythemia: cause or consequence of abnormal platelet production? *Annals of Hematology*, 77(5), 211–215. <https://doi.org/10.1007/s002770050445>.

Grinfeld, J., Nangalia, J., Green, A. R. (2017). Molecular determinants of pathogenesis and clinical phenotype in myeloproliferative neoplasms. *Haematologica*, 102(1), 7–17. <https://doi.org/10.3324/haematol.2014.113845>.

Gurbuxani, S., Vyas, P., Crispino, J.D. (2004). Recent insights into the mechanisms of myeloid leukemogenesis in Down syndrome. *Blood*, 103(2), 399–406. <https://doi.org/10.1182/blood-2003-05-1556>.

Haas, S., Hansson, J., Klimmeck, D., Loeffler, D., Velten, L., Uckelmann, H., Wurzer, S., Prendergast, Á. M., Schnell, A., Hexel, K., Santarella-Mellwig, R., Blaszkiewicz, S., Kuck, A., Geiger, H., Milsom, M.D., Steinmetz, L.M., Schroeder, T., Trumpp, A., Krijgsveld, J, Essers, M.A.G. (2015). Inflammation-induced emergency megakaryopoiesis driven by hematopoietic stem cell-like megakaryocyte progenitors. *Cell Stem Cell*, 17(4), 422–434. <https://doi.org/10.1016/j.stem.2015.07.007>.

- Hann, I.M., Evans, D.I., Marsden, H.B., Jones, P.M., Palmer, M.K. (1978). Bone marrow fibrosis in acute lymphoblastic leukaemia of childhood. *Journal of Clinical Pathology*, 31(4), 313–315. <https://doi.org/10.1136/jcp.31.4.313>.
- Hashimoto, S., Yoda, M., Yamada, M., Yanai, N., Kawashima, T., Motoyoshi, K. (1996). Macrophage colony-stimulating factor induces interleukin-8 production in human monocytes. *Experimental Hematology*, 24(2), 123–128. <http://europepmc.org/abstract/MED/8641333>.
- Herbertz, S., Sawyer, J.S., Stauber, A.J., Gueorguieva, I., Driscoll, K.E., Estrem, S.T., Cleverly, A.L., Desai, D., Guba, S.C., Benhadji, K.A., Slapak, C.A., Lahn, M.M. (2015). Clinical development of galunisertib (Ly2157299 monohydrate), a small molecule inhibitor of transforming growth factor-beta signaling pathway. In *Drug Design, Development and Therapy* (Vol. 9, pp. 4479–4499). Dove Medical Press Ltd. <https://doi.org/10.2147/DDDT.S86621>.
- Hofbauer, L.C. (1999). Osteoprotegerin ligand and osteoprotegerin: novel implications for osteoclast biology and bone metabolism. *European Journal of Endocrinology*, 141(3), 195–210. <https://doi.org/10.1530/eje.0.1410195>.
- Imai, M., Araki, M., Komatsu, N. (2017). Somatic mutations of calreticulin in myeloproliferative neoplasms. *International Journal of Hematology*, 105(6), 743–747. <https://doi.org/10.1007/s12185-017-2246-9>.
- Iwasaki, H., Mizuno, S., Wells, R. A., Cantor, A. B., Watanabe, S., Akashi, K. (2003). GATA-1 converts lymphoid and myelomonocytic progenitors into the megakaryocyte/erythrocyte lineages. *Immunity*, 19(3), 451–462. [https://doi.org/10.1016/S1074-7613\(03\)00242-5](https://doi.org/10.1016/S1074-7613(03)00242-5).
- James, C., Ugo, V., Le Couédic, J.-P., Staerk, J., Delhommeau, F., Lacout, C., Garçon, L., Raslova, H., Berger, R., Bennaceur-Griscelli, A., Villeval, J.L., Constantinescu, S.N., Casadevall, N., Vainchenker, W. (2005). A unique clonal JAK2 mutation leading to constitutive signalling causes polycythaemia vera. *Nature*, 434(7037), 1144–1148. <https://doi.org/10.1038/nature03546>.
- Kacena, M.A., Shivdasani, R.A., Wilson, K., Xi, Y., Troiano, N., Nazarian, A., Gundberg, C. M., Bouxsein, M.L., Lorenzo, J.A., Horowitz, M.C. (2004). Megakaryocyte-osteoblast interaction revealed in mice deficient in transcription factors GATA-1 and NF-E2. *Journal of Bone and Mineral Research*, 19(4), 652–660. <https://doi.org/10.1359/JBMR.0301254>.
- Kakumitsu, H., Kamezaki, K., Shimoda, K., Karube, K., Haro, T., Numata, A., Shide, K., Matsuda, T., Oshima, K., Harada, M. (2005). Transgenic mice overexpressing murine thrombopoietin develop myelofibrosis and osteosclerosis. *Leukemia Research*, 29(7), 761–769. <https://doi.org/10.1016/j.leukres.2004.12.009>.
- Kaplanski, G., Farnarier, C., Kaplanski, S., Porat, R., Shapiro, L., Bongrand, P., Dinarello, C. A. (1994). Interleukin-1 induces interleukin-8 secretion from endothelial cells by a juxtacrine mechanism. *Blood*, 84(12), 4242–4248. <http://europepmc.org/abstract/MED/7994038>.
- Kirsammer, G., Jilani, S., Liu, H., Davis, E., Gurbuxani, S., Le Beau, M.M., Crispino, J.D. (2008). Highly penetrant myeloproliferative disease in the Ts65Dn mouse model of Down syndrome. *Blood*, 111(2), 767–775. <https://doi.org/10.1182/blood-2007-04-085670>.

- Klampfl, T., Gisslinger, H., Harutyunyan, A.S., Nivarthi, H., Rumi, E., Milosevic, J.D., Them, N.C.C., Berg, T., Gisslinger, B., Pietra, D., Chen, D., Vladimer, G.I., Bagienski, K., Milanesi, C., Casetti, I.C., Sant'Antonio, E., Ferretti, V., Elena, C., Schischlik, F., Cleary, C., Six, M., Schalling, M., Schönegger, A., Bock, C., Malcovati, L., Pascutto, C., Superti-Furga, G., Cazzola, M., Kralovics, R. (2013). Somatic mutations of calreticulin in myeloproliferative neoplasms. *New England Journal of Medicine*, 369(25), 2379–2390. <https://doi.org/10.1056/NEJMoa1311347>.
- Kleppe, M., Kwak, M., Koppikar, P., Riester, M., Keller, M., Bastian, L., Hricik, T., Bhagwat, N., McKenney, A. S., Papalexi, E., Abdel-Wahab, O., Rampal, R., Marubayashi, S., Chen, J. J., Romanet, V., Fridman, J.S., Bromberg, J., Teruya-Feldstein, J., Murakami, M., Radimerski, T., Michor, F., Fan, R., Levine, R.L. (2015). JAK–STAT pathway activation in malignant and nonmalignant cells contributes to mpn pathogenesis and therapeutic response. *Cancer Discovery*, 5(3), 316–331. <https://doi.org/10.1158/2159-8290.CD-14-0736>.
- Koch, C.A., Li, C.Y., Mesa, R.A., Tefferi, A. (2003). Non-hepatosplenic extramedullary hematopoiesis: associated diseases, pathology, clinical course, and treatment. *Mayo Clinic Proceedings*, 78(10), 1223–1233. <https://doi.org/10.4065/78.10.1223>.
- Koppikar, P., Abdel-Wahab, O., Hedvat, C., Marubayashi, S., Patel, J., Goel, A., Kucine, N., Gardner, J.R., Combs, A.P., Vaddi, K., Haley, P.J., Burn, T.C., Rupar, M., Bromberg, J.F., Heaney, M.L., de Stanchina, E., Fridman, J.S., Levine, R.L. (2010). Efficacy of the JAK2 inhibitor INCB16562 in a murine model of MPL^{W515L}-induced thrombocytosis and myelofibrosis. *Blood*, 115(14), 2919–2927. <https://doi.org/10.1182/blood-2009-04-218842>.
- Kozma, G.T., Martelli, F., Verrucci, M., Gutiérrez, L., Migliaccio, G., Sanchez, M., Alfani, E., Philipsen, S., Migliaccio, A.R. (2010). Dynamic regulation of Gata1 expression during the maturation of conventional dendritic cells. *Experimental Hematology*, 38(6), 489-503.e1. <https://doi.org/10.1016/j.exphem.2010.03.006>.
- Kralovics, R., Passamonti, F., Buser, A. S., Teo, S.S., Tiedt, R., Passweg, J.R., Tichelli, A., Cazzola, M., Skoda, R.C. (2005). A gain-of-function mutation of JAK2 in myeloproliferative disorders. *New England Journal of Medicine*, 352(17), 1779–1790. <https://doi.org/10.1056/NEJMoa051113>.
- Kuter, D.J., Bain, B., Mufti, G., Bagg, A., Hasserjian, R.P. (2007). Bone marrow fibrosis: Pathophysiology and clinical significance of increased bone marrow stromal fibres. In *British Journal of Haematology* (Vol. 139, Issue 3, pp. 351–362). <https://doi.org/10.1111/j.1365-2141.2007.06807.x>.
- Lacout, C., Pisani, D.F., Tulliez, M., Gachelin, F.M., Vainchenker, W., Villeval, J.L. (2006). JAK2^{V617F} expression in murine hematopoietic cells leads to MPD mimicking human PV with secondary myelofibrosis. *Blood*, 108(5), 1652–1660. <https://doi.org/10.1182/blood-2006-02-002030>.
- Lamprecht Tratar, U., Horvat, S., Cemazar, M. (2018). Transgenic mouse models in cancer research. *Frontiers in Oncology*, 8. <https://doi.org/10.3389/fonc.2018.00268>.
- Lanikova, L., Babosova, O., Prchal, J.T. (2019). Experimental Modeling of Myeloproliferative Neoplasms. *Genes*, 10(10). <https://doi.org/10.3390/genes10100813>.

- Lee, W.Y., Weinberg, O.K., Pinkus, G.S. (2017). GATA1 is a sensitive and specific nuclear marker for erythroid and megakaryocytic lineages. *American Journal of Clinical Pathology*, 147(4), 420–426. <https://doi.org/10.1093/ajcp/aqx018>.
- Leiva, O., Ng, S.K., Matsuura, S., Chitalia, V., Lucero, H., Findlay, A., Turner, C., Jarolimek, W., Ravid, K. (2019). Novel lysyl oxidase inhibitors attenuate hallmarks of primary myelofibrosis in mice. *International Journal of Hematology*, 110(6), 699–708. <https://doi.org/10.1007/s12185-019-02751-6>.
- Levine, R.L., Wadleigh, M., Cools, J., Ebert, B.L., Wernig, G., Huntly, B.J.P., Boggon, T.J., Wlodarska, I., Clark, J.J., Moore, S., Adelsperger, J., Koo, S., Lee, J.C., Gabriel, S., Mercher, T., D'Andrea, A., Fröhling, S., Döhner, K., Marynen, P., Vandenberghe, P., Mesa, R.A., Tefferi, A., Griffin, J.D., Eck, M.J., Sellers, W.R., Meyerson, M., Golub, T.R., Lee, S.J., Gilliland, D.G. (2005). Activating mutation in the tyrosine kinase JAK2 in polycythemia vera, essential thrombocythemia, and myeloid metaplasia with myelofibrosis. *Cancer Cell*, 7(4), 387–397. <https://doi.org/10.1016/j.ccr.2005.03.023>.
- Li, J., Prins, D., Park, H.J., Grinfeld, J., Gonzalez-Arias, C., Loughran, S., Dovey, O.M., Klampfl, T., Bennett, C., Hamilton, T.L., Pask, D.C., Sneade, R., Williams, M., Aungier, J., Ghevaert, C., Vassiliou, G.S., Kent, D.G., Green, A.R. (2018). Mutant calreticulin knockin mice develop thrombocytosis and myelofibrosis without a stem cell self-renewal advantage. *Blood*, 131(6), 649–661. <https://doi.org/10.1182/blood-2017-09-806356>.
- Li, J., Spensberger, D., Ahn, J.S., Anand, S., Beer, P. A., Ghevaert, C., Chen, E., Forrai, A., Scott, L.M., Ferreira, R., Campbell, P.J., Watson, S.P., Liu, P., Erber, W.N., Huntly, B.J.P., Ottersbach, K., Green, A.R. (2010). JAK2^{V617F} impairs hematopoietic stem cell function in a conditional knock-in mouse model of JAK2^{V617F}-positive essential thrombocythemia. *Blood*, 116(9), 1528–1538. <https://doi.org/10.1182/blood-2009-12-259747>.
- Lin, C., Kaushansky, K., Zhan, H. (2016). JAK2^{V617F}-mutant vascular niche contributes to JAK2^{V617F} clonal expansion in myeloproliferative neoplasms. *Blood Cells, Molecules & Diseases*, 62, 42–48. <https://doi.org/10.1016/j.bcmd.2016.09.004>.
- Ling, T., Crispino, J.D., Zingariello, M., Martelli, F., Migliaccio, A.R. (2018). GATA1 insufficiencies in primary myelofibrosis and other hematopoietic disorders: consequences for therapy. *Expert Review of Hematology*, 11(3), 169–184. <https://doi.org/10.1080/17474086.2018.1436965>.
- Lu, X., Levine, R., Tong, W., Wernig, G., Pikman, Y., Zarnegar, S., Gilliland, D.G., Lodish, H. (2005). Expression of a homodimeric type I cytokine receptor is required for JAK2^{V617F}-mediated transformation. *PNAS*, 102(52), 18962–18967. <https://doi.org/10.1073/pnas.0509714102>.
- Manoharan, A., Horsley, R., Pitney, W.R. (1979). The reticulin content of bone marrow in acute leukaemia in adults. *British Journal of Haematology*, 43(2), 185–190. <https://doi.org/10.1111/j.1365-2141.1979.tb03740.x>.
- Marty, C., Lacout, C., Martin, A., Hasan, S., Jacquot, S., Birling, M.C., Vainchenker, W., Villeval, J.L. (2010). Myeloproliferative neoplasm induced by constitutive expression of JAK2V617F in knock-in mice. *Blood*, 116(5), 783–787. <https://doi.org/10.1182/blood-2009-12-257063>.

Marty, C., Pecquet, C., Nivarthi, H., El-Khoury, M., Chachoua, I., Tulliez, M., Villeval, J.L., Raslova, H., Kralovics, R., Constantinescu, S.N., Plo, I., Vainchenker, W. (2016). Calreticulin mutants in mice induce an MPL-dependent thrombocytosis with frequent progression to myelofibrosis. *Blood*, 127(10), 1317–1324. <https://doi.org/10.1182/blood-2015-11-679571>.

Mascarenhas, J., Kosiorek, H.E., Bhave, R., Palmer, J.M., Kuykendall, A.T., Mesa, R.A., Rampal, R., Gerds, A.T., Yacoub, A., Pettit, K.M., Talpaz, M., Komrokji, R.S., Kremyanskaya, M., Gonzalez, A., Fabris, F., Sandy, L., Johnson, K., Dougherty, M., MCGovern, E., Hoffman, R. (2021). Treatment of myelofibrosis patients with the TGF- β 1/3 inhibitor AVID200 (MPN-RC 118) induces a profound effect on platelet production. *Blood*, 138(Supplement 1), 142. <https://doi.org/10.1182/blood-2021-148995>.

Massagué, J. (2008). TGF β in Cancer. *Cell*, 134(2), 215–230. <https://doi.org/10.1016/j.cell.2008.07.001>.

Matsushima, K., Oppenheim, J.J. (1989). Interleukin 8 and MCAF: novel inflammatory cytokines inducible by IL1 and TNF. *Cytokine*, 1(1), 2–13. [https://doi.org/https://doi.org/10.1016/1043-4666\(89\)91043-0](https://doi.org/https://doi.org/10.1016/1043-4666(89)91043-0).

Mcdevitt, M. A., Fujiwara, Y., Shivdasani, R. A., Orkin, S.H. (1997). An upstream, DNase I hypersensitive region of the hematopoietic-expressed transcription factor GATA-1 gene confers developmental specificity in transgenic mice. *Proceedings of the National Academy of Sciences of the United States of America*, 94(15), 7976–7981. <https://doi.org/10.1073/pnas.94.15.7976>.

McDevitt, M.A., Shivdasani, R.A., Fujiwara, Y., Yang, H., Orkin, S.H. (1997). A “knockdown” mutation created by cis-element gene targeting reveals the dependence of erythroid cell maturation on the level of transcription factor GATA-1. *Proceedings of the National Academy of Sciences*, 94(13), 6781–6785. <https://doi.org/10.1073/pnas.94.13.6781>.

Mehta, J., Wang, H., Iqbal, S. U., Mesa, R. (2014). Epidemiology of myeloproliferative neoplasms in the United States. *Leukemia & Lymphoma*, 55(3), 595–600. <https://doi.org/10.3109/10428194.2013.813500>.

Melo-Cardenas, J., Migliaccio, A.R., Crispino, J. D. (2021). The role of megakaryocytes in myelofibrosis. *Hematology/Oncology Clinics of North America*, 35(2), 191–203. <https://doi.org/10.1016/j.hoc.2020.11.004>.

Meng, X.M., Nikolic-Paterson, D.J., Lan, H.Y. (2016). TGF- β : the master regulator of fibrosis. *Nature Reviews. Nephrology*, 12(6), 325–338. <https://doi.org/10.1038/nrneph.2016.48>.

Mesa, R.A., Li, C.Y., Ketterling, R.P., Schroeder, G.S., Knudson, R.A., Tefferi, A. (2005). Leukemic transformation in myelofibrosis with myeloid metaplasia: a single-institution experience with 91 cases. *Blood*, 105(3), 973–977. <https://doi.org/10.1182/blood-2004-07-2864>.

Messina, G., Blasi, C., Anna, S., Rocca, L., Pompili, M., Calconi, A., Grossi, M. (2005). p27Kip1 acts downstream of N-cadherin-mediated cell adhesion to promote myogenesis beyond cell cycle regulation. *Molecular Biology of the Cell*, 16, 1469–1480. <https://doi.org/10.1091/mbc.E04>.

Migliaccio, A.R., Martelli, F., Verrucci, M., Sanchez, M., Valeri, M., Migliaccio, G., Vannucchi, A.M., Zingariello, M., Di Baldassarre, A., Ghinassi, B., Rana, R. A., Van Hensbergen, Y., Fibbe, W.E. (2009). Gata1 expression driven by the alternative HS2 enhancer in the spleen rescues the hematopoietic failure induced by

- the hypomorphic *Gata1*^{low} mutation. *Blood*, 114(10), 2107–2120. <https://doi.org/10.1182/blood-2009-03-211680>.
- Migliaccio, A.R., Migliaccio, G., Ashihara, E., Moroni, E., Giglioni, B., Ottolenghi, S. (1996). Erythroid-specific activation of the distal (testis) promoter of GATA1 during differentiation of purified normal murine hematopoietic stem cells. *Acta Haematologica*, 95(3–4), 229–235. <https://doi.org/10.1159/000203883>.
- Migliaccio, A.R., Rana, R.A., Sanchez, M., Lorenzini, R., Centurione, L., Bianchi, L., Vannucchi, A.M., Migliaccio, G., Orkin, S.H. (2003). GATA-1 as a regulator of mast cell differentiation revealed by the phenotype of the *Gata1*^{low} Mouse Mutant. *Journal of Experimental Medicine*, 197(3), 281–296. <https://doi.org/10.1084/jem.20021149>.
- Mondet, J., Hussein, K., Mossuz, P. (2015). Circulating cytokine levels as markers of inflammation in philadelphia negative myeloproliferative neoplasms: diagnostic and prognostic interest. *Mediators of Inflammation*, 2015, 670580. <https://doi.org/10.1155/2015/670580>.
- Mughal, T. I., Vaddi, K., Sarlis, N. J., Verstovsek, S. (2014). Myelofibrosis-associated complications: pathogenesis, clinical manifestations, and effects on outcomes. *International Journal of General Medicine*, 7, 89–101. <https://doi.org/10.2147/IJGM.S51800>.
- Mullally, A., Lane, S. W., Ball, B., Megerdichian, C., Okabe, R., Al-Shahrour, F., Paktinat, M., Haydu, J.E., Housman, E., Lord, A.M., Wernig, G., Kharas, M.G., Mercher, T., Kutok, J.L., Gilliland, D.G., Ebert, B.L. (2010). Physiological JAK2V^{617F} expression causes a lethal myeloproliferative neoplasm with differential effects on hematopoietic stem and progenitor cells. *Cancer Cell*, 17(6), 584–596. <https://doi.org/10.1016/j.ccr.2010.05.015>.
- Nadrous, H.F., Krowka, M.J., McClure, R.F., Tefferi, A., Lim, K.G. (2004). Agnogenic myeloid metaplasia with pleural extramedullary leukemic transformation. *Leukemia & Lymphoma*, 45(4), 815–818. <https://doi.org/10.1080/1042819032000141329>.
- Nangalia, J., Massie, C.E., Baxter, E.J., Nice, F.L., Gundem, G., Wedge, D.C., Avezov, E., Li, J., Kollmann, K., Kent, D.G., Aziz, A., Godfrey, A.L., Hinton, J., Martincorena, I., Van Loo, P., Jones, A.V, Guglielmelli, P., Tarpey, P., Harding, H. P., Fitzpatrick, J.D., Goudie, C.T., Ortmann, C.A., Loughran, S.J., Raine, K., Jones, D.R., Butler, A.P., Teague, J.W., O'Meara, S., McLaren, S., Bianchi, M., Silber, Y., Dimitropoulou, D., Bloxham, D., Mudie, L., Maddison, M., Robinson, B., Keohane, C., Maclean, C., Hill, K., Orchard, K., Tauro, S., Du, M.Q., Greaves, M., Bowen, D., Huntly, B.J.P., Harrison, C.N., Cross, N.C.P., Ron, D., Vannucchi, A.M., Papaemmanuil, E., Campbell, P.J., Green, A.R. (2013). Somatic CALR mutations in myeloproliferative neoplasms with nonmutated JAK2. *New England Journal of Medicine*, 369(25), 2391–2405. <https://doi.org/10.1056/NEJMoa1312542>.
- Nguyen, T.K., Morse, S.J., Fleischman, A.G. (2016). Transduction-Transplantation mouse model of myeloproliferative neoplasm. *Journal of Visualized Experiments*, 118. <https://doi.org/10.3791/54624>.

- O'Malley, D.P., Sen, J., Juliar, B.E., Orazi, A. (2005). Evaluation of stroma in human immunodeficiency virus/acquired immunodeficiency syndrome-affected bone marrows and correlation with CD4 counts. *Archives of Pathology & Laboratory Medicine*, 129(9), 1137–1140. <https://doi.org/10.5858/2005-129-1137-EOSIHI>.
- Ouellette, D.R. (2005). The impact of anemia in patients with respiratory failure. *Chest*, 128(5 Suppl 2), 576S–582S. https://doi.org/10.1378/chest.128.5_suppl_2.576S.
- Pardanani, A.D., Levine, R.L., Lasho, T., Pikman, Y., Mesa, R.A., Wadleigh, M., Steensma, D.P., Elliott, M.A., Wolanskyj, A.P., Hogan, W.J., McClure, R.F., Litzow, M.R., Gilliland, D.G., Tefferi, A. (2006). MPL515 mutations in myeloproliferative and other myeloid disorders: a study of 1182 patients. *Blood*, 108(10), 3472–3476. <https://doi.org/10.1182/blood-2006-04-018879>.
- Pardanani, A., Tefferi, A., Guglielmelli, P., Bogani, C., Bartalucci, N., Rodríguez, J., Extremera, S., Pérez, I., Alfaro, V., Vannucchi, A.M. (2015). Evaluation of plitidepsin in patients with primary myelofibrosis and post polycythemia vera/essential thrombocythemia myelofibrosis: Results of preclinical studies and a phase II clinical trial. *Blood Cancer Journal*, 5(3). <https://doi.org/10.1038/bcj.2015.5>.
- Pettit, K., Odenike, O. (2017). Novel therapies for myelofibrosis. *Current Hematologic Malignancy Reports*, 12(6), 611–624. <https://doi.org/10.1007/s11899-017-0403-0>.
- Pietra, D., Rumi, E., Ferretti, V.V., Di Buduo, C.A., Milanese, C., Cavalloni, C., Sant'Antonio, E., Abbonante, V., Moccia, F., Casetti, I.C., Bellini, M., Renna, M.C., Roncoroni, E., Fugazza, E., Astori, C., Boveri, E., Rosti, V., Barosi, G., Balduini, A., Cazzola, M. (2016). Differential clinical effects of different mutation subtypes in CALR-mutant myeloproliferative neoplasms. *Leukemia*, 30(2), 431–438. <https://doi.org/10.1038/leu.2015.277>.
- Pikman, Y., Lee, B. H., Mercher, T., McDowell, E., Ebert, B. L., Gozo, M., Cuker, A., Wernig, G., Moore, S., Galinsky, I., DeAngelo, D.J., Clark, J.J., Lee, S.J., Golub, T.R., Wadleigh, M., Gilliland, D.G., Levine, R.L. (2006). MPL^{W515L} is a novel somatic activating mutation in myelofibrosis with myeloid metaplasia. *PLoS Medicine*, 3(7), e270. <https://doi.org/10.1371/journal.pmed.0030270>.
- Pitsilos, S., Hunt, J., Mohler, E. R., Prabhakar, A.M., Poncz, M., Dawicki, J., Khalapyan, T. Z., Wolfe, M.L., Fairman, R., Mitchell, M., Carpenter, J., Golden, M.A., Cines, D.B., Sachais, B.S. (2003). Platelet factor 4 localization in carotid atherosclerotic plaques: correlation with clinical parameters. *Thrombosis and Haemostasis*, 90(6), 1112–1120. <https://doi.org/10.1160/TH03-02-0069>.
- Prentice, C.R. (1985). Acquired coagulation disorders. *Clinics in Haematology*, 14(2), 413–442.
- Puchtler, H., Waldrop, F.S. (1978). Silver impregnation methods for reticulum fibers and reticulin: A re-investigation of their origins and specificity. *Histochemistry*, 57(3), 177–187. <https://doi.org/10.1007/BF00492078>.
- Reeder, T.L., Bailey, R.J., Dewald, G.W., Tefferi, A. (2003). Both B and T lymphocytes may be clonally involved in myelofibrosis with myeloid metaplasia. *Blood*, 101(5), 1981–1983. <https://doi.org/10.1182/blood-2002-07-2341>.

- Riches, P.L., McRorie, E., Fraser, W.D., Determann, C., Van't Hof, R., Ralston, S.H. (2009). Osteoporosis associated with neutralizing autoantibodies against osteoprotegerin. *The New England Journal of Medicine*, 361(15), 1459–1465. <https://doi.org/10.1056/NEJMoa0810925>.
- Roizen, N.J., Amarose, A.P. (1993). Hematologic abnormalities in children with Down syndrome. *American Journal of Medical Genetics*, 46(5), 510–512. <https://doi.org/10.1002/ajmg.1320460509>.
- Schmitt, A., Drouin, A., Massé, J.M., Guichard, J., Shagraoui, H., Cramer, E.M. (2002). Polymorphonuclear neutrophil and megakaryocyte mutual involvement in myelofibrosis pathogenesis. *Leukemia & Lymphoma*, 43(4), 719–724. <https://doi.org/10.1080/10428190290016809>.
- Schmitt, A., Jouault, H., Guichard, J., Wendling, F., Drouin, A., Cramer, E.M. (2000). Pathologic interaction between megakaryocytes and polymorphonuclear leukocytes in myelofibrosis. *Blood*, 96(4), 1342–1347. <http://www.ncbi.nlm.nih.gov/pubmed/10942376>.
- Schneider, R.K., Mullally, A., Dugourd, A., Peisker, F., Hoogenboezem, R., Van Strien, P. M.H., Bindels, E.M., Heckl, D., Büsche, G., Fleck, D., Müller-Newen, G., Wongboonsin, J., Ventura Ferreira, M., Puelles, V. G., Saez-Rodriguez, J., Ebert, B.L., Humphreys, B.D., Kramann, R. (2017). Gli1+ mesenchymal stromal cells are a key driver of bone marrow fibrosis and an important cellular therapeutic target. *Cell Stem Cell*, 20(6), 785–800.e8. <https://doi.org/10.1016/j.stem.2017.03.008>.
- Shide, K., Kameda, T., Yamaji, T., Sekine, M., Inada, N., Kamiunten, A., Akizuki, K., Nakamura, K., Hidaka, T., Kubuki, Y., Shimoda, H., Kitanaka, A., Honda, A., Sawaguchi, A., Abe, H., Miike, T., Iwakiri, H., Tahara, Y., Sueta, M., Hasuike, S., Yamamoto, S., Nagata, K., Shimoda, K. (2017). Calreticulin mutant mice develop essential thrombocythemia that is ameliorated by the JAK inhibitor ruxolitinib. *Leukemia*, 31(5), 1136–1144. <https://doi.org/10.1038/leu.2016.308>.
- Shimizu, R., Kuroha, T., Ohneda, O., Pan, X., Ohneda, K., Takahashi, S., Philipsen, S., Yamamoto, M. (2004). Leukemogenesis caused by incapacitated GATA-1 function. *Molecular and Cellular Biology*, 24(24), 10814–10825. <https://doi.org/10.1128/MCB.24.24.10814-10825.2004>.
- Shivdasani, R.A., Fujiwara, Y., McDevitt, M.A., Orkin, S.H. (1997). A lineage-selective knockout establishes the critical role of transcription factor GATA-1 in megakaryocyte growth and platelet development. *The EMBO Journal*, 16(13), 3965–3973. <https://doi.org/10.1093/emboj/16.13.3965>.
- Simonet, W. S., Lacey, D. L., Dunstan, C. R., Kelley, M., Chang, M. S., Lüthy, R., Nguyen, H. Q., Wooden, S., Bennett, L., Boone, T., Shimamoto, G., DeRose, M., Elliott, R., Colombero, A., Tan, H. L., Trail, G., Sullivan, J., Davy, E., Bucay, N., Renshaw-Gegg, L., Hughes, T.M., Hill, D., Pattison, W., Campbell, P., Sander, S., Van, G., Tarpley, J., Derby, P., Lee, R., Boyle, W.J. (1997). Osteoprotegerin: a novel secreted protein involved in the regulation of bone density. *Cell*, 89(2), 309–319. [https://doi.org/10.1016/s0092-8674\(00\)80209-3](https://doi.org/10.1016/s0092-8674(00)80209-3).
- Singh, M. K., Li, Y., Li, S., Cobb, R. M., Zhou, D., Lu, M.M., Epstein, J.A., Morrissey, E.E., Gruber, P.J. (2010). Gata4 and Gata5 cooperatively regulate cardiac myocyte proliferation in mice. *Journal of Biological Chemistry*, 285(3), 1765–1772. <https://doi.org/10.1074/jbc.M109.038539>.

- Skoda, R.C., Duek, A., Grisouard, J. (2015). Pathogenesis of myeloproliferative neoplasms. *Experimental Hematology*, 43(8), 599–608. <https://doi.org/10.1016/j.exphem.2015.06.007>.
- Song, J., Hussaini, M., Zhang, H., Shao, H., Qin, D., Zhang, X., Ma, Z., Hussain Naqvi, S. M., Zhang, L., Moscinski, L. C. (2017). Comparison of the mutational profiles of primary myelofibrosis, polycythemia vera, and essential thrombocytosis. *American Journal of Clinical Pathology*, 147(5), 444–452. <https://doi.org/10.1093/ajcp/aqw222>.
- Spangrude, G.J., Lewandowski, D., Martelli, F., Marra, M., Zingariello, M., Sancillo, L., Rana, R.A., Migliaccio, A.R. (2016). P-Selectin sustains extramedullary hematopoiesis in the *Gata1*^{low} model of myelofibrosis. *Stem Cells*, 34(1), 67–82. <https://doi.org/10.1002/stem.2229>.
- Srouf, S.A., Devesa, S.S., Morton, L.M., Check, D.P., Curtis, R.E., Linet, M.S., Dore, G.M. (2016). Incidence and patient survival of myeloproliferative neoplasms and myelodysplastic/myeloproliferative neoplasms in the United States, 2001-12. *British Journal of Haematology*, 174(3), 382–396. <https://doi.org/10.1111/bjh.14061>.
- Suzuki, M., Kobayashi-Osaki, M., Tsutsumi, S., Pan, X., Ohmori, S., Takai, J., Moriguchi, T., Ohneda, O., Ohneda, K., Shimizu, R., Kanki, Y., Kodama, T., Aburatani, H., Yamamoto, M. (2013). GATA factor switching from GATA2 to GATA1 contributes to erythroid differentiation. *Genes to Cells*, 18(11), 921–933. <https://doi.org/10.1111/gtc.12086>.
- Takeuchi, K., Higuchi, T., Yamashita, T., Koike, K. (1999). Chemokine production by human megakaryocytes derived from cd34-positive cord blood cells. *Cytokine*, 11(6), 424–434. <https://doi.org/10.1006/cyto.1998.0455>.
- Tefferi, A. (2005). Pathogenesis of myelofibrosis with myeloid metaplasia. *Journal of Clinical Oncology: Official Journal of the American Society of Clinical Oncology*, 23(33), 8520–8530. <https://doi.org/10.1200/JCO.2004.00.9316>.
- Tefferi, A. (2021). Primary myelofibrosis: 2021 update on diagnosis, risk-stratification and management. *American Journal of Hematology*, 96(1), 145–162. <https://doi.org/10.1002/ajh.26050>.
- Tefferi, A., Vaidya, R., Caramazza, D., Finke, C., Lasho, T., Pardanani, A. (2011). Circulating interleukin (IL)-8, IL-2R, IL-12, and IL-15 levels are independently prognostic in primary myelofibrosis: a comprehensive cytokine profiling study. *Journal of Clinical Oncology*, 29(10), 1356–1363. <https://doi.org/10.1200/JCO.2010.32.9490>.
- Teman, C.J., Wilson, A.R., Perkins, S.L., Hickman, K., Prchal, J.T., Salama, M.E. (2010). Quantification of fibrosis and osteosclerosis in myeloproliferative neoplasms: A computer-assisted image study. *Leukemia Research*, 34(7), 871–876. <https://doi.org/10.1016/j.leukres.2010.01.005>.
- Terui, T., Niitsu, Y., Mahara, K., Fujisaki, Y., Urushizaki, Y., Mogi, Y., Kohgo, Y., Watanabe, N., Ogura, M., Saito, H. (1990). The production of transforming growth factor-beta in acute megakaryoblastic leukemia and its possible implications in myelofibrosis. *Blood*, 75(7), 1540.
- Thiele, J., Grashof, K., Fisher, R. (1991). Follow-up study on bone marrow reticulin fibrosis in AML. *Analytical Cellular Pathology: The Journal of the European Society for Analytical Cellular Pathology*, 3(4), 225–231.

- Thiele, J., Kvasnicka, H. M. (2006). Grade of bone marrow fibrosis is associated with relevant hematological findings—a clinicopathological study on 865 patients with chronic idiopathic myelofibrosis. *Annals of Hematology*, 85(4), 226–232. <https://doi.org/10.1007/s00277-005-0042-8>.
- Thiele, J., Kvasnicka, H.M., Facchetti, F., Franco, V., van der Walt, J., Orazi, A. (2005). European consensus on grading bone marrow fibrosis and assessment of cellularity. *Haematologica*, 90(8), 1128–1132.
- Thiele, J., Lorenzen, J., Manich, B., Kvasnicka, H.M., Zirbes, T.K., Fischer, R. (1997). Apoptosis (programmed cell death) in idiopathic (primary) osteo-/myelofibrosis: naked nuclei in megakaryopoiesis reveal features of para-apoptosis. *Acta Haematologica*, 97(3), 137–143. <https://doi.org/10.1159/000203671>.
- Tsai, F.Y., Orkin, S.H. (1997). Transcription factor GATA-2 is required for proliferation/survival of early hematopoietic cells and mast cell formation, but not for erythroid and myeloid terminal differentiation. *Blood*, 89(10), 3636–3643.
- Tsai, S.F., Martin, D.I.K., Zon, L.I., D’Andrea, A.D., Wong, G.G., Orkin, S.H. (1989). Cloning of cDNA for the major DNA-binding protein of the erythroid lineage through expression in mammalian cells. *Nature*, 339(6224), 446–451. <https://doi.org/10.1038/339446a0>.
- Vainchenker, W., Constantinescu, S.N., Plo, I. (2016). Recent advances in understanding myelofibrosis and essential thrombocythemia. *F1000Research*, 5. <https://doi.org/10.12688/f1000research.8081.1>.
- Vainchenker, W., Kralovics, R. (2017). Genetic basis and molecular pathophysiology of classical myeloproliferative neoplasms. *Blood*, 129(6), 667–679. <https://doi.org/10.1182/blood-2016-10-695940>.
- Van Bon, L., Affandi, A. J., Broen, J., Christmann, R. B., Marijnissen, R.J., Stawski, L., Farina, G. A., Stifano, G., Mathes, A.L., Cossu, M., York, M., Collins, C., Wenink, M., Huijbens, R., Hesselstrand, R., Saxne, T., DiMarzio, M., Wuttge, D., Agarwal, S. K., Radstake, T.R.D.J. (2014). Proteome-wide analysis and CXCL4 as a biomarker in systemic sclerosis. *The New England Journal of Medicine*, 370(5), 433–443. <https://doi.org/10.1056/NEJMoa1114576>.
- Vannucchi, A.M., Barbui, T., Cervantes, F., Harrison, C., Kiladjan, J.J., Kröger, N., Thiele, J., Buske, C. (2015). Philadelphia chromosome-negative chronic myeloproliferative neoplasms: ESMO Clinical Practice Guidelines for diagnosis, treatment and follow-up. *Annals of Oncology*, 26, v85–v99. <https://doi.org/10.1093/annonc/mdv203>.
- Vannucchi, A.M., Bianchi, L., Cellai, C., Paoletti, F., Carrai, V., Calzolari, A., Centurions, L., Lorenzini, R., Carta, C., Alfani, E., Sanchez, M., Migliaccio, G., Migliaccio, A. R. (2001). Accentuated response to phenylhydrazine and erythropoietin in mice genetically impaired for their GATA-1 expression (*Gata1^{low}* mice). *Blood*, 97(10), 3040–3050. <https://doi.org/10.1182/blood.V97.10.3040>.
- Vannucchi, A.M., Bianchi, L., Cellai, C., Paoletti, F., Rana, R.A., Lorenzini, R., Migliaccio, G., Migliaccio, A.R. (2002). Development of myelofibrosis in mice genetically impaired for GATA-1 expression (*Gata1^{low}* mice). *Blood*, 100(4), 1123–1132. <https://doi.org/10.1182/blood-2002-06-1913>.
- Vannucchi, A. M., Lasho, T. L., Guglielmelli, P., Biamonte, F., Pardanani, A., Pereira, A., Finke, C., Score, J., Gangat, N., Mannarelli, C., Ketterling, R. P., Rotunno, G., Knudson, R. A., Susini, M. C., Laborde, R. R.,

- Spolverini, A., Pancrazzi, A., Pieri, L., Manfredini, R., Tefferi, A. (2013). Mutations and prognosis in primary myelofibrosis. *Leukemia*, 27(9), 1861–1869. <https://doi.org/10.1038/leu.2013.119>.
- Vannucchi, A. M., Pancrazzi, A., Guglielmelli, P., Di Lollo, S., Bogani, C., Baroni, G., Bianchi, L., Migliaccio, A. R., Bosi, A., Paoletti, F. (2005). Abnormalities of GATA-1 in megakaryocytes from patients with idiopathic myelofibrosis. *American Journal of Pathology*, 167(3), 849–858. [https://doi.org/10.1016/S0002-9440\(10\)62056-1](https://doi.org/10.1016/S0002-9440(10)62056-1).
- Varricchio, L., Iancu-Rubin, C., Upadhyaya, B., Zingariello, M., Martelli, F., Verachi, P., Clementelli, C., Denis, J.F., Rahman, A.H., Tremblay, G., Mascarenhas, J., Mesa, R.A., O'Connor-McCourt, M., Migliaccio, A.R., Hoffman, R. (2021). TGF- β 1 protein trap AVID200 beneficially affects hematopoiesis and bone marrow fibrosis in myelofibrosis. *JCI Insight*, 6(18). <https://doi.org/10.1172/jci.insight.145651>.
- Varricchio, L., Mancini, A., Migliaccio, A.R. (2009). Pathological interactions between hematopoietic stem cells and their niche revealed by mouse models of primary myelofibrosis. *Expert Rev Hematol*, 2(3), 315–334. <https://doi.org/10.1586/ehm.09.17>.
- Verrucci, M., Pancrazzi, A., Aracil, M., Martelli, F., Guglielmelli, P., Zingariello, M., Ghinassi, B., D'Amore, E., Jimeno, J., Vannucchi, A.M., Migliaccio, A.R. (2010). CXCR4-independent rescue of the myeloproliferative defect of the Gata1low myelofibrosis mouse model by Aplidin. *J Cell Physiol*, 225(2), 490–499. <https://doi.org/10.1002/jcp.22228>.
- Villevall, J.L., Cohen-Solal, K., Tulliez, M., Giraudier, S., Guichard, J., Burstein, S., Cramer, E.M., Vainchenker, W., Wendling, F. (1997). High thrombopoietin production by hematopoietic cells induces a fatal myeloproliferative syndrome in mice. *Blood*, 90(11), 4369–4383.
- Vrij, A.A., Rijken, J., Van Wersch, J.W., Stockbrügger, R.W. (2000). Platelet factor 4 and beta-thromboglobulin in inflammatory bowel disease and giant cell arteritis. *European Journal of Clinical Investigation*, 30(3), 188–194. <https://doi.org/10.1046/j.1365-2362.2000.00616.x>.
- Vyas, P., Ault, K., Jackson, C.W., Orkin, S.H., Shivdasani, R.A. (1999). Consequences of GATA-1 deficiency in megakaryocytes and platelets. *Blood*, 93(9), 2867–2875.
- Wang, J.C. (2005). Importance of plasma matrix metalloproteinases (MMP) and tissue inhibitors of metalloproteinase (TIMP) in development of fibrosis in agnogenic myeloid metaplasia. *Leukemia & Lymphoma*, 46(9), 1261–1268. <https://doi.org/10.1080/10428190500126463>.
- Wang, J. C., Chen, C., Lou, L. H., Mora, M. (1997). Blood thrombopoietin, IL-6 and IL-11 levels in patients with agnogenic myeloid metaplasia. *Leukemia*, 11(11), 1827–1832. <https://doi.org/10.1038/sj.leu.2400846>.
- Wang, J. C., Chen, C., Novetsky, A. D., Lichter, S. M., Ahmed, F., Friedberg, N. M. (1998). Blood thrombopoietin levels in clonal thrombocytosis and reactive thrombocytosis. *The American Journal of Medicine*, 104(5), 451–455. [https://doi.org/10.1016/s0002-9343\(98\)00090-4](https://doi.org/10.1016/s0002-9343(98)00090-4).
- Waugh, D.J.J., Wilson, C. (2008). The Interleukin-8 Pathway in Cancer. *Clinical Cancer Research*, 8(21), 6735–6742. <https://doi.org/10.1158/1078-0432.CCR-07-4843>.

- Wernig, G., Kharas, M.G., Mullally, A., Leeman, D.S., Okabe, R., George, T., Clary, D.O., Gilliland, D.G. (2012). EXEL-8232, a small-molecule JAK2 inhibitor, effectively treats thrombocytosis and extramedullary hematopoiesis in a murine model of myeloproliferative neoplasm induced by MPLW515L. *Leukemia*, 26(4), 720–727. <https://doi.org/10.1038/leu.2011.261>.
- Wernig, G., Mercher, T., Okabe, R., Levine, R.L., Lee, B.H., Gilliland, D.G. (2006). Expression of Jak2^{V617F} causes a polycythemia vera–like disease with associated myelofibrosis in a murine bone marrow transplant model. *Blood*, 107(11), 4274–4281. <https://doi.org/10.1182/blood-2005-12-4824>.
- Wilkins, B.S., Erber, W.N., Bareford, D., Buck, G., Wheatley, K., East, C.L., Paul, B., Harrison, C.N., Green, A.R., Campbell, P.J. (2008). Bone marrow pathology in essential thrombocythemia: interobserver reliability and utility for identifying disease subtypes. *Blood*, 111(1), 60–70. <https://doi.org/10.1182/blood-2007-05-091850>.
- Yan, X. Q., Lacey, D., Fletcher, F., Hartley, C., McElroy, P., Sun, Y., Xia, M., Mu, S., Saris, C., Hill, D., Hawley, R. G., McNiece, I. K. (1995). Chronic exposure to retroviral vector encoded MGDF (mpl-ligand) induces lineage-specific growth and differentiation of megakaryocytes in mice. *Blood*, 86(11), 4025–4033.
- Yin, T. (2006). The stem cell niches in bone. *Journal of Clinical Investigation*, 116(5), 1195–1201. <https://doi.org/10.1172/JCI28568>.
- Yu, C., Cantor, A.B., Yang, H., Browne, C., Wells, R. A., Fujiwara, Y., Orkin, S.H. (2002). Targeted deletion of a high-Affinity GATA-binding site in the GATA-1 promoter leads to selective loss of the eosinophil lineage in vivo. *Journal of Experimental Medicine*, 195(11), 1387–1395. <https://doi.org/10.1084/jem.20020656>.
- Zahr, A.A., Salama, M.E., Carreau, N., Tremblay, D., Verstovsek, S., Mesa, R., Hoffman, R., Mascarenhas, J. (2016). Bone marrow fibrosis in myelofibrosis: pathogenesis, prognosis and targeted strategies. *Haematologica*, 101(6), 660–671. <https://doi.org/10.3324/haematol.2015.141283>.
- Zaldivar, M.M., Pauels, K., von Hundelshausen, P., Berres, M.L., Schmitz, P., Bornemann, J., Kowalska, M.A., Gassler, N., Streetz, K.L., Weiskirchen, R., Trautwein, C., Weber, C., Wasmuth, H.E. (2010). CXC chemokine ligand 4 (Cxcl4) is a platelet-derived mediator of experimental liver fibrosis. *Hepatology (Baltimore, Md.)*, 51(4), 1345–1353. <https://doi.org/10.1002/hep.23435>.
- Zaleskas, V.M., Krause, D.S., Lazarides, K., Patel, N., Hu, Y., Li, S., Van Etten, R. A. (2006). Molecular pathogenesis and therapy of polycythemia induced in mice by JAK2^{V617F}. *PLoS ONE*, 1(1), e18. <https://doi.org/10.1371/journal.pone.0000018>.
- Zingariello, M., Fabucci, M.E., Bosco, D., Migliaccio, A.R., Martelli, F., Rana, R.A., Zetterberg, E. (2010). Differential localization of P-selectin and von Willebrand factor during megakaryocyte maturation. *Biotechnic & Histochemistry: Official Publication of the Biological Stain Commission*, 85(3), 157–170. <https://doi.org/10.3109/10520290903149612>.
- Zingariello, M., Martelli, F., Ciaffoni, F., Masiello, F., Ghinassi, B., D'Amore, E., Massa, M., Barosi, G., Sancillo, L., Li, X., Goldberg, J. D., Rana, R. A., Migliaccio, A. R. (2013). Characterization of the TGF-β1

signaling abnormalities in the *Gata1*^{low} mouse model of myelofibrosis. *Blood*, 121(17), 3345–3363. <https://doi.org/10.1182/blood-2012-06-439661>.

Zingariello, M., Martelli, F., Verachi, P., Bardelli, C., Gobbo, F., Mazzarini, M., Migliaccio, A.R. (2019). Novel targets to cure primary myelofibrosis from studies on *Gata1*^{low} mice. *IUBMB Life*, 72(October 2019), 131–141. <https://doi.org/10.1002/iub.2198>.

Zingariello, M., Ruggeri, A., Martelli, F., Marra, M., Sancillo, L., Ceglia, I., Rana, R. A., Migliaccio, A.R. (2015). A novel interaction between megakaryocytes and activated fibrocytes increases TGF- β bioavailability in the *Gata1*^{low} mouse model of myelofibrosis. *American Journal of Blood Research*, 5(2), 34–61. <http://www.ncbi.nlm.nih.gov/pubmed/27069753>.

Zingariello, M., Sancillo, L., Martelli, F., Ciaffoni, F., Marra, M., Varricchio, L., Rana, R.A., Zhao, C., Crispino, J. D., Migliaccio, A.R. (2017). The thrombopoietin/MPL axis is activated in the *Gata1*^{low} mouse model of myelofibrosis and is associated with a defective RPS14 signature. *Blood Cancer Journal*, 7(6), 572. <https://doi.org/10.1038/bcj.2017.51>.

Zucker-Franklin D. (1974). Ultrastructural studies of hematopoietic elements in relation to the myelofibrosis-osteosclerosis syndrome, megakaryocytes and platelets (MMM or MOS). *Advances in Bioscience and Biotechnology*, 16, 127–143.

Chapter II. Experimental section

Abstract

Primary myelofibrosis (PMF) is the most severe form of Philadelphia-negative myeloproliferative neoplasms (MPNs), characterized by anemia, progressive splenomegaly, extramedullary hematopoiesis and bone marrow (BM) fibrosis, with disease progression to leukemia and low survival. The best therapy currently available for myelofibrosis includes treatment with a JAK inhibitor (Ruxolitinib), which, however, only ameliorates symptoms. Unfortunately, the pathogenesis of the disease is still poorly understood. It has been hypothesized that its progression may be determined by the presence of inflammatory cytokines produced by the bone marrow microenvironment that promote the development of fibrosis. The three aims of this PhD thesis, using the *Gata1*^{low} mouse model of myelofibrosis, were: 1. To investigate the presence of different cytokines in the bone marrow microenvironment; 2. To test the efficacy of treatment with Reparixin, a CXCR1/2 receptor inhibitor of CXCL1 (the murine homolog of human IL-8); 3. To test the efficacy of treatment with RB40.34 (P-selectin inhibitor), alone and in combination with Ruxolitinib. In the first study, we demonstrated by immunohistochemistry (IHC) the presence in the BM of *Gata1*^{low} mice of elevated levels of CXCL1, and its receptors CXCR1/2, and TGF- β 1. In particular, the cells with higher expression of these cytokines and receptors were the megakaryocytes. In the second study, we found that treatment with Reparixin in *Gata1*^{low} mice showed dose-dependent efficacy in reducing bone marrow and splenic fibrosis. Furthermore, by IHC analysis we demonstrated that the treatment induced a decrease in the expression of TGF- β 1, while the expression levels of CXCL1 and CXCR1/2 were similar to those of untreated mice. In the third study, we found that treatment with RB40.34 in combination with Ruxolitinib normalizes the phenotype of *Gata1*^{low} mice, reducing fibrosis and the content of TGF- β and CXCL1 in the bone marrow, and restoring the architecture of hematopoiesis in the bone marrow and spleen. In summary, these data provide preclinical evidence that treatment with Reparixin and RB40.34 in combination with Ruxolitinib are effective on reversing the myelofibrotic trait in the *Gata1*^{low} mouse model and encourage clinical trials to validate these compounds in human patients with PMF.

1. Introduction

Primary myelofibrosis (PMF) is the most severe form of Philadelphia-negative myeloproliferative neoplasms (MPN) (Marcellino et al., 2020) characterized by anemia, progressive splenomegaly, extra-medullary hematopoiesis, bone marrow (BM) fibrosis, osteosclerosis, neoangiogenesis, leukemia progression and low survival (Harrison et al., 2020; Masarova et al., 2017). The best therapy currently available for myelofibrosis includes treatment with the Jak inhibitor (Ruxolitinib), which, however, only relieves disease symptoms, reducing splenomegaly and improving patient survival, and also reducing the likelihood of transformation into leukemia (Cervantes & Pereira,

2017; Deininger et al., 2015; Iurlo & Cattaneo, 2017; Verstovsek et al., 2012; Verstovsek, Gotlib, et al., 2017; Verstovsek, Mesa, et al., 2017).

Driver mutations in one or more hematopoietic lines in the thrombopoietin (TPO) axis have been described in the literature. These are somatic mutations in one of these 3 genes-JAK2, CALR, or MPL which alter JAK-STAT signaling causing proinflammatory cytokine release and bone marrow remodeling (Barbui et al., 2018; Zahr et al., 2016). MPN progress from a pre-fibrotic stage to myelofibrosis by a mechanism still poorly understood not associated with the acquisition of specific second mutations (Dunbar et al., 2023; Marcellino et al., 2020). It has been hypothesized that the progression of MPN could be determined by the presence of inflammatory cytokines produced by the bone marrow microenvironment that sustains fibrosis (Koschmieder & Chatain, 2020; Migliaccio, 2018).

PMF has a unique cellular signature: both BM and spleen contain numerous megakaryocytes (MKs) exhibiting distinctive abnormalities that include reduced expression of the transcription factor Gata1 (Vannucchi et al., 2005) and increased proliferation with delayed maturation (Centurione et al., 2004; Schmitt et al., 2000). The MKs of PMF patients express high levels of the adhesion receptor P-selectin (P-sel) in the cytoplasmic membrane of MKs. Such expression induces an abnormal interaction with its ligand P-selectin glycoprotein ligand-1 expressed by neutrophils (Evangelista et al., 1999; Moore et al., 1992) precisely triggering a process of pathological emperipolesis between the neutrophils and MKs, leading to the death of MKs for paraptosis and release of factors contained in the cytoplasm of MKs in the microenvironment, such as TGF- β (Thiele et al., 1997; Zingariello et al., 2010).

Previous studies have identified several proinflammatory cytokines whose plasma levels have increased in patients with PMF compared to non-diseased patients. Specifically, the plasma of these patients contains greater levels of TGF- β , both as total and activated form (Campanelli et al., 2011), and interleukin-8 (IL-8), the latter being associated with more serious symptoms, leukocytosis and progression to leukemic diseases (Barabanshikova et al., 2017; Tefferi et al., 2011). These cytokines are abnormally produced by megakaryocytes present in the bone marrow of PMF patients, but also by other cells present in the bone marrow microenvironment, such as monocytes, macrophages, and endothelial cells in response to proinflammatory stimuli (Batlle & Massagué, 2019; Dunbar et al., 2023; Martyré, 1995; Waugh & Wilson, 2008). The discovery of the production of pro-inflammatory cytokines by megakaryocytes of PMF patients, such as TGF- β and IL-8, is of considerable interest, as it has been hypothesized that they drive the fibrosis as they activate other cell types, such as fibrocytes, to produce collagen (Dongre & Weinberg, 2019; Zingariello et al., 2015).

Previous studies have shown that TGF- β and IL-8 stimulate megakaryocyte proliferation by keeping these cells in an immature state (Bruno et al., 1998; Dunbar et al., 2023; Emadi et al., 2005). Moreover, IL-8 increases emperipolesis (Köhler et al., 2011), which is believed to be responsible for

the increased release of TGF- β by megakaryocytes into the microenvironment (Centurione et al., 2004).

Gata1^{low} mice carrying the hypomorphic *Gata1*^{low} mutation, which specifically deletes the first hypersensitive site (HS1) upstream of the *Gata1* gene, express the same MKs alterations observed in MF patients and develop progressive MF closely resembling human disease. These mice, although they do not carry driver mutations for MF, are considered a bona fide animal model of MF because they express an activated TPO/MPL axis, which can be drugged by JAK inhibitors (such as Ruxolitinib), and an RSP14 ribosomopathy, which is responsible for the altered maturation of the megakaryocytes and expression of P-sel. The altered expression of P-sel is responsible for pathological emperipolesis that increases the bioavailability of proinflammatory cytokines and drives fibrosis (Spangrude et al., 2016; Zingariello et al., 2019).

Using this mouse model of the disease, I collaborated during my three years of PhD Programme to investigations on the presence of abnormal content of different cytokines in the bone marrow microenvironment of these mice and to experimental administration of two different compounds to better characterize this disease. Specifically, we aimed:

1. To study the relationship between serum levels of pro-inflammatory cytokines and their bioavailability in the bone marrow microenvironment in *Gata1*^{low} mice. The final goal was to identify in the bone marrow microenvironment the cell populations responsible for the increased bioavailability of these cytokines and to identify the consequences of their alteration, which, in addition to fibrosis, include profound remodeling of the microenvironment architecture that alters the distribution of hematopoietic stem cells within the bone marrow architecture.

2. Based on the previous data in which we demonstrated that BM megakaryocytes of *Gata1*^{low} mice express not only high levels of TGF- β 1, but also high levels of CXCL1, the murine equivalent of human IL-8, the aim was to evaluate whether MKs of *Gata1*^{low} mice express CXCR1 and CXCR2, receptors of CXCL1, and thus the efficacy of Reparixin treatment in this mouse model.

3. In previous studies, it has been shown that *Gata1*^{low} mice lacking the *P-selectin* gene do not develop myelofibrosis. Therefore, the aim was to test the hypothesis that pharmacological inhibition of P-selectin with RB40.34, alone and in combination with Ruxolitinib, is effective in reversing the myelofibrotic phenotype expressed by *Gata1*^{low} mice.

1.1 References

Barabanshikova, M.V., Dubina, I.A., Lapin, S.V., Morozova, E.V., Vlasova, J.J., Ivanova, M.O., Moiseev, I.S., Afanasyev, B.V. (2017). Clinical correlates and prognostic significance of IL-8, sIL-2R, and immunoglobulin-free light chain levels in patients with myelofibrosis. *Oncology Research and Treatment*, 40(10), 574–579. <https://doi.org/10.1159/000477253>.

- Barbui, T., Tefferi, A., Vannucchi, A.M., Passamonti, F., Silver, R.T., Hoffman, R., Verstovsek, S., Mesa, R., Kiladjian, J.J., Hehlmann, R., Reiter, A., Cervantes, F., Harrison, C., Mc Mullin, M.F., Hasselbalch, H.C., Koschmieder, S., Marchetti, M., Bacigalupo, A., Finazzi, G., Kroeger, N., Griesshammer, M., Birgegard, G., Barosi, G. (2018). Philadelphia chromosome-negative classical myeloproliferative neoplasms: revised management recommendations from European LeukemiaNet. *Leukemia*, 32(5), 1057–1069. <https://doi.org/10.1038/s41375-018-0077-1>.
- Batlle, E., Massagué, J. (2019). Transforming Growth Factor- β signaling in immunity and cancer. *Immunity*, 50(4), 924–940. <https://doi.org/10.1016/j.immuni.2019.03.024>
- Bruno, E., Horrigan, S.K., Van Den Berg, D., Rozler, E., Fitting, P.R., Moss, S.T., Westbrook, C., Hoffman, R. (1998). The Smad5 gene is involved in the intracellular signaling pathways that mediate the inhibitory effects of transforming growth factor-beta on human hematopoiesis. *Blood*, 91(6), 1917–1923. <http://www.ncbi.nlm.nih.gov/pubmed/9490674>.
- Campanelli, R., Rosti, V., Villani, L., Castagno, M., Moretti, E., Bonetti, E., Bergamaschi, G., Balduini, A., Barosi, G., Massa, M. (2011). Evaluation of the bioactive and total transforming growth factor β 1 levels in primary myelofibrosis. *Cytokine*, 53(1), 100–106. <https://doi.org/https://doi.org/10.1016/j.cyto.2010.07.427>.
- Centurione, L., Di Baldassarre, A., Zingariello, M., Bosco, D., Gatta, V., Rana, R.A., Langella, V., Di Virgilio, A., Vannucchi, A.M., Migliaccio, A.R. (2004). Increased and pathologic emperipolesis of neutrophils within megakaryocytes associated with marrow fibrosis in GATA-1^{low} mice. *Blood*, 104(12), 3573–3580. <https://doi.org/10.1182/blood-2004-01-0193>.
- Cervantes, F., Pereira, A. (2017). Does ruxolitinib prolong the survival of patients with myelofibrosis? *Blood*, 129(7), 832–837. <https://doi.org/10.1182/blood-2016-11-731604>.
- Deininger, M., Radich, J., Burn, T.C., Huber, R., Paranagama, D., Verstovsek, S. (2015). The effect of long-term ruxolitinib treatment on JAK2^{V617F} allele burden in patients with myelofibrosis. *Blood*, 126(13), 1551–1554. <https://doi.org/10.1182/blood-2015-03-635235>.
- Dongre, A., Weinberg, R.A. (2019). New insights into the mechanisms of epithelial–mesenchymal transition and implications for cancer. *Nature Reviews Molecular Cell Biology*, 20(2), 69–84. <https://doi.org/10.1038/s41580-018-0080-4>.
- Dunbar, A.J., Kim, D., Lu, M., Farina, M., Bowman, R.L., Yang, J.L., Park, Y., Karzai, A., Xiao, W., Zaroogian, Z., O'Connor, K., Mowla, S., Gobbo, F., Verachi, P., Martelli, F., Sarli, G., Xia, L., Elmansy, N., Kleppe, M., Chen, Z., Xiao, Y., McGovern, E., Snyder, J., Krishnan, A., Hill, C., Cordner, K., Zouak, A., Salama, M.E., Yohai, J., Tucker, E., Chen, J., Zhou, J., McConnell, T., Migliaccio, A.R., Koche, R., Rampal, R., Fan, R., Levine, R.L., Hoffman, R. (2023). CXCL8/CXCR2 signaling mediates bone marrow fibrosis and is a therapeutic target in myelofibrosis. *Blood*, 141(20), 2508–2519. <https://doi.org/10.1182/blood.2022015418>.
- Emadi, S., Clay, D., Desterke, C., Guerton, B., Maquarre, E., Jasmin, C. (2005). IL-8 and its CXCR1 and CXCR2 receptors participate in the control of megakaryocytic proliferation, differentiation, and ploidy in myeloid metaplasia with myelofibrosis. *Blood*, 105(2), 464–473. <https://doi.org/10.1182/blood-2003-12-4415>.

- Evangelista, V., Manarini, S., Sideri, R., Rotondo, S., Martelli, N., Piccoli, A., Totani, L., Piccardoni, P., Vestweber, D., de Gaetano, G., Cerletti, C. (1999). Platelet/Polymorphonuclear leukocyte interaction: P-Selectin triggers protein-tyrosine phosphorylation-dependent CD11b/CD18 adhesion: role of PSGL-1 as a signaling molecule. *Blood*, 93(3), 876–885. <https://doi.org/10.1182/blood.V93.3.876>.
- Harrison, C.N., Schaap, N., Mesa, R.A., Harrison, C.N. (2020). Management of myelofibrosis after ruxolitinib failure. *Annals of Hematology*, 16, 1–13. <https://doi.org/10.1007/s00277-020-04002-9>.
- Iurlo, A., Cattaneo, D. (2017). Treatment of myelofibrosis: old and new strategies. *Clinical Medicine Insights: Blood Disorders*, 10, 1–10. <https://doi.org/10.1177/1179545X17695233>.
- Köhler, A., De Filippo, K., Hasenberg, M., van den Brandt, C., Nye, E., Hosking, M. P., Lane, T.E., Männ, L., Ransohoff, R.M., Hauser, A.E., Winter, O., Schraven, B., Geiger, H., Hogg, N., Gunzer, M. (2011). G-CSF-mediated thrombopoietin release triggers neutrophil motility and mobilization from bone marrow via induction of CXCR2 ligands. *Blood*, 117(16), 4349–4357. <https://doi.org/10.1182/blood-2010-09-308387>.
- Koschmieder, S., Chatain, N. (2020). Role of inflammation in the biology of myeloproliferative neoplasms. *Blood Reviews*, 42, 100711. <https://doi.org/10.1016/j.blre.2020.100711>.
- Marcellino, B.K., Verstovsek, S., Mascarenhas, J. (2020). The myelodepletive phenotype in myelofibrosis: clinical relevance and therapeutic implication. *Clinical Lymphoma, Myeloma and Leukemia*, 1–7. <https://doi.org/doi:10.1016/j.clml.2020.01.008>.
- Martyré, M.C. (1995). TGF- β and megakaryocytes in the pathogenesis of myelofibrosis in myeloproliferative disorders. *Leukemia & Lymphoma*, 20(1–2), 39–44. <https://doi.org/10.3109/10428199509054751>.
- Masarova, L., Bose, P., Daver, N., Pemmaraju, N., Newberry, K.J., Cortes, J., Kantarjian, H.M., Verstovsek, S. (2017). Patients with post-essential thrombocythemia and post-polycythemia vera differ from patients with primary myelofibrosis. *Leukemia Research*, 59, 110–116. <https://doi.org/10.1016/j.leukres.2017.06.001>.
- Migliaccio, A.R. (2018). A vicious interplay between genetic and environmental insults in the etiology of blood cancers. *Experimental Hematology*, 59, 9–13. <https://doi.org/10.1016/j.exphem.2017.12.004>.
- Moore, K.L., Stults, N.L., Diaz, S., Smith, D.F., Cummings, R.D., Varki, A., McEver, R.P. (1992). Identification of a specific glycoprotein ligand for P-selectin (CD62) on myeloid cells. *The Journal of Cell Biology*, 118(2), 445–456. <https://doi.org/10.1083/jcb.118.2.445>.
- Schmitt, A., Jouault, H., Guichard, J., Wendling, F., Drouin, A., Cramer, E.M. (2000). Pathologic interaction between megakaryocytes and polymorphonuclear leukocytes in myelofibrosis. *Blood*, 96(4), 1342–1347. <http://www.ncbi.nlm.nih.gov/pubmed/10942376>.
- Spangrude, G.J., Lewandowski, D., Martelli, F., Marra, M., Zingariello, M., Sancillo, L., Rana, R.A., Migliaccio, A.R. (2016). P-Selectin sustains extramedullary hematopoiesis in the *Gata1^{low}* model of myelofibrosis. *Stem Cells*, 34(1), 67–82. <https://doi.org/10.1002/stem.2229>.
- Tefferi, A., Vaidya, R., Caramazza, D., Finke, C., Lasho, T., Pardanani, A. (2011). Circulating interleukin (IL)-8, IL-2R, IL-12, and IL-15 levels are independently prognostic in primary myelofibrosis: a comprehensive

cytokine profiling study. *Journal of Clinical Oncology*, 29(10), 1356–1363. <https://doi.org/10.1200/JCO.2010.32.9490>.

Thiele, J., Lorenzen, J., Manich, B., Kvasnicka, H.M., Zirbes, T.K., Fischer, R. (1997). Apoptosis (programmed cell death) in idiopathic (primary) osteo-/myelofibrosis: naked nuclei in megakaryopoiesis reveal features of para-apoptosis. *Acta Haematologica*, 97(3), 137–143. <https://doi.org/10.1159/000203671>.

Vannucchi, A.M., Pancrazzi, A., Guglielmelli, P., Di Lollo, S., Bogani, C., Baroni, G., Bianchi, L., Migliaccio, A.R., Bosi, A., Paoletti, F. (2005). Abnormalities of GATA-1 in megakaryocytes from patients with idiopathic myelofibrosis. *American Journal of Pathology*, 167(3), 849–858. [https://doi.org/10.1016/S0002-9440\(10\)62056-1](https://doi.org/10.1016/S0002-9440(10)62056-1).

Verstovsek, S., Gotlib, J., Mesa, R.A., Vannucchi, A.M., Kiladjan, J.J., Cervantes, F., Harrison, C.N., Paquette, R., Sun, W., Naim, A., Langmuir, P., Dong, T., Gopalakrishna, P., Gupta, V. (2017). Long-term survival in patients treated with ruxolitinib for myelofibrosis: COMFORT-I and -II pooled analyses. *Journal of Hematology & Oncology*, 10(1), 156. <https://doi.org/10.1186/s13045-017-0527-7>.

Verstovsek, S., Kantarjian, H.M., Estrov, Z., Cortes, J.E., Thomas, D.A., Kadia, T., Pierce, S., Jabbour, E., Borthakur, G., Rumi, E., Pungolino, E., Morra, E., Caramazza, D., Cazzola, M., Passamonti, F. (2012). Long-term outcomes of 107 patients with myelofibrosis receiving JAK1/JAK2 inhibitor ruxolitinib: survival advantage in comparison to matched historical controls. *Blood*, 120(6), 1202–1209. <https://doi.org/10.1182/blood-2012-02-414631>.

Verstovsek, S., Mesa, R.A., Gotlib, J., Gupta, V., DiPersio, J.F., Catalano, J.V., Deininger, M.W.N., Miller, C.B., Silver, R.T., Talpaz, M., Winton, E.F., Harvey Jr, J.H., Arcasoy, M.O., Hexner, E.O., Lyons, R.M., Paquette, R., Raza, A., Jones, M., Kornacki, D., Sun, K., Kantarjian, H. (2017). Long-term treatment with ruxolitinib for patients with myelofibrosis: 5-year update from the randomized, double-blind, placebo-controlled, phase 3 COMFORT-I trial. *Journal of Hematology & Oncology*, 10(1), 55. <https://doi.org/10.1186/s13045-017-0417-z>.

Waugh, D.J.J., Wilson, C. (2008). The Interleukin-8 pathway in cancer. *Clinical Cancer Research*, 8(21), 6735–6742. <https://doi.org/10.1158/1078-0432.CCR-07-4843>.

Zahr, A.A., Salama, M.E., Carreau, N., Tremblay, D., Verstovsek, S., Mesa, R., Hoffman, R., Mascarenhas, J. (2016). Bone marrow fibrosis in myelofibrosis: pathogenesis, prognosis and targeted strategies. *Haematologica*, 101(6), 660–671. <https://doi.org/10.3324/haematol.2015.141283>.

Zingariello, M., Fabucci, M.E., Bosco, D., Migliaccio, A.R., Martelli, F., Rana, R.A., Zetterberg, E. (2010). Differential localization of P-selectin and von Willebrand factor during megakaryocyte maturation. *Biotechnic & Histochemistry: Official Publication of the Biological Stain Commission*, 85(3), 157–170. <https://doi.org/10.3109/10520290903149612>.

Zingariello, M., Martelli, F., Verachi, P., Bardelli, C., Gobbo, F., Mazzarini, M., Migliaccio, A.R. (2019). Novel targets to cure primary myelofibrosis from studies on *Gata1*^{low} mice. *IUBMB Life*, 131–141. <https://doi.org/10.1002/iub.2198>.

Zingariello, M., Ruggeri, A., Martelli, F., Marra, M., Sancillo, L., Ceglia, I., Rana, R. A., Migliaccio, A.R. (2015). A novel interaction between megakaryocytes and activated fibrocytes increases TGF- β bioavailability in the *Gata1*^{low} mouse model of myelofibrosis. American Journal of Blood Research, 5(2), 34–61. <http://www.ncbi.nlm.nih.gov/pubmed/27069753>.

2. Results

Aim 1: The pro-inflammatory milieu in the bone marrow of *Gata1*^{low} was studied in the paper titled: “Resident self-tissue of proinflammatory cytokines rather than their systemic levels correlates with development of myelofibrosis in *Gata1*^{low} mice”, published in Biomolecules in 2022.

Aim2: The efficacy of Reparixin treatment on *Gata1*^{low} mice was studied and published in the article titled: “The CXCR1/CXCR2 inhibitor reparixin alters the development of myelofibrosis in the *Gata1*^{low} mice” in Frontiers in Oncology in 2022.

Aim 3: The efficacy of treatment with RB40.34, alone and in combination with Ruxolitinib, on *Gata1*^{low} mice was studied in the work titled: “Preclinical studies on the use of a P-selectin-blocking monoclonal antibody to halt progression of myelofibrosis in the *Gata1*^{low} mouse model” published in Experimental Hematology in 2023.

2.1. Resident Self-Tissue of Proinflammatory Cytokines Rather Than Their Systemic Levels Correlates with Development of Myelofibrosis in *Gata1*^{low} Mice

Adapted from: Article

Microenvironmental bioavailability of pro-inflammatory cytokines rather than their serum levels correlates with development of myelofibrosis in *Gata1*^{low} mice

Maria Zingariello¹, Paola Verachi², Francesca Gobbo^{2,3}, Fabrizio Martelli⁴, Mario Falchi⁵, Maria Mazzarini², Mauro Valeri⁶, Giuseppe Sarli², Christian Marinaccio⁷, Johanna Melo-Cardenas⁸, John D. Crispino⁸ and Anna Rita Migliaccio^{9,10*}

¹ Department of Medicine, Campus Biomedico, Rome, Italy. m.zingariello@unicampus.it

² Department of Biomedical and Neuromotorial Sciences, Alma Mater University, Bologna, Italy. paola.verachi@unibo.it, francesca.gobbo3@unibo.it, maria.mazzarini4@unibo.it

³ Department of Veterinary Medical Sciences, University of Bologna, Ozzano dell'Emilia, Bologna, Italy. francesca.gobbo3@unibo.it, giuseppe.sarli@unibo.it

⁴ National Center for Drug Research and Evaluation, Istituto Superiore di Sanità, Rome, Italy. fabrizio.martelli@iss.it

⁵ National Center HIV/AIDS Research, Istituto Superiore di Sanità, Rome, Italy. mario.falchi@iss.it

⁶ Center for animal experimentation and well-being, Istituto Superiore di Sanità, Rome, Italy. mauro.valeri@iss.it

⁷ Dana-Farber Cancer Institute, Harvard Medical School, Boston, MA, USA. christian_marinaccio@dfci.harvard.edu

⁸ Department of Hematology, St. Jude Children's Research Hospital, Memphis, TN, USA. johanna.melo-cardenas@stjude.org, john.crispino@stjude.org

⁹ Altius Institute for Biomedical Sciences, Seattle, WA, USA. amigliaccio@altius.org

¹⁰ Center for Integrated Biomedical Research, Campus Bio-medico, Rome, Italy. a.migliaccio@unicampus.it

* Correspondence: Anna Rita Migliaccio, Altius Institute for Biomedical Sciences, Seattle, WA, USA.

amigliaccio@altius.org

Abstract: Serum levels of inflammatory-cytokines are currently investigated as prognosis markers in myelofibrosis, the most severe Philadelphia-negative myeloproliferative neoplasm. We tested this hypothesis in the *Gata1*^{low} model of myelofibrosis. *Gata1*^{low} mice, and age-matched wild-type littermates, were analyzed before and after disease onset. We assessed cytokine serum levels by Luminex-bead-assay and ELISA, frequency and cytokine content of stromal cells by flow-cytometry and immune-histochemistry and bone marrow (BM) localization of GFP-tagged hematopoietic stem cells (HSC) by confocal-microscopy. Differences in serum levels of 32 inflammatory-cytokines between pre-fibrotic and fibrotic *Gata1*^{low} mice and their wild-type littermates were modest. However, BM from fibrotic *Gata1*^{low} mice contained higher levels of lipocalin-2, CXCL1 and TGF- β 1 than wild-type BM. Although frequencies of endothelial cells, mesenchymal cells, osteoblasts and megakaryocytes were higher than normal in *Gata1*^{low} BM, the cells which expressed these cytokines

the most were malignant megakaryocytes. This increased bioavailability of pro-inflammatory cytokines was associated with altered HSC localization: *Gata1*^{low} HSC were localized in the femur diaphysis in areas surrounded by micro-vessels, neo-bones and megakaryocytes while wild-type HSC were localized in the femur epiphysis around adipocytes. In conclusions, bioavailability of inflammatory cytokines in BM, rather than blood levels, possibly by reshaping the HSC niche, correlates with myelofibrosis in *Gata1*^{low} mice.

Keywords: myelofibrosis, GATA1, pro-inflammatory cytokines, TGF- β 1, interleukin 8, megakaryocytes, microenvironment

1. Introduction

The Philadelphia-negative Myeloproliferative Neoplasms (MPN) represent a continuum of diseases characterized by hyperproliferation of one or more blood lineages sustained by driver mutations in the thrombopoietin (TPO) axis (either in *MPL*, encoding the receptor for TPO, in *JAK2*, encoding the first element of the signal for MPL and other receptors of the cytokine superfamily, or in *Calreticulin*, encoding a chaperon protein that when mutated constitutively activates MPL) (Barbui et al., 2018; Zahr et al., 2016). By a mechanism still poorly understood, MPN progress to myelofibrosis (MF), the most severe form of these disease and to myeloid leukemia (Marcellino et al., 2020). Since the progression of MPN to MF is not associated with the acquisition of specific second mutations (A. J. Dunbar et al., 2020), it has been hypothesized that it is driven by the establishment of a pro-inflammatory milieu in the bone marrow microenvironment which sustains fibrosis and hematopoietic failure in this organ and establishes hematopoiesis in extramedullary sites (Koschmieder & Chatain, 2020; Migliaccio, 2018). To test this hypothesis, the pro-inflammatory cytokines expressed at altered levels in myelofibrosis is the subject of extensive investigation, with the aim to identify and validate specific cytokine alterations that may be used as markers for prognosis of disease progression or targeted for patient-specific therapies. These studies are under the assumption that the level of a cytokine in the blood predicts its bioavailability in the bone marrow microenvironment and are fostered by the technical limitation that, due to the underlying fibrosis, bone marrow samples from MF patients suited for analyses are limited.

Previous studies have identified that the serum (and/or plasma) of patients with MF contain greater levels of several pro-inflammatory cytokines than that of non-diseased individuals. More specifically, the plasma of these patients contains greater levels of TGF- β , both as total and activated form (Campanelli et al., 2011), and interleukin-8 (IL-8) and the plasma levels of IL-8 were found to predict the severity of the symptoms and progression to leukemic transformation (Barabanshikova et al., 2017; Tefferi et al., 2011). Both TGF- β and IL-8 are abnormally produced at high levels by the megakaryocytes present in the bone marrow of myelofibrosis patients (A. Dunbar et al., 2021; Martyr ,

1995). However, these cytokines are also produced by monocytes, macrophages and endothelial cells in response to pro-inflammatory stimuli (Batlle & Massagué, 2019; Waugh & Wilson, 2008). *In vitro* studies have also shown that they can also be produced by other cell types present in the bone marrow microenvironment such as fibroblasts, neutrophils, and megakaryocytes (Batlle & Massagué, 2019; Hashimoto et al., 1996; Kaplanski et al., 1994; Matsushima & Oppenheim, 1989; Takeuchi et al., 1999). The comparison of the production and response to these cytokines by normal and malignant megakaryocytes is of specific interest. The numerous malignant megakaryocytes found in the bone marrow of these patients are hypothesized as driver of the fibrosis (Malara et al., 2018). However, it is currently debated whether they drive the process by producing altered levels of inflammatory cytokines which activate other cell types (fibrocytes or fibrocytes possibly of macrophage origin)(Zingariello et al., 2015, 2019) to produce collagen and/or because by responding to these cytokines by acquiring altered functions (Emadi et al., 2005). In fact, both TGF- β and IL-8 have been shown to increase the proliferation of megakaryocytes by retaining these cells in an immature state(Bruno et al., 1998; A. Dunbar et al., 2021; Emadi et al., 2005) In addition, IL-8 has been reported to increase the interaction between megakaryocytes and neutrophils (Köhler et al., 2011), the emperipolesis of which is thought to be responsible for increasing the release of TGF- β in the microenvironment (Centurione et al., 2004). These studies are of direct clinical interests since preclinical data indicating that TGF- β trap and IL-8 inhibitors rescue the myelofibrosis phenotype in animal models (Centurione et al., 2004; A. Dunbar et al., 2021) and clinical trials with these drugs are currently under investigation (Mascarenhas et al., 2021).

In the present study we clarify the relationship between the serum levels of pro-inflammatory cytokines and their bioavailability in the bone marrow microenvironment using the well characterized *Gata1*^{low} mouse model of myelofibrosis (Zingariello et al., 2019) . We also investigate the cell populations in the bone marrow microenvironment which is responsible for their increased bioavailability and the consequences of their alterations which, in addition to fibrosis, include a profound reshaping of the microenvironment architecture that alters the distribution of the hematopoietic stem cells within the bone marrow architecture.

2. Materials and Methods

2.1. Mice

Transgenic mice were bred in the animal facility of Istituto Superiore di Sanità as described (Martelli et al., 2005; Vannucchi et al., 2002). Littermates were genotyped at birth by PCR (Martelli et al., 2005) and those found not to carry the expected mutation(s) were used as wild-type controls. We analyzed the following transgenic lines: *Gata1*^{low} mice, mice lacking *P-selectin* (*Psel*^{null}) (Frenette et al., 2000) and double *Gata1*^{low}*Psel*^{null} mice mice(Spangrude et al., 2016). To study the HSC localization within the bone marrow architecture, we analyzed double *huCD34tTA/TetO-H2BGFP*

mice carrying the *histone H2B* gene fused with *GFP* under the control of the regulatory sequences of *human CD34* which in mice are active only in hematopoietic stem cells (HSC) (Qiu et al., 2014; Radomska et al., 2002) (defined as *huCD34-GFP^{H2B}* from now on) and triple *huCD34^{tTA}/TetO-H2BGFP/Gata1^{low}* mice (defined *huCD34-GFP^{H2B}/Gata1^{low}*) generated according to standard genetic approaches in the animal facility of Istituto Superiore di Sanità. All the mutations had been carried in the CD1 background for more than 10 generations. Mice were divided into two groups based on age: 5-7 months (adult) and 12-14 months (old) group, unless otherwise indicated. In selected experiments, wild-type and *Gata1^{low}* littermates were treated with *SB431542* (cat# S4317-5GM, Sigma Aldrich, Darmstadt, DE), an inhibitor of the first tyrosine kinase of the TGF- β 1 receptor type I signaling (Zingariello et al., 2013). In these experiments, 12-mo-old mice (12 mice/experiment) were intraperitoneally injected with *SB431542* (60 μ g/kg/day) or vehicle (same volume) for 1 month. Wild-type (WT) CD1, DBA2 and C57BL6 mice were purchased from Charles River (Calco, Lecco, Italy). Gender was considered as independent variable and results obtained with females and males were combined because found not to be statistically different.

2.2. Blood collection

Blood was collected from the retro-orbital plexus into ethylen-diamino-tetracetic acid-coated micro-capillary tubes (20-40 μ L/sampling) from mice that had previously topically anesthetized with lidocaine (one drop/eye) (EDRA S.p.A., Milan, Italy). Serum was prepared by allowing blood clotting for 2 hours at room temperature and centrifugation for 20min at 2000xg. Serum samples were stored in aliquots at -80°C, thawed once and analyzed within 20 min from thawing. Serum from 5-7 months (adult) and 12-14 months (old) wild-type CD1, C57BL-6 and DBA2 mice were purchased from Charles River Laboratories.

2.3. Cytokine profiling

The serum was spun at 10.000xg for 10min at 4°C to remove particulates. Cytokine levels were quantified using the mouse cytokine/chemokine magnetic bead panel for 32 cytokines from Millipore (cat# MCYTMAG70PMX32BK, Darmstadt, DE) according to manufacturer's instructions. Data were acquired using a Luminex® 200™, and cytokine concentrations were calculated using xPONENT® software (Luminex Corporation, Auxin, TX, USA) against a standard curve.

2.4. Enzyme-Linked Immunosorbent Assay (ELISA)

Serum levels of lipocalin-2 (LCN2), CXCL1 and TGF- β 1 were determined in duplicate with the Quantikine ELISA Kits (cat# MLCN20, MKC00B and DB100B, respectively, R&D Systems, Minneapolis, MN, USA), as described by the manufacturer. Optical densities were determined using a microplate reader set to 450nm (VICTOR® Nivo™, Perkin Elmer, Milan, Italy).

2.5. Flow cytometry determination of microenvironmental cells and HSC

The frequency of endothelial cells (ECs), mesenchymal stem cells (MSCs) and osteoblasts (OBCs) was determined by analyzing hematopoietic cell-depleted bone marrow cells obtained by carefully crushing the femurs in Iscove's Modified Dulbecco's Medium according to flow cytometry criteria defined by the Passegué laboratory (Schepers et al., 2013). Briefly, ECs were defined as Lin⁻/CD45⁻/CD31⁺/Sca-1⁺ cells, MSCs as Lin⁻/CD45⁻/CD31⁻/CD51⁺/Sca-1⁺ cells and OBCs as Lin⁻/CD45⁻/CD31⁻/CD51⁺/Sca-1⁻ cells. The frequency of megakaryocytes (MKs) and neutrophils (Neu) was instead determined by analyzing bone marrow cells labeled with FITC-A CD61/PE-A CD41 or PE-A Gr1/PE-Cy7-A CD11b, as described (Ghinassi et al., 2007; Zingariello et al., 2013). For HSC determinations, mononuclear bone marrow cells were incubated with a cocktail of the following antibodies: APC-CD117, APC-Cy7-Sca1, PE-Cy7-CD150, biotin-labeled anti-mouse CD48, and biotin-labeled anti-lineage antibodies. After 30 minutes of incubation on ice, cells were washed once and stained with streptavidin-PE-Cy5, and cell fluorescence was analyzed with a Gallios analyzer (Beckman Coulter, Brea, CA, USA). The total HSC population was defined as LSK (Lin⁻/CD48⁻/c-kit⁺/Sca-1⁺) while long-term repopulating HSC were defined by the SLAM phenotype (Lin⁻/CD48⁻/c-kit⁺/Sca-1⁺/CD150⁺) as previously described (Oguro et al., 2013; Spangrude et al., 2016). Nonspecific signals and dead cells were excluded by appropriate fluorochrome-conjugated isotype and propidium iodide staining, respectively. All the antibodies were purchased from BD-Pharmingen (San Diego, CA, USA). Fluorescent signals were measured with the FACS Aria (Becton Dickinson, Franklin Lakes, NJ, USA), dead cells were excluded by Sytox Blue staining (0.002mM, Molecular Probes, Eugene, OR, USA). Results were analyzed with the Kaluza analysis version 2.1 (Beckman Coulter). Examples of the gates used to identify the stromal cells and the HSC are presented in Figures S1.

2.6. Histological and Immunohistochemical Analyses

Femurs were fixed in formaldehyde (10% v/v with neutral buffer), treated for 1h with bone marrow biopsy decalcifying solution (Osteodec; Bio-Optica, Milan, Italy) and included in paraffin. Sections (3µm) were stained either with hematoxylin-eosin (H&E; Hematoxylin cat# 01HEMH2500; Eosin cat# 01EOY101000; Histo-Line Laboratories, Pantigliate, MI, Italy) or reticulin (both from Bio-Optica, Milan, Italy) or subjected to immunohistochemistry with anti-TGF-β1 (cat# sc-130348, Santa Cruz Biotechnology, Santa Cruz, CA, USA), anti-LCN2 (cat# MBS178180, MyBioSource, San Diego, CA, USA), anti-CXCL1 (cat# ab86436, Abcam, Cambridge, UK), anti-CXCR1 (cat# GTX100389, Genetex, Irvine, CA, USA), anti-CXCR2 (cat# catalog ab14935, Abcam) and anti-BMP-4 (cat# ab235114, Abcam) antibodies. Immunoreactions were detected with avidin-biotin immunoperoxidase (Vectastain Elite ABC Kit, Vector Laboratories, Burlingame, CA, USA) and the chromogen 3,3'-diaminobenzidine (0.05% w/v, cat# ACB999, Histo-Line Laboratories). Slides were counterstained with Papanicolaou's hematoxylin (Histo-Line Laboratories). Images were acquired with an optical

microscope (Eclipse E600; Nikon, Shinjuku, Japan) equipped with the Imaging Source "33" Series USB 3.0 Camera (cat# DFK 33UX264; Bremen, DE). Reticulin fibers were quantified on 5 different areas/femur/mouse from at least 4 mice per group using the ImageJ program (version 1.52t) (National Institutes of Health, Bethesda, MD, USA) (see **Figure S2A** for detail). The level of the expressions of LCN2, TGF- β 1, CXCL1, CXCR1 and CXCR2 per cell was also evaluated with the ImageJ program by counting the number of cells that exceeded the intensity set as threshold (see **Figure S2B** for detail).

2.7. Confocal microscopy determinations

Femurs were fixed, decalcified and included in paraffin as described above. Sections (5 μ m) were stained with DAPI (D9542-5MG, Sigma Aldrich) and analyzed with the confocal microscope Zeiss LSM 900 (Carl Zeiss GmbH, Jena, DE) in the Airyscan mode. Excitation light was obtained by a Laser Dapi (405nm) for DAPI and the Argon Ion Laser (488nm) for GFP. Optical thickness varied from 0.50 μ m for the 20x objective to 0.20 μ m for the 63x objective. Images were process and analyzed with the Zen Blue (3.2) software (Carl Zeiss GmbH) and the ImageJ (version 1.53t) software (National Institutes of Health, <http://imagej.nih.gov/ij>) (see movie 1 and 2, for detail). 3D reconstructions were obtained by the full set of stack images, 15 images for the 20x objective and 34 images for 63 x objective, by the Zen Blue software.

2.8. Expression profiling

For microarray analyses, total RNA was extracted from the bone marrow and spleen of 8- to 10-month-old *Gatal*^{low} and wild-type littermates, purified with Rneasy Mini Kit (Qiagen, Germantown, MD, USA) and hybridized to the Illumina Mouse WG-6V2 Bead Chip gene expression array as described(Zingariello et al., 2017). Functional Annotation Clustering was performed with the David Bioinformatic Database (David Bioinformatics Resources 6.7 NIAID/NIH). Microarray data have been deposited in the Gene Expression Omnibus database (GSE89630) <https://www.ncbi.nlm.nih.gov/geo/query/acc.cgi?token=ijgpwgsyjhwpoj&acc=GSE89630> (Zingariello et al., 2017). Gene Set Enrichment Analysis (GSEA) was performed with the GSEA application version 4.1.0 (<https://www.gsea-msigdb.org/gsea/index.jsp>) with gene set setting for the permutation parameter and Signal2Noise for the metric parameter.

2.8. Statistical Analyses

All the data have a normal distribution, as assessed by Shapiro and Wilk's W test (Graph Pad Software, La Jolla, CA) and are presented either as Mean (\pm SD) or as Median (min–max) of at least three separate experiments, as indicated. Statistical analyses among groups were done either by T-test (comparisons among two groups) or by Tukey for multiple comparison test (comparisons among >three groups), as appropriate. Differences among groups were considered statistically significant with a $p < 0.05$.

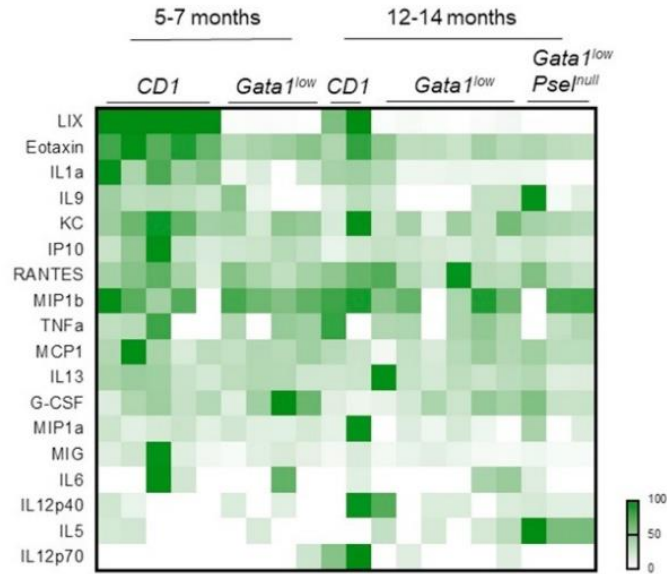
3. Results

3.1. Modest differences in the cytokine profile of *Gata1*^{low} mice with age

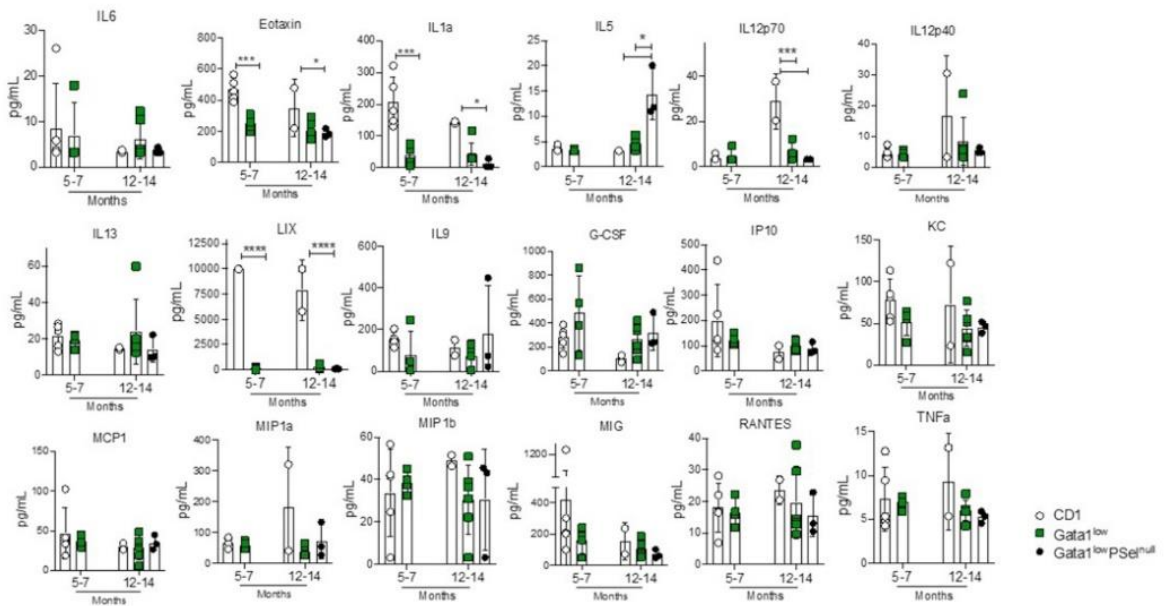
The levels of 32 cytokines in the serum from *Gata1*^{low} mice at 5-7 (when they have not developed myelofibrosis) and 12-14 (with bone marrow fibrosis) months of age were studied. Of the 32 cytokines analyses, only 18 were present at detectable levels in the serum of the mice (IL-6, Eotaxin, IL1a, IL5, IL12p70, IL12p40, IL13, LIX, IL9, G-CSF, IP10, KC, MCP1, MIP1a, MIP1b, MIG, RANTES, TNF α) while the concentration of 14 cytokines (GM-CSF, IFN γ , IL2, IL4, IL10, IL3, IL7, LIF, VEGF, IL1 β , IL15, IL17 and M-CSF) was below the levels detectable with this assay (3.2pg/ml). Detectable cytokines are presented in **Figure 1A** and **B**. Results were compared with those observed in CD1 mice of comparable age and with 12–14-month *Gata1*^{low} mice lacking the *P-selectin* gene (*Psel*^{null}), as negative control. Both wild-type mice and double *Gata1*^{low}*Psel*^{null} mice do not develop fibrosis in bone marrow (Martelli et al., 2005; Spangrude et al., 2016; Vannucchi et al., 2002). The results showed changes in a few cytokines with mostly decreased levels of LIX, IL1a and Eotaxin in young and old *Gata1*^{low} animals, and decreased levels of IL12p70 in old *Gata1*^{low} mice compared to wild-type controls.

Given the great interest in TGF- β 1, LCN2 and CXCL1 in the pathobiology of myelofibrosis (Agarwal et al., 2016; Tefferi et al., 2011; Tillmann et al., 2021), the serum levels of these three inflammatory cytokines were compared by ELISA using larger cohorts of mice. Also, in these set of experiments, *Gata1*^{low}*Psel*^{null} (and *Psel*^{null} mice) were analyzed as additional negative control. Age and sex did not affect the values observed in the different experimental groups. Therefore, results obtained with young and old or males and females were combined. The serum of *Gata1*^{low} mice contained levels of LCN2 and CXCL1 significantly lower than that of CD1 mice or of mice lacking *Psel* with or without the *Gata1*^{low} mutations (**Figure 1C**). In a previous publication, we demonstrated that the serum of *Gata1*^{low} mice contains TGF- β 1 levels modestly (2-fold) higher than that of CD1 mice (2.4 vs 1.5ng/mL, respectively) (Zingariello et al., 2013). Here we confirm that these levels are slightly higher also from that of *Psel*^{null} and *Gata1*^{low}*Psel*^{null} mice.

A



B



C

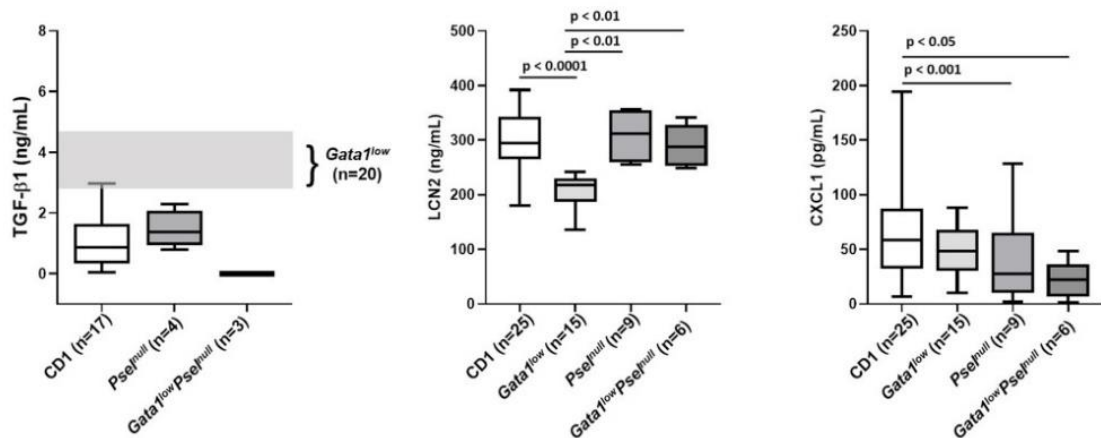


Figure 1. Modest changes in inflammatory cytokine profilings of sera from *Gata1*^{low} mice with age and with respect to CD1 littermates wild-type at the *Gata1* locus and to *Gata1*^{low}*Psel*^{null} mice. **A)** Heatmap of detectable cytokines. **B)** Concentration values for each cytokine detected. p values were calculated with multiple comparison t-tests for each cytokine. **C)** Serum levels determined by ELISA of TGF-β1 (left), CXCL1 (middle) and LCN2 (right) in CD1 mice wild-

type at the *Gata1* locus, in *Gata1*^{low} mice and in mice lacking the *Psel* gene with and without the *Gata1*^{low} mutation. The number of mice analysed in each experimental group is indicated by n. Statistical Analyses was performed with multiple comparison test. Since when age and sex were analysed as independent variable did not reveal any statistically significant difference, results obtained at different ages in females and males were pooled. The levels of TGF-β1 in the serum from *Gata1*^{low} mice which were previously reported (Zingariello et al., 2013) and are indicated as shaded areas in the left panel.

3.2. The genetic background is a confounding factor in determining the normal levels of TGF-β1, LCN2 and CXCL1 in mice

Given the great importance of the pro-inflammatory cytokines in the development of myelofibrosis (Koschmieder & Chatain, 2020; Migliaccio, 2018), the modest differences found in the serum levels among CD1 mice harboring the *Gata1*^{low} mutation or wild-type at this locus was puzzling. It has been previously shown that the mouse strain plays an important role in the manifestation of myelofibrosis induced by the *Gata1*^{low} mutation (Martelli et al., 2005). In the C57BL/6 background, the *Gata1*^{low} mutation is lethal at birth with the few (~5%) surviving mice developing myelofibrosis within the first 1-2 months (Eliades et al., 2011; McDevitt et al., 1997). In the CD1 background, *Gata1*^{low} mice are viable at birth because rapidly recruit the spleen as extramedullary site but slowly develop myelofibrosis while aging (Martelli et al., 2005; Vannucchi et al., 2002). By contrast, in the DBA/2 background, *Gata1*^{low} mice are born viable and develop thrombocytopenia and anemia with age but never develop myelofibrosis (Martelli et al., 2005).

A careful analysis of the pathobiology of laboratory mice with age and of the cause of their natural death indicates the existence of a vast variegation of inflammatory manifestations among different strains (Brayton et al., 2012). In fact, in addition to neoplasms of the hematopoietic, lung, liver and mammary glands which are developed by mice of most strains, CD1 mice die more frequently of pathologies associated with inflammatory signatures such as amyloidosis, arteritis, glomerulonephritis, ulcerative dermatitis, fatty liver and pneumonia than C57BL/6 and DBA/2 mice (Brayton et al., 2012). These results suggest that the absence of differences between the levels of cytokines present in the serum between *Gata1*^{low} and wild-type littermates described in **Figure 1** may be confounded by the fact that the serum of mice in the CD1 background contains basal levels of pro-inflammatory cytokines higher than that of other strains. To test this hypothesis, we compared the levels of TGF-β1, LCN2 and CXCL1 in the sera from CD1, C57BL/6 and DBA2 mice obtained from commercial sources (**Figure 2**). Serum was collected from both males and females at 5-7 months (adult) and 12-14 months (old) of age and since the results from females and males or young and adult mice were similar, they were pooled. Indeed, there was a good correlation between the reported manifestation of inflammatory diseases (Brayton et al., 2012) and serum levels of TGF-β1, LCN2 and CXCL1 among different strains. CD1 mice expressed levels of all three inflammatory cytokines significantly greater than those expressed by DBA/2 mice while C57BL/6 mice expressed only levels of LCN2 and CXCL1 greater than DBA/2 mice.

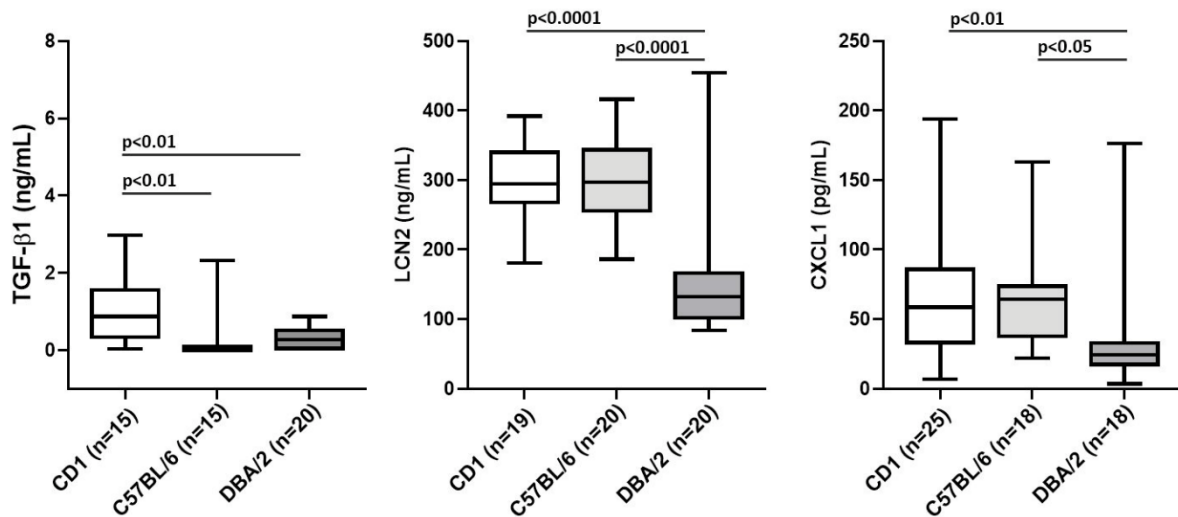


Figure 2. The serum from CD1 mice contains greater levels of pro-inflammatory cytokines than that from C57BL/6 or DBA/2 mice. The number of mice analyzed per experimental group is indicated by n. p values were calculated with Tukey multiple comparison test and statistically significant differences ($p < 0.05$) indicated in the panels.

To assess whether the wild-type littermates of *Gatal*^{low} mice develop with age pathological conditions associated with inflammation, we conducted histopathological examinations of sections from their organs (**Figure 3**). Hematoxylin-eosin-stained sections of lungs, hearts, kidneys, spleens, livers and skins from 6 mice (4 males and 2 females) below 6 months old and from 15 mice (9 males and 6 females) above of 11 months of age were analyzed (**Figure 3** and data not shown). None of the mice younger than 6 months showed detectable changes in the tissues observed (data not shown) while chronic inflammation, often involving more than one organ, was often apparent in samples from older animals. The most frequent lesion was interstitial pneumonia (7/15 mice) (**Figure 3A and B**), followed by nephritis (5/15 mice) with a mixed expression of chronic glomerulonephritis associated to interstitial nephritis (**Figure 3C**). Arteriopathy with mural calcification was apparent in kidneys of two mice (**Figure 3D**), while only in one mouse it was observed amyloidosis in the spleen (**Figure 3E**), interstitial hepatitis (**Figure 3F**), chronic dermatitis (**Figure 3G**) and steatonecrosis (**Figure 3H**). The mouse with amyloidosis showed interstitial hepatitis as associated lesion.

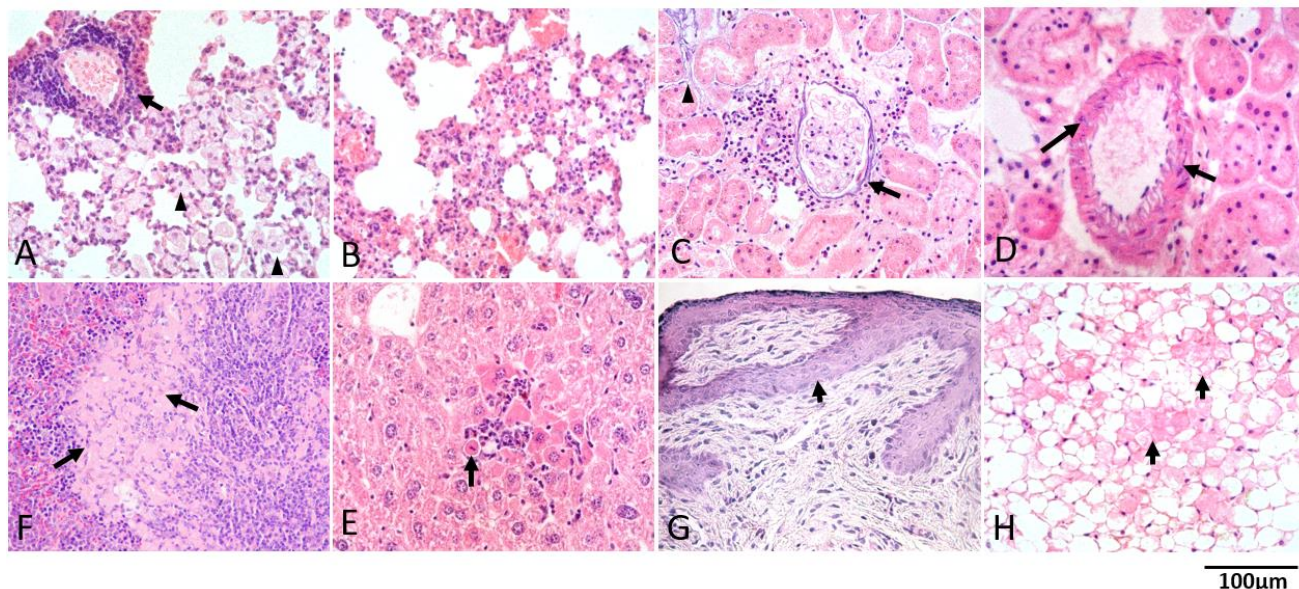


Figure 3. The organs from 12-14-months old wild-type littermates of *Gata1*^{low} mice present a histopathological signature consistent with multisite inflammation. Hematoxylin/Eosin staining of representative sections showing the presence of interstitial pneumonia with lymphocytes infiltrating the peri-broncho-vascular space (arrow), macrophages collection in alveoli (arrowheads) (A) and irregular thickening of alveolar septa by lymphocytes (B); Nephritis with a mixed expression of chronic glomerulonephritis (hypocellular glomerulus) and interstitial nephritis with lymphocytes infiltrating the inter-tubular and perivascular space with basophilic linear deposits along the basement membrane of Bowman's capsule (arrow) and of tubules (arrowhead) (C); Arteriopathy with mural calcification: basophilic granular deposits beneath endothelial cells and between leiomyocytes, i.e. smooth muscle cells around the vessels (arrows) (D). Interstitial hepatitis with intralobular collection of lymphocytes surrounding shrunken and hyper-eosinophilic hepatocytes undergoing apoptosis (arrow) (E); Interstitial collection of faintly eosinophilic homogeneous material referable to amyloid (arrows) in the spleen (F), chronic dermatitis with dermal fibrosis, lack of adnexa and hyperplasia of epidermis (arrow) with acanthosis in the skin (G) and steatonecrosis of the perirenal fat (arrows) (H). Magnification 40x. Results are representative of those observed in 15 mice (age \geq 11 months, 9 males and 6 females).

3.3. The bone marrow microenvironment of *Gata1*^{low} mice contain abnormally high levels of megakaryocytes, endothelial cells, mesenchymal cells and osteoblasts.

HSC are sustained by specific niche cells of the bone marrow microenvironment, namely by endothelial cells present in the microvasculature (Szade et al., 2018). Evidence is emerging, however that the nature of the supporting niche changes with age and/or under inflammatory states, although the identity of the cells supporting the HSC under these conditions has not been clarified as yet (Raaijmakers, 2019; Yang & de Haan, 2021). In addition, MPN is associated with profound differences in the composition of the cells of the microenvironment. The Passegué laboratory had demonstrated that the malignant hematopoietic cells of the Bcr/Abl-driven mouse model of chronic MPN progressively remodels the endosteal BM niche into a self-reinforcing leukemic niche that impairs normal hematopoiesis, favoring the leukemic stem cell function and contributing to bone marrow fibrosis (Schepers et al., 2013). This remodeling requires direct cell-cell interaction and changes in the expression levels of TGF- β , Notch, and other inflammatory signaling. In addition, in the case of JAK2-

driven MPN, it has been shown that in patients and in animal models the disease is driven by a consistent reduction in the numbers of sympathetic nerve fibers, supporting Schwann cells, which regulates the HSC supporting functions of a subpopulation of nestin⁺ mesenchymal stem cells (Arranz et al., 2014; Drexler et al., 2019). To clarify the cell population(s) responsible for establishing a pro-inflammatory milieu in the bone marrow of *Gata1*^{low} mice, we first compared the frequency of stromal cells, and of hematopoietic cells (megakaryocytes and neutrophils) with microenvironmental shaping functions (Schmitt et al., 2002; Wolach et al., 2018), in the bone marrow from *Gata1*^{low} and wild-type littermates (**Figure 4**).

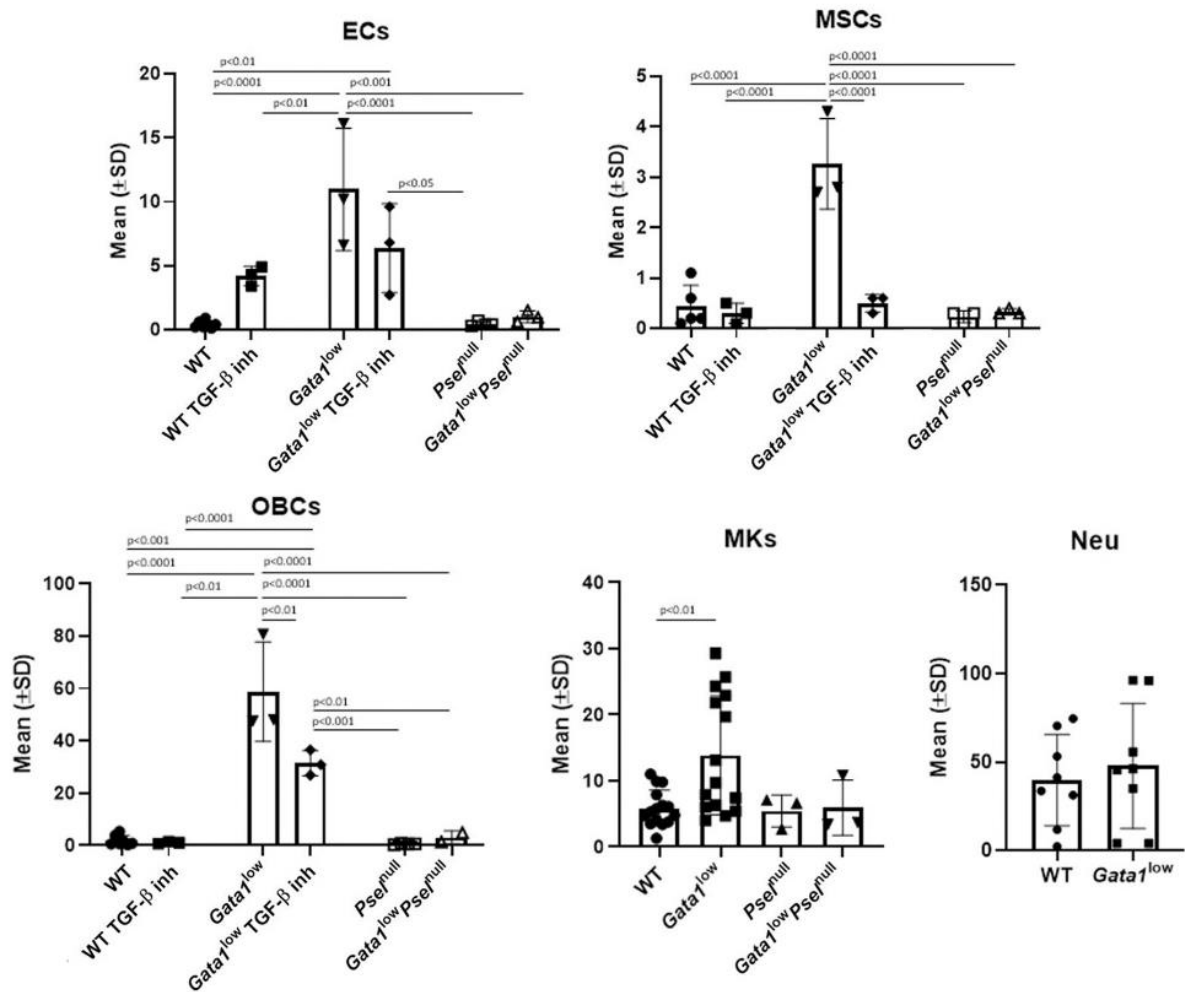


Figure 4. The bone marrow from *Gata1*^{low} mice (12-14- months of age) contains levels of endothelial cells, mesenchymal stem cells, osteoblasts and megakaryocytes greater than those present in the bone marrow from wild-type littermates. The levels of these cells in the mutant mice were greatly reduced by treatment with a TGF-β1 inhibitor and/or by deletion of the *P-sel* gene. Cells were identified according to previously described flow cytometry criteria (Ghinassi et al., 2007; Schepers et al., 2013) (see Figure S1 for the detail of the gates). Results are presented as Mean (±SD) and as values of individual mice (each dot an individual mouse). P-values were calculated with Tukey multiple comparison and those statistically significant are indicated in the panels.

The frequencies of megakaryocytes, endothelial and mesenchymal cells, and osteoblasts in the bone marrow from *Gata1*^{low} mice are all greater than normal while those of the neutrophils are within normal ranges (**Figure 4**). The greater frequency of megakaryocytes is consistent with previous reports

(Vannucchi et al., 2005) while that of endothelial cells and of osteoblasts is consistent with the increased vascularization and osteogenesis observed in these mice (Kacena et al., 2004; Vannucchi et al., 2005) which recapitulate that seen in myelofibrosis patients (Barosi & Hoffman, 2005). Deletion of *Psel* and pharmacological inhibition of TGF- β normalized the frequency of endothelial cells, of mesenchymal cells and osteoblasts found in *Gata1*^{low} bone marrow. These observations are consistent with the finding that deletion of *Psel*, probably by reducing TGF- β bioavailability, and inhibition of TGF- β both reduces osteopetrosis and neo-vascularization in *Gata1*^{low} mice (Spangrude et al., 2016; Varricchio et al., 2021; Zingariello et al., 2013).

These results indicate that the microenvironment of the bone marrow from *Gata1*^{low} mice contains altered levels of stromal and hematopoietic cells which can all be targets and/or producers of pro-inflammatory cytokines.

*3.4. The bone marrow from *Gata1*^{low} mice contains high levels of TGF- β 1, LCN2 and CXCL1 produced by the malignant megakaryocytes*

By contrast with the modest differences in pro-inflammatory cytokines in the serum of *Gata1*^{low} mice and wild-type littermates (**Figure 1C**), in previous publications, we reported immunohistochemistry studies indicating that the bone marrow from *Gata1*^{low} mice contains levels of TGF- β 1, LCN2 and CXCL1 greater than normal ((A. Dunbar et al., 2021; Zingariello et al., 2013) and **Figure S4**). These cytokines may be produced by several cell types present in the bone marrow microenvironment: TGF- β 1 may be produced by endothelial cells (Yousef et al., 2015) and megakaryocytes (Zingariello et al., 2013), LCN2 by neutrophils (Schmidt-Ott et al., 2006) and CXCL1 by megakaryocytes, endothelial cells, osteoblasts and neutrophils (Eash et al., 2010; Köhler et al., 2011).

The increased frequencies of stromal cells described above raise then the question whether the increased cytokine bioavailability in the bone marrow of *Gata1*^{low} mice is a consequence of altered numbers of producing cells and/or by altered levels of cytokine produced by a specific cell type. To answer this question, we compared the levels of cytokine expressed by individual cell types identified on the basis of morphological criteria in bone marrow sections immune-stained with antibodies against the three different cytokines. Endothelial cells were recognized as flat cells surrounding structures resembling vessels (i.e. optically empty channels containing red blood cells); osteoblasts were identified as cuboidal cells on the endosteum of the bones; megakaryocytes on the basis of their size (10 times greater than that of any other cell type) and the polylobate morphology of their nuclei and neutrophils on the basis of their small size (9 μ m) and kidney shaped nuclei (**Figure 5**).

As expected (Yousef et al., 2015; Zingariello et al., 2013), in the bone marrow of wild-type mice, TGF- β 1 was expressed at detectable levels by endothelial cells and megakaryocytes (**Figure 5A**). Also, in the bone marrow from *Gata1*^{low} mice, TGF- β 1 was expressed by endothelial cells and

megakaryocytes but, as previously reported (Zingariello et al., 2013), the TGF- β 1 immunostaining of the malignant megakaryocytes is significantly stronger than that of the corresponding wild-type cells. These results suggest that the increased bioavailability of TGF- β 1 in the bone marrow microenvironment of the mutant mice is due both to the increased number of megakaryocytes and to the greater amount of TGF- β 1 they produce at the single cell level (**Figure 5B**).

As expected (Schmidt-Ott et al., 2006), in the bone marrow of wild-type mice, LCN2 is contained mostly in neutrophils (**Figure 5A**). By contrast in the bone marrow of *Gata1*^{low} mice, LCN2 is expressed at detectable levels both by neutrophils and megakaryocytes (**Figure 5B**). The expression of LCN2 in the malignant megakaryocytes is consistent with the great levels of LCN2 previously reported in megakaryocytes expanded *in vitro* from MF patients (Lu et al., 2015). Therefore, the increased bioavailability of LCN2 in the microenvironment of *Gata1*^{low} mice is due to production by a novel cell type, i.e. the malignant megakaryocytes.

As expected (Eash et al., 2010; Köhler et al., 2011), in the bone marrow of wild-type mice, CXCL1 is expressed at detectable levels by endothelial cells, osteoblasts, megakaryocytes and neutrophils (**Figure 5A**). In the bone marrow of *Gata1*^{low} mice, CXCL1 is expressed by the same cells which express this growth factor in the wild-type organ but the expression in the malignant megakaryocytes is much greater levels than in their corresponding wild-type cells (**Figure 5B**). Therefore, as for TGF- β 1, the increased bioavailability of CXCL1 in the microenvironment of *Gata1*^{low} mice is due to the increased numbers of megakaryocytes that produce greater levels of this growth factor per cell.

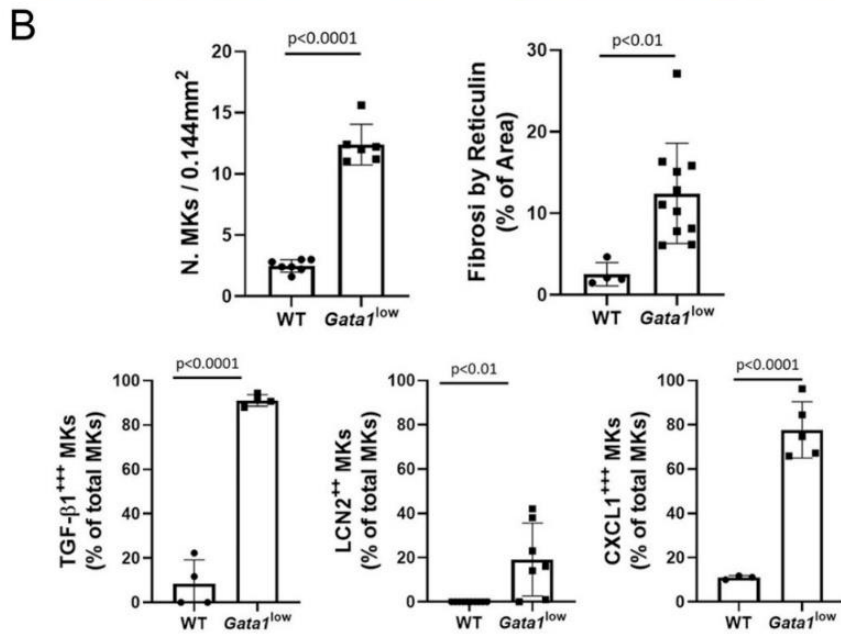
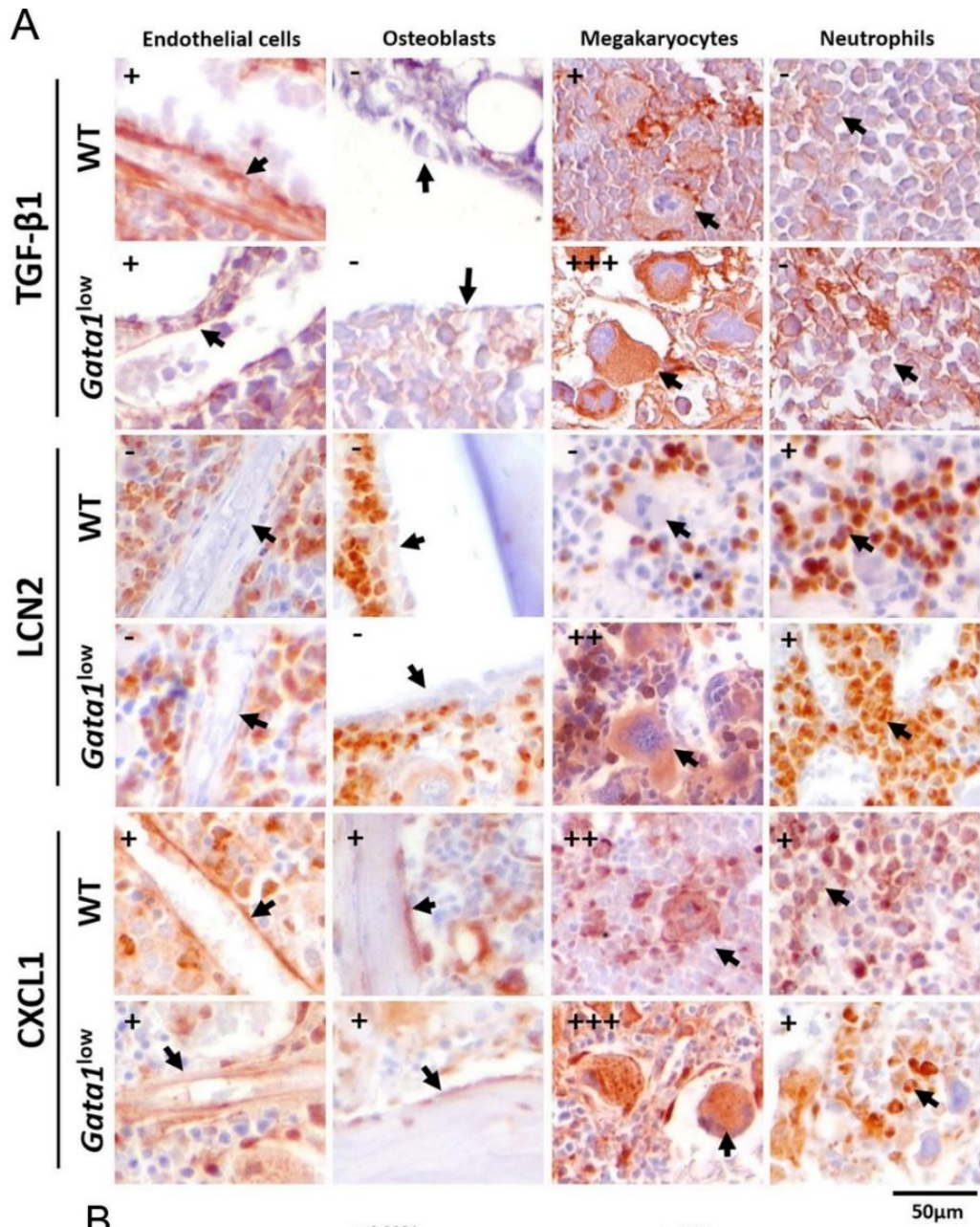


Figure 5. Megakaryocytes from the bone marrow of *Gata1*^{low} mice contain more TGF- β 1, LCN2 and CXCL1 than the

corresponding cells from the wild-type littermates. **A**) Representative sections from the bone marrow of wild-type and *Gata1*^{low} littermates immuno-stained with antibodies per TGF- β 1, LCN2 and CXCL1 showing the level of these cytokines in endothelial cells, osteoblasts, megakaryocytes and neutrophils (all indicated by arrows) recognized by morphological criteria as indicated. Semi-quantitative estimates (-, +, ++ or +++) of the intensity of the staining in each population is indicated on the top left. Original magnification 40x. **B**) Quantification of TGF- β 1, LCN2 and CXCL1 expressing MKs of wild-type and *Gata1*^{low} mice. Frequency of total megakaryocytes, levels of fibrosis (as control) and percent of megakaryocytes expressing high levels of TGF- β 1, LCN2 and CXCL1 in bone marrow section from *Gata1*^{low} and wild type littermates, as indicated. The content of pro-inflammatory cytokines in the megakaryocytes was quantified as described in Figure S2 using 5 randomly selected areas per femur from three-four mice per experimental group. Statistical analysis was done by t-test and statistically significant p-values among groups are indicated within the panels.

3.5. Megakaryocytes from the bone marrow of *Gata1*^{low} mice express greater levels of CXCR1 and CXCR2

CXCL1 has been described to exert its biological effects by activating CXCR1 expressed by endothelial cells, osteoblasts and megakaryocytes (Hoshino et al., 2013; Kowalska et al., 1999; Li et al., 2003; Teijeira et al., 2020) while CXCR2 is specifically expressed by neutrophils (Eash et al., 2010; Teijeira et al., 2020). To clarify which cell type may be responding to the greater levels of CXCL1 observed in the bone marrow of *Gata1*^{low} mice, immunostaining studies with anti-CXCR1 and CXCR2 antibodies were performed (**Figure 6**). In wild-type bone marrow, CXCR1 expression was detectable at great levels on endothelial cells and neutrophils and at lower levels on osteoblasts and megakaryocytes while CXCR2 was detectable at high levels on neutrophils, at low levels on endothelial cells and megakaryocytes and levels barely detectable on osteoblasts. By contrast, as previously reported (A. Dunbar et al., 2021), the bone marrow from *Gata1*^{low} mice expressed total levels of CXCR1 greater than normal (**Figure S5**). At the single cell levels, CXCR1 and CXCR2 were expressed at levels similar to those found in wild-type mice in the endothelial cells, osteoblasts and neutrophils of the mutant mice but it was expressed at levels much greater than normal in megakaryocytes (**Figure 6**), indicating that the great content of receptors observed in the bone marrow is likely a reflection of its great megakaryocyte content.

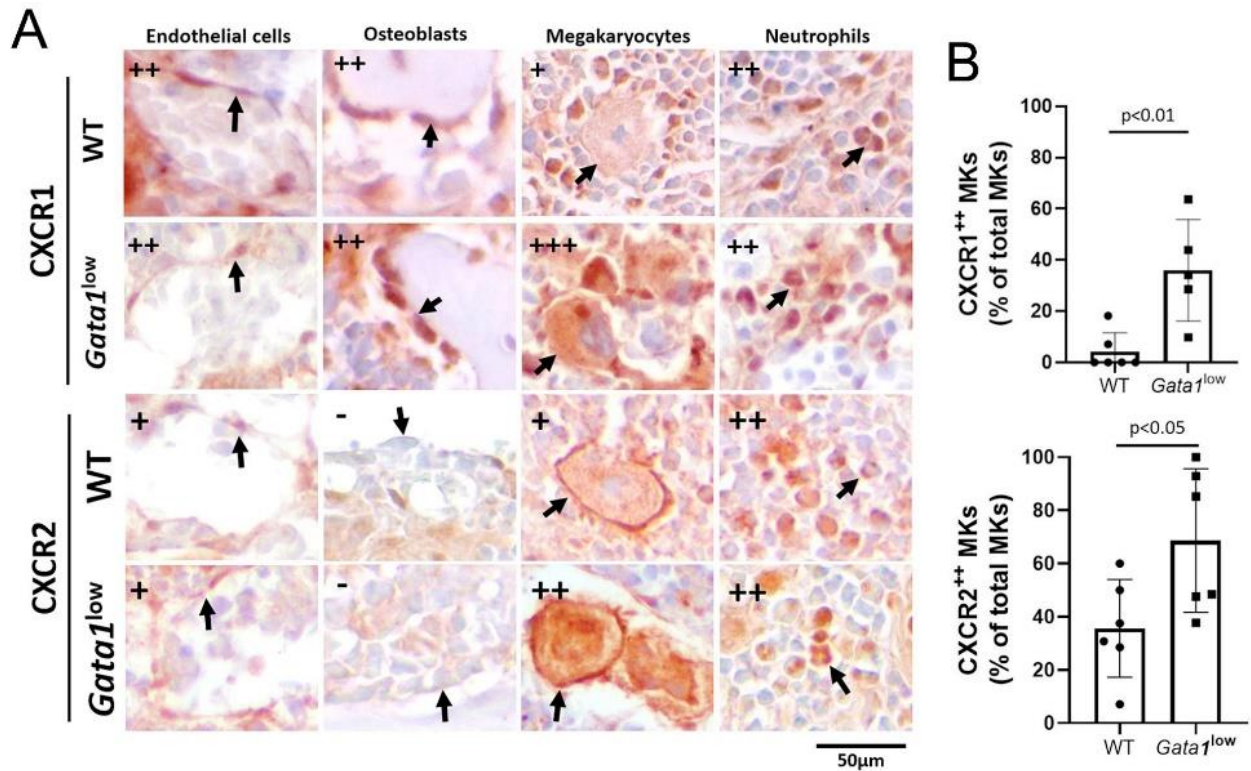


Figure 6. Malignant megakaryocytes express great levels of CXCR1 and CXCR2. **A)** Representative sections from the bone marrow of wild-type and *Gata1*^{low} littermates immunostained with antibodies per CXCR1 and CXCR2 showing the level of these receptors in endothelial cells, osteoblasts, megakaryocytes and neutrophils (indicated with arrows). Semiquantitative estimates (-, + or ++) of the intensity of the staining in the different cells are provided on the top left. Original magnification 40x. **B)** Percentage of megakaryocytes expressing high levels of CXCR1 and CXCR2. The pro-inflammatory cytokines were quantified as described in **Figure S2B** on 5 randomly selected areas per femur from three-four mice per experimental group. Statistical analysis was done by t-test and statistically significant p values among groups are indicated within the panels.

In previous publications, we have demonstrated that increased TGF- β bioavailability activates a TGF- β expression signature in the bone marrow from *Gata1*^{low} mice (Zingariello et al., 2013). Since LCN2 activates CXCL1 expression (Jeon et al., 2013), the greater levels of CXCL1 observed in the bone marrow of the mutant mice (**Figure 5** and **S4**) provides indirect proof that the LCN2 signaling is also activated in this organ. However, there is no indication so far that increased CXCL1 bioavailability activates this pathway in the bone marrow from *Gata1*^{low} mice. To fill this gap, we combed the published expression profile of *Gata1*^{low} bone marrow (Ling et al., 2018) for genes downstream to the two receptors of CXCL1, CXCR1 and CXCR2 (**Figure 7**). This analysis demonstrated a statistically significant activation of genes downstream to both CXCR1 and CXCR2.

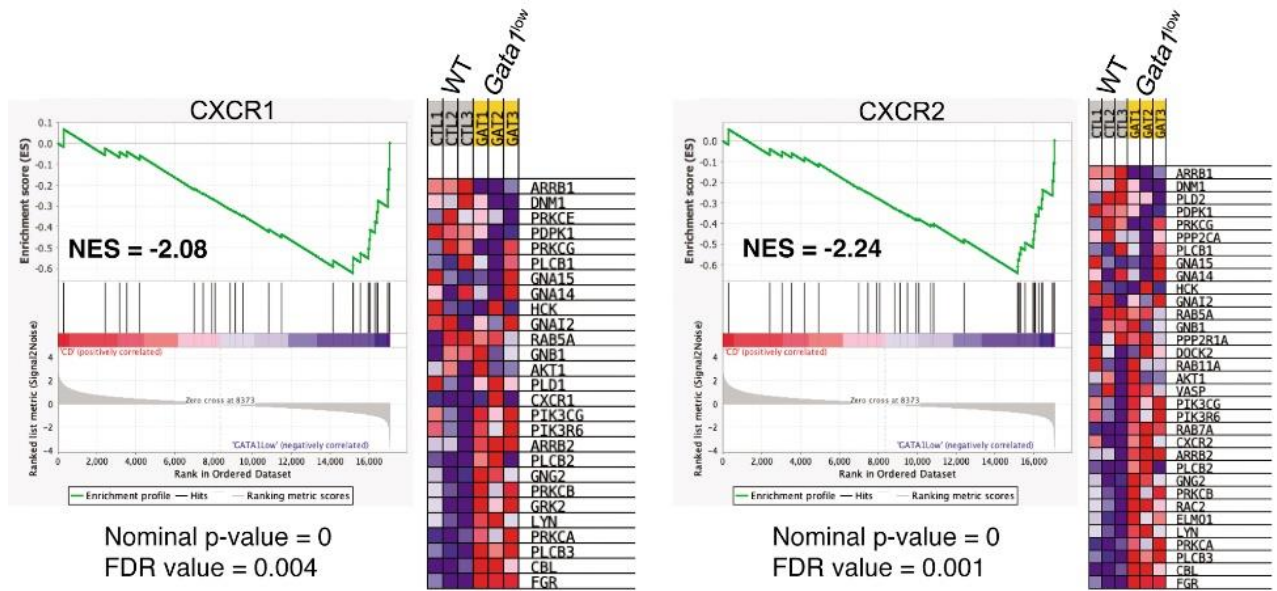


Figure 7. Both CXCR1 and CXCR2 gene signatures are enriched in *Gata1*^{low} bone marrow. Gene set enrichment analysis (GSEA) for the CXCR1 and CXCR2 signatures and heat maps of differentially expressed genes of the CXCR1 and CXCR2 pathway.

3.4. In the bone marrow from old wild-type mice, HSC are distributed around adipocytes while in that from *Gata1*^{low} mice HSC are localized in areas of the medulla between bone trabeculae and vessels which contain great numbers of megakaryocytes

The *huCD34-GFPH2B* mice were generated by the Moore Lemischka laboratory to track the changes occurring in HSC properties when these cells divide (Qiu et al., 2014). Since the expression of *GFPH2B* is driven by the regulatory sequences of the human *CD34* gene which in mice are active only in HSC (Radomska et al., 2002), the *GFPH2B* transgene is expressed only by HSC with the stringent SLAM phenotype which correspond to cells with long term repopulation potential (Qiu et al., 2014). Since the GFPH2B protein is a histone incorporated in the chromosomes in stoichiometrically constant ration with the amount of their DNA, the levels of GFP expressed by the HSC in each mouse is extremely constant. However, since *hCD34* is no longer active as soon as the progeny of the HSC are committed to differentiate, only the immediate committed HSC progeny (short term repopulating HSC and multi-lineage progenitor cells) retain some GFP signal inherited from the chromatids of their mother (Qiu et al., 2014). Studies on prospective cell isolation based on levels of GFP expression combined with functional analyses have demonstrated that only long-term repopulating HSC are GFP^{high} while short term repopulating HSC are GFP^{medium}, multipotent progenitor cells are GFP^{low} and lineage restricted progenitor cells no longer express detectable levels of GFP (Qiu et al., 2014).

By flow cytometry, we confirmed that GFP is not expressed by the cKIT⁻ cell fraction which does not contain HSC/progenitor cells of the bone marrow from *huCD34-GFPH2B* mice while it is expressed over a good range of intensities by the LSK cells with the greatest levels expressed by the 18% of LSK with the SLAM phenotype, which identified the long-term repopulating HSC (**Figure 8**).

To a surprise, however, GFP was expressed by the cKIT⁻ cells from the bone marrow of *huCD34-GFPH2B/Gata1^{low}* mice although it is expressed over a good range of intensity by LSK with the greatest levels detected in the very few (1%) of the LSK with a SLAM phenotype (**Figure 8**). The reduced numbers of SLAM cells detected in the bone marrow of *huCD34-GFPH2B/Gata1^{low}* mice is consistent with previous publications which have demonstrated that in *Gata1^{low}* mice most of the SLAM cells are in the spleen(Spangrude et al., 2016).

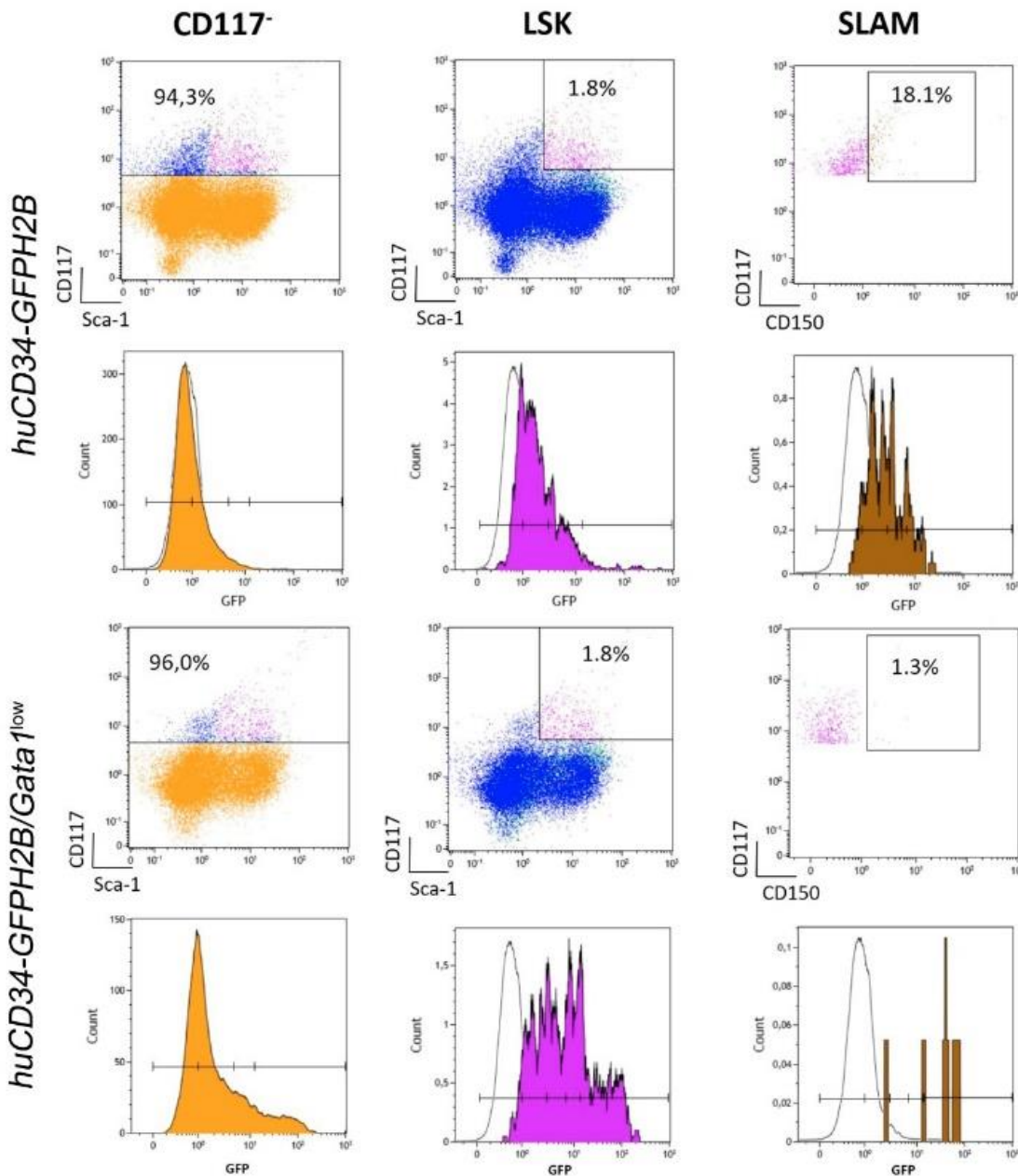


Figure 8. By flow cytometry, in the bone marrow of wild type mice GFP is expressed only by cells in the LSK gate while in that from *Gata1^{low}* mice GFP is expressed both by non LSK and LSC cells. Scatter plots of bone marrow cells from representative *huCD34-GFPH2B* and *huCD34-GFPH2B/Gata1^{low}* littermates showing the gates used to identify cKIT⁻ cells (orange events), LSK (purple events) and SLAM (brown events) cells, as indicated. The intensity of the GFP expressed in the different populations is shown as colour coded histograms below each panel. The dotted histogram included in each panel indicate the signal in the GFP channels from the corresponding cells from the bone marrow of *hCD34* and *hCD34/Gata1^{low}* mice, used as negative controls.

By confocal microscopy, cells expressing GFP were clearly detectable in the bone marrow from both *huCD34-GFPH2B* and *huCD34-GFPH2B/Gata1^{low}* littermates (**Figure 9 and 10**). Stacking analyses indicated that in wild-type mice GFP was mostly detectable in small cells where it was localized in the nucleus and in very few large cells where it was localized in the cytoplasm (**Figure S3A**). GFP was mostly localized in the nucleus of small cells also in the bone marrow from *huCD34-GFPH2B/Gata1^{low}* mice, but, by contrast with *huCD34-GFPH2B* mice, in this case the GFP was localized in the cytoplasm of a great numbers of large cells that had the morphology of macrophages (**Figure S3B** and data not shown). These results suggest that the large proportion of *huCD34-GFPH2B/Gata1^{low}* cKIT⁻ bone marrow cells that had been found to express GFP by flow cytometry (**Figure 8**) are likely macrophages that have phagocytized malignant the HSC which had likely died by apoptosis induced by the pro-inflammatory environment of the *huCD34-GFPH2B/Gata1^{low}* bone marrow (Caiado et al., 2021).

Using these data as a foundation, we determined the localization of small GFP-tagged cells (which represent long- and short-term repopulating HSC and multilineage progenitor cells) within the bone marrow architecture of *huCD34-GFPH2B* and *huCD34-GFPH2B/Gata1^{low}* mice (**Figure 9 and 10**). In the femur from old wild-type mice, GFP-tagged cells were localized either in clusters in the epiphysis of the femur or in the diaphysis area within the medulla (**Figure 9**). The brightest GFP-cells were found in the epiphysis and lined optically empty circles, a feature that characterizes areas occupied by adipocytes (**Figure 9 and S3B**). Interestingly, the cells around each cluster expressed homogenous level of GFP intensity (either high or low), suggesting that in old *huCD34-GFPH2B* mice cells HSC with similar potency tend to remain localized together.

In agreement with the flow cytometry data indicating that in the bone marrow of *huCD34-GFPH2B/Gata1^{low}* mice GFP^{high} SLAM cells are very few, the spleen from *Gata1^{low}* mice contained much more GFP⁺ cell than that from *huCD34-GFPH2B* mice (data not shown). In addition, in *huCD34-GFPH2B/Gata1^{low}* mice, the nuclear fluorescent intensity in the cells from the spleen was significantly greater than that from the cells of the bone marrow (17.85 ± 12.98 vs 6.88 ± 4.47 mean fluorescent intensity/cell in the spleen and in bone marrow, respectively). These data confirm previous observations indicating that in *Gata1^{low}* mice a vast majority of the SLAM are in the spleen (Spangrude et al., 2016).

By contrast with the localization of GFP cells observed in the bone marrow from *huCD34-GFPH2B* mice, although the femur of *huCD34-GFPH2B/Gata1^{low}* mice contain more adipocytes than that of their *huCD34-GFPH2B* littermates (**Figure 10** and data not shown), cells expressing GFP were rarely associated with the optically empty circles but instead were localized mostly in the medulla in areas containing micro-vessels and neo-formed bone trabeculae (**Figure 10**). These areas also contained megakaryocytes.

huCD34-GFPH2B

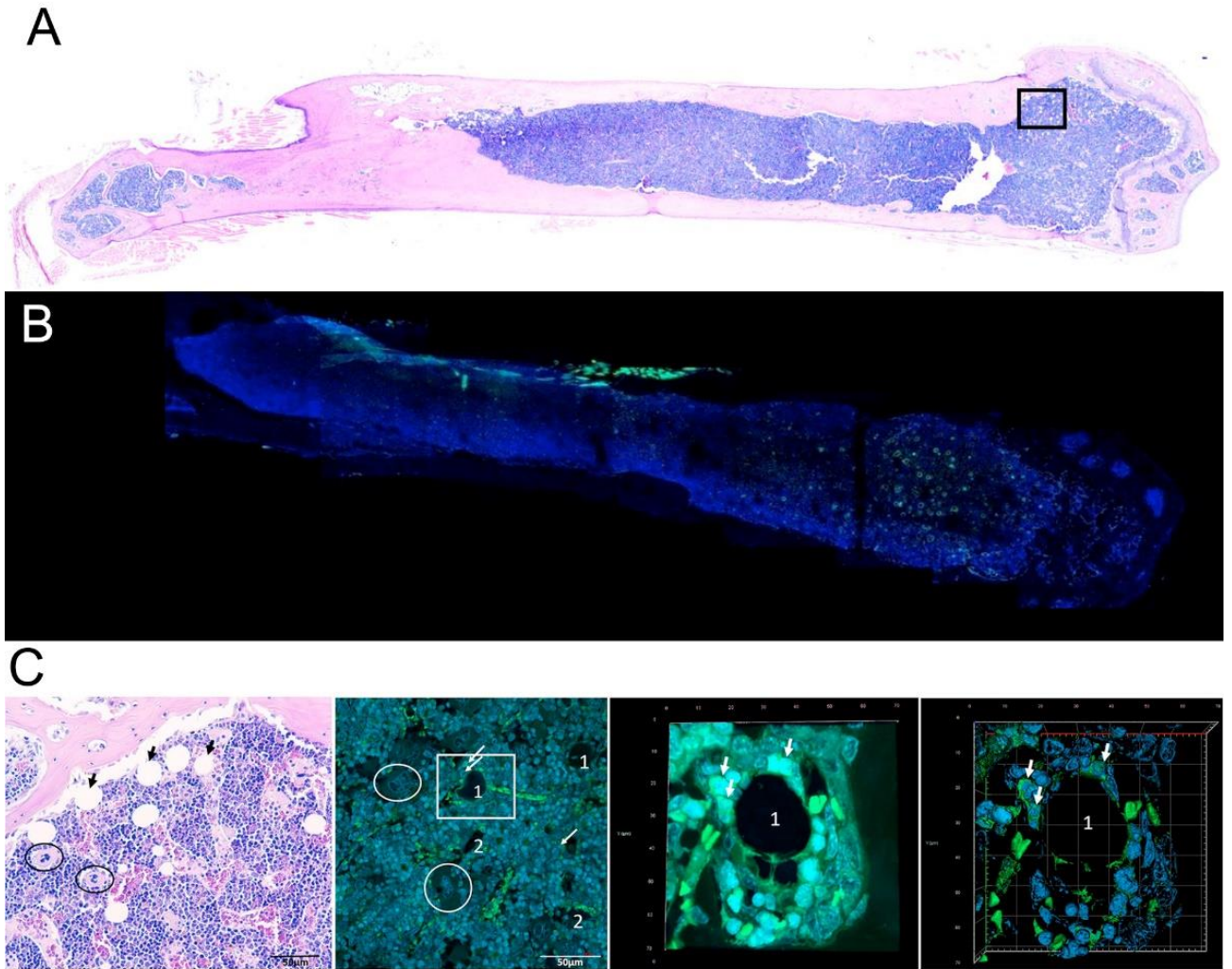


Figure 9. Confocal microscopy analyses of the distribution of GFP-positive cells within the bone marrow architecture of *huCD34-GFPH2B* mice. **A)** The H&E staining of a femur section from one representative *huCD34-GFPH2B* mouse reveals hypercellular bone marrow with scant residual adipocytes well visible in H&E figure in C. **B)** Confocal microscopy analyses with GFP and DAPI of a femur from one representative *huCD34-GFPH2B* mouse revealing that GFP+ cells are mostly distributed in the epiphysis of the femur. **C)** Representative panels showing at larger magnification the areas indicated in rectangles in A (H&E staining, left panel) and in B (confocal microscopy, second panel of the left). The rectangle on the second panel on the left is shown as stack image and as tridimensional reconstruction on the right. The tridimensional reconstruction is shown in detail in Video 3. Black arrows in A indicate adipocytes, circles indicate megakaryocyte clusters, white arrows indicate GFP-positive cells. A and B are photomerge of 4x magnification pictures, in C the magnifications are 20x for the first and second panel, 40x for the third and fourth panel.

huCD34-GFPH2B/Gata1^{low}

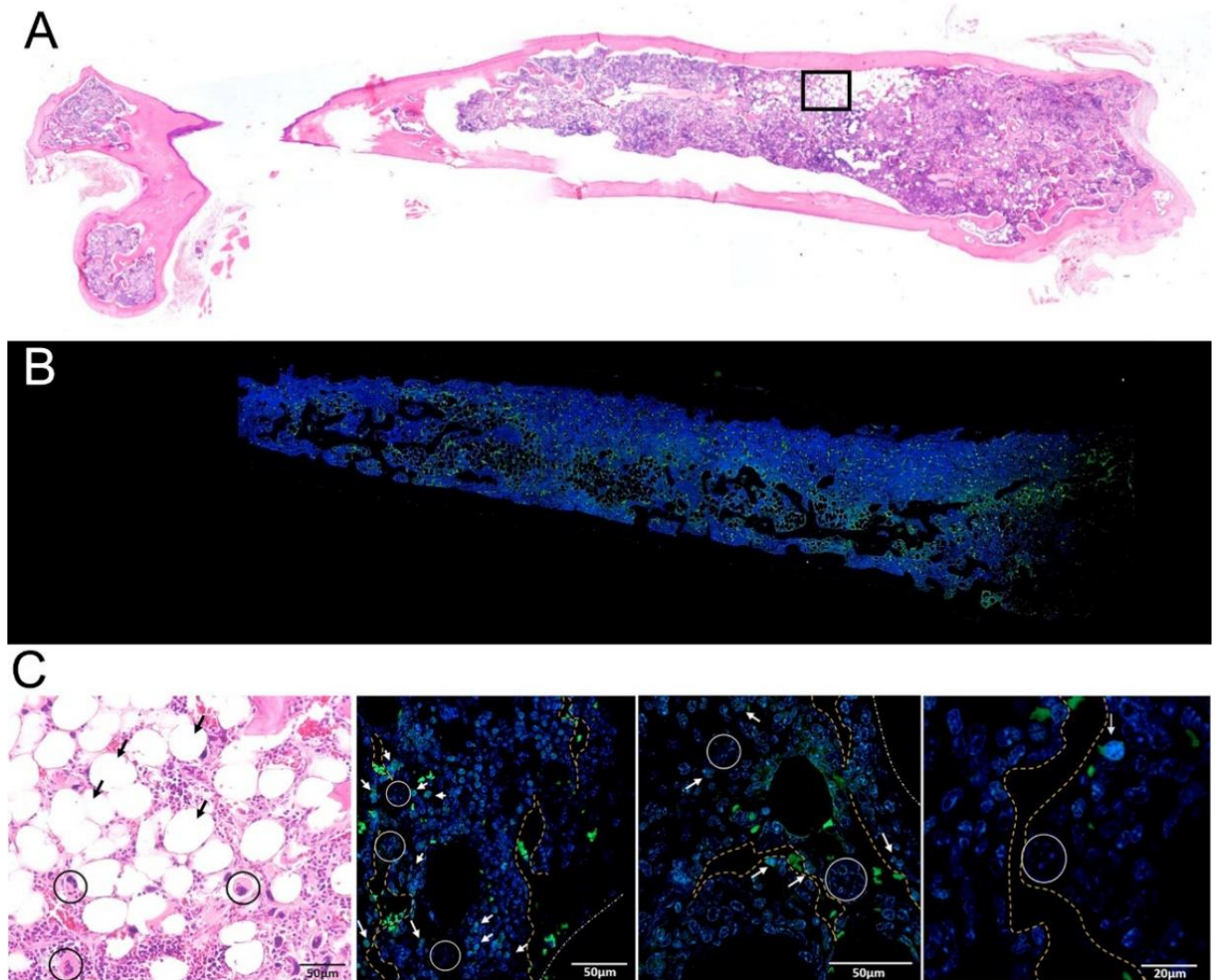


Figure 10. Confocal microscopy analyses of the distribution of GFP-positive HSC within the bone marrow architecture of *huCD34-GFPH2B/Gata1^{low}* mice. **A)** H&E staining of a femur section from a representative *huCD34-GFPH2B/Gata1^{low}* reveals hypocellular bone marrow with adipocyte hyperplasia associated with fibrosis and abundance of megakaryocytes. **B)** Confocal microscopy analyses with GFP and DAPI of a femur section from one representative *huCD34-GFPH2B* mouse revealing that GFP+ cells are distributed both in the epiphysis and in the diaphysis of the femur. **C)** Left panel: larger magnification of the rectangle in the H&E-stained section in A showing the great numbers of adipocytes (black arrows) and megakaryocytes (circles) present in the femur of the mutant mice. Other panels, larger magnifications of the confocal microscopy analyses of the femur shown in B indicating the localization of the GFP+ cells within the bone marrow architecture. White arrows indicate GFP-positive cells, circles indicate megakaryocyte clusters, white dashed lines indicate the contour of micro-vessels while yellow dashed lines indicate the contour of the neo-formed bones. A and B are photomerge of 4x magnification pictures, in C the magnifications are 20x for the first and second panel, 40x for the third panel and 60x for the fourth panel.

Angiogenesis and neo-bone formation are sustained by the interplay between TGF- β , VEGF and BMP-4 (Hankenson et al., 2015; Lin et al., 2015; Nguyen et al., 2013; Shen et al., 2009). We have previously shown that the bone marrow of *Gata1^{low}* mice contain high levels of VEGF (Vannucchi et al., 2005) and TGF- β (Zingariello et al., 2013). We show here that this bone marrow expresses also

high levels of BMP4, especially at the levels of the megakaryocytes (**Figure 11**). In a previous publication, it has been shown that megakaryocytes are responsible for the osteopetrosis observed in *Gata1*^{low} mice by secreting the bone matrix proteins osteonectin, bone sialoprotein, and osteopontin (Kacena et al., 2004). It is possible then that the megakaryocytes present within the cluster, which engulf the GFP+ cells are releasing the growth factors (TGF- β , VEGF and BMP-4) which, by inducing neo-angiogenesis and bone formation, are shaping the microenvironment of the *Gata1*^{low} femur increasing the niches for short-term repopulation HSC and multilineage progenitor cells. These cells, however, are induced into apoptosis by the pro-inflammatory milieu of this microenvironment resulting in hematopoietic failure.

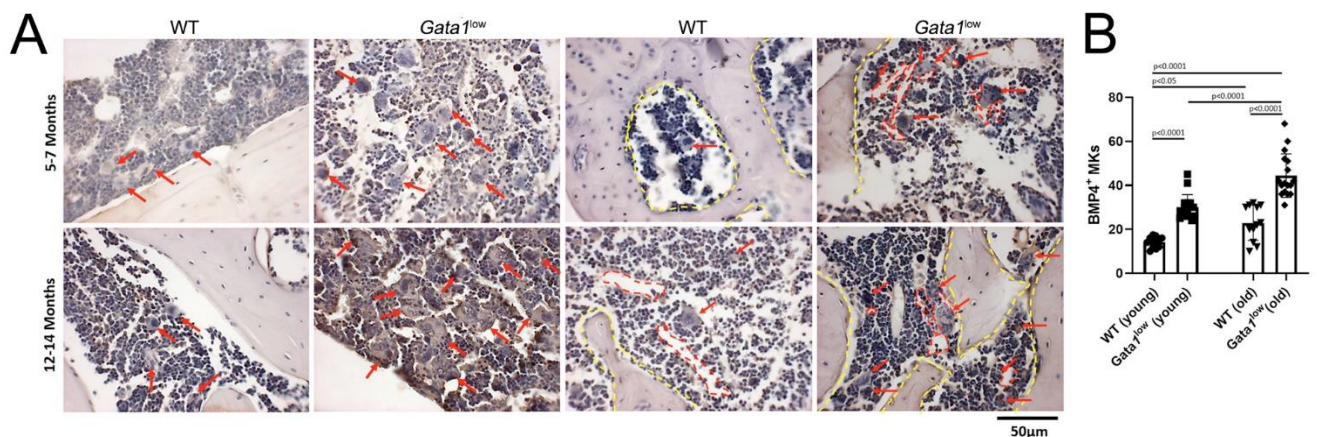


Figure 11. The megakaryocytes in the femur of *Gata1*^{low} mice contain express high levels of BMP-4 and are localized in close proximity of microvessels and bone trabeculae. **A)** Representative sections of the femur from two representative wild-type and *Gata1*^{low} mice immunostained for BMP-4 and counterstained with hematoxylin-eosin. Arrows indicate megakaryocytes, red dashed lines indicate the contour of the micro-vessels, yellow dashed lines indicate the contour of the bones. Magnification 40x. **B)** Quantification of the megakaryocytes expressing BMP-4 in the bone marrow of young and old wild-type and *Gata1*^{low} littermates, as indicated. Results are presented as Mean (\pm SD) and as values of individual mice (each dot an individual mouse). p values were calculated with Tukey multiple comparison and those statistically significant are indicated in the panels.

4. Discussion

Numerous studies are currently analyzing the changes occurring at the level of HSC with aging under the assumption that these changes may predispose to the development of myeloproliferative disorders and possibly to leukemia. Aging affects the HSC directly, by inducing epigenetic changes, and indirectly by altering the supportive role of the microenvironment (Pang et al., 2011; Raaijmakers, 2019; Yang & de Haan, 2021). These effects are supposed to be mediated by pro-inflammatory cytokines produced by the organism in response to environmental insults (Mitroulis et al., 2020). The inflammatory, aging and HSC alteration circuit is usually investigated using animal models harboring loss or gain of function mutations in key genes. Here we elucidated whether the pro-inflammatory milieu of the bone marrow microenvironment is correctly reflected by the cytokine content in the blood

and the effects of this milieu on the development of myelofibrosis and of bone marrow failure using a mouse strain naturally predisposed to develop pathologies driven by inflammation.

We first demonstrated that mice of the CD1 strain (both males and females), a strain known to exhibit pathologies associated with inflammation at the greatest frequency among mouse strains used as experimental models in the laboratory (Brayton et al., 2012), express serum levels of the pro-inflammatory cytokines TGF- β 1, LCN2 and CXCL1, the murine equivalent of human IL-8, greater than that expressed by the serum from mice which instead more rarely develop inflammatory diseases in the protected environment of an animal facility such as C57BL6 or DBA2. These results indicate that the baseline serum concentration may represent a confounding factor when establishing the normal range of pro-inflammatory cytokines in a mouse strain and raise a cautionary note on the range of their concentrations which should be considered normal in the human population, which also shown a great baseline genetic heterogeneity.

The great level of pro-inflammatory cytokines present in the sera of CD1 mice with respect to that of other strains was associated with histopathological alterations in multiple organs predictive of pathologies associated with chronic inflammation (interstitial pneumonia, arteritis, glomerulonephritis, amyloidosis in the spleen, epidermis hyperplasia). However, in over 60 old CD1 mice analyzed over the course of the years, we never observed myelofibrosis in the bone marrow (ARM, unpublished observation). Therefore, serum levels of pro-inflammatory cytokine per se do not predispose to the development of myelofibrosis in the absence of a driver mutation. This concept was further tested by determining that there is little difference in serum levels of a large panel of pro-inflammatory cytokines, including TGF- β 1, LCN2 and CXCL1, between *Gata1*^{low} mice and their wild-type littermates. There was also little difference between the serum levels of these cytokines between young, which do not express myelofibrosis, and old, when mice have developed myelofibrosis, *Gata1*^{low} mice. By contrast, the levels of TGF- β 1, LCN2 and CXCL1 (and of BMP-4) were found greatly increased in the bone marrow of *Gata1*^{low} mice with respect to their wild-type littermates. Therefore, once leading mutations have appeared, the microenvironmental bioavailability of pro-inflammatory cytokine is of great importance for the development of myelofibrosis.

TGF- β 1, LCN2 and CXCL1 are known to be expressed by multiple cell types. Our histochemistry studies indicated that they were expressed at comparable levels in most of the wild-type and *Gata1*^{low} microenvironmental cells analyzed apart from megakaryocytes in which they were all expressed at levels greater than normal. These observations re-enforce the knowledge that the malignant megakaryocytes play a major role on the development of myelofibrosis. Up to now, it was believed that this role was limited to secreting cytokines responsible to activate other cells (fibroblasts, monocytes-derived fibrocytes or even other megakaryocytes) to synthesize proteins of the extracellular matrix, inducing fibrosis. Whether fibrosis is then a by-standing effect or is responsible for hematopoietic failure in the marrow is a matter of debate. The observation that myelofibrosis can be

cured by bone marrow transplantation (Rondelli et al., 2014) provides a strong clinical indication that normal hematopoietic stem cells are capable to exert their functions even in the altered microenvironment of a myelofibrosis patients, suggesting that fibrosis per se does not reduce the supporting HSC niches in the bone marrow of these patients.

The last few years have seen a great increase in our understanding of the niches supporting hematopoiesis in the bone marrow. The HSC niches in the murine bone marrow are defined based on their anatomical location (in the diaphysis or in the epiphysis of the femur), the type of blood vessels (sinusoids, arterioles of transition zone vessels) they contain and the proximity with the endosteal zone (Raaijmakers, 2019; Szade et al., 2018; Yang & de Haan, 2021). Based on their anatomical site, at least two different types of HSC have been recognized: the central niche, which contains sinusoids and arterioles and hosts the majority (>90%) of the HSC, and the endosteal niche, in close proximity to the bone surface, which hosts the rest of the HSC. In both locations, HSC resides in close proximity with endothelial and mesenchymal stem cells (Anthony & Link, 2014). It was Dr. Lord that first proved that the long-term repopulating HSC are localization in the most external niches of the bones within niches going toward the central area of the medulla hosting progressively more differentiated HSC and finally progenitor cells (Lord, 1990). Recent data indicate that the HSC niches are reshaped during aging and inflammation and these changes are thought to determine the changes of HSC functions observed with age (HSC bias, exhaustion and clonality) (Ho & Méndez-Ferrer, 2020; Mitroulis et al., 2020). However, although it is well known that, in addition to microenvironmental clue, the effects exerted by aging on the property of HSC has a strong strain-specificity linked to the polymorphism of the polycomb gene among laboratory strains (de Haan & Van Zant, 1999; Klauke et al., 2013), our knowledge on the changes in the HSC niche with age in different strains is limited. By contrast with the human bone marrow, the mouse bone marrow contains very few adipocytes. It is debated whether these cells derive from mesenchymal stem cells or have HSC origin (Guerrero-Juarez et al., 2019). Whatever their origin is, by contrast with the adipocytes found in other tissues, the ones present in the bone marrow are capable to produce SCF and other HSC supportive growth factors (Zhang et al., 2019) and have been proposed to be putative HSC niche which becomes relevant with age. In agreement with this hypothesis, in old wild-type mice of the CD1 background, the small cells expressing the greatest levels of GFP were found localized in clusters surrounding the adipocytes. These results suggest that in this strain adipocytes play important niche functions with age.

The bone marrow from *Gata1*^{low} mice contained number of adipocytes greater than that of their wild-type littermates. This observation is consistent with the notion that, in addition to fibrosis, the bone marrow from MF patients often contains great numbers of adipocytes, numbers that may be so high to let to the identification of a MF subtype, MF with fatty bone marrow, the etiology of which is still poorly understood (Polino et al., 1986). It is possible that the driver mutations increase the proliferation potential to those adipocytes derived from the malignant HSC. In spite of their great

number, adipocytes were seldomly associated with small cells expressing GFP in the bone marrow of *Gata1*^{low} mice. GFP+ cells were instead located in areas of the medulla surrounded by micro-vessels and bones and containing great numbers of megakaryocytes. These results suggest that the abnormal megakaryocytes increase the niches supporting short-term HSC and progenitor cells in the bone marrow. The hypothesis that the hematopoietic niches in an organ, which is experiencing hematopoietic failure, are increased is counterintuitive. This apparent paradox is partially explained by the observation that the bone marrow from *Gata1*^{low} mice contain great numbers of macrophages containing high levels of GFP in their cytoplasm. Since pro-inflammatory cytokines are well known to increase the apoptotic rates of HSC/progenitor cells (Caiado et al., 2021), we suggest that megakaryocytes induce hematopoietic failure by secreting factors inducing HSC in apoptosis, which are then phagocytized by macrophages.

An important conclusion from this study is that the resident self-tissue, also defined as microenvironmental bioavailability, of BM proinflammatory cytokine, rather than their systemic levels, plays a key role in the development of myelofibrosis in the *Gata1*^{low} mouse model. The major cytokines/chemokines identified are TGF- β 1, LCN2, and CXCL1, and emperipoiesis seems to be one of the major drivers of LCN2 secretion in the microenvironment.

Supplementary Materials: Supplementary Figures S1 to S8 and Supplementary Tables S1 to S4 are available at: 10.5281/zenodo.5914546 (link: <https://zenodo.org/record/5914546#.YfQkberMJPY>) while movies 1, 2 and 3 are available at doi: 10.5281/zenodo.5833120 (link: https://zenodo.org/record/5833120#.YfF75_7MJPY). Movie 1. Tridimensional image of GFP localization in the nucleus. Movie 2. Tridimensional image of GFP localization in the cytoplasm. Movie 3. Tridimensional reconstruction of GFPpositive cells localized around an adipocyte.

Author Contributions: MZ, FG, and MF performed the histological experiments and wrote the manuscript. PV performed the ELISA experiments and wrote the manuscript. FM performed the flow cytometry determinations and wrote the manuscript. MM performed the statistical analyses and wrote the manuscript. CM performed the GSEA analysis and JMC performed the cytokine analysis and wrote the manuscript. GS, JC and ARM designed the study, interpreted data, and wrote the manuscript. All authors contributed to the article and approved its submitted version.

Funding: This study was supported by grants from the National Cancer Institute (P01-CA108671), the Heart, Lung and Blood Institute (1R01-HL134684) and Associazione Italiana Ricerca Cancro (AIRC 17608).

Institutional Review Board Statement: All the experiments were performed according to protocol n. 419/2015-PR approved by the Italian Ministry of Health and according to the directive 2010/63/EU

of the European Parliament and of the Council of 22 September 2010 on the protection of animals used for scientific purposes.

Informed Consent Statement: Not applicable. No human studies.

Data Availability Statement: Microarray data have been deposited in the Gene Expression Omnibus database (GSE89630)

<https://www.ncbi.nlm.nih.gov/geo/query/acc.cgi?token=ijgpwgsyjhwpdoj&acc=GSE89630>.

Acknowledgments: The support of Yvan Gilardi, Enrico Cardarelli and Andrea Giovannelli, of the Animal Facility of Istituto Superiore di Sanità is gratefully acknowledged. Francesca Arciprete is also acknowledged for technical support. Single *huCD34tTA* and *TetO-H2BGFP* mutant mice were gently provided by Dr. Kateri Moore Lemischka.

Conflicts of Interest: The authors declare no conflict of interest.

5. References

Agarwal, A., Morrone, K., Bartenstein, M., Zhao, Z. J., Verma, A., Goel, S. (2016). Bone marrow fibrosis in primary myelofibrosis: pathogenic mechanisms and the role of TGF- β . *Stem Cell Investigation*, 3, 5. <https://doi.org/10.3978/j.issn.2306-9759.2016.02.03>.

Anthony, B.A., Link, D.C. (2014). Regulation of hematopoietic stem cells by bone marrow stromal cells. *Trends in Immunology*, 35(1), 32–37. <https://doi.org/10.1016/j.it.2013.10.002>.

Arranz, L., Sánchez-Aguilera, A., Martín-Pérez, D., Isern, J., Langa, X., Tzankov, A., Lundberg, P., Muntión, S., Tzeng, Y.S., Lai, D.M., Schwaller, J., Skoda, R.C., Méndez-Ferrer, S. (2014). Neuropathy of haematopoietic stem cell niche is essential for myeloproliferative neoplasms. *Nature*, 512(7512), 78–81. <https://doi.org/10.1038/nature13383>.

Barabanshikova, M.V, Dubina, I.A., Lapin, S.V, Morozova, E.V, Vlasova, J.J., Ivanova, M.O., Moiseev, I.S., Afanasyev, B.V. (2017). Clinical correlates and prognostic significance of IL-8, sIL-2R, and immunoglobulin-free light chain levels in patients with myelofibrosis. *Oncology Research and Treatment*, 40(10), 574–578. <https://doi.org/10.1159/000477253>.

Barbui, T., Tefferi, A., Vannucchi, A. M., Passamonti, F., Silver, R.T., Hoffman, R., Verstovsek, S., Mesa, R., Kiladjan, J.J., Hehlmann, R., Reiter, A., Cervantes, F., Harrison, C., Mc Mullin, M.F., Hasselbalch, H.C., Koschmieder, S., Marchetti, M., Bacigalupo, A., Finazzi, G., Kroeger, N., Griesshammer, M., Birgegard, G., Barosi, G. (2018). Philadelphia chromosome-negative classical myeloproliferative neoplasms: revised management recommendations from European LeukemiaNet. *Leukemia*, 32(5), 1057–1069. <https://doi.org/10.1038/s41375-018-0077-1>.

Barosi, G., Hoffman, R. (2005). Idiopathic myelofibrosis. *Seminars in Hematology*, 42(4), 248–258. <https://doi.org/10.1053/J.SEMINHEMATOL.2005.05.018>.

- Battle, E., Massagué, J. (2019). Transforming growth factor- β signaling in immunity and cancer. *Immunity*, 50(4), 924–940. <https://doi.org/10.1016/j.immuni.2019.03.024>.
- Brayton, C.F., Treuting, P.M., Ward, J.M. (2012). Pathobiology of aging mice and GEM. *Veterinary Pathology*, 49(1), 85–105. <https://doi.org/10.1177/0300985811430696>.
- Bruno, E., Horrigan, S. K., Van Den Berg, D., Rozler, E., Fitting, P. R., Moss, S.T., Westbrook, C., Hoffman, R. (1998). The Smad5 gene is involved in the intracellular signaling pathways that mediate the inhibitory effects of transforming growth factor-beta on human hematopoiesis. *Blood*, 91(6), 1917–1923.
- Caiado, F., Pietras, E. M., Manz, M. G. (2021). Inflammation as a regulator of hematopoietic stem cell function in disease, aging, and clonal selection. *The Journal of Experimental Medicine*, 218(7). <https://doi.org/10.1084/jem.20201541>.
- Campanelli, R., Rosti, V., Villani, L., Castagno, M., Moretti, E., Bonetti, E., Bergamaschi, G., Balduini, A., Barosi, G., Massa, M. (2011). Evaluation of the bioactive and total transforming growth factor β 1 levels in primary myelofibrosis. *Cytokine*, 53(1), 100–106. <https://doi.org/10.1016/j.cyto.2010.07.427>.
- Centurione, L., Di Baldassarre, A., Zingariello, M., Bosco, D., Gatta, V., Rana, R. A., Langella, V., Di Virgilio, A., Vannucchi, A.M., Migliaccio, A.R. (2004). Increased and pathologic emperipolesis of neutrophils within megakaryocytes associated with marrow fibrosis in GATA-1^{low} mice. *Blood*, 104(12), 3573–3580. <https://doi.org/10.1182/blood-2004-01-0193>.
- De Haan, G., Van Zant, G. (1999). Dynamic changes in mouse hematopoietic stem cell numbers during aging. *Blood*, 93(10), 3294–3301.
- Drexler, B., Passweg, J.R., Tzankov, A., Bigler, M., Theocharides, A.P., Cantoni, N., Keller, P., Stussi, G., Ruefer, A., Benz, R., Favre, G., Lundberg, P., Nienhold, R., Fuhrer, A., Biaggi, C., Manz, M. G., Bargetzi, M., Mendez-Ferrer, S., Skoda, R.C. (2019). The sympathomimetic agonist mirabegron did not lower JAK2^{V617F} allele burden, but restored nestin-positive cells and reduced reticulin fibrosis in patients with myeloproliferative neoplasms: results of phase II study SAKK 33/14. *Haematologica*, 104(4), 710–716. <https://doi.org/10.3324/haematol.2018.200014>.
- Dunbar, A.J., Rampal, R.K., Levine, R. (2020). Leukemia secondary to myeloproliferative neoplasms. *Blood*, 136(1), 61–70. <https://doi.org/10.1182/blood.2019000943>.
- Dunbar, A.J., Kim, D., Lu, M., Farina, M., Bowman, R.L., Yang, J.L., Park, Y., Karzai, A., Xiao, W., Zaroogian, Z., O'Connor, K., Mowla, S., Gobbo, F., Verachi, P., Martelli, F., Sarli, G., Xia, L., Elmansy, N., Kleppe, M., Chen, Z., Xiao, Y., McGovern, E., Snyder, J., Krishnan, A., Hill, C., Cordner, K., Zouak, A., Salama, M.E., Yohai, J., Tucker, E., Chen, J., Zhou, J., McConnell, T., Migliaccio, A.R., Koche, R., Rampal, R., Fan, R., Levine, R.L., Hoffman, R. (2023). CXCL8/CXCR2 signaling mediates bone marrow fibrosis and is a therapeutic target in myelofibrosis. *Blood*, 141(20), 2508–2519. <https://doi.org/10.1182/blood.2022015418>.
- Eash, K.J., Greenbaum, A.M., Gopalan, P.K., Link, D.C. (2010). CXCR2 and CXCR4 antagonistically regulate neutrophil trafficking from murine bone marrow. *Journal of Clinical Investigation*, 120(7), 2423–2431. <https://doi.org/10.1172/JCI41649>.

- Eliades, A., Papadantonakis, N., Bhupatiraju, A., BurrIDGE, K.A., Johnston-Cox, H.A., Migliaccio, A. R., Crispino, J.D., Lucero, H.A., Trackman, P.C., Ravid, K. (2011). Control of megakaryocyte expansion and bone marrow fibrosis by lysyl oxidase. *Journal of Biological Chemistry*, 286(31), 27630–27638. <https://doi.org/10.1074/jbc.M111.243113>.
- Emadi, S., Clay, D., Desterke, C., Guerton, B., Maquarre, E., Jasmin, C. (2005). IL-8 and its CXCR1 and CXCR2 receptors participate in the control of megakaryocytic proliferation, differentiation, and ploidy in myeloid metaplasia with myelofibrosis. *Blood*, 105(2), 464–473. <https://doi.org/10.1182/blood-2003-12-4415>.
- Frenette, P.S., Denis, C.V., Weiss, L., Jurk, K., Subbarao, S., Kehrel, B., Hartwig, J.H., Vestweber, D., Wagner, D.D. (2000). P-selectin glycoprotein ligand 1 (PSGL-1) is expressed on platelets and can mediate platelet-endothelial interactions in vivo. *Journal of Experimental Medicine*, 191(8), 1413–1422. <https://doi.org/10.1084/jem.191.8.1413>.
- Ghinassi, B., Sanchez, M., Martelli, F., Amabile, G., Vannucchi, A.M., Migliaccio, G., Orkin, S.H., Migliaccio, A.R. (2007). The hypomorphic *Gata1^{low}* mutation alters the proliferation/differentiation potential of the common megakaryocytic-erythroid progenitor. *Blood*, 109(4), 1460–1471. <https://doi.org/10.1182/blood-2006-07-030726>.
- Guerrero-Juarez, C.F., Dedhia, P.H., Jin, S., Ruiz-Vega, R., Ma, D., Liu, Y., Yamaga, K., Shestova, O., Gay, D.L., Yang, Z., Kessenbrock, K., Nie, Q., Pear, W. S., Cotsarelis, G., Plikus, M. V. (2019). Single-cell analysis reveals fibroblast heterogeneity and myeloid-derived adipocyte progenitors in murine skin wounds. *Nature Communications*, 10(1), 650. <https://doi.org/10.1038/s41467-018-08247-x>.
- Hankenson, K.D., Gagne, K., Shaughnessy, M. (2015). Extracellular signaling molecules to promote fracture healing and bone regeneration. *Advanced Drug Delivery Reviews*, 94, 3–12. <https://doi.org/10.1016/j.addr.2015.09.008>.
- Hashimoto, S., Yoda, M., Yamada, M., Yanai, N., Kawashima, T., Motoyoshi, K. (1996). Macrophage colony-stimulating factor induces interleukin-8 production in human monocytes. *Experimental Hematology*, 24(2), 123–128.
- Ho, Y.H., Méndez-Ferrer, S. (2020). Microenvironmental contributions to hematopoietic stem cell aging. *Haematologica*, 105(1), 38–46. <https://doi.org/10.3324/haematol.2018.211334>.
- Hoshino, A., Ueha, S., Hanada, S., Imai, T., Ito, M., Yamamoto, K., Matsushima, K., Yamaguchi, A., Iimura, T. (2013). Roles of chemokine receptor CXCR1 in maintaining murine bone homeostasis through the regulation of both osteoblasts and osteoclasts. *Journal of Cell Science*, 126(Pt 4), 1032–1045. <https://doi.org/10.1242/jcs.113910>.
- Jeon, S., Jha, M. K., Ock, J., Seo, J., Jin, M., Cho, H., Lee, W.-H., Suk, K. (2013). Role of lipocalin-2-chemokine axis in the development of neuropathic pain following peripheral nerve injury. *The Journal of Biological Chemistry*, 288(33), 24116–24127. <https://doi.org/10.1074/jbc.M113.454140>.
- Kacena, M.A., Shivdasani, R.A., Wilson, K., Xi, Y., Troiano, N., Nazarian, A., Gundberg, C.M., Bouxsein, M.L., Lorenzo, J.A., Horowitz, M.C. (2004). Megakaryocyte-osteoblast interaction revealed in mice deficient

- in transcription factors GATA-1 and NF-E2. *Journal of Bone and Mineral Research*, 19(4), 652–660. <https://doi.org/10.1359/JBMR.0301254>.
- Kaplanski, G., Farnarier, C., Kaplanski, S., Porat, R., Shapiro, L., Bongrand, P., Dinarello, C.A. (1994). Interleukin-1 induces interleukin-8 secretion from endothelial cells by a juxtacrine mechanism. *Blood*, 84(12), 4242–4248.
- Klauke, K., Radulović, V., Broekhuis, M., Weersing, E., Zwart, E., Olthof, S., Ritsema, M., Bruggeman, S., Wu, X., Helin, K., Bystrykh, L., de Haan, G. (2013). Polycomb Cbx family members mediate the balance between haematopoietic stem cell self-renewal and differentiation. *Nature Cell Biology*, 15(4), 353–362. <https://doi.org/10.1038/ncb2701>.
- Köhler, A., De Filippo, K., Hasenberg, M., van den Brandt, C., Nye, E., Hosking, M. P., Lane, T. E., Männ, L., Ransohoff, R. M., Hauser, A. E., Winter, O., Schraven, B., Geiger, H., Hogg, N., Gunzer, M. (2011). G-CSF-mediated thrombopoietin release triggers neutrophil motility and mobilization from bone marrow via induction of CXCR2 ligands. *Blood*, 117(16), 4349–4357. <https://doi.org/10.1182/blood-2010-09-308387>.
- Koschmieder, S., Chatain, N. (2020). Role of inflammation in the biology of myeloproliferative neoplasms. *Blood Reviews*, 42, 100711. <https://doi.org/10.1016/j.blre.2020.100711>.
- Kowalska, M.A., Ratajczak, J., Hoxie, J., Brass, L.F., Gewirtz, A., Poncz, M., Ratajczak, M.Z. (1999). Megakaryocyte precursors, megakaryocytes and platelets express the HIV co-receptor CXCR4 on their surface: determination of response to stromal-derived factor-1 by megakaryocytes and platelets. *British Journal of Haematology*, 104(2), 220–229. <https://doi.org/10.1046/j.1365-2141.1999.01169.x>.
- Li, A., Dubey, S., Varney, M. L., Dave, B.J., Singh, R.K. (2003). IL-8 directly enhanced endothelial cell survival, proliferation, and matrix metalloproteinases production and regulated angiogenesis. *Journal of Immunology (Baltimore, Md. : 1950)*, 170(6), 3369–3376. <https://doi.org/10.4049/jimmunol.170.6.3369>.
- Lin, S., Xie, J., Gong, T., Shi, S., Zhang, T., Fu, N., Ye, L., Wang, M., Lin, Y. (2015). TGFβ signalling pathway regulates angiogenesis by endothelial cells, in an adipose-derived stromal cell/endothelial cell co-culture 3D gel model. *Cell Proliferation*, 48(6), 729–737. <https://doi.org/10.1111/cpr.12222>.
- Ling, T., Crispino, J.D., Zingariello, M., Martelli, F., Migliaccio, A.R. (2018). GATA1 insufficiencies in primary myelofibrosis and other hematopoietic disorders: consequences for therapy. *Expert Review of Hematology*, 11(3), 169–184. <https://doi.org/10.1080/17474086.2018.1436965>.
- Lord, B.I. (1990). The architecture of bone marrow cell populations. *International Journal of Cell Cloning*, 8(5), 317–331. <https://doi.org/10.1002/stem.5530080501>.
- Lu, M., Xia, L., Liu, Y. C., Hochman, T., Bizzari, L., Aruch, D., Lew, J., Weinberg, R., Goldberg, J. D., Hoffman, R. (2015). Lipocalin produced by myelofibrosis cells affects the fate of both hematopoietic and marrow microenvironmental cells. *Blood*, 126(8), 972–982. <https://doi.org/10.1182/blood-2014-12-618595>.
- Malara, A., Abbonante, V., Zingariello, M., Migliaccio, A., Balduini, A. (2018). Megakaryocyte contribution to bone marrow fibrosis: many arrows in the quiver. *Mediterranean Journal of Hematology and Infectious Diseases*, 10(1), e2018068. <https://doi.org/10.4084/MJHID.2018.068>.

- Marcellino, B. K., Verstovsek, S., Mascarenhas, J. (2020). The myelodepletive phenotype in myelofibrosis: clinical relevance and therapeutic implication. *Clinical Lymphoma, Myeloma and Leukemia*, 1–7. <https://doi.org/doi: 10.1016/j.clml.2020.01.008>.
- Martelli, F., Ghinassi, B., Panetta, B., Alfani, E., Gatta, V., Pancrazzi, A., Bogani, C., Vannucchi, A. M., Paoletti, F., Migliaccio, G., Migliaccio, A.R. (2005). Variegation of the phenotype induced by the *Gata1*^{low} mutation in mice of different genetic backgrounds. *Blood*, 106(13), 4102–4113. <https://doi.org/10.1182/blood-2005-03-1060>.
- Martyré, M.C. (1995). TGF- β and megakaryocytes in the pathogenesis of myelofibrosis in myeloproliferative disorders. *Leukemia & Lymphoma*, 20(1–2), 39–44. <https://doi.org/10.3109/10428199509054751>.
- Mascarenhas, J., Kosiorek, H. E., Bhave, R., Palmer, J. M., Kuykendall, A. T., Mesa, R. A., Rampal, R., Gerds, A. T., Yacoub, A., Pettit, K. M., Talpaz, M., Komrokji, R. S., Kremyanskaya, M., Gonzalez, A., Fabris, F., Sandy, L., Johnson, K., Dougherty, M., MCGovern, E., Hoffman, R. (2021). Treatment of myelofibrosis patients with the TGF- β 1/3 inhibitor AVID200 (MPN-RC 118) induces a profound effect on platelet production. *Blood*, 138(Supplement 1), 142. <https://doi.org/10.1182/blood-2021-148995>.
- Matsushima, K., Oppenheim, J.J. (1989). Interleukin 8 and MCAF: novel inflammatory cytokines inducible by IL1 and TNF. *Cytokine*, 1(1), 2–13. [https://doi.org/https://doi.org/10.1016/1043-4666\(89\)91043-0](https://doi.org/https://doi.org/10.1016/1043-4666(89)91043-0).
- McDevitt, M.A., Shivdasani, R.A., Fujiwara, Y., Yang, H., Orkin, S. H. (1997). A “knockdown” mutation created by cis-element gene targeting reveals the dependence of erythroid cell maturation on the level of transcription factor GATA-1. *Proceedings of the National Academy of Sciences*, 94(13), 6781–6785. <https://doi.org/10.1073/pnas.94.13.6781>.
- Migliaccio, A.R. (2018). A vicious interplay between genetic and environmental insults in the etiology of blood cancers. *Experimental Hematology*, 59, 9–13. <https://doi.org/10.1016/j.exphem.2017.12.004>
- Mitroulis, I., Kalafati, L., Bornhäuser, M., Hajishengallis, G., Chavakis, T. (2020). Regulation of the bone marrow niche by inflammation. *Frontiers in Immunology*, 11, 1540. <https://doi.org/10.3389/fimmu.2020.01540>.
- Nguyen, J., Tang, S.Y., Nguyen, D., Alliston, T. (2013). Load regulates bone formation and Sclerostin expression through a TGF β -dependent mechanism. *PloS One*, 8(1), e53813. <https://doi.org/10.1371/journal.pone.0053813>.
- Oguro, H., Ding, L., Morrison, S.J. (2013). SLAM family markers resolve functionally distinct subpopulations of hematopoietic stem cells and multipotent progenitors. *Cell Stem Cell*, 13(1), 102–116. <https://doi.org/10.1016/j.stem.2013.05.014>.
- Pang, W.W., Price, E.A., Sahoo, D., Beerman, I., Maloney, W.J., Rossi, D.J., Schrier, S.L., Weissman, I.L. (2011). Human bone marrow hematopoietic stem cells are increased in frequency and myeloid-biased with age. *Proceedings of the National Academy of Sciences of the United States of America*, 108(50), 20012–20017. <https://doi.org/10.1073/pnas.1116110108>.

- Polino, G., Barosi, G., Berzuini, A., Castelli, G., Isernia, P., Palestra, P., Riccardi, A., Rossi, F., Magrini, U. (1986). Fatty bone marrow with severe myeloid hypoplasia in idiopathic myelofibrosis. *Haematologica*, 71(2), 117–121.
- Qiu, J., Papatsenko, D., Niu, X., Schaniel, C., Moore, K. (2014). Divisional history and hematopoietic stem cell function during homeostasis. *Stem Cell Reports*, 2(4), 473–490. <https://doi.org/10.1016/j.stemcr.2014.01.016>.
- Raaijmakers, M.H.G.P. (2019). Aging of the hematopoietic stem cell niche: an unnerving matter. *Cell Stem Cell*, 25(3), 301–303. <https://doi.org/10.1016/j.stem.2019.08.008>.
- Radomska, H.S., Gonzalez, D.A., Okuno, Y., Iwasaki, H., Nagy, A., Akashi, K., Tenen, D.G., Huettner, C. S. (2002). Transgenic targeting with regulatory elements of the human CD34 gene. *Blood*, 100(13), 4410–4419. <https://doi.org/10.1182/blood-2002-02-0355>.
- Rondelli, D., Goldberg, J. D., Isola, L., Price, L. S., Shore, T. B., Boyer, M., Bacigalupo, A., Rambaldi, A., Scarano, M., Klisovic, R. B., Gupta, V., Andreasson, B., Mascarenhas, J., Wetzler, M., Vannucchi, A. M., Prchal, J. T., Najfeld, V., Orazi, A., Weinberg, R. S., Miller, C., Barosi, G., Silverman, L.R., Prosperini, G., Marchioli, R., Hoffman, R. (2014). MPD-RC 101 prospective study of reduced-intensity allogeneic hematopoietic stem cell transplantation in patients with myelofibrosis. *Blood*, 124(7), 1183–1191. <https://doi.org/10.1182/blood-2014-04-572545>.
- Schepers, K., Pietras, E. M., Reynaud, D., Flach, J., Binnewies, M., Garg, T., Wagers, A. J., Hsiao, E. C., Passegue, E. (2013). Myeloproliferative neoplasia remodels the endosteal bone marrow niche into a self-reinforcing leukemic niche. *Cell Stem Cell*, 13(3), 285–299. <https://doi.org/10.1016/j.stem.2013.06.009>.
- Schmidt-Ott, K. M., Mori, K., Kalandadze, A., Li, J.-Y., Paragas, N., Nicholas, T., Devarajan, P., Barasch, J. (2006). Neutrophil gelatinase-associated lipocalin-mediated iron traffic in kidney epithelia. *Current Opinion in Nephrology and Hypertension*, 15(4), 442–449. <https://doi.org/10.1097/01.mnh.0000232886.81142.58>.
- Schmitt, A., Drouin, A., Massé, J.-M., Guichard, J., Shagraoui, H., Cramer, E. M. (2002). polymorphonuclear neutrophil and megakaryocyte mutual involvement in myelofibrosis pathogenesis. *Leukemia & Lymphoma*, 43(4), 719–724. <https://doi.org/10.1080/10428190290016809>.
- Shen, Q., Zhu, S., Hu, J., Geng, N., Zou, S. (2009). Recombinant human bone morphogenetic protein-4 (BMP-4)-stimulated cell differentiation and bone formation within the expanding calvarial suture in rats. *The Journal of Craniofacial Surgery*, 20(5), 1561–1565. <https://doi.org/10.1097/SCS.0b013e3181b09cc1>.
- Spangrude, G.J., Lewandowski, D., Martelli, F., Marra, M., Zingariello, M., Sancillo, L., Rana, R.A., Migliaccio, A.R. (2016). P-Selectin Sustains Extramedullary Hematopoiesis in the *Gata1*^{low} Model of Myelofibrosis. *Stem Cells*, 34(1), 67–82. <https://doi.org/10.1002/stem.2229>.
- Szade, K., Gulati, G.S., Chan, C.K.F., Kao, K.S., Miyanishi, M., Marjon, K.D., Sinha, R., George, B. M., Chen, J.Y., Weissman, I.L. (2018). Where hematopoietic stem cells live: the bone marrow niche. *Antioxidants & Redox Signaling*, 29(2), 191–204. <https://doi.org/10.1089/ars.2017.7419>.

- Takeuchi, K., Higuchi, T., Yamashita, T., Koike, K. (1999). Chemokine production by human megakaryocytes derived from cd34-positive cord blood cells. *Cytokine*, 11(6), 424–434. <https://doi.org/https://doi.org/10.1006/cyto.1998.0455>.
- Tefferi, A., Vaidya, R., Caramazza, D., Finke, C., Lasho, T., Pardanani, A. (2011). Circulating interleukin (IL)-8, IL-2R, IL-12, and IL-15 levels are independently prognostic in primary myelofibrosis: a comprehensive cytokine profiling study. *Journal of Clinical Oncology*, 29(10), 1356–1363. <https://doi.org/10.1200/JCO.2010.32.9490>.
- Teijeira, Á., Garasa, S., Gato, M., Alfaro, C., Migueliz, I., Cirella, A., de Andrea, C., Ochoa, M. C., Otano, I., Etxeberria, I., Andueza, M.P., Nieto, C.P., Resano, L., Azpilikueta, A., Allegretti, M., de Pizzol, M., Ponz-Sarvisé, M., Rouzaut, A., Sanmamed, M.F., Schalper, K., Carleton, M., Mellado, M., Rodriguez-Ruiz, M.E., Berraondo, P., Perez-Gracia, J.L., Melero, I. (2020). CXCR1 and CXCR2 Chemokine Receptor Agonists Produced by Tumors Induce Neutrophil Extracellular Traps that Interfere with Immune Cytotoxicity. *Immunity*, 52(5), 856-871.e8. <https://doi.org/10.1016/j.immuni.2020.03.001>.
- Tillmann, S., Olschok, K., Schröder, S.K., Bütow, M., Baumeister, J., Kalmer, M., Preußger, V., Weinbergerova, B., Kricheldorf, K., Mayer, J., Kubsova, B., Racil, Z., Wessiepe, M., Eschweiler, J., Isfort, S., Brümmendorf, T.H., Becker, W., Schemionek, M., Weiskirchen, R., Chatain, N. (2021). The unfolded protein response is a major driver of LCN2 expression in BCR-ABL- and JAK2V617F-positive MPN. *Cancers*, 13(16). <https://doi.org/10.3390/cancers13164210>.
- Vannucchi, A.M., Bianchi, L., Cellai, C., Paoletti, F., Rana, R. A., Lorenzini, R., Migliaccio, G., Migliaccio, A.R. (2002). Development of myelofibrosis in mice genetically impaired for GATA-1 expression (GATA-1^{low} mice). *Blood*, 100(4), 1123–1132. <https://doi.org/10.1182/blood-2002-06-1913>.
- Vannucchi, A.M., Bianchi, L., Paoletti, F., Pancrazzi, A., Torre, E., Nishikawa, M., Zingariello, M., Di Baldassarre, A., Rana, R.A., Lorenzini, R., Alfani, E., Migliaccio, G., Migliaccio, A.R. (2005). A pathobiologic pathway linking thrombopoietin, GATA-1, and TGF- β 1 in the development of myelofibrosis. *Blood*, 105(9), 3493–3501. <https://doi.org/10.1182/blood-2004-04-1320>.
- Varricchio, L., Iancu-Rubin, C., Upadhyaya, B., Zingariello, M., Martelli, F., Verachi, P., Clementelli, C., Denis, J.-F., Rahman, A. H., Tremblay, G., Mascarenhas, J., Mesa, R. A., O’Connor-McCourt, M., Migliaccio, A.R., Hoffman, R. (2021). TGF- β 1 protein trap AVID200 beneficially affects hematopoiesis and bone marrow fibrosis in myelofibrosis. *JCI Insight*, 6(18). <https://doi.org/10.1172/jci.insight.145651>.
- Waugh, D. J. J., & Wilson, C. (2008). The interleukin-8 pathway in cancer. *Clinical Cancer Research*, 8(21), 6735–6742. <https://doi.org/10.1158/1078-0432.CCR-07-4843>.
- Wolach, O., Sellar, R.S., Martinod, K., Cherpokova, D., McConkey, M., Chappell, R.J., Silver, A.J., Adams, D., Castellano, C. A., Schneider, R. K., Padera, R. F., DeAngelo, D.J., Wadleigh, M., Steensma, D.P., Galinsky, I., Stone, R.M., Genovese, G., McCarroll, S.A., Iliadou, B., Hultman, C., Neubergh, D., Mullally, A., Wagner, D.D., Ebert, B.L. (2018). Increased neutrophil extracellular trap formation promotes thrombosis in

- myeloproliferative neoplasms. *Science Translational Medicine*, 10(436).
<https://doi.org/10.1126/scitranslmed.aan8292>.
- Yang, D., de Haan, G. (2021). Inflammation and aging of hematopoietic stem cells in their niche. *Cells*, 10(8).
<https://doi.org/10.3390/cells10081849>.
- Yousef, H., Conboy, M. J., Morgenthaler, A., Schlesinger, C., Bugaj, L., Paliwal, P., Greer, C., Conboy, I.M., Schaffer, D. (2015). Systemic attenuation of the TGF- β pathway by a single drug simultaneously rejuvenates hippocampal neurogenesis and myogenesis in the same old mammal. *Oncotarget*, 6(14), 11959–11978.
<https://doi.org/10.18632/oncotarget.3851>.
- Zahr, A.A., Salama, M.E., Carreau, N., Tremblay, D., Verstovsek, S., Mesa, R., Hoffman, R., Mascarenhas, J. (2016). Bone marrow fibrosis in myelofibrosis: pathogenesis, prognosis and targeted strategies. *Haematologica*, 101(6), 660–671. <https://doi.org/10.3324/haematol.2015.141283>.
- Zhang, Z., Huang, Z., Ong, B., Sahu, C., Zeng, H., Ruan, H.B. (2019). Bone marrow adipose tissue-derived stem cell factor mediates metabolic regulation of hematopoiesis. *Haematologica*, 104(9), 1731–1743.
<https://doi.org/10.3324/haematol.2018.205856>.
- Zingariello, M., Martelli, F., Ciaffoni, F., Masiello, F., Ghinassi, B., D'Amore, E., Massa, M., Barosi, G., Sancillo, L., Li, X., Goldberg, J.D., Rana, R.A., Migliaccio, A.R. (2013). Characterization of the TGF- β 1 signaling abnormalities in the *Gata1*^{low} mouse model of myelofibrosis. *Blood*, 121(17), 3345–3363.
<https://doi.org/10.1182/blood-2012-06-439661>.
- Zingariello, M., Martelli, F., Verachi, P., Bardelli, C., Gobbo, F., Mazzarini, M., Migliaccio, A.R. (2019). Novel targets to cure primary myelofibrosis from studies on *Gata1*^{low} mice. *IUBMB Life*, 72,131–141.
<https://doi.org/10.1002/iub.2198>.
- Zingariello, M., Ruggeri, A., Martelli, F., Marra, M., Sancillo, L., Ceglia, I., Rana, R.A., Migliaccio, A.R. (2015). A novel interaction between megakaryocytes and activated fibrocytes increases TGF- β bioavailability in the *Gata1*^{low} mouse model of myelofibrosis. *American Journal of Blood Research*, 5(2), 34–61.
- Zingariello, M., Sancillo, L., Martelli, F., Ciaffoni, F., Marra, M., Varricchio, L., Rana, R.A., Zhao, C., Crispino, J.D., Migliaccio, A.R. (2017). The thrombopoietin/MPL axis is activated in the *Gata1*^{low} mouse model of myelofibrosis and is associated with a defective RPS14 signature. *Blood Cancer Journal*, 7(6), 1–11.
<https://doi.org/10.1038/bcj.2017.51>.

6. Supplementary Figures

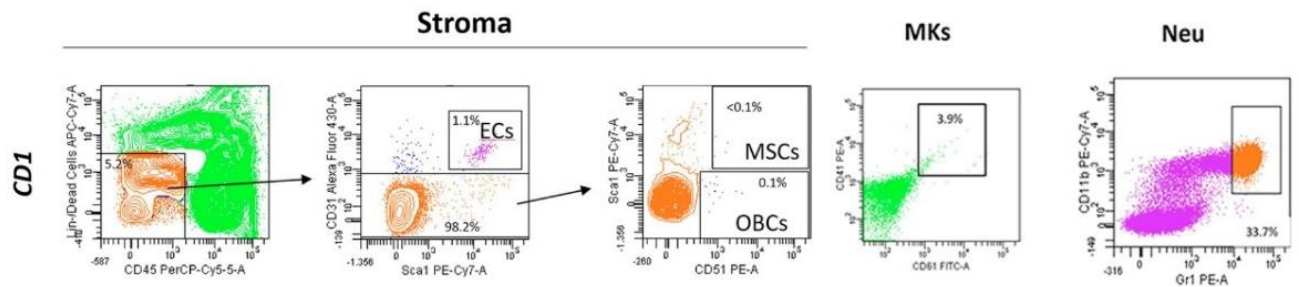


Figure S1. Gating used to identify endothelial cells (ECs), mesenchymal cells (MSCs), osteoblasts (OBCs), megakaryocytes (MKs) and neutrophils (Neu) in the bone marrow from a wild type mouse. In order to correctly estimate the frequency of all the cell populations, the monocellular cell suspension used for the analyses were prepared by carefully crushing the femurs of the mice (see (Schepers et al., 2013) and (Ghinassi et al., 2007) for detail).

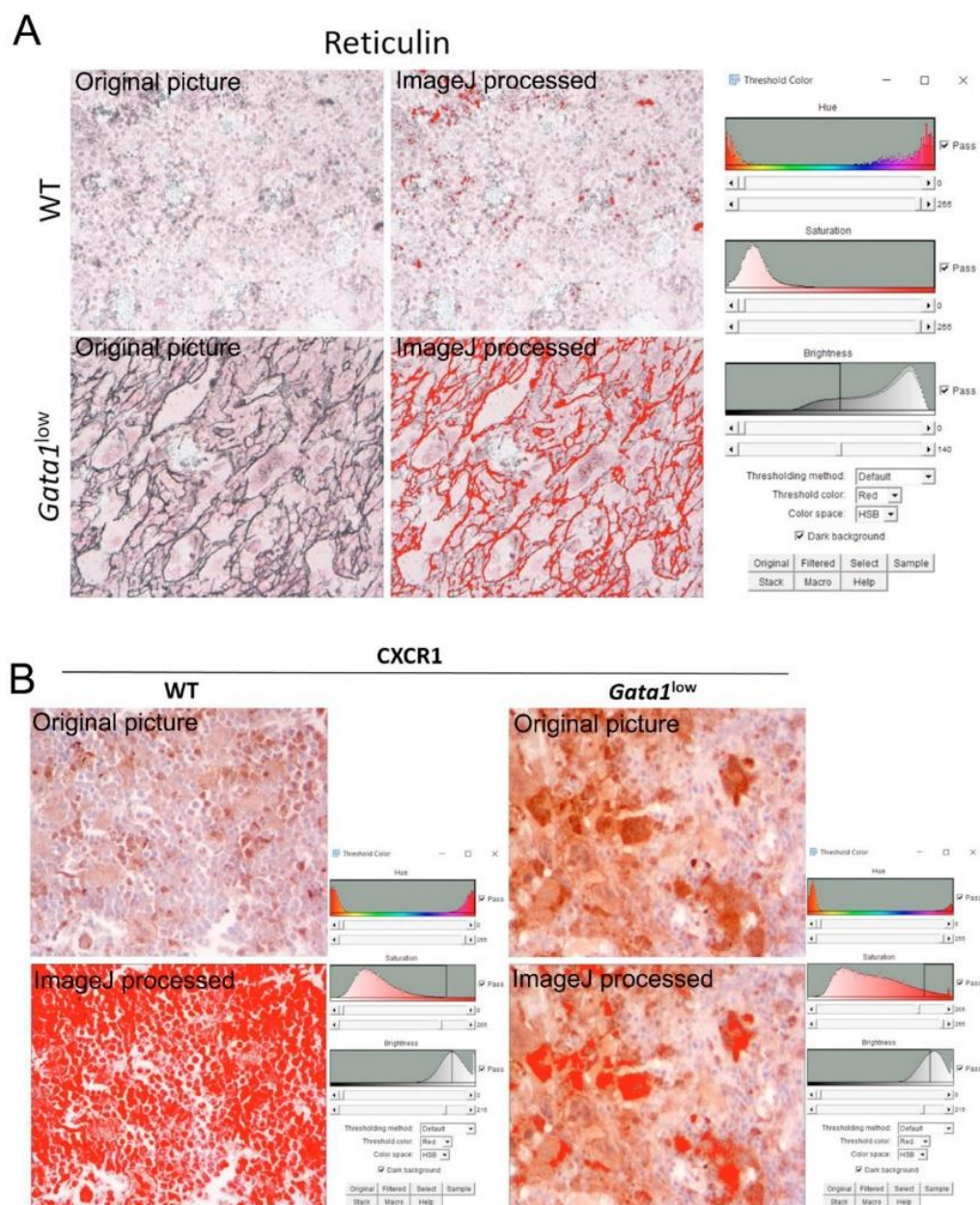


Figure S2. (A) Example of the computer assisted image analysis used to quantify the level of fibrosis in bone marrow sections stained by Reticulin (black fibers) from representative wild-type (WT) and *Gata1*^{low} mice. The ImageJ program-assisted quantification process includes selection of the color channel (black histogram, Hue), determination of the

threshold (Saturation histogram) and quantification of the areas which exceed the threshold (in %) (Brightness histogram). **(B)** Example of the computer assisted image analysis used to quantify the number of megakaryocytes positive per CXCR1 in in bone marrow sections from wild-type (WT) and *Gata1*^{low} mice. In this case, the conditions to quantify the signal in wild-type and *Gata1*^{low} mice were set separately. The ImageJ program-assisted quantification process includes selection of the cell type, determination of the threshold per cell (Saturation histogram) and quantification of the number of cells which exceed the threshold (Brightness histogram). Magnification 40x.

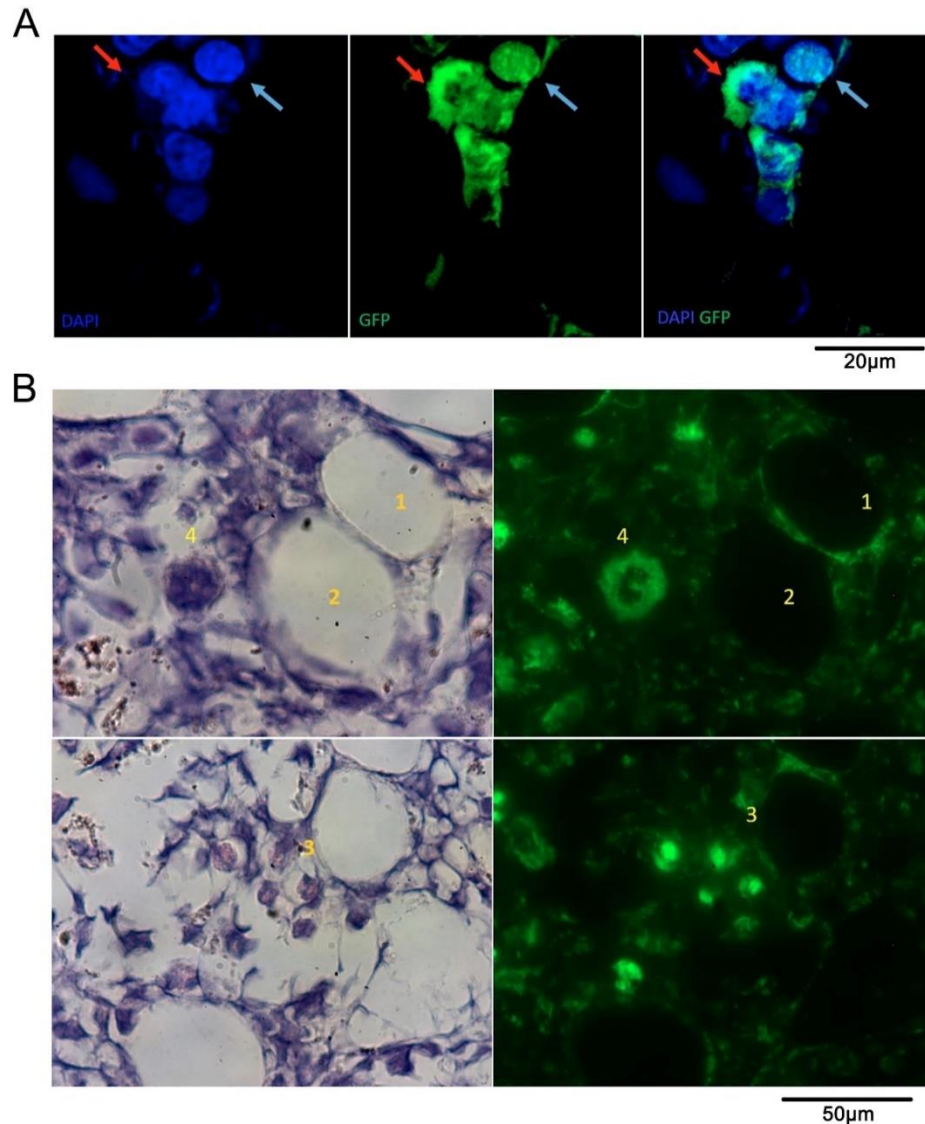


Figure S3. A) Median optical slice of a confocal stack microscopy obtained with a 63x objective. The blue arrow indicates a GFP signal present inside nucleus (shown as tridimensional image in movie 1), whereas the red arrow indicates a cell where the GFP signal is localized in the cytoplasm (shown as tridimensional image in movie 2). DAPI and GFP signals are shown separately and combined. **B)** Hematoxylin-eosin staining (left) and fluorescent microscopy (right) of two representative sections from the bone marrow of one huCD34-GFP^{H2B} mouse. The GFP staining labels either the nuclear areas of cells with small size (1, 2 and 3) or, very rarely, the cytoplasm of large cells (4), possibly macrophages. Slides were counter stained with DAPI. Magnification 40x.

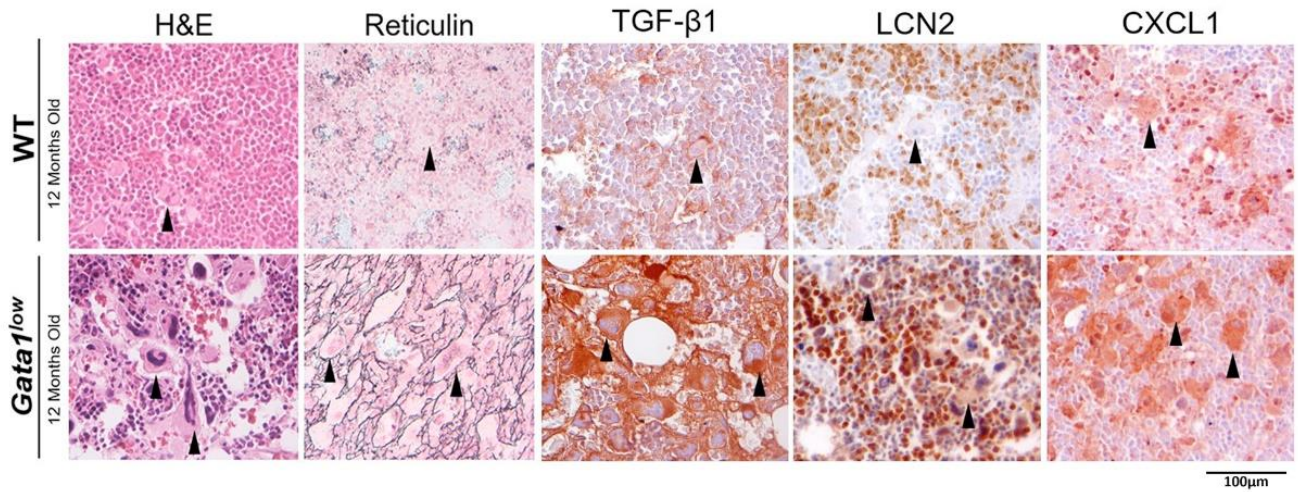


Figure S4. Hematoxylin/Eosin (H&E) and reticulin staining and TGF- β 1, LCN2 and CXCL1 immunostaining of bone marrow sections from representative wild-type (WT) and *Gata1*^{low} littermates showing the fibrosis and increased cytokine bioavailability in microenvironment of the mutant mice. Results are representative of those observed in 12-month-old mice randomly selected from male and female, at least were analyzed 6 mice each staining. The arrows indicate individual megakaryocytes in wild-type mice and megakaryocyte clusters in *Gata1*^{low} mice. Magnification 40x. Similar results were previously published in Dunbar et al, 2021(A. Dunbar et al., 2021).

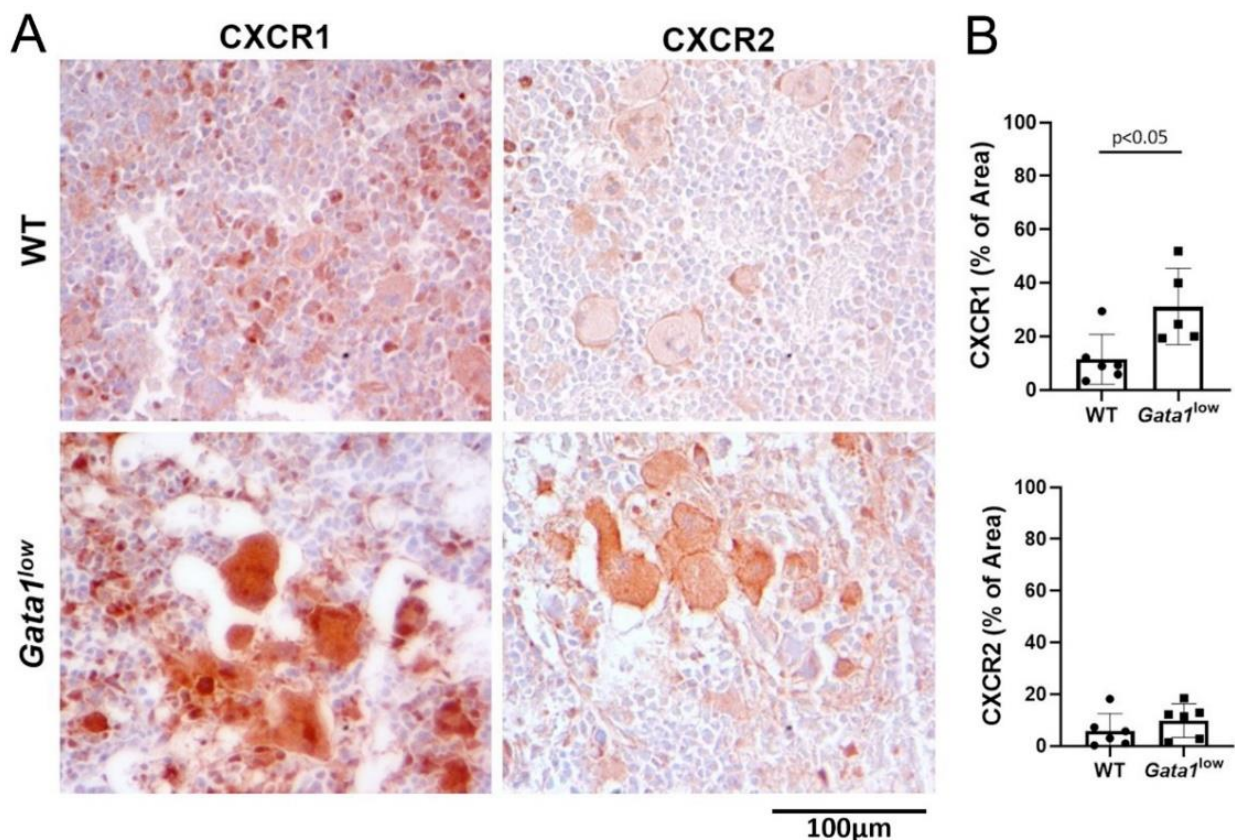


Figure S5. The bone marrow from *Gata1*^{low} mice contain great levels of CXCR1. High levels of CXCR1 and CXCR2 in bone marrow sections from *Gata1*^{low} mice. A) Representative sections from the bone marrow of wild-type and *Gata1*^{low} littermates immunostained with antibodies per CXCR1 and CXCR2. Magnification 40x. B) Computer assisted quantification of the content of the CXCR1 and CXCR2 in 5 randomly selected areas per femur from three-four mice per experimental group. Statistical analysis was done by t-test and statistically significant p values among groups are indicated within the panels. Similar results were reported in Dunbar et al (A. Dunbar et al., 2021).

Adapted from: *Article*

The CXCR1/CXCR2 inhibitor Reparixin Alters the Development of Myelofibrosis in the *Gata1*^{low} Mice

Paola Verachi¹, Francesca Gobbo^{1,2}, Fabrizio Martelli³, Andrea Martinelli⁴, Giuseppe Sarli², Andrew Dunbar^{5,6,7}, Ross L. Levine^{5,6,7,8}, Ronald Hoffman^{7,9}, Maria Teresa Massucci¹⁰, Laura Brandolini¹⁰, Cristina Giorgio¹¹, Marcello Allegretti¹⁰ and Anna Rita Migliaccio^{12,13}

¹ Department of Biomedical and Neuromotor Sciences, Alma Mater Studiorum University, Bologna, Italy;

² Department of Veterinary Medical Sciences, University of Bologna, Ozzano dell'Emilia, Bologna, Italy;

³ National Center for Drug Research and Evaluation, Istituto Superiore di Sanità, Rome, Italy;

⁴ Center for animal experimentation and well-being, Istituto Superiore di Sanità, Rome, Italy.;

⁵ Human Oncology & Pathogenesis Program, Memorial Sloan Kettering Cancer Center, New York, NY, USA;

⁶ Leukemia Service, Department of Medicine and Center for Hematologic Malignancies, Memorial Sloan Kettering Cancer Center, New York, NY, USA;

⁷ Myeloproliferative Neoplasm Research Consortium;

⁸ Center for Epigenetics Research, Memorial Sloan Kettering Cancer Center, New York, NY, USA;

⁹ Division of Hematology/Oncology, Tisch Cancer Institute and Department of Medicine, Icahn School of Medicine at Mount Sinai, New York, NY, USA;

¹⁰ Dompé Farmaceutici Spa R&D, L'Aquila, Italy;

¹¹ Dompé Farmaceutici Spa R&D, Napoli, Italy;

¹² Center for Integrated Biomedical Research, Campus Bio-medico, Rome, Italy;

¹³ Altius Institute for Biomedical Sciences, Seattle, WA, USA.

* Correspondence: Anna Rita Migliaccio, Altius Institute for Biomedical Sciences, Seattle, WA, USA. amigliaccio@altius.org and Marcello Allegretti, Chief Scientific Officer; Dompé Farmaceutici Spa; email: marcello.allegretti@dompe.com

Abstract. A major role for human (h)CXCL8 (interleukin-8) in the pathobiology of myelofibrosis (MF) has been suggested by observations indicating that MF megakaryocytes express increased levels of hCXCL8 and that plasma levels of this cytokine in MF patients are predictive of poor patient outcomes. Here, we demonstrate that, in addition to high levels of TGF- β , the megakaryocytes from the bone marrow of the *Gata1*^{low} mouse model of myelofibrosis express high levels of murine (m)CXCL1, the murine equivalent of hCXCL8, and its receptors CXCR1 and CXCR2. Treatment with the CXCR1/R2 inhibitor, Reparixin in aged-matched *Gata1*^{low} mice demonstrated reductions in bone marrow and splenic fibrosis. Of note, the levels of fibrosis detected using two independent methods (Gomori and Reticulin staining) were inversely correlated with plasma levels of Reparixin.

Immunostaining of marrow sections indicated that the bone marrow from the Reparixin-treated group expressed lower levels of TGF- β 1 than those expressed by the bone marrow from vehicle-treated mice while the levels of mCXCL1, and expression of CXCR1 and CXCR2, were similar to that of vehicle-treated mice. Moreover, immunofluorescence analyses performed on bone marrow sections from *Gata1*^{low} mice indicated that treatment with Reparixin induced expression of GATA1 while reducing expression of collagen III in megakaryocytes. These data suggest that in *Gata1*^{low} mice, Reparixin reduces fibrosis by reducing TGF- β 1 and collagen III expression while increasing GATA1 in megakaryocytes. Our results provide a preclinical rationale for further evaluation of this drug alone and in combination with current JAK inhibitor therapy for the treatment of patients with myelofibrosis.

Keywords: Myelofibrosis, megakaryocytes, TGF- β , GATA1, CXCL8 (interleukin-8)

1. Introduction

Primary Myelofibrosis (MF) is due to both a primary clonal myeloproliferation as a result of activating mutations of the JAK/STAT pathway and a secondary inflammatory response characterized by micro-environmental changes and aberrant release of multiple pro-inflammatory cytokines (Tefferi, 2005). Abnormal megakaryocytes (MKs) play a crucial role in the development of the MF stromal reaction (Vannucchi et al., 2005), which includes bone marrow (BM) reticulin fibrosis, osteosclerosis, increased microvessel density, a proinflammatory milieu, anemia, splenomegaly and extramedullary hematopoiesis (Tefferi, 2005; Tefferi et al., 2011). Current JAK1/2 inhibitor therapy improves clinical symptoms but does not alter the clinical progression to more overt phases of MF or blast phase (Verstovsek et al., 2017; Harrison et al., 2016). Therefore, novel therapeutic strategies aiming to reduce the inflammatory microenvironment that contributes to the sustained proliferation of the malignant hematopoietic stem cells (HSCs) are currently being investigated (Zimran et al., 2019).

Human (h)CXCL8 (C-X-C Motif Chemokine Ligand 8) is a member of the chemokine family and exerts its biological activities by signaling through the CXCR1 and CXCR2 receptors. The chemokine family also includes CXCL1, CXCL2, CXCL3, CXCL5, CXCL6, and CXCL7, and together they share an ELR (glutamic, leucine, arginine) motif that mediates CXCR1/2 binding. Most of the studies published until now have investigated the biological effects exerted by hCXCL8 and its receptors on polymorphonuclear leukocytes. However, the effects exerted by hCXCL8 on other cell types, such as endothelial, epithelial and fibroblasts, known also to express CXCR1/CXCR2, are still poorly defined (Russo et al., 2014). hCXCL8 is produced by several bone marrow cells, including megakaryocytes (MKs) (Takeuchi et al., 1999), and exhibits many biological functions in inflammation, hematopoietic stem cell (HSC) proliferation, mobilization, and neo-angiogenesis. A previous study demonstrated that hCXCL8 contributes to altered MK proliferation, differentiation, and ploidy in myeloid metaplasia with MF (Emadi et al., 2005). Moreover, high levels of circulating

hCXCL8 were detected in patients with MF and were predictive of inferior survival (Tefferi et al., 2011). In addition, Dunbar et al have demonstrated that the malignant CD34+ clones from a subset of MF patients secrete high levels of hCXCL8 in vitro which is associated with adverse clinical outcome and increased marrow fibrosis (Dunbar et al., 2020).

Full understanding of the pathophysiological role of hCXCL8 has been limited by known differences between human and rodents. In humans, hIL-8/CXCL8 (and CXCL6, also known as GCP-2) exerts its activity by activating both CXCR1 and CXCR2 (Murphy et al., 1991, Holmes et al., 1991), whereas the other ELR-CXC chemokines selectively bind CXCR2 (Wuyts et al., 1997). For many years, only one functional ELR-CXC receptor was identified in mice and was characterized as the homologue of human CXCR2 (Bozic et al., 1994; Cerretti et al., 1993). This receptor, showing high affinity for the murine counterparts of hCXCL8, mCXCL1(KC) and MIP-2, was believed to be responsible for the functions attributed to the two human receptors. Consistent with this, gene ablation of mouse CXCR2 impairs neutrophil responses to murine MIP-2 and to hIL-8/CXCL8 (Cacalano et al., 1994; Lee et al., 1995) confirming a critical role for CXCR2 in neutrophil recruitment and activation. The orthologous murine CXCR1 (mCXCR1) (Fu et al., 2005; Moepps et al., 2006) was subsequently identified and found to be expressed by BM, peripheral mononuclear cells, CD4+ and CD8+ T cells, and certain lymphoid cell types but was first considered to be a non-functional receptor due to the repeated failure of any attempt to identify its cognate ligand/s. More recently, mCXCR1 has been confirmed to behave as a functional receptor (Fan et al., 2006), specifically activated by mGCP-2, hGCP-2/CXCL6, and hIL-8/CXCL8, and to play a key role in collagen-induced arthritis (mCIA). This discovery paved the way for novel studies on the biology of CXCR1/2 using mouse models. These studies support the notion that mCXCR1 is the functional murine orthologue of hCXCR1 and that hIL-8/CXCL8 is functionally replaced, in addition by mCXCL1, by CXCL6 in mice (Wuyts et al., 1996).

Reparixin is a dual, non-competitive allosteric antagonist of the hCXCL1 receptors hCXCR1/R2 with a marked selectivity for hCXCR1 ($IC_{50} = 1\text{nM}$ for hCXCR1; $IC_{50} = 400\text{ nM}$ for hCXCR2) and cross-reactivity with mCXCR1/2 (Bertini et al., 2004; Citro et al., 2014). In particular, the allosteric modulation exerted by Reparixin inhibits human and murine CXCR1/R2 activation independently of the cognate ligand (Allegretti et al., 2008) and without blocking binding of the ligand to its receptors (Stipo J et al., 2015). The mechanism of action of Reparixin accounts for the functional selectivity of the drug that allows it to switch off G-protein mediated pathway activation without impairing ligand-induced internalization and scavenging thus not affecting the extracellular levels of mCXCL1. The *in vivo* activity of Reparixin was originally evaluated in animal models of ischemia/reperfusion injury (Bertini et al., 2004) and the therapeutic potential of CXCR1/R2 inhibition was further investigated in several mouse models of airway inflammation. In particular, Reparixin was shown to ameliorate pulmonary fibrosis caused by the administration of particulate matter and bleomycin in mice (Cheng et al., 2019). Similarly, the CXCR1/R2 inhibition exerted by ladarixin, a dual allosteric blocker of

CXCR1/R2 structurally similar to Reparixin, has been shown to reduce neutrophil infiltration and collagen deposition in the bleomycin-induced mouse model of pulmonary fibrosis (Mattos et al., 2020). These data suggest CXCR1/2 inhibition might have anti-fibrotic effects across numerous organs.

Mice carrying the hypomorphic *Gata1*^{low} mutation express the same MKs alterations observed in MF patients and develop progressive MF closely resembling human disease, including a BM failure syndrome and development of extramedullary hematopoiesis (Centurione et al., 2004; Vyas et al., 1999; Vannucchi et al., 2002). Previous studies have demonstrated that MKs from the BM of *Gata1*^{low} mice express not only high levels of TGF- β 1 (Zingariello et al., 2013), but also high levels of mCXCL1, the murine equivalent of hCXCL8 (Zingariello et al., 2022). Using these data as a foundation, in the current study we have evaluated whether MKs from *Gata1*^{low} mice express CXCR1 and CXCR2 and tested whether treatment with Reparixin affects the development of MF in this mouse model.

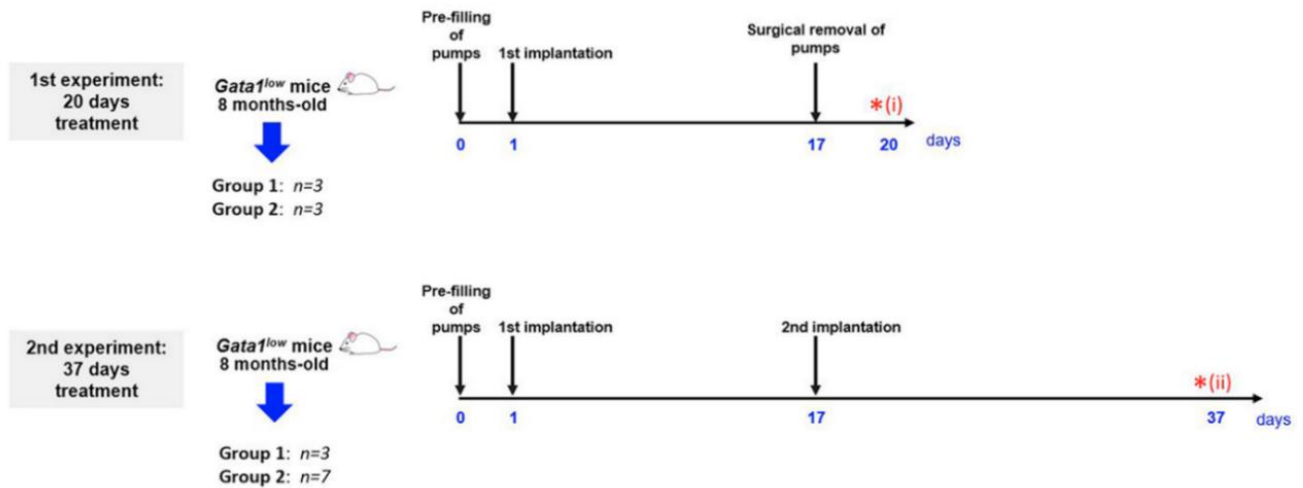
2. Materials and methods

2.1. Mice

Gata1^{low} mice were originally obtained from Dr S Orkin and bred in the animal facility of Istituto Superiore di Sanità as described (Vannucchi et al., 2002). Littermates were genotyped at birth by PCR as previously described (Martelli et al., 2005) and those found not to carry the mutation were used as wild-type (WT) controls. All the experiments were performed according to the protocols approved by the institutional animal care committee according to the European Directive 86/609/EEC.

2.2. Treatment

Sixteen eight-months-old *Gata1*^{low} mice were then anesthetized with 2-to-3% isoflurane and implanted subcutaneously with an ALZET® Osmotic Pump (model 2002) pre-filled with 200 μ L of vehicle (sterile saline) or Reparixin (7.5mg/h/Kg in sterile saline) as described by the manufacturer's instructions. The concentration of Reparixin was chosen on the basis of previous concentration-response and efficacy studies in which the selected concentration of 7.5 mg/h/kg administered by continuous infusion was proven to be able to reduce pathological outcomes in preclinical models of liver ischemia and reperfusion, neuropathic pain and acquired epilepsy (Cavalieri et al., 2005; Brandolini et al., 2017; Di Sapia et al, 2021) Before treatment, the mouse genotype had been confirmed by PCR as described (Martelli et al., 2005). The scheme of the two experiments and of their end-points is outlined in **Figure 1**.



Group 1: Vehicle (sterile saline) administered subcutaneously by ALZET® Osmotic Pumps

Group 2: Reparixin (7.5mg/h/Kg in sterile saline) administered subcutaneously by ALZET® Osmotic Pumps

Figure 1. Scheme of the two treatments of *Gata1*^{low} mice with either vehicle or Reparixin for 20 (experiment 1) or 37 (experiment 2) days. In experiment 1, mini-pumps were removed at day 17 and three mice per experimental group were sacrificed at day 17 for end-point determination. In experiment 2, mini-pumps were removed at day 17 from three vehicles and six Reparixin-treated mice and the mini-pumps were replaced with a second implant. These mice were then treated for 17 additional days and sacrificed at day 37. Red asterisks indicate the timing of the sacrifice in the first (i) and second (ii) experiment.

In the first experiment, mini-pumps were removed on day 17, and three mice per experimental group were weighed, bled for blood count determinations and plasma collection, and sacrificed for histopathological evaluation of the BM and spleen at day 20. Since the manufacturer guarantees that the Alzet model 2002 mini-pumps deliver the drug with the predicted rates only for 14 days, to mimic the clinical situation in which Reparixin is likely to be administered to patients for long time, in the second experiment, mini-pumps were removed from three mice treated with vehicle and seven mice treated with Reparixin and replaced with newly filled devices. These mice were then treated for 17 additional days and analyzed on day 37, when they were weighed, bled for blood count determinations and plasma collection, and sacrificed for histopathological analyses.

2.3. Blood collection

Mice were topically anesthetized with lidocaine (one drop/eye) and blood was collected from the retro-orbital plexus into microcapillary tubes using sodium citrate 3.2% (ratio 1:9) as an anticoagulant. Hematocrit (Hct), platelets (Plts) and white blood cells (WBC) counts were evaluated by an accredited commercial laboratory which provides diagnostic services on laboratory animals (Plaisant Laboratory). For drug concentration determinations, plasma was separated from whole blood by centrifugation for 20 min at 10000 rpm and stored at -20°.

2.4. Determination of the plasma concentration of Reparixin

Determinations of Reparixin levels in plasma samples involved protein precipitation by the addition of acetonitrile (Sigma-Aldrich, S. Louis, MO, USA) (ratio 1:3). Samples were then centrifuged (20000 x g for 15 min at 4°C) and supernatants analyzed by high-performance liquid chromatography (HPLC, Dionex-Thermo Fisher Scientific, Sunnyvale, CA, USA) using an electrospray ionization (ESI) source for detection. The chromatographic column was a Gemini C18 100 x 2.0 mm, 5µm (Phenomenex, Torrance, CA, USA) and the lower limit of quantification is 0.05 µg/mL.

2.5. Histological analyses

Femurs were fixed in formaldehyde (10% v/v with neutral buffer), treated for 1h with a decalcifying solution (Osteodec; Bio-Optica, Milan, Italy) and paraffin embedded. Spleens were fixed in formaldehyde as previously described (Zingariello et al, 2013) and embedded in paraffin. Paraffin-embedded tissues were cut into consecutive 3µm sections and stained either with Hematoxylin-Eosin (H&E; Hematoxylin cat no. 01HEMH2500; Eosin cat no. 01EOY101000; Histo-Line Laboratories, Pantigliate, MI, Italy), Gomori silver (cat no. 04-040801; Bio-Optica) or Reticulin (cat no. 04-040802; Bio-Optica) staining. These two last staining both reveal the presence of reticulin fibers and were used as independent evaluations of fibrosis to increase the rigor of the assessment of the findings. BM sections were immune-stained with anti-CXCL1 (cat# ab86436, Abcam, Cambridge, UK), anti-CXCR1 (cat# GTX100389, Genetex, Irvine, CA, USA), anti-CXCR2 (cat# catalog ab14935, Abcam) or anti-TGF-β1 (cat no. sc-130348, Santa Cruz Biotechnology, Santa Cruz, CA, USA, from now on we use TGF-β1 or TGF-β, depending whether results were obtained with reagents which recognize the TGF-β1 isoform or all the three TGF-β isoforms), antibodies. Immunoreactions were detected with avidin-biotin immune-peroxidase (Vectastain Elite ABC Kit, Vector Laboratories, Burlingame, CA, USA) and the chromogen 3,3'-diaminobenzidine (0.05% w/v). Slides were counterstained with Papanicolaou's hematoxylin (Histo-Line Laboratories). Images were acquired with an optical microscope (Eclipse E600; Nikon, Shinjuku, Japan) equipped with the Imaging Source "33" Series USB 3.0 Camera (cat no. DFK 33UX264; Bremen, DE). Images were processed and the intensity of the immunostaining quantified with the software ImageJ (version 1.52t) (National Institutes of Health).

2.6. Immunofluorescence analysis

Three micron-thick BM sections were dewaxed in xylene and treated with EDTA buffer pH=8 for 20' in a pressure cooker (110-120°C, high pressure) for antigen retrieval. Sections were labeled with antibody against CD42b (a rat monoclonal antibody that recognizes the alpha chain of platelet glycoprotein I, cat no. ab183345, Abcam), GATA1 (rat monoclonal, cat no. sc-265, Santa Cruz) and Collagen III (rabbit polyclonal, cat no. ab7778, Abcam) over night at 4°C. Detection of primary antibodies was visualized with a secondary antibody goat anti rat Alexa Fluor 488 (cat no. ab150165,

Abcam) and goat anti rabbit Alexa Fluor 555 (cat no. ab150078, Abcam). Sections were counterstained with DAPI (cat no. D9542-5MG, Sigma-Aldrich, Darmstadt, DE) and mounted with Fluor-shield histology mounting medium (Catalog F6182-10MG, Sigma-Aldrich). Slides were examined using a Nikon Eclipse Ni microscope equipped with filters appropriate for the fluorochrome to be analyzed. Images were recorded with a Nikon DS-Qi1Nc digital camera and NIS Elements software BR 4.20.01. Confocal microscopy determinations were performed at 40x magnification on at least 120 CD42b positive cells (MKs) per area (0.720mm^2) of bone marrow section per mouse. We have analyzed a total of 6 mice treated with vehicle, three mice treated with Reparixin for three days and 7 mice treated with Reparixin for 37 days.

2.7. Data analysis

Data were analyzed and plotted using GraphPad Prism 8.0.2 software (GraphPad Software, San Diego, California United States) and presented as Mean (\pm SD) or as box charts, when appropriate. Shapiro-Wilk test was used to confirm that the data are normally distributed. Comparisons between the two groups were performed with one way Anova while comparisons between multiple groups were performed with the Tukey's multiple comparisons test. Linear correlations were calculated by the Pearson *R* test. Differences were considered statistically significant with a $p < 0.05$.

3. Results

3.1. Treatment with Reparixin is well tolerated without significant changes in body weight and blood counts

The body weight of the mice included in the two experiments and its variations during treatment are shown in **Figure 2**. Probably due to sampling bias, before treatment the weight of the mice included in the vehicle and Reparixin group is statistically different ($p < 0.01$). The difference in weight of the Reparixin-treated mice remains statistically different from that of the vehicle mice at days 20 ($p < 0.05$). However, there is no statistically significant difference between the Reparixin-treated mice and the corresponding vehicle group both at days 20 and 37 (**Figure 2**). The wellbeing of the treated mice was monitored daily by a veterinarian. Death was not recorded and the mice remained active with no significant changes in behavior (no lethargy, no excessive grooming, no change in coat luster) during all the period of observation. The Htc and WBC counts remained within normal ranges in all experimental groups, while Plt counts were low as has been previously observed in *Gata1*^{low} mice (**Table 1**). In-depth analyses of the WBC populations, revealed significant greater neutrophil counts at day 37 versus days 20 (**Table 1**), while the lymphocyte and monocyte counts remained similar among groups (**Figure S1**).

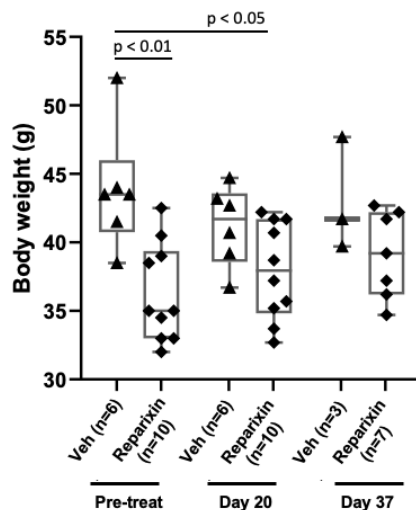


Figure 2. Treatment with Reparixin did not affect animal weights. Body weight determinations performed before (Pre-treat) and after 20 or 37 days of treatment with Reparixin. Data are presented as box charts and as value per individual mouse (each symbol a different mouse). The data are normally distributed by Shapiro-Wilk test and the Reparixin pre-treatment ($p < 0.01$) and at day 20 ($p < 0.05$) group are statistically different from the vehicle group by Turkey's multiple comparison test.

Table 1. Blood parameters observed in mice treated with vehicle or with Reparixin for 20 or 37 days. Data are presented as Mean (\pm SD) and p values are calculated by Tukey's multiple comparisons test. Abbreviations: Htc, hematocrit; Plt, platelet count; WBC, white blood cells count. The number of mice included in each experimental group is indicated by n.

	Htc (%)	WBC ($\times 10^3/\mu\text{L}$)	Neutrophils ($\times 10^3/\mu\text{L}$)	Plt ($\times 10^3/\mu\text{L}$)
Vehicle ($n=5$)	34.32 \pm 3.87	2.78 \pm 0.55	0.35 \pm 0.32	187.80 \pm 26.12
Reparixin day 20 ($n=3$)	35.63 \pm 3.45	3.27 \pm 0.72	0.30 \pm 0.18	181.30 \pm 53.30
p values (versus vehicle)	0.8771	0.8103	0.9868	0.9862
Reparixin day 37 ($n=6$)	30.92 \pm 3.58	3.57 \pm 1.43	1.02 \pm 0.52	99.83 \pm 71.92
p values (versus vehicle)	0.3136	0.4684	0.0465	0.0591
p values (versus Reparixin day 20)	0.2082	0.9173	0.0691	0.1429

3.3. Plasma levels of Reparixin

According to the specification provided by the manufacturer, Alzet model 2002 mini-pumps have an approximate 0.2mL reservoir that delivers a preloaded drug or vehicle solutions continuously for at least 14 days at a rate of 5 $\mu\text{L}/\text{h}$. To confirm that mice remained to the drug at the time of sacrifice, the plasma levels of Reparixin at day 20 and 37 were determined. Plasma levels ranged from 3.24 to

17.87 $\mu\text{g}/\text{mL}$. These levels are similar to those observed in previous experiments using the same device (Di Sapia et al., 2021). Notably, plasma levels of Reparixin were significantly higher in mice treated for 20 days (13.90 \pm 4.18) compared to those that underwent a second implantation and were treated for 17 additional days (6.71 \pm 4.18) (**Figure 3**). Although the levels of drug detected at the second time-point were similar to those determined in prior studies (Di Sapia et al., 2021), the observation that mice treated with the same concentration for longer time have plasma level of the drug lower than those treated for lower times is puzzling. It is possible that changes in the cell composition of the longer treated mice lead to greater amounts of tissue-bound Reparixin reducing the free levels of the drug found in plasma. However, it is also possible that the plasma levels of Reparixin at the two time points reflect differences in the efficiency of the derma to absorb the drug. This alternative hypothesis is supported by the observation that, since GATA1 regulates the differentiation of dermal mast cells, derma of *Gata1*^{low} mice contains great numbers of these cells (Migliaccio et al., 2003). In addition, wild-type CD1 mice, the background in which we harbor the *Gata1*^{low} mutations express a systemic pro-inflammatory signature which determines chronic dermatitis with dermal fibrosis (Zingariello et al., 2022). This baseline dermal fibrosis is also present in *Gata1*^{low} mice (ARM, unpublished observations) and it is possibly exacerbated once the mast cells are activated by the mechanical stress induced by the mini-pumps implanted subcutaneously, reducing the efficiency of the dermal absorption and of the plasma levels of the drug. Therefore, the plasma levels of Reparixin are a true reflection of the concentration of the drug delivered by the mini-pumps to the animals.

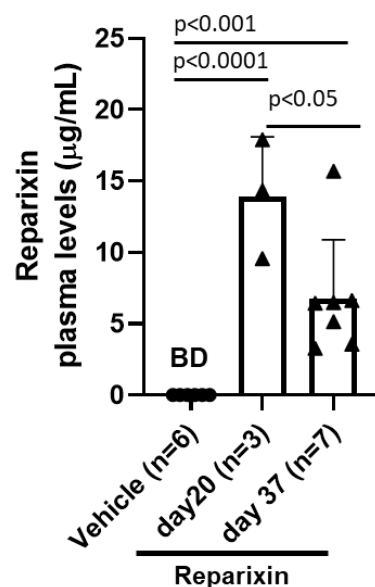


Figure 3. Plasma levels ($\mu\text{g}/\text{mL}$) of Reparixin detected at days 20 and 37. Plasma levels of Reparixin were significantly higher in *Gata1*^{low} mice scarified at day 20 as compared to those scarified at day 37. Data are presented as Mean (\pm SD) and are analyzed by Tukey's multiple comparisons test. Dots represents values observed in the individual mice. $p<0.05$ was considered statistically significant. Abbreviations: BD, below detectable levels (i.e. $< 20\%$ of the lower limit of quantitation ($0.2\mu\text{g}/\text{mL}$)).

3.4. The reduction of fibrosis in the BM of *Gata1^{low}* mice induced by Reparixin correlates with the concentration of the drug in the blood

The BM from *Gata1^{low}* mice is characterized by reduced cellularity due to accumulation of reticulin fibers with age (Vannucchi et al., Blood 2002). Overall, the treatment had modest effects on BM cellularity (**Table 2**).

Table 2. Bone marrow cellularity and spleen weight determined in *Gata1^{low}* mice treated either with vehicle or with Reparixin for 20 or 37 days. Data are presented as Mean (\pm SD) and p-values were calculated with respect to vehicles by Tukey's multiple comparisons test.

	Cells/femur ($\times 10^6$)	Spleen weight (g)
Vehicle ($n=6$)	20.55 \pm 5.83	0.33 \pm 0.13
Reparixin day 20 ($n=3$)	22.24 \pm 0.85 ($p=0.91$)	0.26 \pm 0.05 ($p=0.51$)
Reparixin day 37 ($n=7$)	21.68 \pm 6.49 ($p=0.93$)	0.35 \pm 0.06 ($p=0.93$)

However, a reduction in BM fibrosis was observed by both Gomori and Reticulin staining in mice treated with Reparixin compared to those treated with vehicle alone to a statistically significant degree on day 20 (**Figure 4A-B**). Since mice treated for 20 days had higher concentrations of the drug in the plasma, we assessed whether the effects exerted by Reparixin on fibrosis was concentration-dependent rather than time-dependent by performing concentration/effect correlation analyses. Notably, this analysis revealed that the levels of fibrosis were inversely correlated with the plasma levels of the drug in individual mice (**Figure 4C**).

3.4. The reduction of fibrosis in the spleen of *Gata1^{low}* mice induced by Reparixin correlates with the levels of the drug in the blood

Gata1^{low} mice develop extramedullary hematopoiesis with fibrosis in the spleen and associated splenomegaly. Despite the fact that treatment with Reparixin did not induce significant changes in spleen volumes (**Table 2**), histological analyses indicated a remarkable reduction in the fibrosis expressed by the spleen in the Reparixin-treated mice (**Figure 5A**). As for BM, the reductions observed in the spleen were statistically significant only at day 20 (**Figure 5B**) but analyses of all the time points revealed a significant inverse correlation between fibrosis detected by reticulin staining and plasma levels of Reparixin in individual mice (**Figure 5C**).

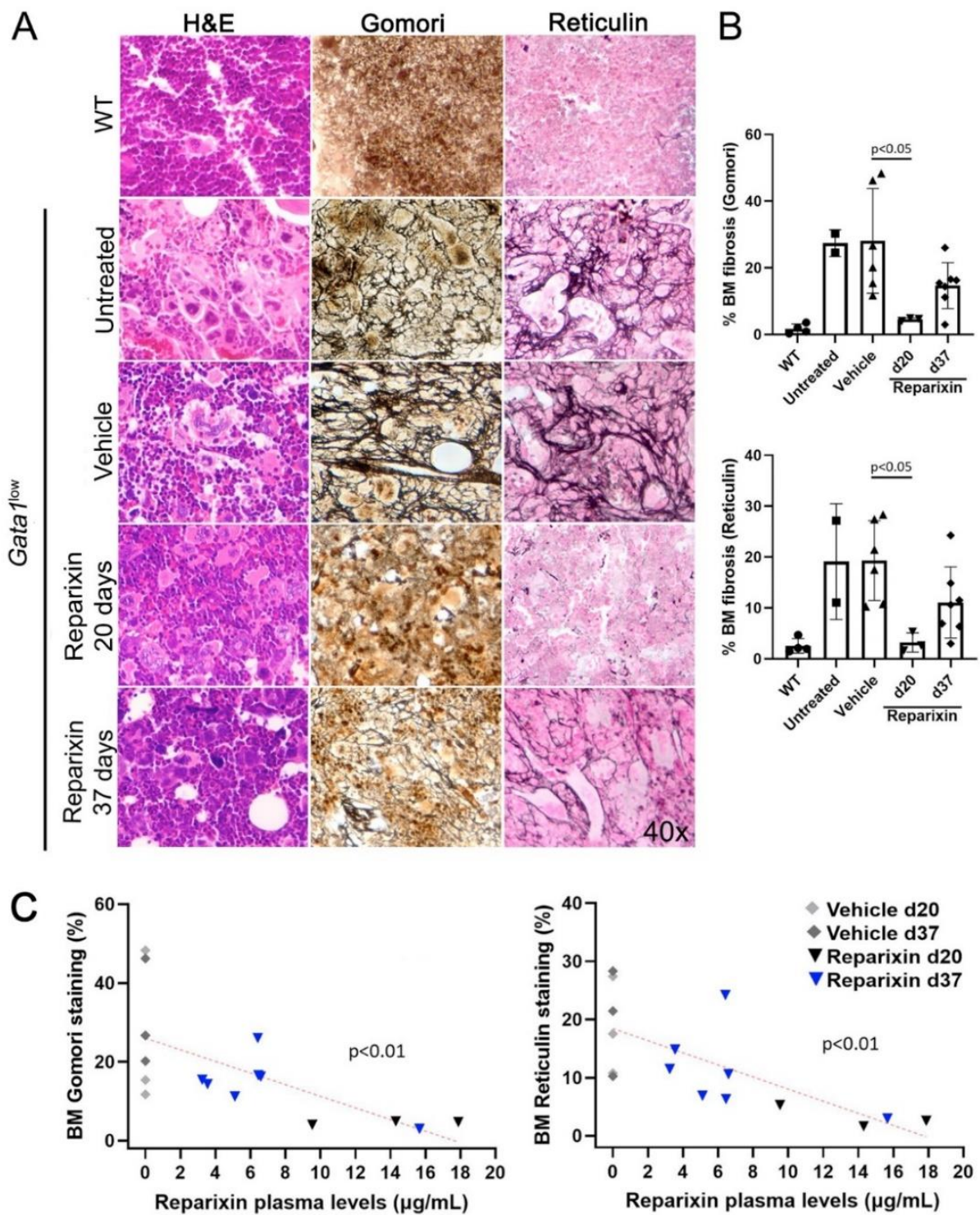


Figure 4. Reparixin decreases in a concentration-dependent fashion the fibrosis present in the BM from *Gata1*^{low} mice. **A)** H&E, Reticulin, and Gomori staining of BM sections from representative *Gata1*^{low} mice treated either with vehicle or Reparixin for 20 or 37 days, as indicated. Untreated *Gata1*^{low} and WT littermates are presented as positive and negative controls, respectively. Magnification 400x. **B)** Levels of fibrosis quantified by computer image analyses on BM sections stained with Gomori or Reticulin from multiple *Gata1*^{low} mice treated either with vehicle or Reparixin, as indicated. Data are presented as Mean (\pm SD) and are analyzed by Tukey's multiple comparisons test. $p < 0.05$ was considered statistically significant. **C)** Linear regression analyses between fibrosis plasma concentration or Reparixin in individual mice (Pearson $R = -0.66$, $p < 0.01$ for Gomori staining; Pearson $R = -0.71$, $p < 0.01$ for Reticulin staining). Each dot represents an individual mouse.

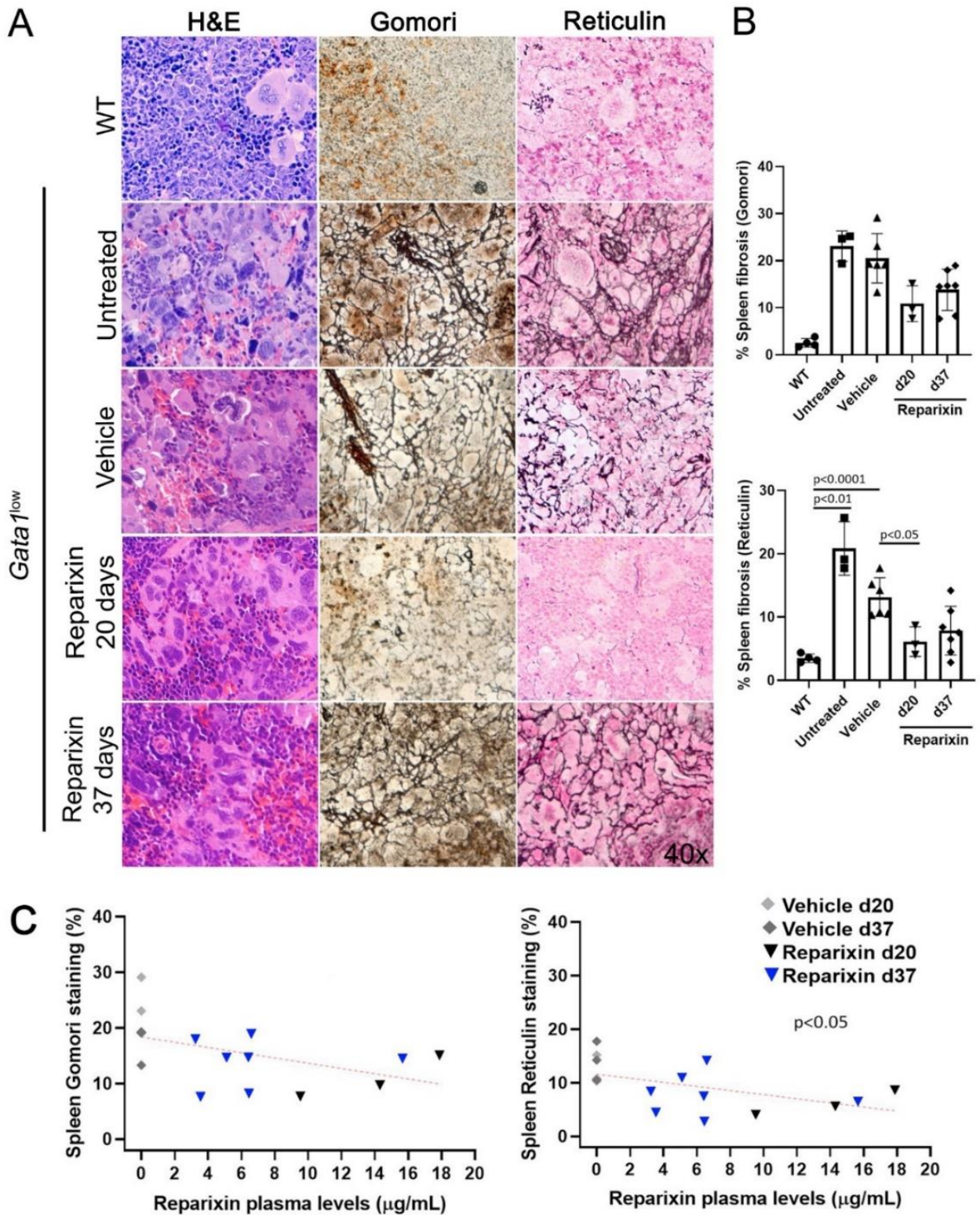


Figure 5. Reparixin decreased in a concentration-dependent fashion the degree of fibrosis present in the spleen of *Gata1^{low}* mice. **A)** H&E, Reticulin, Gomori and reticulin staining of spleen sections from representative *Gata1^{low}* mice treated either with vehicle or Reparixin for 20 or 37 days, as indicated. Untreated *Gata1^{low}* and WT littermates are presented as positive and negative controls, respectively. Magnification 400x. **B)** Levels of fibrosis quantified by image analyses in spleen sections stained with Gomori or Reticulin from *Gata1^{low}* mice treated either with vehicle or Reparixin, as indicated. Data were presented as Mean (\pm SD) and were analyzed by Tukey's multiple comparisons test. $p < 0.05$ was considered statistically significant. **C)** Linear regression analyses of fibrosis and plasma levels of Reparixin in individual mice (Pearson $R = -0.48$, not significant for Gomori staining; Pearson $R = -0.53$, $p < 0.05$ for Reticulin staining). Each dot represents a single mouse.

3.5. Treatment with Reparixin reduced the levels of TGF- β 1, but not that of mCXCL1 or its receptors CXCR1/2 in the BM of *Gata1*^{low} mice

To gain greater insights on the effects of Reparixin on fibrosis reduction in *Gata1*^{low} mice, we determined by immunohistochemistry the content of CXCL1, and of its receptors CXCR1 and CXCR2, in the BM of *Gata1*^{low} mice treated either with Reparixin or with vehicle. We had previously demonstrated that the BM from *Gata1*^{low} mice contain high levels of TGF- β and express an altered TGF- β signature which was thought to be the cause of the marrow fibrosis since treatment of the mice with the receptor-1(R1) kinase inhibitor SB431542 (Zingariello et al., 2013) or with a TGF- β trap (Varricchio et al., 2021) reversed both the abnormal TGF- β signature and the increase in marrow fibrosis, restoring hematopoiesis in BM, of these mice. On the basis of these data, the content of TGF- β in the BM of *Gata1*^{low} mice treated either with Reparixin or with vehicle was determined. These analyses indicated that the MKs from the Reparixin-treated mice express significantly lower levels of TGF- β 1 than the corresponding cells from animals receiving vehicle alone. By contrast the levels of CXCL1, CXCR1 and CXCR2 expressed by the Reparixin-treated MKs remained comparable to that of the vehicle-treated cells (**Figure 6**). Although the reductions in TGF- β 1 content were not correlated with the plasma levels of Reparixin of individual mice (data not shown), these results suggest that Reparixin may decrease fibrosis by reducing the levels of TGF- β 1.

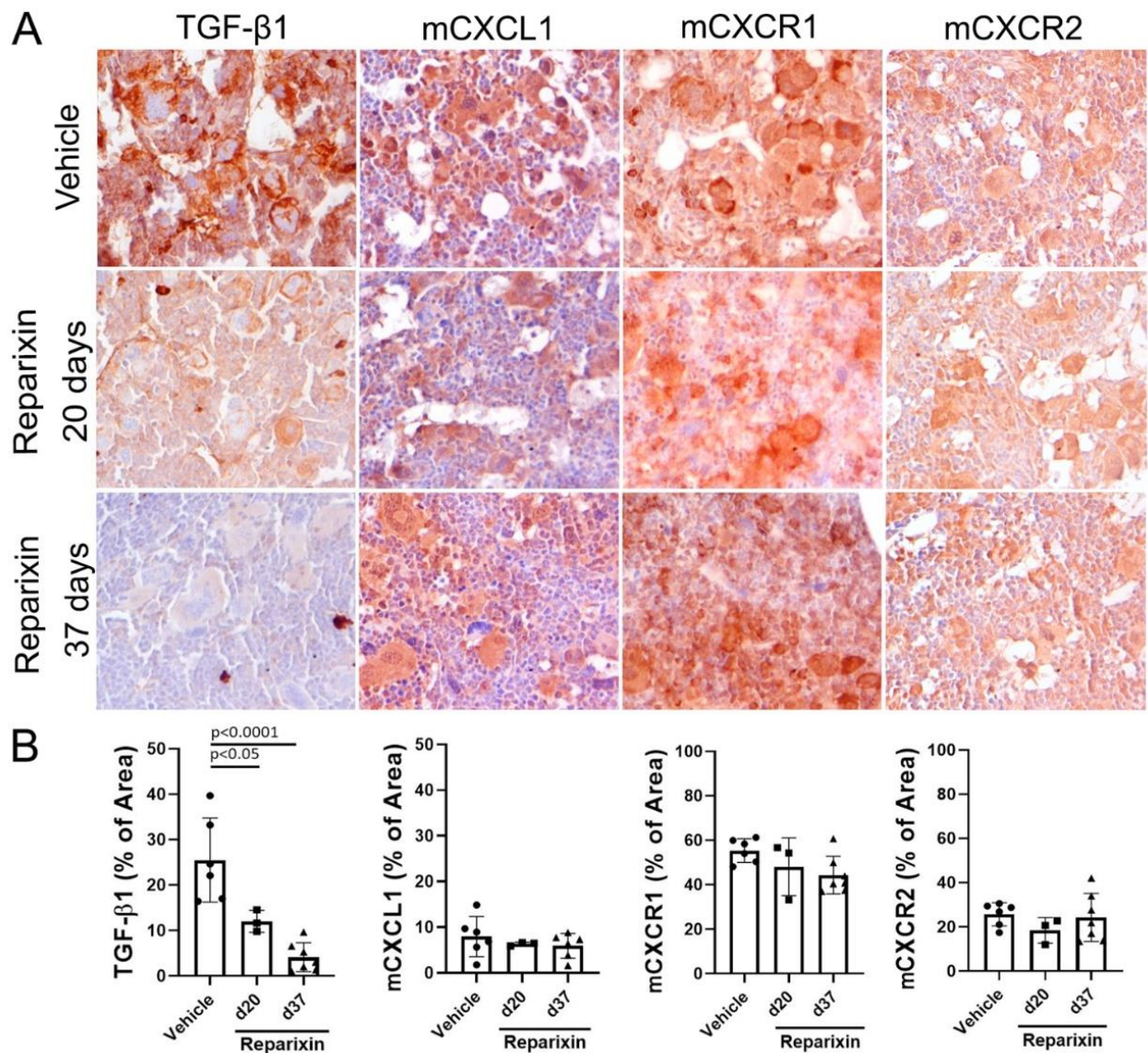


Figure 6. Treatment with Reparixin decreases the TGF-β1 content of the BM from *Gata1*^{low} mice. **A)** Immunohistochemical staining for TGF-β1, mCXCL1, mCXCR1, and mCXCR2 of BM sections from representative *Gata1*^{low} mice treated either with vehicle or Reparixin for 20 or 37 days, as indicated. Magnifications 40X. **B)** Quantification by computer assisted imaging of the TGF-β1, mCXCL1, mCXCR1 and mCXCR2 content in the BM from *Gata1*^{low} mice treated with either with vehicle or Reparixin for 20 or 37 days, as indicated. Data are presented as Mean (±SD) and were analyzed by Tukey's multiple comparisons test. Values observed in individual mice are presented as dots. $p < 0.05$ were considered statistically significant.

3.6. Reparixin increases the GATA1 content while reducing that of collagen III in MKs from the bone marrow of *Gata1*^{low} mice

Previous studies have established that both in MF patients and in MPN driver mutation animal models of myelofibrosis the reduced levels of GATA1 is due to a ribosomopathy that reduces the GATA1 content in the malignant MKs (Vannucchi et al., 2005; Gilles et al., 2017). In addition, MK-restricted expression of *JAK2*^{V617F}, the most common driver mutation of MF, is sufficient to induce myelofibrosis in mice (Zhan et al., 2016). The finding from the Balduini laboratory that a large proportion of the malignant MKs in the BM of MF patients express collagen, suggests that

hypomorphic GATA1 MKs are directly responsible for the fibrosis observed in these patients (Abbonante et al., 2016). This hypothesis is supported by recent single cell profiling of BM cells that has identified a previously unrecognized population of MKs poised to exert niche-functions by secreting collagen and other extracellular matrix proteins. These niche supporting MKs morphologically resemble immature MKs (low ploidy levels with reduced presence of granules and platelet-territories in their cytoplasm) the maturation of which is sustained by low levels of GATA1 and high levels of TGF- β signaling (Migliaccio and Hoffman, 2021; Sun et al., 2021; Wang et al., 2021).

Since the hypomorphic *Gata1*^{low} mutation are characterized by reduced expression of GATA1 in MKs and the BM from these mice express high levels of TGF- β (Vyas et al.,1999; Zingariello et al.,2013), we hypothesized that this fibrosis may be sustained by increased numbers of niche-poised MKs with low levels of GATA1 due to the increase in BM TGF- β and that the reduced levels of TGF- β induced by Reparixin would reduce the degree of marrow fibrosis by reducing the frequency of this niche-poised MKs present in BM. To test this hypothesis, we first analyzed the content of GATA1 in MKs from BM sections of mice treated either with vehicle or with Reparixin (**Figure 7**). This analysis confirmed that the BM from *Gata1*^{low} mice contained greater numbers of MKs and that the GATA1 content of these MKs was reduced (**Figure 7A**). Although the number of MKs in both vehicle- and Reparixin-treated mice remained greater than normal, the GATA1 content of the MKs from the Reparixin-treated mice was greatly increased (**Figure 7B,C**). Of note, the percentage of MKs expressing high GATA1 levels was directly correlated with the plasma levels of Reparixin detected in individual mice (**Figure 7D**).

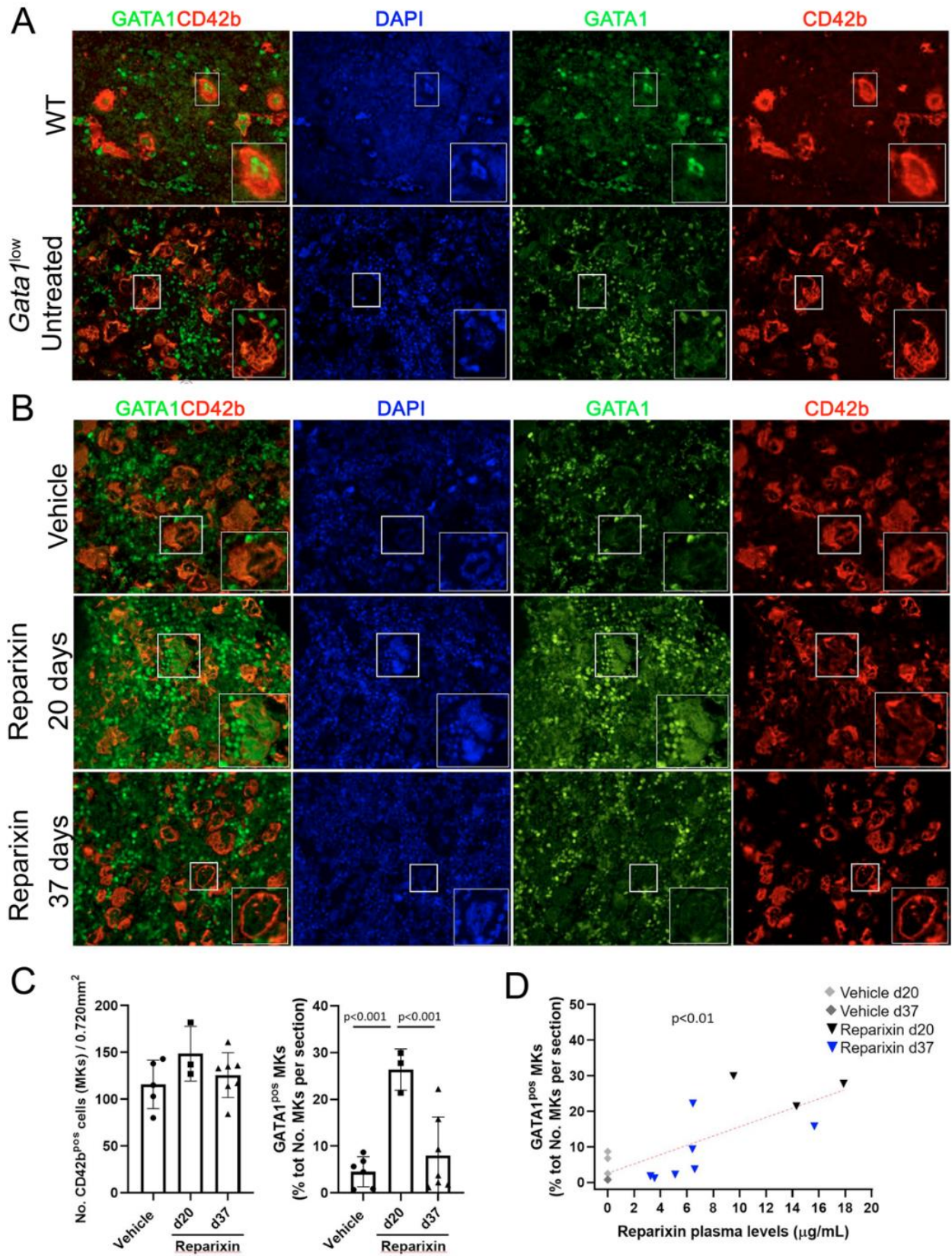


Figure 7. Reparixin restores in a concentration-dependent fashion the GATA1 content of the MKs in the BM of *Gata1*^{low} mice. **A**) Double immunofluorescence staining with GATA1 (FITCH-green) and CD42b (TRITCH-red), as a marker of MKs (Sim et al., 2017), antibodies of BM sections from representative wild-type (WT) and untreated *Gata1*^{low} mice, as indicated. The hypomorphic *Gata1*^{low} mutation selectively reduces expression of GATA1 in the MKs from the BM of *Gata1*^{low} mice compared to the correspondent cells from WT littermates. Magnification 400x. **B**) Double immunofluorescence staining with GATA1 (FITCH-green) and CD42b (TRITCH-red) of BM sections from representative

mice treated either with vehicle or Reparixin for 20 or 37 days, as indicated. Magnification 400x. The boxes in A and B indicate the MKs shown at greater magnification on the bottom of the panels. C) Frequency of MKs and percentage of MKs positive for GATA1 in BM sections from multiple treated mice. Data are presented as Mean (\pm SD) and as values in individual mice (each symbol a mouse). Results were analyzed by Tukey's multiple comparisons test. $p < 0.05$ were considered statistically significant. D) Correlation between the percent of MKs positive for GATA1 and plasma levels of the Reparixin in individual mice (Pearson $R = 0.76$, $p < 0.01$). Each dot represents a single mouse.

We then compared the percent of MKs expressing Collagen III in the BM of *Gata1*^{low} and WT mice (**Figure 8A,B**). Since the anti-ColIII antibody is conjugated with the same fluorochrome that labels most of the commercially available mouse CD42b antibodies, in these studies MKs were recognized on the basis of their large size and their polylobulated nuclei as revealed by DAPI staining. Greater number of the MKs in the BM from *Gata1*^{low} expressed increased levels of collagen III while these cells were rare in WT mice, suggesting that the BM from *Gata1*^{low} mice was enriched for niche-poised MKs.

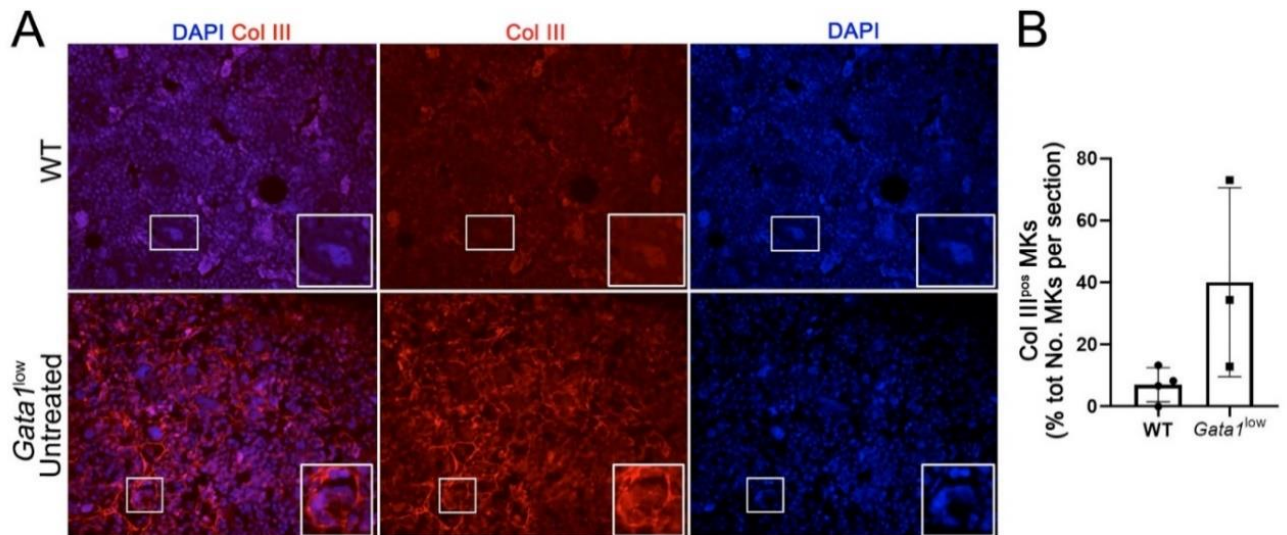


Figure 8. The bone marrow from *Gata1*^{low} mice contains great numbers of megakaryocytes that express Collagen III. **A)** Representative immunofluorescence staining with an anti-Col III (TRITCH-red) antibody showing that the MKs from *Gata1*^{low} mice express higher levels of Col III than those from their WT littermates. Megakaryocytes were recognized on the basis of their morphology (size and morphology of the nucleus). Magnification 400x. The white boxes indicate representative MKs shown at greater magnification on the right bottom side of each panel. **B)** Percent of MKs positive for Coll III (Col III^{pos} MKs) over the total numbers of MKs observed in BM sections from WT and *Gata1*^{low} littermates. Data are presented as Mean (\pm SD) and as frequency per individual mouse (dots) and were analyzed by One-way ANOVA. Each dot represents a single mouse. $p < 0.05$ was considered statistically significant.

Notably, we then demonstrated that treatment with Reparixin reduced in a concentration-dependent fashion the frequency of MKs expressing collagen III in the BM from *Gata1*^{low} mice while the frequency of these cells in the BM of the vehicle treated mice remained increased (**Figure 9**).

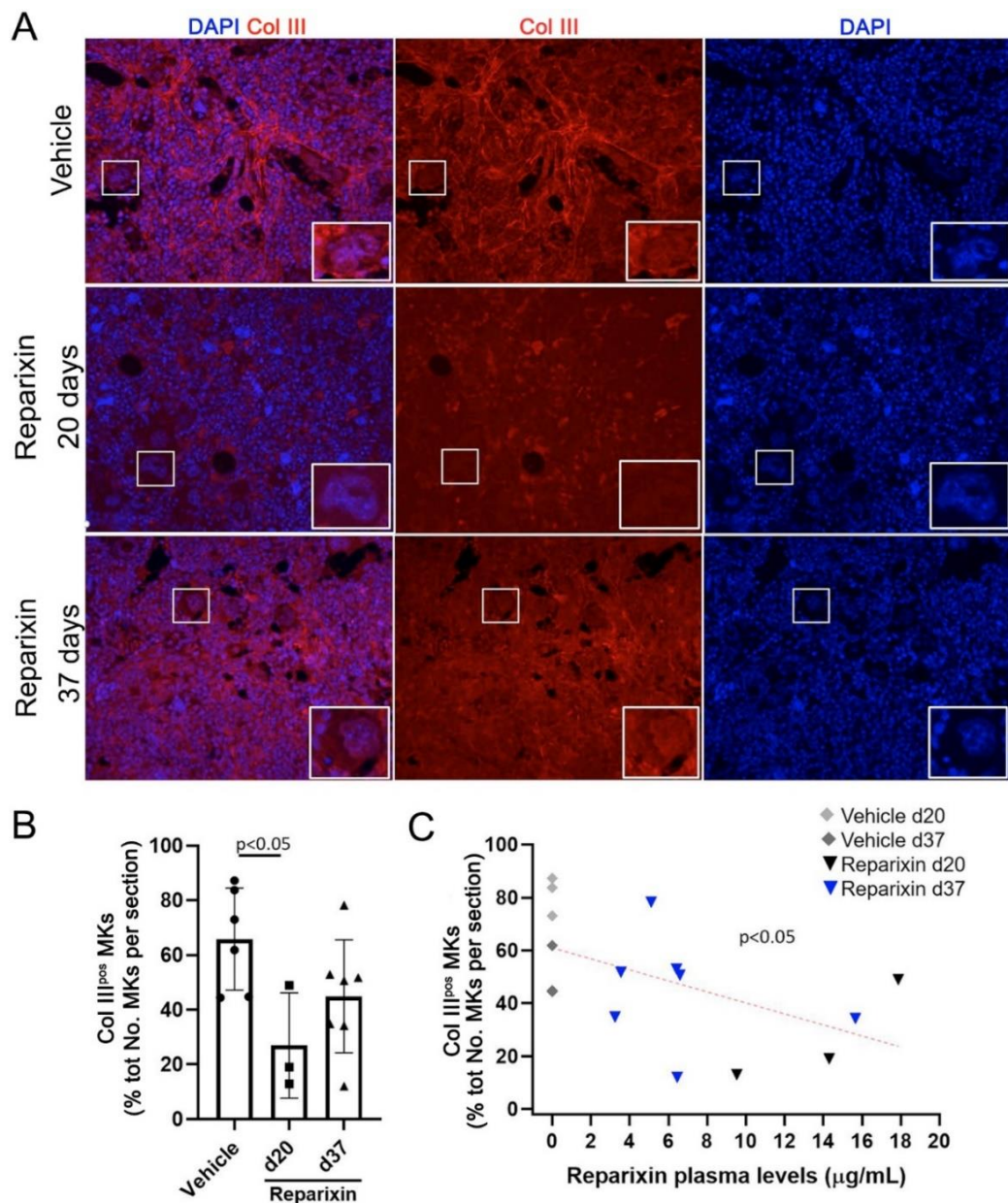


Figure 9. Reparixin reduces in a concentration-dependent fashion the frequency of Col III^{pos} MKs in the bone marrow of *Gata1*^{low} mice. **A)** Immunofluorescence analyses with an anti-Col III (TRITCH-red) antibody of BM sections from representative *Gata1*^{low} mice treated either with vehicle or with Reparixin for 20 or 37 days, as indicated. Megakaryocytes were recognized by morphology. Magnification 400x. The white rectangles indicate representative MKs shown at greater magnification on the bottom right of each panel. **B)** Frequency of MKs positive for Col III over the total number of MKs per sections quantified by computer image analyses. Data are presented as Mean (\pm SD) and as values per single mouse (each dot a mouse) and were analyzed by Tukey's test multiple comparisons test. $p < 0.05$ was considered statistically significant. **C)** Linear regression analyses between the frequency of Col III^{pos} MKs and plasma levels of Reparixin in individual mice (Pearson $R = -0.53$, $p < 0.05$). Each dot represents a single mouse.

Niche-poised and platelet-poised MK have distinctive morphologies. On average, niche-poised MKs are smaller than platelet-poised cells and their nuclei contains lower number of lobes (Sun et al., 2021). The analyses of the morphology of the MKs shown in **Figure 7** at greater magnification revealed that the MKs from the Reparixin-treated mice that contained GATA1 are on average smaller and with less lobated nuclei than those that were negative for GATA1 (**Figure S2**). These results

suggest that Reparixin may have specifically increased the GATA1 content in the niche-poised MKs, explaining why, in spite of the increase of GATA1 in the MKs, the Plts numbers of the treated mice did not increase (**Table 1**). This hypothesis was tested by performing immunofluorescence studies to assess whether Reparixin increased the GATA1 content in the same MK population that expresses collagen (**Figure 10**). This analysis was performed only on the mice that had been treated for day 20 which exhibited the greatest reduction of fibrosis. The frequency of MKs expressing collagen III which were also positive for GATA1 was significantly greater in mice treated with Reparixin suggesting that Reparixin had specifically increased GATA1 content in niche-poised MKs, possibly hampering their pro-fibrotic functions.

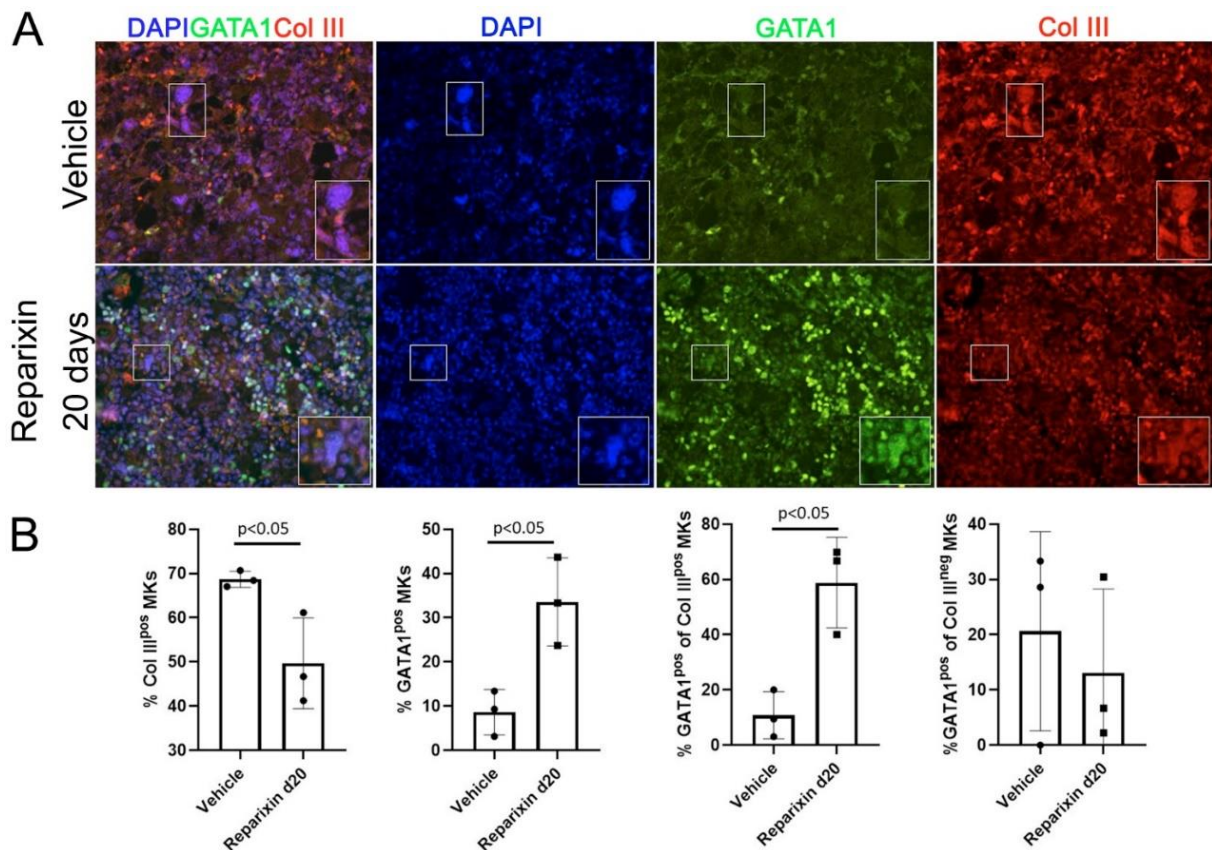


Figure 10. Reparixin increases the GATA1 content in the MK subpopulation that express high levels of Col III. **A)** Double immunofluorescence staining with anti-GATA1 (FITC-green) and Col III (TRITC-red) antibodies of BM sections from representative *Gata1*^{low} mice treated with either vehicle or Reparixin for 20 days. Magnification 400x. The rectangles indicate a representative MK shown at greater magnification on the bottom right of each panel. **B)** Frequency of MKs positive for Col III (Col III^{pos} MKs), for GATA1 (Gata1^{pos} MKs) and of the subsets of MKs positive or negative for Col III that were also positive for GATA1, respectively. Data are presented as Mean (\pm SD) and as values for individual mouse (each mouse a dot). Statistical analyses were performed by One-way ANOVA. $p < 0.05$ was considered statistically significant.

4. Discussion

hCXCL8 is one of the pro-inflammatory cytokines expressed at high levels in MF and is associated with the poorest patient outcomes (Tefferi et al., 2011). In addition, malignant CD34⁺ cells and MKs from MF patients express high levels of hCXCL8 (Dunbar et al., 2020). We have now

determined that the BM from the *Gata1*^{low} MF mouse model contains MKs that not only express increased levels of TGF- β , but also of mCXCL1, the murine equivalent of hCXCL8, and that the MKs from these mice express higher levels of CXCR1 and CXCR2 receptors. The recent consideration of CXCR1/R2 allosteric inhibitors for therapy of inflammatory lung diseases associated with fibrosis (Cheng et al., 2020; Mattos et al., 2020) suggests that these inhibitors might be effective in treating BM fibrosis. This hypothesis was tested in the present study that assessed the effects of the CXCR1/R2 inhibitor Reparixin on the myelofibrotic phenotype expressed by *Gata1*^{low} mice.

In accordance with the observations that allosteric modulation of CXCR1/2 is well tolerated (Goldstein et al., 2020; Maffi et al., 2020; Opfermann et al., 2015), treatment with Reparixin showed no significant changes in body weight and in blood parameters in *Gata1*^{low} mice, and no deaths were recorded during the entire period of observation.

Having found that an intrinsic variability in circulating drug levels was associated with prolonged administration of Reparixin by mini-pumps (Di Sapia et al., 2021 and this manuscript), we performed correlative analyses to assess concentration-dependent treatment effects. Notably, by histological analysis we observed that Reparixin reduced in a concentration-dependent fashion the degree of BM and splenic fibrosis of *Gata1*^{low} mice. Since CXCL1 and its CXCR1 and CXCR2 receptors contribute to the control of megakaryocytic proliferation, differentiation, and ploidy in MF (Emadi et al., 2005), we evaluated whether inhibition of the CXCR1/R2 signaling might reduce the fibrosis by restoring the MKs abnormalities observed in *Gata1*^{low} mice.

First, immunohistochemistry staining showed for the first time that mCXCR1, the recently characterized murine orthologue of hCXCR1 is highly expressed, together with mCXCR2 specifically in the MKs from *Gata1*^{low} mice. Consistent with the fact that allosteric modulation does not block the binding of the endogenous ligand to its receptors or alter its constitutive activity (Bertini et al., 2004), we observed that Reparixin treatment did not alter the expression of CXCL1 or CXCR1/R2 receptors by MKs from the BM of *Gata1*^{low} mice. Since CXCR1/CXCR2 are also activated by CXCL6 and MIP2, we may not formally exclude that altered levels of these two chemokines are also involved in the development of myelofibrosis in our model and that their levels were normalized by treatment with Reparixin. This hypothesis will be tested as part of a separate study.

We observed, however, that the BM of Reparixin-treated mice expressed lower levels of TGF- β as compared to vehicle treated mice. The effect of Reparixin on TGF- β expression was independent of the plasma concentration of Reparixin. Since Reparixin is a >100 fold more potent inhibitor of CXCR1 (both h and m) than CXCR2 (both h and m), (Bertini et al., 2004; Citro et al., 2015), we hypothesize that TGF- β production by murine MKs is primarily regulated by mCXCR1 and therefore is not influenced by the variability in circulating drug levels. The suggested role of mCXCR1 in the regulation of TGF- β content is supported by recent data highlighting the prominent role of the CXCL6/CXCR1 axis in the release of TGF- β by liver Kupffer cells both in patients with liver fibrosis

and in a mouse model of carbon tetrachloride-induced chronic liver injury and fibrosis (Cai X et al., 2018). We may not exclude however, that Reparixin reduced TGF- β content in the bone marrow indirectly by reducing the frequency of pathological MKs emperipolesis with the neutrophils which triggers the release of this factor in the bone marrow. In fact, since it is well known that CXCL1 induces neutrophil chemotaxis (Teijeira et al., 2021), it is possible that Reparixin, by decreasing neutrophil chemotaxis toward the MKs reduces their pathological emperipolesis with these cells reducing the amount of TGF- β they release in the microenvironment. This hypothesis is currently under investigation as part of a separate study (Dunbar et al., under revision). In conclusion, our results indicate that, in addition to CXCR2 indicated by loss of function studies in mouse models, (Dunbar et al., under review), also CXCR1 is involved in the regulation of profibrotic signaling at least in *Gata1*^{low} mice.

We previously reported that pharmacological inhibition of TGF- β signaling in *Gata1*^{low} mice restored the maturation of MKs and increased their content of GATA1 (Zingariello et al., 2013). Since we observed a significant decrease of the TGF- β expressed by MKs following Reparixin-treatment, we hypothesized that Reparixin might restore MK functions by reducing TGF- β content. This hypothesis is counterintuitive since Reparixin did not increase platelets numbers, which are typically low in *Gata1*^{low} mice. This apparent paradox was explained by recent single cell profiling analyses indicating that murine BM contains three distinctive MK populations, each one exerting a different function. In addition to MKs poised to generate platelets, the BM contains MK poised to exert immune functions in the lungs (Pariser et al., 2021) or niche functions during the embryogenesis but possibly also in adult organs undergoing tissue repair (Migliaccio and Hoffman, 2021; Sun et al., 2021; Wang et al., 2021; Pariser et al., 2021). The BMs from *Gata1*^{low} mice, as well as that of MF patients, are characterized by an increased proportion of immature MKs that express increased levels of collagen (Abbonante et al., 2016, Malara et al., 2014 and this manuscript). By immunostaining, we observed that Reparixin increased GATA1 expression while reducing the collagen III content in *Gata1*^{low} mouse MKs. Notably, we demonstrated that the increase of GATA1 levels was most evident in the subpopulation of MKs expressing collagen, suggesting that Reparixin may target the niche-poised MKs reducing their ability to mediate collagen deposition and fibrosis in this animal model. At the moment, there is little experimental indication on the mechanism(s) that increased GATA1 content in the MKs from the Reparixin-treated mice. On the basis of published data, we suggest that this increase is mediated by the decreased TGF- β levels observed in these mice. In fact, it is well known that TGF- β , through a mechanism still poorly identified, retains MK immature (Kuter et al., 1992). Since MK maturation requires GATA1 upregulation (with consequently down regulation of GATA2, a maturation mechanism defined the GATA1 to GATA2 switch (Bresnick et al., 2010)), it is conceivable that TGF- β reduces MK maturation by reducing expression of GATA1 and increasing that of GATA2. This hypothesis has been directly tested by the finding that a small TGF- β inhibitor rescues the

abnormal maturation (and myelofibrosis) in *Gata1^{low}* mice by increasing the levels of *Gata1* mRNA while reducing those of *Gata2* (Zingariello et al., 2013; Yue et al., 2017). Due to the hypomorphic mutation, *Gata1^{low}* cells lack one of the three major hypersensitive sites of the gene but still contain two other important regulatory sequences (McDevitt et al., 1997; Migliaccio et al., 2009), which may be the target of the TGF- β inhibitors which have been demonstrated to be capable to upregulate its expression (Zingariello et al., 2013). Although drugs that increase GATA1 in MKs, such as Aurora kinase inhibitors, have been shown to be effective in reduce fibrosis in myelofibrosis patients (Wen et al., 2015), it may be debated whether drugs, such as Reparixin, that increase GATA1 protein in a mouse model in which the transcription of the gene is reduced by deletion of its regulatory sequence, will be effective in patients where the GATA1 content is reduced by inefficient translation of GATA1 mRNA (Gilles et al., 2013). However, since Reparixin appears to act via TGF- β and the TGF- β TRAP AVID200 is capable to downregulate GATA2 (and therefore presumably to upregulates GATA1), restoring the maturation of MKs expanded in vitro from CD34+ cells in the subset of patients who are responsive to the drug (Varricchio et al., 2021), we believe that Reparixin will be effective also in patients.

In conclusion, these results indicate that treatment with Reparixin rescues the MF phenotype of *Gata1^{low}* mice and provides a rationale for considering Reparixin as a therapeutic option to treat MF patients.

Funding: This study was supported by grants from the National Cancer Institute (P01-CA108671), the National Heart, Lung and Blood Institute (1R01-HL134684), Associazione Italiana Ricerca Cancro (AIRC, IG23525), by funds from Italian Ministry of Economic Development DM 02/08/2019 and DD 02/10/2019 grant proposal number 1410, and by Dompé Farmaceutici Spa R&D.

Institutional Review Board Statement: All the experiments were performed according to protocol n. 419/2015-PR approved by the Italian Ministry of Health and according to the directive 2010/63/EU of the European Parliament and of the Council of 22 September 2010 on the protection of animals used for scientific purposes.

Informed Consent Statement: Not applicable. No human studies

Authors contribution statement: PV, FG, FM, MTM, LB and CG performed experiments and analyzed the data. PV and FG performed statistical analyses. GS reviewed all the histopathological determinations. ARM and MA designed the study, interpreted the data and wrote the manuscript. All the authors read the manuscript and concur with its content.

Data Availability Statement: The individual data for each mouse are available on request.

Acknowledgments: The technical support of Mrs. Yvan Gilardi, Enrico Cardarelli and Andrea Giovannelli, of the Animal Facility of Istituto Superiore di Sanità and the editorial assistance of Dr. Gisella Gaspari are gratefully acknowledged.

Conflicts of Interest: PV, FG, FM, AM and GS declare no conflict. MTM, LB, CG and MA are employee of Dompè Farmaceutici SPA and ARM received research funds from Dompè Farmaceutici SPA.

Disclosure. The content of the manuscript was presented as a poster at the 63rd ASH Annual Meeting & Exposition (Blood (2021) 138 (Supplement 1): 3579. doi: 10.1182/blood-2021-147261). The effects of Reparixin on fibrosis at day 20 are included in the manuscript entitled “CXCL8/CXCR2 signaling mediates bone marrow fibrosis and represents a therapeutic target in myelofibrosis” by Dunbar et al (2021, bioRxiv preprint doi: <https://doi.org/10.1101/2021.12.08.471791>) under review in Blood. The correlation between the effects on fibrosis and the Reparixin concentration and the mechanistic insights on the effect of Reparixin in myelofibrosis are unpublished and have not been submitted for publication to any other journal.

5. References

- Abbonante, V., Di Buduo, C.A., Gruppi, C., Malara, A., Gianelli, U., Celesti, G., Anselmo, A., Laghi, L., Vercellino, M., Visai, L., Iurlo, A., Moratti, R., Barosi, G., Rosti, V., Balduini, A. (2016). Thrombopoietin/TGF- β 1 loop regulates megakaryocyte extracellular matrix component synthesis. *Stem Cells*, 34 (4), 1123–1133. <https://doi.org/10.1002/stem.2285>.
- Allegretti, M., Bertini, R., Bizzarri, C., Beccari, A., Mantovani, A., Locati, M. (2008). Allosteric inhibitors of chemoattractant receptors: opportunities and pitfalls. *Trends in Pharmacological Sciences*, 29(6):280-6. <https://doi.org/10.1016/j.tips.2008.03.005>.
- Bresnick, E.H., Lee, H.Y., Fujiwara, T., Johnson, K.D., Keles, S. (2010). GATA switches as developmental drivers. *The Journal of Biological Chemistry*, 285(41):31087-31093. <https://doi.org/10.1074/jbc.R110.159079>.
- Bertini, R., Allegretti, M., Bizzarri, C., Moriconi, A., Locati, M., Zampella, G., Cervellera, M.N., Di Cioccio, V., Cesta, M.C., Galliera, E., Martinez, F.O., Di Bitondo, R., Troiani, G., Sabbatini, V., D'Anniballe, G., Anacardio, R., Cutrin, J.C., Cavalieri, B., Mainiero, F., Strippoli, R., Villa, P., Di Girolamo, M., Martin, F., Gentile, M., Santoni, A., Corda, D., Poli, G., Mantovani, A., Ghezzi, P., Colotta, F. (2004). Noncompetitive allosteric inhibitors of the inflammatory chemokine receptors CXCR1 and CXCR2: prevention of reperfusion injury. *PNAS*, 101(32), 11791-6. <https://doi.org/10.1073/pnas.0402090101>.
- Bozic, C. R., Gerard, N. P., Von Uexkull-Guldenband, C., Kolakowski, L. F., Jr., Conklyn, M. J., Breslow, R., Showell, H.J., Gerard, C. (1994). The murine interleukin 8 type B receptor homologue and its ligands. Expression and biological characterization. *The Journal of Biological Chemistry*, 269, 29355–29358.

- Brandolini, L., Benedetti, E., Ruffini, P.A., Russo, R., Cristiano, L., Antonosante, A., d'Angelo, M., Castelli, V., Giordano, A., Allegretti, M., Cimini, A. (2017). CXCR1/2 pathways in paclitaxel-induced neuropathic pain. *Oncotarget*, 8(14):23188-23201. <https://doi.org/10.18632/oncotarget.15533>.
- Cacalano, G., Lee, J., Kikly, K., Ryan, A. M., Pitts-Meek, S., Hultgren, B., Wood, W.I., Moore, M.W. (1994). Neutrophil and B cell expansion in mice that lack the murine IL-8 receptor homolog. *Science*, 265, 682–684. <https://doi.org/10.1126/science.8036519>.
- Cai, X., Li, Z., Zhang, Q., Qu, Y., Xu, M., Wan, X., Lu, L. (2018). CXCL6-EGFR-induced Kupffer cells secrete TGF- β 1 promoting hepatic stellate cell activation via the SMAD2/BRD4/C-MYC/EZH2 pathway in liver fibrosis. *Journal of Cellular and Molecular Medicine*, 22(10):5050-5061. <https://doi.org/10.1111/jcmm.13787>.
- Cavalieri, B., Mosca, M., Ramadori, P., Perrelli, M.-G., De Simone, L., Colotta, F., Bertini, R., Poli, G., Cutrì, J.C. (2005). Neutrophil recruitment in the reperfused-injured rat liver was effectively attenuated by repertaxin, a novel allosteric noncompetitive inhibitor of CXCL8 receptors: a therapeutic approach for the treatment of post-ischemic hepatic syndromes. *International Journal of Immunopathology and Pharmacology*, 18(3):475-486. <https://doi.org/10.1177/039463200501800307>.
- Centurione, L., Di Baldassarre, A., Zingariello, M., Bosco, D., Gatta, V., Rana, R.A., Langella, V., Di Virgilio, A., Vannucchi, A.M., Migliaccio, A.R. (2004). Increased and pathologic emperipolesis of neutrophils within megakaryocytes associated with marrow fibrosis in *Gata1*^{low} mice. *Blood*, 104(12), 3573–3580. <https://doi.org/10.1182/blood-2004-01-0193>.
- Cerretti, D.P., Nelson, N., Kozlosky, C.J., Morrissey, P.J., Copeland, N. G., Gilbert, D.J., Jenkins, N.A., Dosik, J.K., Mock, B.A. (1993). The murine homologue of the human interleukin-8 receptor type B maps near the *Ity-Lsh-Bcg* disease resistance locus. *Genomics*, 18, 410–413. <https://doi.org/10.1006/geno.1993.1486>.
- Cheng, I.Y., Liu, C.C., Lin, J.H., Hsu, T.W., Hsu, J.W., Li, A.F., Ho, W.C., Hung, S.C., Hsu, H.S. (2019). Particulate matter increases the severity of bleomycin-induced pulmonary fibrosis through KC-Mediated neutrophil chemotaxis. *International Journal of Molecular Sciences*, 21(1):227. <https://doi.org/10.3390/ijms21010227>.
- Citro, A., Valle, A., Cantarelli, E., Mercalli, A., Pellegrini, S., Liberati, D. (2015). CXCR1/2 inhibition blocks and reverses type 1 diabetes in mice. *Diabetes*, 64(4), 1329-40. <https://doi.org/10.2337/db14-0443>.
- Di Sapia, R., Zimmer, T.S., Kebede, V., Balosso, S., Ravizza, T., Sorrentino, D., Castillo, M.A.M., Porcu, L., Cattani, F., Ruocco, A., Aronica, E., Allegretti, M., Brandolini, L., Vezzani, A. (2021). CXCL1-CXCR1/2 signaling is induced in human temporal lobe epilepsy and contributes to seizures in a murine model of acquired epilepsy. *Neurobiology of Disease*, 158:105468. <https://doi.org/10.1016/j.nbd.2021.105468>.
- Dunbar, A., Lu, M., Farina, M., Park, Y., Yang, J., Kim, D., Karzai, A., Salama, M., Snyder, J., Krishnan, A., Koche, R.P., Fan, R., Levine, R.L., Hoffman, R. (2020). Increased Interleukin-8 (IL8)-CXCR2 Signaling Promotes Progression of Bone Marrow Fibrosis in Myeloproliferative Neoplasms. *Blood*, 136(Supplement 1):6–7. <https://doi.org/10.1182/blood-2020-138843>.

- Emadi, S., Clay, D., Desterke, C., Guerton, B., Maquarre, E., Charpentier, A. (2005). IL-8 and its CXCR1 and CXCR2 receptors participate in the control of megakaryocytic proliferation, differentiation, and ploidy in myeloid metaplasia with myelofibrosis. *Blood*, 105, 464. <https://doi.org/10.1182/blood-2003-12-4415>.
- Fan, X., Patera, A.C., Pong-Kennedy, A., Deno, G., Gonsiorek, W., Manfra, D.J., Vassileva, G., Zeng, M., Jackson, C., Sullivan, L., Sharif-Rodriguez, W., Opdenakker, G., Van Damme, J., Hedrick, J.A., Lundell, D., Lira, S.A., Hipkin, R.W. (2007). Murine CXCR1 is a functional receptor for GCP-2/CXCL6 and interleukin-8/CXCL8. *Journal of Biological Chemistry*, 282(16), 11658-66. <https://doi.org/10.1074/jbc.M607705200>.
- Fu, W., Zhang, Y., Zhang, J., and Chen, W.F. (2005). Cloning and characterization of mouse homolog of the CXC chemokine receptor CXCR1. *Cytokine*, 31, 9–17. <https://doi.org/10.1016/j.cyto.2005.02.005>.
- Gilles, L., Arslan, A.D., Marinaccio, C., Wen, Q.J., Arya, P., McNulty, M., Yang, Q., Zhao, J.C., Konstantinoff, K., Lasho, T., Pardanani, A., Stein, B., Plo, I., Sundaravel, S., Wickrema, A., Migliaccio, A., Gurbuxani, S., Vainchenker, W., Plataniias, L.C., Tefferi, A., Crispino, J.D. (2017). Downregulation of GATA1 drives impaired hematopoiesis in primary myelofibrosis. *Journal of Clinical Investigation*, 127(4), 1316–1320. <https://doi.org/10.1172/jci82905>.
- Goldstein, L.J., Perez, R.P., Yardley, D., Han, L.K., Reuben, J.M., Gao, H., McCanna, S., Butler, B., Ruffini, P.A., Liu, Y., Rosato, R.R., Chang, J.C. (2020). A window-of-opportunity trial of the CXCR1/2 inhibitor reparixin in operable HER-2-negative breast cancer. *Breast Cancer Research*, 22(1):4. <https://doi.org/10.1186/s13058-019-1243-8>.
- Harrison, C.N., Vannucchi, A.M., Kiladjian, J.J., Al-Ali, H.K., Gisslinger, H., Knoop, L., Cervantes, F., Jones, M.M., Sun, K., McQuitty, M., Stalbovskaya, V., Gopalakrishna, P., Barbui, T. (2016). Long-term findings from COMFORT-II, a phase 3 study of ruxolitinib vs best available therapy for myelofibrosis. *Leukemia* 30, 1701. <https://doi.org/10.1038/leu.2016.323>.
- Holmes, W.E., Lee, J., Kuang, W.J., Rice, G.C., Wood, W.I. (1991). Structure and functional expression of a human interleukin-8 receptor. *Science*, 253, 1278–1280. <https://doi.org/10.1126/science.1840701>.
- Jurcevic, S., Humfrey, C., Uddin, M., Warrington, S., Larsson, B., Keen, C. (2015). The effect of a selective CXCR2 antagonist (AZD5069) on human blood neutrophil count and innate immune functions. *British Journal of Clinical Pharmacology*, 80(6):1324-36. <https://doi.org/10.1111/bcp.12724>.
- Kuter, D.J., Gminski, D.M., Rosenberg, R.D. (1992). Transforming growth factor beta inhibits megakaryocyte growth and endomitosis. *Blood*, 79(3):619-626.
- Lee, J., Cacalano, G., Camerato, T., Toy, K., Moore, M.W., and Wood, W.I. (1995). Chemokine binding and activities mediated by the mouse IL-8 receptor. *Journal of Immunology*, 155, 2158–2164.
- Maffi, P., Lundgren, T., Tufveson, G., Rafael, E., Shaw, J.A.M., Liew, A., Saudek, F., Witkowski, P., Golab, K., Bertuzzi, F., Gustafsson, B., Daffonchio, L., Ruffini, P.A., Piemonti, L.; REP0211 Study Group. (2020). Targeting CXCR1/2 does not improve insulin secretion after pancreatic islet transplantation: a phase 3, double-blind, randomized, placebo-controlled trial in type 1 diabetes. *Diabetes Care*, 43(4):710-718. <https://doi.org/10.2337/dc19-1480>.

- Malara, A., Currao, M., Gruppi, C., Celesti, G., Viarengo, G., Buracchi, C., Laghi, L., Kaplan, D.L., Balduini, A. (2014). Megakaryocytes contribute to the bone marrow-matrix environment by expressing fibronectin, type IV collagen, and laminin. *Stem Cells*, 32(4), 926–937. <https://doi.org/10.1002/stem.1626>.
- Martelli, F., Ghinassi, B., Panetta, B., Alfani, E., Gatta, V., Pancrazzi, A., Bogani, C., Vannucchi, A.M., Paoletti, F., Migliaccio, G., Migliaccio, A.R. (2005). Variegation of the phenotype induced by the *Gata1*^{low} mutation in mice of different genetic backgrounds. *Blood*, 106(13):4102-13. <https://doi.org/10.1182/blood-2005-03-1060>.
- Mattos, M.S., Ferrero, M.R., Kraemer, L., Lopes, G.A.O., Reis, D.C., Cassali, G.D., Oliveira, F.M.S., Brandolini, L., Allegretti, M., Garcia, C.C., Martins, M.A., Teixeira, M.M., Russo, R.C. (2020). CXCR1 and CXCR2 inhibition by ladarixin improves neutrophil-dependent airway inflammation in mice. *Frontiers in Immunology*, 11:566953. <https://doi.org/10.3389/fimmu.2020.566953>.
- McDevitt, M.A., Shivdasani, R.A., Fujiwara, Y., Yang, H., and Orkin, S.H. (1997). A "knockdown" mutation created by cis-element gene targeting reveals the dependence of erythroid cell maturation on the level of transcription factor GATA-1. *PNAS*, 94 (13), 6781–6785. <https://doi.org/10.1073/pnas.94.13.6781>
- Migliaccio, A.R., Rana, R.A., Sanchez, M., Lorenzini, R., Centurione, L., Bianchi, L., Vannucchi, A. M., Migliaccio, G., Orkin, S.H. (2003). GATA-1 as a regulator of mast cell differentiation revealed by the phenotype of the *Gata1*^{low} Mouse Mutant. *Journal of Experimental Medicine*, 197(3), 281–296. <https://doi.org/10.1084/jem.20021149>.
- Migliaccio, A.R., Martelli, F., Verrucci, M., Sanchez, M., Valeri, M., Migliaccio, G., Vannucchi, A.M., Zingariello, M., Di Baldassarre, A., Ghinassi, B., Rana, R.A., Van Hensbergen, Y., Fibbe, W.E. (2009). *Gata1* expression driven by the alternative HS2 enhancer in the spleen rescues the hematopoietic failure induced by the hypomorphic *Gata1*^{low} mutation. *Blood*, 114(10), 2107–2120. <https://doi.org/10.1182/blood-2009-03-211680>.
- Migliaccio, A.R., and Hoffman, R. (2021). An outline of the outset of thrombopoiesis in human embryos at last. *Cell Stem Cell*, 28 (3), 363–365. <https://doi.org/10.1016/j.stem.2021.02.007>.
- Moepps, B., Nuessler, E., Braun, M., and Gierschik, P. (2006). A homolog of the human chemokine receptor CXCR1 is expressed in the mouse. *Molecular Immunology*, 43, 897–914. <https://doi.org/10.1016/j.molimm.2005.06.043>.
- Murphy, P.M., and Tiffany, H.L. (1991). Cloning of complementary DNA encoding a functional human interleukin-8 receptor. *Science*, 253, 1280–1283. <https://doi.org/10.1126/science.1891716>.
- Takeuchi, K., Higuchi, T., Yamashita, T., and Koike, K. (1999). Chemokine production by human megakaryocytes derived from CD34-positive cord blood cells. *Cytokine*, 11, 424-434. <https://doi.org/10.1006/cyto.1998.0455>.
- Opfermann, P., Derhaschnig, U., Felli, A., Wenisch, J., Santer, D., Zuckermann, A., Dworschak, M., Jilma, B., Steinlechner, B. (2015). A pilot study on reparixin, a CXCR1/2 antagonist, to assess safety and efficacy in attenuating ischaemia-reperfusion injury and inflammation after on-pump coronary artery bypass graft surgery. *Clinical & Experimental Immunology*, 180(1):131-42. <https://doi.org/10.1111/cei.12488>.

- Pariser, D. N., Hilt, Z. T., Ture, S. K., Blick-Nitko, S. K., Looney, M. R., Cleary, S. J., Roman-Pagan, E., Saunders, J. 2nd, Georas, S.N., Veazey, J., Madere, F., Santos, L.T., Arne, A., Huynh, N.P., Livada, A.C., Guerrero-Martin, S.M., Lyons, C., Metcalf-Pate, K.A., McGrath, K.E., Palis, J., Morrell, C.N. (2021). Lung megakaryocytes are immune modulatory cells. *Journal of clinical investigation*, 131(1), e137377. <https://doi.org/10.1172/JCI137377>.
- Russo, R.C., Garcia, C.C., Teixeira, M.M., and Amaral, F.A. (2014). The CXCL8/IL-8 chemokine family and its receptors in inflammatory diseases. *Expert Review of Clinical Immunology*, 10(5), 593-619. <https://doi.org/10.1586/1744666X.2014.894886>.
- Sim, X., Jarocha, D., Hayes, V., Hanby, H.A., Marks, M.S., Camire, R.M., French, D.L., Poncz, M., Gadue, P. (2017). Identifying and enriching platelet-producing human stem cell-derived megakaryocytes using factor V uptake. *Blood*, 130(2):192-204. <https://doi.org/10.1182/blood-2017-01-761049>.
- Sun, S., Jin, C., Si, J., Lei, Y., Chen, K., Cui, Y., Liu, Z., Liu, J., Zhao, M., Zhang, X., Tang, F., Rondina, M.T., Li, Y., Wang, Q.F. (2021). Single-cell analysis of ploidy and the transcriptome reveals functional and spatial divergency in murine megakaryopoiesis. *Blood*, 138(14):1211-1224. <https://doi.org/10.1182/blood.2021010697>.
- Tefferi, A. (2005). Pathogenesis of myelofibrosis with myeloid metaplasia. *Journal of Clinical Oncology*, 23(33):8520-30. <https://doi.org/10.1200/JCO.2004.00.9316>.
- Tefferi, A., Vaidya, R., Caramazza, D., Finke, C., Lasho, T., Pardanani, A. (2011). Circulating interleukin (IL)-8, IL-2R, IL-12, and IL-15 levels are independently prognostic in primary myelofibrosis: a comprehensive cytokine profiling study. *Journal of Clinical Oncology*, 29(10): 1356–1363. <https://doi.org/10.1200/JCO.2010.32.9490>.
- Teijeira, A., Garasa, S., Ochoa, M.D.C., Cirella, A., Olivera, I., Glez-vaz, J., Andueza, M.P., Migueliz, I., Alvarez, M., Rodríguez-Ruiz, M.E., Rouzaut, A., Berraondo, P., Sanmamed, M.F., Perez Gracia, J.L., Melero, I. (2021). Differential Interleukin-8 thresholds for chemotaxis and netosis in human neutrophils. *European Journal of Immunology*, 51(9):2274-2280. <https://doi.org/10.1002/eji.202049029>.
- Vannucchi, A.M., Bianchi, L., Cellai, C., Paoletti, F., Rana, R.A., Lorenzini, R., et al. (2002). Development of myelofibrosis in mice genetically impaired for GATA-1 expression (GATA-1low mice). *Blood*, 100(4), 1123–1132. <https://doi.org/10.1182/blood-2002-06-1913>.
- Vannucchi, A.M., Pancrazzi, A., Guglielmelli, P., Di Lollo, S., Bogani, C., Baroni, G., Bianchi, L., Migliaccio, A.R., Bosi, A., Paoletti, F. (2005). Abnormalities of GATA-1 in megakaryocytes from patients with idiopathic myelofibrosis. *American Journal of Pathology*, 167(3), 849–858. [https://doi.org/10.1016/S0002-9440\(10\)62056-1](https://doi.org/10.1016/S0002-9440(10)62056-1).
- Varricchio, L., Iancu-Rubin, C., Upadhyaya, B., Zingariello, M., Martelli, F., Verachi, P., Clementelli, C., Denis, J.F., Rahman, A.H., Tremblay, G., Mascarenhas, J., Mesa, R. A., O'Connor-McCourt, M., Migliaccio, A.R., Hoffman, R. (2021). TGF- β 1 protein trap AVID200 beneficially affects hematopoiesis and bone marrow fibrosis in myelofibrosis. *JCI Insight*, 6(18). <https://doi.org/10.1172/jci.insight.145651>.

Verstovsek, S., Mesa, R.A., Gotlib, J., Gupta, V., DiPersio, J., Catalano, J.V., Deininger, M.W., Miller, C.B., Silver, R.T., Talpaz, M., Winton, E.F., Harvey, J.H., Arcasoy, M.O., Hexner, E.O., Lyons, R.M., Paquette, R., Raza, A., Jones, M., Kornacki, D., Sun, K., Kantarjian, H. (2017). Long-term treatment with ruxolitinib for patients with myelofibrosis: 5-year update from the randomized, double-blind, placebo-controlled, phase 3 COMFORT-I trial. *Journal of Hematology & Oncology*, 10(1):55. <https://doi.org/10.1186/s13045-017-0417-z>.

Vyas, P., Ault, K., Jackson, C.W., Orkin, S.H., Shivdasani, R.A. (1999). Consequences of GATA-1 deficiency in megakaryocytes and platelets. *Blood*, 93, 2867–2875.

Wang, H., He, J., Xu, C., Chen, X., Yang, H., Shi, S., Liu, C., Zeng, Y., Wu, D., Bai, Z., Wang, M., Wen, Y., Su, P., Xia, M., Huang, B., Ma, C., Bian, L., Lan, Y., Cheng, T., Shi, L., Liu, B., Zhou, J. (2021). Decoding human megakaryocyte development. *Cell Stem Cell*, 28(3), 535–549.e8. <https://doi.org/10.1016/j.stem.2020.11.006>.

Wen, Q.J., Yang, Q., Goldenson, B., Malinge, S., Lasho, T., Schneider, R.K., Breyfogle, L.J., Schultz, R., Gilles, L., Koppikar, P., Abdel-Wahab, O., Pardanani, A., Stein, B., Gurbuxani, S., Mullally, A., Levine, R.L., Tefferi, A., Crispino, J.D. (2015). Targeting megakaryocytic-induced fibrosis in myeloproliferative neoplasms by AURKA inhibition. *Nature Medicine*, 21(12):1473-1480. <https://doi.org/10.1038/nm.3995>.

Wuyts, A., Van Osselaer, N., Haelens, A., Samson, I., Herdewijn, P., Ben-Baruch, A., Oppenheim, J.J., Proost, P., Van Damme, J. (1997). Characterization of synthetic human granulocyte chemotactic protein 2: usage of chemokine receptors CXCR1 and CXCR2 and in vivo inflammatory properties. *Biochemistry*, 36, 2716–2723. <https://doi.org/10.1021/bi961999z>.

Wuyts, A., Haelens, A., Proost, P., Lenaerts, J. P., Conings, R., Opdenakker, G., Van Damme, J. (1996). Identification of mouse granulocyte chemotactic protein-2 from fibroblasts and epithelial cells. Functional comparison with natural KC and macrophage inflammatory protein-2. *Journal of Immunology*, 157, 1736–1743.

Yue, L., Bartenstein, M., Zhao, W., Ho, W.T., Han, Y., Murdun, C., Mailloux, A.W., Zhang, L., Wang, X., Budhathoki, A., Pradhan, K., Rapaport, F., Wang, H., Shao, Z., Ren, X., Steidl, U., Levine, R.L., Zhao, Z.J., Verma, A., Epling-Burnette, P.K. (2017). Efficacy of ALK5 inhibition in myelofibrosis. *JCI Insight*, 2(7):e90932. <https://doi.org/10.1172/jci.insight.90932>

Zhan, H., Ma, Y., Lin, C.H.S., Kaushansky, K. (2016). JAK2^{V617F}-mutant megakaryocytes contribute to hematopoietic stem/progenitor cell expansion in a model of murine myeloproliferation. *Leukemia*, 30(12), 2332–2341. <https://doi.org/10.1038/leu.2016.114>.

Zimran A, Durán G, Giraldo P, Rosenbaum H, Giona F, Petakov M, Terreros Muñoz E, Solorio-Meza SE, Cooper PA, Varughese S, Alon S, Chertkoff R. (2019). Long-term efficacy and safety results of taliglucerase alfa through 5years in adult treatment-naïve patients with Gaucher disease. *Blood Cells Molecules and Diseases*, 78:14-21. <https://doi.org/10.1016/j.bcmed.2016.07.002>.

Zingariello, M., Martelli, F., Ciaffoni, F., Masiello, F., Ghinassi, B., D'Amore, E., Massa, M., Barosi, G., Sancillo, L., Li, X., Goldberg, J. D., Rana, R. A., & Migliaccio, A. R. (2013). Characterization of the TGF-β1

signaling abnormalities in the *Gata1*^{low} mouse model of myelofibrosis. *Blood*, 121(17), 3345–3363. <https://doi.org/10.1182/blood-2012-06-439661>.

Zingariello, M., Verachi, P., Gobbo, F., Martelli, F., Falchi, M., Valeri, M., Sarli, G., Marinaccio, C., Melo-Cardenas, J., Crispino, J.D., Migliaccio, A.R. (2022). Resident self-tissue of pro-inflammatory cytokines rather than their systemic levels correlates with development of myelofibrosis in *Gata1*^{low} mice. *Biomolecules*, 12(2):234. <https://doi.org/10.3390/biom12020234>.

6. Supplementary Figures

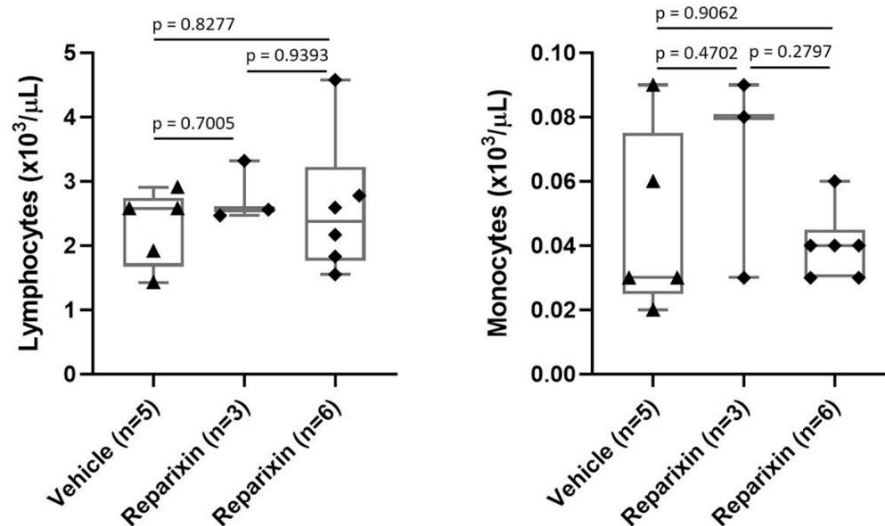


Figure S1. Lymphocyte and Monocyte counts in the blood from mice treated with vehicle or with Reparixin for 20 or 37 days. Data are presented as box charts and as value per individual mouse (each symbol a different mouse) and p values are calculated by Tukey's multiple comparisons test. The number of mice included in each experimental group is indicated by n.

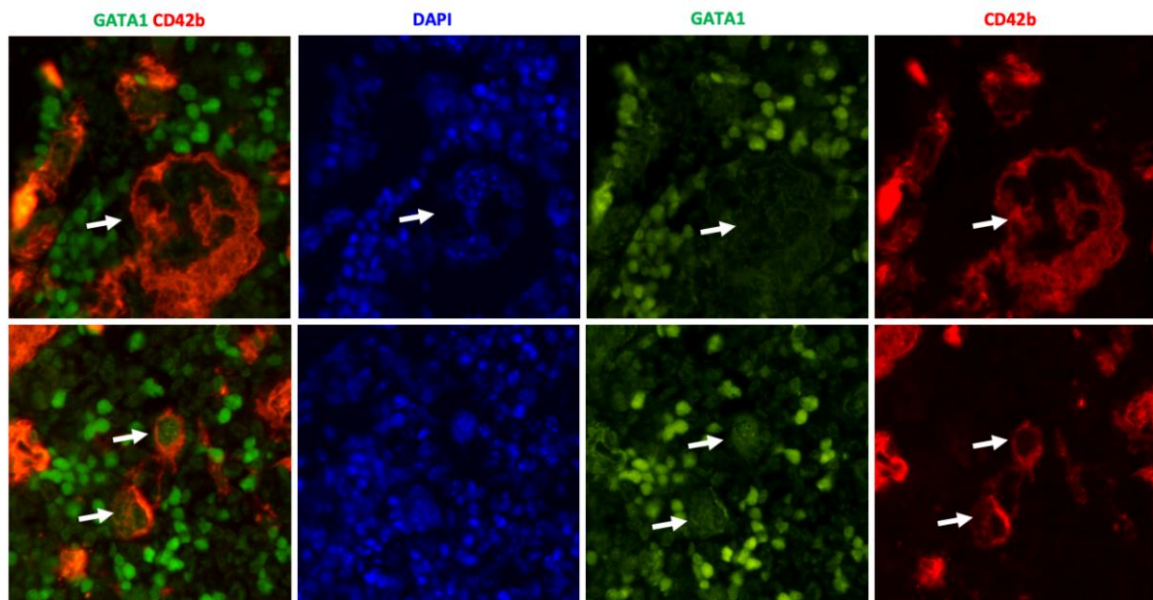


Figure S2. Morphology at 100x magnification of two representative MKs from the Reparixin-treated day 20 group showing that while the MK that does not contain GATA1 is clearly bigger and its nucleus has more lobes than that that contains GATA1.

2.3. Preclinical studies on the use of a P-selectin-blocking monoclonal antibody to halt progression of myelofibrosis in the *Gata1*^{low} mouse model

Adapted from: *Article*

Preclinical studies on the use of a P-selectin blocking monoclonal antibody to halt progression of myelofibrosis in the *Gata1*^{low} mouse model

Paola Verachi¹, Francesca Gobbo^{1,2}, Fabrizio Martelli³, Mario Falchi⁴, Antonio di Virgilio⁵, Giuseppe Sarli², Celine Wilke⁶, Andreas Bruederle⁶, Anirudh Prahallad⁶, Francesca Arciprete⁷, Maria Zingariello⁷ and Anna Rita Migliaccio^{7,8,*}

¹ Department of Biomedical and Neuromotor Sciences, University of Bologna, Italy;

² Department of Veterinary Medical Sciences, University of Bologna, Italy;

³ National Center for Preclinical and Clinical Research and Evaluation of Pharmaceutical Drugs, Istituto Superiore di Sanità, Rome, Italy;

⁴ National Center for HIV/AIDS Research, Istituto Superiore di Sanità, Rome, Italy;

⁵ Center for animal experimentation and well-being, Istituto Superiore di Sanità, Rome, Italy;

⁶ Novartis (United States), East Hanover, USA;

⁷ Unit of Microscopic and Ultrastructural Anatomy, University Campus Bio-Medico, Rome, Italy;

⁸ Altius Institute for Biomedical Sciences, Seattle, WA, USA.

*Corresponding Author: Anna Rita Migliaccio, PhD; Altius Institute for Biomedical Sciences, 2211 Elliott Avenue - 6th Floor - Suite 410 Seattle, WA 98121 – USA. Email: amigliaccio@altius.org

Abstract. The bone marrow (BM) and spleen from patients with myelofibrosis (MF), as well as those from the *Gata1*^{low} mouse model of the disease contain increased number of abnormal megakaryocytes. These cells express high levels of the adhesion receptor P-selectin on their surface, which triggers a pathologic neutrophil emperipolesis, leading to increased bioavailability of transforming growth factor- β (TGF- β) in the microenvironment and disease progression. With age, *Gata1*^{low} mice develop a phenotype similar to that of patients with MF, which is the most severe of the Philadelphia-negative myeloproliferative neoplasms. We previously demonstrated that *Gata1*^{low} mice lacking the P-selectin gene do not develop MF. In the current study, we tested the hypothesis that pharmacologic inhibition of P-selectin may normalize the phenotype of *Gata1*^{low} mice that have already developed MF. To test this hypothesis, we have investigated the phenotype expressed by aged *Gata1*^{low} mice treated with the antimouse monoclonal antibody RB40.34, alone and also in combination with ruxolitinib. The results indicated that RB40.34 in combination with ruxolitinib normalizes the phenotype of *Gata1*^{low} mice with limited toxicity by reducing fibrosis and the content of TGF- β and CXCL1 (two drivers of fibrosis in this model) in the BM and spleen and by restoring hematopoiesis in the BM and the architecture of the spleen. In conclusion, we provide preclinical evidence that treatment with an antibody against P-

selectin in combination with Ruxolitinib may be more effective than ruxolitinib alone to treat MF in patients

Keywords: Myeloproliferative Neoplasms, P-selectin, Fibrosis, megakaryocytes, TGF- β

1. Introduction

Myelofibrosis (MF) is the most severe of Philadelphia chromosome negative myeloproliferative neoplasms (MPN). The complex phenotype of the MF patients includes fibrosis and hematopoietic failure in bone marrow (BM), stem/progenitor cell mobilization, development of extramedullary hematopoiesis with splenomegaly and their clinical course is associated with increased risk of thrombosis, bleeding and evolution to acute leukemia (Barbui et al., 2018; Dunbar et al., 2020; Marcellino et al., 2020; Zahr et al., 2016). MF may be driven by gain of function mutations in several genes of the thrombopoietin axes such as MPL, the thrombopoietin receptor, JAK2, the first element of the MPL signaling, and calreticulin, a chaperon protein that when mutated binds MPL on the cell surface, inducing conformational changes which lead to ligand independent constitutive activation of the receptor (Vainchenker & Constantinescu, 2013). Regardless of the driver mutation, it has been recognized that MF has a distinctive cellular signature. In fact, both the BM and spleen from these patients contain numerous clusters of morphologically immature megakaryocytes (MK) (Malara et al., 2018) endowed with great proliferation potential (Centurione et al., 2004; Schmitt et al., 2000). In MF, MK are retained immature by a mutation-driven RSP14 ribosomopathy that impairs the translation of the mRNA for GATA1 (Gilles et al., 2017; Vannucchi et al., 2005), the transcription factor which plays a pivotal role in the progression of MK maturation (Crispino & Weiss, 2014). The causative role of the resulting abnormal MK in the pathogenesis of this disease is strongly supported by experiments in mice indicating that those carrying a hypomorphic mutation which selectively reduces GATA1 in MK (*Gata1*^{low} mice) develop myelofibrosis with age (Vannucchi et al., 2002) while transgenic mice expressing JAK2^{V617F}, one of the driver mutations of the disease (Barbui et al., 2018; Dunbar et al., 2020; Marcellino et al., 2020; Zahr et al., 2016), only in MK develop myelofibrosis even if their hematopoietic stem cells are normal (Woods et al., 2019; Zhang et al., 2018). As first hypothesized by Schmitt et al (Schmitt et al., 2000), mechanistically, malignant MK are thought to drive MF by engaging in a pathological process of emperipoiesis with the neutrophils which increases the bioavailability of transforming growth factor- β (TGF- β), and possibly of other pro-inflammatory cytokines, in the BM of MF patients and animal models (Campanelli et al., 2011; Centurione et al., 2004; Chagraoui et al., 2002; Ciurea et al., 2007) The pathobiological role of TGF- β in the development of myelofibrosis has been further confirmed by the observation that in animal models development of myelofibrosis is prevented by genetic ablation of the TGF- β gene (Chagraoui et al., 2002; Gastinne et al., 2007) and reverted by treating myelofibrosis mice with a small TGF- β receptor-1 kinase inhibitors (Zingariello et al., 2013) or with the TGF- β trap AVID200 (Varricchio et al., 2021).

The TGF- β trap AVID200 is currently in clinical phase-1/2 clinical trials for MF who are resistant to therapy with the JAK1/2 inhibitor Ruxolitinib (Rux) (Gerds et al., 2020).

Later studies have indicated that the adhesion receptor P-selectin (P-SEL) may represent an element upstream to TGF- β in the pathobiological pathway leading to MF. In fact, the MK abnormalities observed in this disease include abnormal cytoplasmic trafficking of P-SEL which instead to be partitioned in the granules is displayed on the cell surface (Zetterberg et al., 2014). The high levels of P-SEL on the cell surface, by interacting with its ligand (P-selectin glycoprotein ligand-1, PSGL-1) expressed by the neutrophils (Evangelista et al., 1999; Moore et al., 1992) has been hypothesized to drive a process of pathological emperipolesis between the neutrophils and the MK which leads to death of the MK by para-apoptosis and release of TGF- β in the microenvironment (Thiele et al., 1997; Zingariello et al., 2015). This hypothesis has been mechanistically demonstrated by the observation that the TGF- β bio-availability in the BM of *Gata1*^{low} mice lacking the P-sel gene is normal and that these mice do not develop myelofibrosis with age and live, on average, 2 months longer than their *Gata1*^{low} littermates (Spangrude et al., 2016). These findings support the hypothesis that in MF, the disease is established and progresses thanks to a pathological P-SEL/TGF- β circuit established by the malignant MK (Ceglia et al., 2016). Whether inhibition of P-SEL would also be effective in reverting to normal myelofibrosis once the disease is established has not been demonstrated as yet.

Recently, the P-SEL inhibitor Crizanlizumab (SEG101) has been demonstrated to reduce the frequency of vaso-occlusive crises in patients with Sickle Cell Disease with limited toxicity (Ataga et al., 2017). Based on these observations, in November 2019, the Federal Drug Administration approved the use of Crizanlizumab for the treatment of pain crisis in Sickle Cell Disease. The rationale for the clinical study with Crizanlizumab had been provided by a pre-clinical study that evaluated the effects of the commercially available monoclonal antibody RB40.34 targeting the murine P-SEL as antithrombotic agent in a mouse model of Sickle Cell Disease (Embury et al., 2004). Using the fact that Crizanlizumab had been already approved for clinical use and that conditions for effective treatment of mice with RB40.34 had been already described, we test here the hypothesis that pharmacological inhibition of P-SEL with RB40.34, alone or in combination with Rux, is effective in reverting the myelofibrotic phenotype expressed by *Gata1*^{low} mice.

2. Materials and Methods

2.1. Mice

Gata1^{low} mice are bred in the animal facility of Istituto Superiore di Sanità as described (Martelli et al., 2005). Littermates are genotyped at birth by PCR and those found not to carry the mutation are used as wild-type (WT) controls. All the experiments, including the size of the experimental groups, are performed according to the protocols D9997.121 approved by the Italian Ministry of Health on September 2nd 2021, and according to the European Directive 86/609/EEC.

2.2. Treatments

A total of 47 *Gata1*^{low} mice were implanted with 14mm micro-chips (one chip/mouse) (AVID, Norco, CA, USA) and divided into two separate experiments (**Figure S1**). In the first experiment, 24 11-months-old mice were randomly divided in four groups (3 males and 3 females each) that were treated as follows: Group 1: Vehicle (2% v/v DMSO by gavage, negative control for group 3 and 4); Group 2: Biotinconjugated rat anti-mouse CD62P (RB40.34, Cat. n. 553743, BD Pharmigen, San Diego, CA, USA; 30 µg/mouse per day x three days per week by iv, as described (Embury et al., 2004), until day 45, and then ip); Group 3: Rux (Novartis Pharma AG, Basel, Switzerland; 45mg/Kg twice per day x 5 days a week by gavage as described (Zingariello et al., 2017)); Group 4: biotin-labeled RB40.34 and Rux in combination. On Day 5, all the mice were weighed and bled for blood cell counts determinations and detection of RB34.40 on platelets. Mice were sacrificed at day 5 (males) and day 12 (females) and BM and spleen collected for cell signaling and histopathological determinations. In the second experiment, 23 8-months-old *Gata1*^{low} mice were divided in the same groups described above and treated for 7 weeks. In this experiment, we used the purified RB40.34 (Cat. n. 553742, BD Pharmigen). The treatment was interrupted for two weeks during the holiday break (from day 24 to day 43). On day 54, all the mice were weighed, bled for blood counts determination, and sacrificed for histopathology observations of their BM and spleen.

2.3. Blood counts determination

Mice were topically anesthetized with Novesina (Cat. n. s01ha02, Novartis, Basel, CH, one drop/eye) and blood collected from the retro-orbital plexus into heparinized microcapillary tubes. Blood counts were evaluated on deidentified samples by an accredited commercial laboratory which provide diagnostic services for laboratory animals (Plaisant Laboratory, Rome, Italy).

2.4. Flow cytometry

Binding of RB40.34 to platelets. Platelet-enriched plasma was prepared by centrifugation of 200µL of heparinized blood (10,000rpm for 20min with the Eppendorf™ Centrifuge 5425/5425 R, Eppendorf, Milan, Italy) and the binding of biotinylated RB40.34 to platelets measured by flow cytometry following incubation with PE-Cy7 Streptavidin (ca. no. 557598, BD Pharmingen). Platelets were identified based on size (FS: forward scatter) and internal cell complexity (SS: side scatter), as described (Zetterberg et al., 2014). MK identification and binding to RB40.34. BM and spleen cells were resuspended in Ca⁺⁺ Mg⁺⁺ -free PBS containing 0.5% (v/v) fetal bovine serum (FBS, Cat. n. F7524, Sigma-Aldrich) and incubated with PE-CD41, FITC-CD61 and PE-Cy7-streptavidin. Cells were then divided by flow cytometry into four populations corresponding to non-MK (CD41^{neg}/CD61^{neg}); immature MK (CD41^{neg}/CD61^{high}); mature MK (CD41^{high}/CD61^{high}) and very mature MK (CD41^{high}/CD61^{neg}), as described (Zingariello et al., 2013). The levels of PE-Cy7-streptavidin staining was assessed as a measure of biotinylated-RB40.34 binding to the MK.

Hematopoietic stem/progenitor cell determinations. Mononuclear BM and spleen suspensions were incubated with a cocktail of antibodies including APC-CD117, APC-Cy7-Sca1, PE-Cy7-CD150, biotin-labeled anti-mouse CD48 and biotin-labeled anti-lineage antibodies. After 30min of incubation on ice, cells were washed and incubated with streptavidin-PE-Cy5 (all from BD Pharmingen). Hematopoietic progenitor cells were defined as lineage negative cells (Lin^{neg}). Hematopoietic stem cells were defined as LSK (Lin^{neg}/CD48^{neg}/c-Kit^{pos}/Sca-1^{pos}) while long-term repopulating hematopoietic stem cells were defined as SLAM (Lin^{neg}/CD48^{neg}/c-Kit^{pos}/Sca1^{pos}/CD150^{pos}) as described (Oguro et al., 2013; Spangrude et al., 2016). Non-specific signals and dead cells were excluded, respectively, by appropriate fluorochrome-conjugated isotype and propidium iodide staining. All the flow cytometry analyses were performed with the Gallios analyzer (Beckman Coulter) and the results analyzed with the Kaluza analysis program, version 2.1 (Beckman Coulter).

2.5. Western blot analysis

BM and spleen from *Gata1*^{low} mice treated for 5 days were dissolved in lysis buffer containing protease and phosphatase inhibitors and stored at -80°C. Protein extracts were separated by electrophoresis under denaturing conditions using 7.5-10% mini-Protean TGX pre-casted gels (Bio-Rad, CA, USA) and transferred to nitrocellulose filters with the Transblot-Turbo system (Bio-Rad, Hercules). Filters were probed with antibodies against proteins of the canonical (SMAD2/3, cat no. 8685, Cell Signaling, Boston, MA, USA), p-SMAD2/3 (cat no. 8828, Cell Signaling), TGF-βRII (cat no. ab186838, Abcam, Cambridge, UK) and non-canonical (p38, cat no. 9212; p-p38, cat no. 4511; ERK1/2, cat no. 9102; p-ERK1/2, cat no. 9101; all from Cell Signaling) TGF-β signaling and of the JAK/STAT signaling (JAK2 (cat. No 3230, Cell Signaling), STAT5 (cat no. sc-74442, Santa Cruz, Dallas, Texas, USA), p-JAK2 (Phospho-Tyr1007/1008 JAK2, cat no. 3771, Cell Signaling) and p-STAT5 (cat no, 9351, Cell Signaling). GAPDH (cat no. G9545, Sigma Aldrich) was used as a loading control. The bands were quantified with the ImageJ 1.52q software (National Institutes of Health, Bethesda, MD, USA) and normalized against GAPDH. Stoichiometry determinations of phosphoproteins levels were obtained by normalizing the content of the phosphoprotein with that of the corresponding total protein.

2.6. Histological analyses

Femurs were fixed in formaldehyde (10% v/v with neutral buffer), treated for 1h with a decalcifying kit (Osteodec; Bio-Optica, Milan, Italy) and included in paraffin. Spleens were fixed in formaldehyde and then included in paraffin (Zingariello et al., 2013). Paraffin-embedded tissues were cut into consecutive 3µm sections and stained either with Hematoxylin-Eosin (H&E; cat no. 01HEMH2500 and 01EOY101000, respectively; Histo-Line Laboratories, Pantigliate, MI, Italy), Gomori silver or Reticulin staining and Mallory Trichrome staining (cat no. 04-040801, 04-040802, 04-020802 respectively; Bio-Optica). For immune-microscopy, BM sections were incubated with anti-

CXCL1 (cat no. ab86436, Abcam), anti-TGF- β 1 (cat no. sc-130348, Santa Cruz Biotechnology) antibodies and reactions detected by avidin-biotin immune-peroxidase staining and 3,3'-diaminobenzidine (0.05% w/v) (Vectastain Elite ABC Kit, Vector Laboratories, Burlingame, CA, USA). Slides were counterstained with Papanicolaou's hematoxylin (Histo-Line Laboratories). Images were acquired with the optical microscope Eclipse E600 (Nikon, Shinjuku, Japan) equipped with the Imaging Source "33" Series USB 3.0 Camera (cat no. DFK 33UX264; Bremen, DE) and the signal quantified acquiring at least 5 different areas/femur/mouse from at least 4 mice per group using the ImageJ program (version 1.52t) (National Institutes of Health), as described (Schneider et al., 2012; Zingariello et al., 2022). For Immuno-fluorescence microscopy determinations, three micron-thick BM sections were dewaxed in xylene and antigens were retrieved by treatment with EDTA buffer (pH=8) for 20' in a pressure cooker (110-120°C, high pressure) and incubated with antibodies against CD42b (cat no. ab183345, Abcam), GATA1 (cat no. sc-265, Santa Cruz), CD3 (cat no. ab16669, Abcam) and CD45R/B220 (cat no. 553085, BD-Pharmingen) over night at 4°C. Primary antibodies were visualized with the secondary antibody goat anti rat Alexa Fluor 488 (cat no. ab150165, Abcam) or goat anti rabbit Alexa Fluor 555 (cat no. ab150078, Abcam). All sections were counterstained with DAPI (cat no. D9542-5MG, Sigma-Aldrich, Darmstadt, DE), mounted with Fluor-shield histology mounting medium (cat. F6182-10MG, Sigma-Aldrich), and examined using a Nikon Eclipse Ni microscope equipped with filters appropriate for the fluorochrome to be analyzed. Images were recorded with a Nikon DS-Qi1Nc digital camera and NIS 190 Elements software BR 4.20.01 and quantified with the ImageJ program by counting the number of cells that exceeded the intensity set as threshold, as described (Zingariello et al., 2022). Reconstruction of the image of the all femur was obtained by the combining the entire set of stack images (15 images at 20x or 34 images at 63x) with the Zen Blue software (Zeiss, Oberkochen, DE). Microvessel density was determined by incubating bone marrow and spleen sections with anti-CD34 (cat no. MAB7100, AbNova, Taiwan, primary) and Alexa Fluor 568- conjugated donkey anti-rat (Invitrogen, Carlsbad, CA, USA, secondary) and with Hoechst 33342 (Thermo Fisher Scientific, Waltham, MA, USA).

2.7. Data analysis

Data were analyzed and plotted using GraphPad Prism 8.0.2 software (GraphPad Software, San Diego, CA, USA) and presented as Mean (\pm SD) or as box charts, as more appropriate. All the data had a normal distribution, as assessed by Shapiro Wilk T test. Values between two groups were compared by T test while those among multiple groups were compared by Tukey's multiple comparisons test or Anova, as indicated. Kaplan–Meier survival curves were compared by log-rank (Mantel-Cox) test. Differences were considered statistically significant with a $p < 0.05$.

3. Results

3.1. The RB40.34 antibody readily binds to platelets in the blood and reaches the fibrotic BM of *Gata1*^{low} mice

Because the underlying fibrosis in the BM of *Gata1*^{low} mice may restrain the RB40.34 antibody to reach the BM, we conducted a feasibility study to determine whether the biotinylated-RB40.34 was detectable in BM sections from mice treated for 5 days. In addition, since we, and others, have demonstrated that platelets from *Gata1*^{low} mice express greater levels of P-SEL on their surface (Vyas et al., 1999; Zetterberg et al., 2014), we determined whether biotinylated-RB40.34 was detectable on platelets present in the blood 5 hours after its administration as control of the persistence of the antibody in the circulation after its injection (**Figure 1**). Biotin is produced in the liver and is present, albeit at low levels, in several cell types (Fletcher and Myant, 1960). Therefore, it is not surprising that the APC-Cy7 Streptavidin signal is detected also on platelets and BM sections from mice in the vehicle and Rux groups which did not receive biotinylated-RB40.34. However, the signals on platelets and BM sections from mice which had received biotinylated-RB40.34 is clearly greater than background levels (**Figure 1**).

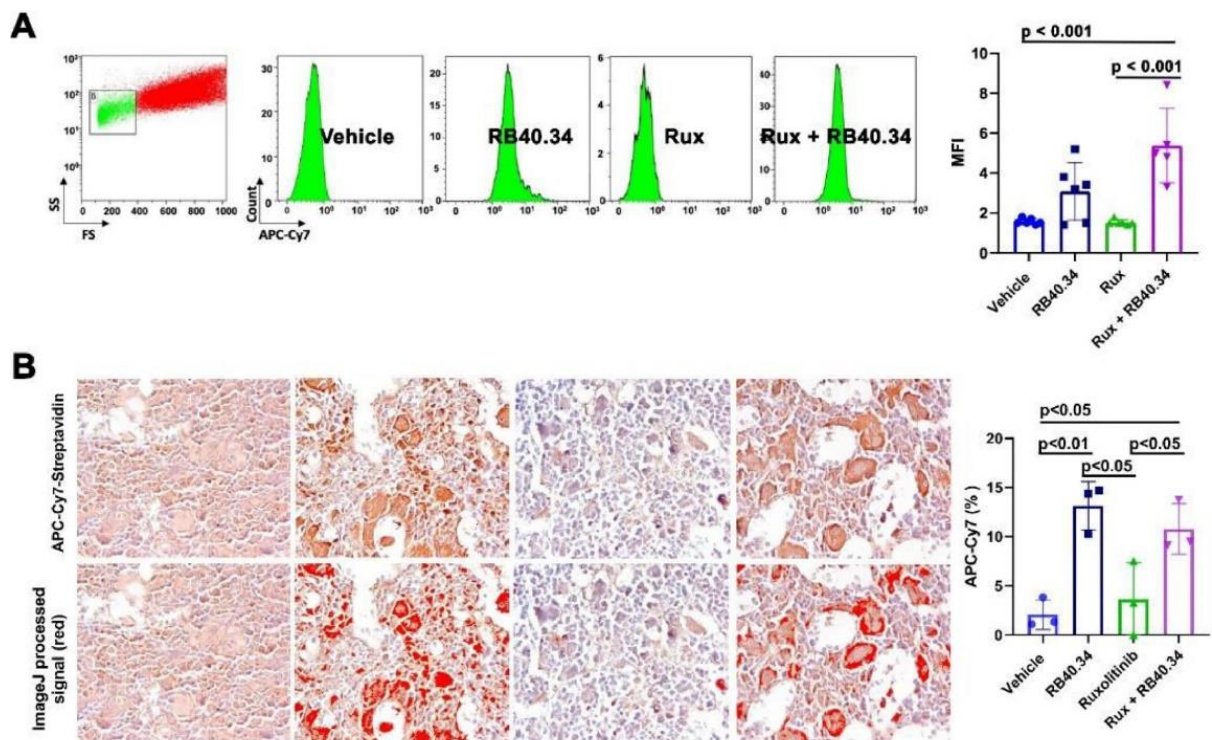


Figure 1. On day 5, RB40.34 is readily detected on the platelets present in the blood and on sections of bone marrow (BM) of *Gata1*^{low} mice. (**A**) Flow cytometry analyses with APC-Cy7-streptavidin of platelets present in the blood of *Gata1*^{low} mice after 5 days of treatment. The different groups of mice had been treated 5 hours earlier with the vehicle, biotinylated-RB40.34, Rux, and the two drugs in combination, as indicated. Platelets are recognized based on size (FS: forward scatter) and internal cell complexity (SS: side scatter). Representative FS or SS gating and histograms of the APC-Cy7-streptavidin staining are presented on the left. The mean fluorescence intensity (\pm SD) of APC-Cy7-streptavidin staining and values in individual mice (each symbol a mouse) are presented on the right. p values were calculated using Tukey's multiple

comparison test, and significant differences are indicated in the panels. **(B)** Representative sections of BM of *Gata1*^{low} mice treated with vehicle (first panel) or biotinylated-RB40.34, Rux, and Rux and biotinylated-RB40.34 incubated with APC–Cy7–streptavidin (top panels). The panel on the bottom shows the computer-generated signal specific for mAb RB40.34 obtained by subtracting the background from the vehicle using ImageJ program. Areas exceeding the threshold are artificially labeled in red. Details of the ImageJ processing of the images are provided in **Supplementary Figure S2**. Magnification, 40X. The intensities of APC–Cy7 staining as a percentage of areas above the threshold in sections from the BM of multiple mice are presented on the right.

*3.2. Five days treatment with RB40.34 in combination with Rux reduces TGF- β signaling in bone marrow and JAK2/STAT5 signaling in the spleen from *Gata1*^{low} mice*

To investigate the effects of the treatments on the signaling state of the BM and spleen from *Gata1*^{low} mice, western-blot analyses of these organs from untreated *Gata1*^{low} mice and from mice treated for 5 days were performed. These studies used a panel of antibodies which target SMAD2/3, and TGF- β RII (canonical TGF- β signaling); p38, p-p38, ERK1/2 and p-ERK1/2 (non-canonical TGF- β signaling) and JAK2 and STAT5 (JAK/STAT signaling). Untreated WT mice were analyzed in parallel as control (**Figures 2,3 and S3**). pJAK2 and pSTAT5 were not investigated because the phosphorylation of these two proteins in extracts from primary tissues is very sensitive to degradation upon storage (**Figure S4**).

The BM from untreated *Gata1*^{low} mice expresses levels of TGF- β RII significantly greater than WT mice, which are likely a reflection of the increased number of MK present in this organ. Treatment with RB40.34 or Rux alone had no effect to the levels of SMAD2/3 and TGF- β RII proteins which remain similar to that of untreated *Gata1*^{low} mice. By contrast, treatment with RB40.34 in combination with Rux reduce the content of SMAD2/3 and of TGF- β RII in the BM down to levels expressed by BM from WT mice, suggesting that the treatment reduced the canonical TGF- β signaling in this organ (**Figure 2A,C**). The levels of total ERK and p38, that are two elements of the MAPK-dependent non-canonical TGF- β signaling (Massagué et al., 2000), and of their phosphorylated forms in the BM of untreated *Gata1*^{low} mice are not significantly greater than normal. Although none of the treatments affected the p38 content/activation state, treatment with RB40.34 in combination with Rux reduces to barely detectable levels the activation of p-ERK, an indication that this treatment is reducing the non-canonical TGF- β signaling possibly responsible for fibrosis in the BM (**Figure 2B,C**). By contrast, the content and activation state of canonical and non-canonical TGF- β signaling in the spleen from untreated *Gata1*^{low} mice are similar to that of spleen from WT mice and are not significantly affected by any of the treatments (**Figure S3**).

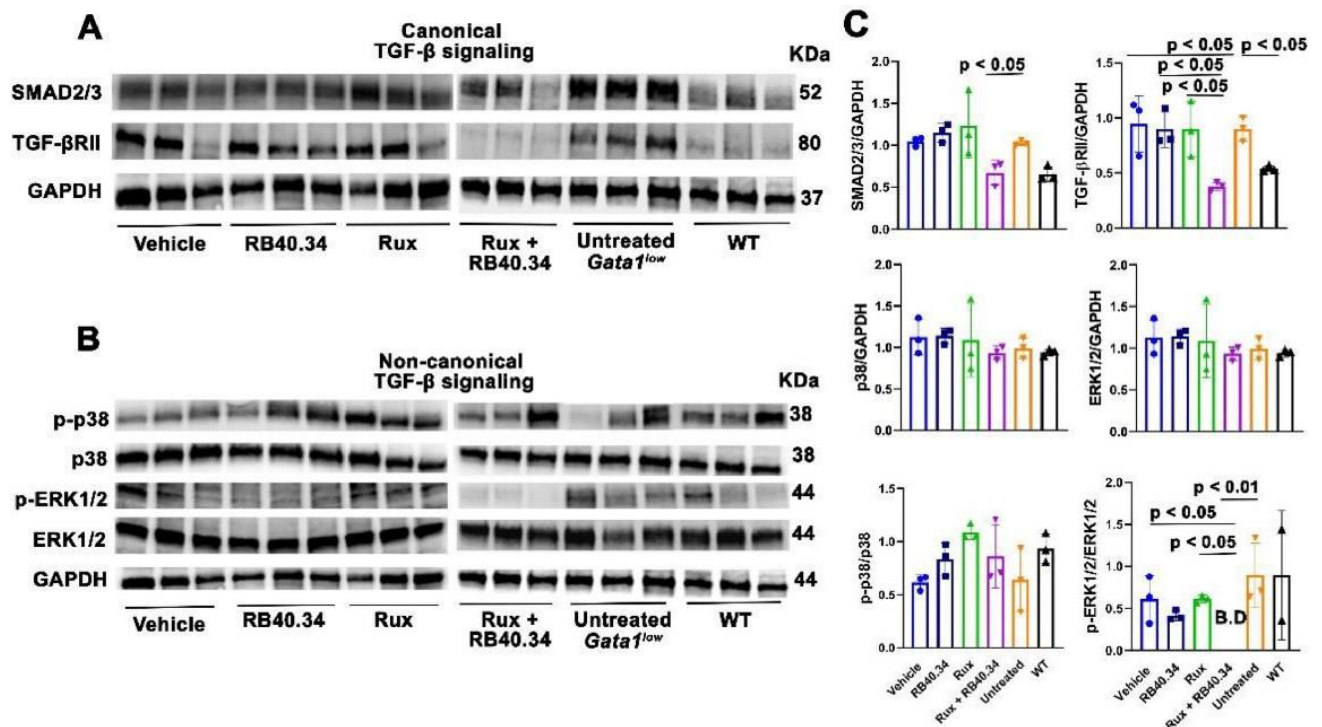


Figure 2. Treatment with RB40.34 in combination with Rux restores the abnormal canonical and noncanonical TGF- β signaling observed in the bone marrow (BM) of *Gata1*^{low} mice. (A–C) Western blot analyses for the content of elements downstream to the canonical and noncanonical TGF- β signaling of the BM of untreated wild-type (WT) and *Gata1*^{low} mice and of *Gata1*^{low} treated with vehicle, RB40.34, Rux, and the two drugs in combination, as indicated. Blots are presented on the right and quantifications on the left. Quantitative values are presented as mean (\pm SD) and as individual values for each mouse. Total protein levels are normalized toward the corresponding GPDH levels, whereas to take into account differences in total protein, the levels of the phosphoproteins are expressed stoichiometrically as a ratio to the total level of the corresponding protein. *P* values were calculated using Tukey's multiple comparison test, and statistically significant differences are indicated in the panels.

JAK2 is not detected in BM from untreated *Gata1*^{low} and WT littermates and, with the exception of two out of three mice in the vehicle and Rux alone groups, remains undetectable in BM from the treated groups as well. The content of STAT5 is instead robust and not statistically different across all groups in BM (**Figure 3A,C**). By contrast, the content of JAK2 and STAT5 in the spleen from untreated *Gata1*^{low} mice is significantly greater than that from WT littermates (**Figure 3B,D**), possibly reflecting the great levels of extramedullary hematopoiesis occurring in the spleen of the mutant animals (Migliaccio et al., 2009). The levels of STAT5 in the spleen from *Gata1*^{low} mice remain robust after treatment with either Rux or RB40.34 alone or in combination. By contrast, the levels of JAK2 in the spleen of the mutant mice are drastically reduced upon the combined treatment with Rux and RB40.34, but not with either of the drugs alone. These data suggest that the combination of Rux+RB40.34 is targeting the extramedullary hematopoiesis in spleen.

These data indicate that treatment for only 5 days with Rux+RB03.34 in combination induces detectable biochemical changes in the BM and spleen from *Gata1*^{low} mice. Additional experiments, associated with expression profiling of individual cell populations, are necessary to assess whether

these biochemical changes are due to alterations in cell composition and/or in the signaling cascade of individual cell populations in these organs.

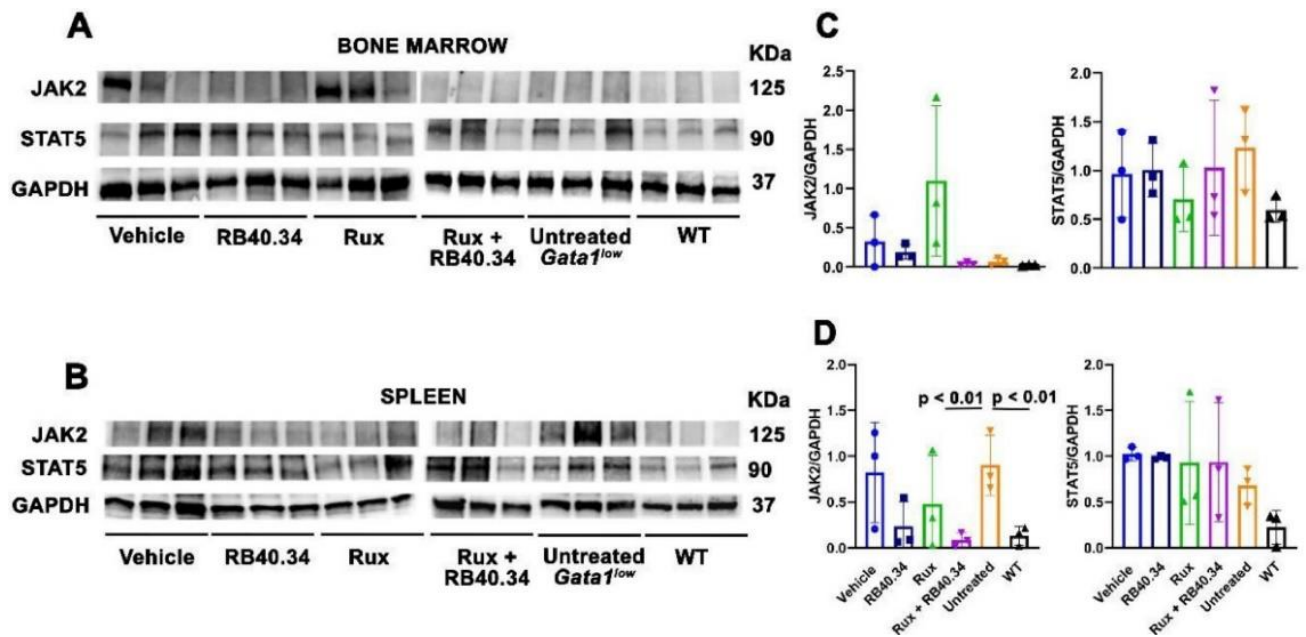


Figure 3. Treatment with RB40.34 in combination with Rux restores the abnormal JAK2/STAT5 signaling observed in the spleen of *Gata1*^{low} mice. Western blot analyses for JAK2, STAT5, and GAPDH (as loading control) of bone marrow (A, C) and spleen (B, D) from untreated wild-type (WT) and *Gata1*^{low} mice and *Gata1*^{low} mice treated with vehicle, RB40.34, and Rux, alone and in combination. Blots are presented on the right and quantifications on the left. In (C, D), quantitative values are presented as mean (\pm SD) and as individual values for each mouse. *P* values were calculated using Tukey's multiple comparison test, and statistically significant differences are indicated in the panels.

3.3. All the treatments are well tolerated with no significant effects on survival and body weight

Encouraged by the results described above, we performed longer treatments (day 12 and day 54) to assess whether these drugs may affect the myelofibrosis phenotype expressed by *Gata1*^{low} mice. To determine safety, all the treated mice were daily monitored by a veterinarian who recorded no significant modifications in physical activity and behavior (no lethargy, no excessive grooming, no change in coat luster) during all the period of observation. None of the treatments affected the weight of the animals which remains similar to that observed before treatment in all the experimental groups (Figure S5A). Although few deaths were recorded during treatment (Table S1), overall log-rank test of the Kaplan-Meier survival curves of the treated *Gata1*^{low} mice showed no significance difference in death rate among groups (Figure S5B).

3.4. RB40.34, alone or in combination with Rux, reduces anisocytosis and lymphocyte counts

Htc levels remained within normal ranges in all experimental groups for all the duration of the treatments (Table 1). A significant raise in red blood cell (RBC) distribution width (RDW) at levels that meet the criteria for anisocytosis is observed in some of the mice treated with vehicle and in all of those treated with Rux for 54 days while the RDW in the groups treated with RB40.34 alone or in combination with Rux is within normal ranges (Figure 4A). None of the treatments rescue the platelet

deficiency of *Gata1*^{low} mice which remains significantly lower than normal in all the groups (**Table 1**).

The difference in WBC counts between untreated *Gata1*^{low} and WT littermates is not statistically significant (**Table 1**) and none of the drugs investigated induces significant changes in the WBC counts since even the two-fold reductions observed at day 54 in the Rux and RB40.54 plus Rux groups are not statistically significant by Tukey multiple comparison test with those of untreated mice. However, a comparison of the frequencies of the different WBC subpopulations reveals that RB40.34 in combination with Rux significantly decreases the lymphocytes counts by day 54 (**Figure 4B**). In conclusion, none of the treatments induced anemia nor rescued thrombocytopenia of *Gata1*^{low} mice. However, treatment for 54 days with RB40.34 in combination with Rux reduced anisocytosis and lymphocyte counts.

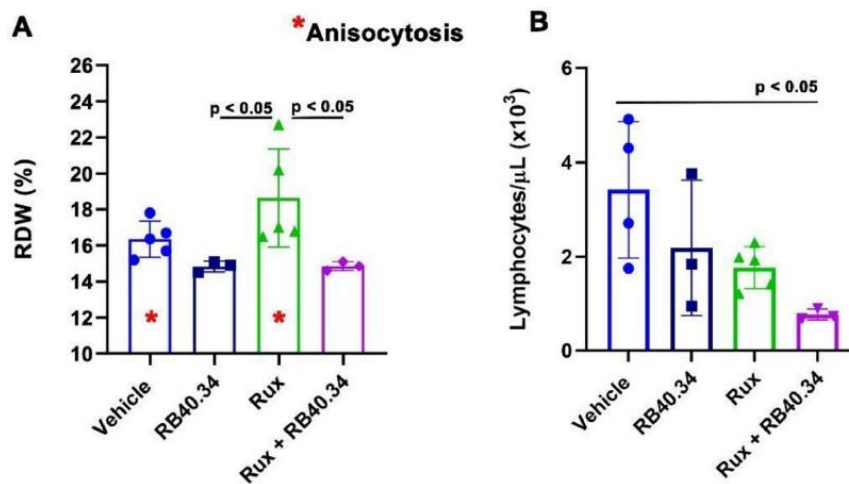


Figure 4. Treatment for 54 days with RB40.34 in combination with Rux reduces the frequency of red blood cell anisocytosis and lymphocyte counts in the blood of *Gata1*^{low} mice. **(A)** Red blood cell distribution width (RDW, in %) detected in the blood of *Gata1*^{low} mice treated with vehicle, RB40.34, Rux, and the two drugs in combination for 54 days, as indicated. Data are presented as mean (\pm SD) and as individual values for each mouse. The asterisks indicate the groups containing the deidentified samples flagged for anisocytosis by the accredited laboratory. **(B)** Lymphocyte counts observed in the blood of *Gata1*^{low} mice treated with vehicle, RB40.34, Rux, and the two drugs in combination for 54 days, as indicated. Data are presented as mean (\pm SD) and as individual values from each mouse. *P* values were calculated using Tukey's multiple comparison test, and statistically significant differences ($p < 0.05$) are indicated in the panels.

3.5. Treatment with RB40.34 in combination with Rux reduces fibrosis and restores hematopoiesis in the bone marrow from *Gata1*^{low} mice

By 8-11 months of age, the femur of *Gata1*^{low} mice is hypocellular and contain great levels of fibrosis (**Figure S6**). None of the treatments alters the BM cellularity (which remains lower than normal) and the level of fibrosis observed by day 5 (data not shown). By day 12, however, although the BM from all the groups remains hypocellular (data not shown), the level of fibrosis in the diaphysis of the femur from mice treated with RB40.34 and Rux in combination is reduced (**Figure S7**), suggesting that this combination is starting to be effective. In agreement with this hypothesis, by day 54, the femur from mice of the RB40.36 plus Rux group appears reddish, a sign of improved

erythropoiesis (**Figure 5A**), and contains significantly greater number of cells than that from the vehicle group (**Figure 5B**). This increased cellularity is also evident by hematoxylin/eosin staining of the BM sections (**Figure 5C**). In addition, reticulin staining indicates strong reductions of fibrosis in the BM of the entire femur of mice treated with RB40.34 plus Rux for 54 days (**Figure 5C,D**). By contrast, single treatment with RB40.34 significantly reduces fibrosis, but does not increase BM cellularity while, as previously reported (Zingariello et al., 2017), treatment with Rux alone does not increase BM cellularity and does not reduce fibrosis in *Gata1*^{low} mice. The reason while, by contrast with our data, Rux is effective in reducing fibrosis in the JAK2^{V617F}-driven mouse model (Li et al., 2022) is unclear and deserves to be further investigated.

The abnormal *Gata1*^{low} MK release several bone morphogenic proteins that are responsible for increased bone formation starting at 1-months of age (Garimella et al., 2007; Kacena et al., 2004; Vannucchi et al., 2002). In spite of the increased collagen deposition, the bone from the *Gata1*^{low} mice remains immature with poor Ca⁺⁺ deposition and, similarly to what observed in MF patients, the mice develop osteopetrosis (Ravid & Karagianni, 2021; Stavnichuk & Komarova, 2022). Differences in the integrity of the femur from mice treated with the different drug combinations (**Figure 5C**) suggest possible differences in the levels of osteopetrosis expressed in the four experimental groups. To test this hypothesis, we analyzed by Mallory trichrome staining femur from untreated WT and *Gata1*^{low} littermates and from *Gata1*^{low} mice treated with the different drug combination (**Figure S8**). As expected, the cortical bone of WT mice is characterized by red-mature lamellar bone with limited blue areas of osteoids rich in collagen fibers but poor in Ca⁺⁺. By contrast, the cortical bone of both the epiphysis and the diaphysis from *Gata1*^{low} mice contains large blue areas with unmineralized osteoids and limited areas of red-mature lamellar bone. The diaphysis of the mutant mice also contains large areas of trabecular unmineralized bone protruding in the medulla. These results are similar to those published in (Li et al., 2022; Ravid & Karagianni, 2021). After 54 days of treatment, the histopathology of the femur from the vehicle and RB40.34 group is similar to that of untreated *Gata1*^{low} mice of comparable age. However, the medulla of the femur from the mice treated with Rux, alone and in combination with RB40.34, contains significant less areas of neo-bone formation while the maturation of the cortical bone from the femurs of mice treated with Rux is normal (**Figure S8**).

Another of the features associated with myelofibrosis which is conserved in animal models is increased neoangiogenesis (Vannucchi et al., 2002). To assess whether the treatments had reduced the neo-angiogenesis in the bone marrow and spleen from *Gata1*^{low} mice, confocal microscopy studies with CD34, which in mice recognize endothelial cells, and Hoechst, to identify the nucleated cells, were performed (**Figure 6**). Indeed, by day 54, the vessel density of all the treatment groups was significantly lower than in the vehicle.

The BM hematopoietic failure associated with the myelofibrotic phenotype of *Gata1*^{low} mice includes barely detectable levels of hematopoietic stem/progenitor cells in this organ (Spangrude et

al., 2016). To confirm that RB40.34 in combination with Rux improves hematopoiesis in BM, the frequency and total numbers of progenitor (Lin^-) and short term (LSK) and long (SLAM) term repopulating stem cells in the BM from mice treated for 54 days with the various drug combination was evaluated (**Figures 5E and S9**). Indeed, the BM from mice treated with RB40.34 in combination with Rux contains significantly greater frequency of Lin^{neg} and LSK and greater total numbers of all three populations than that from the vehicle-treated group.

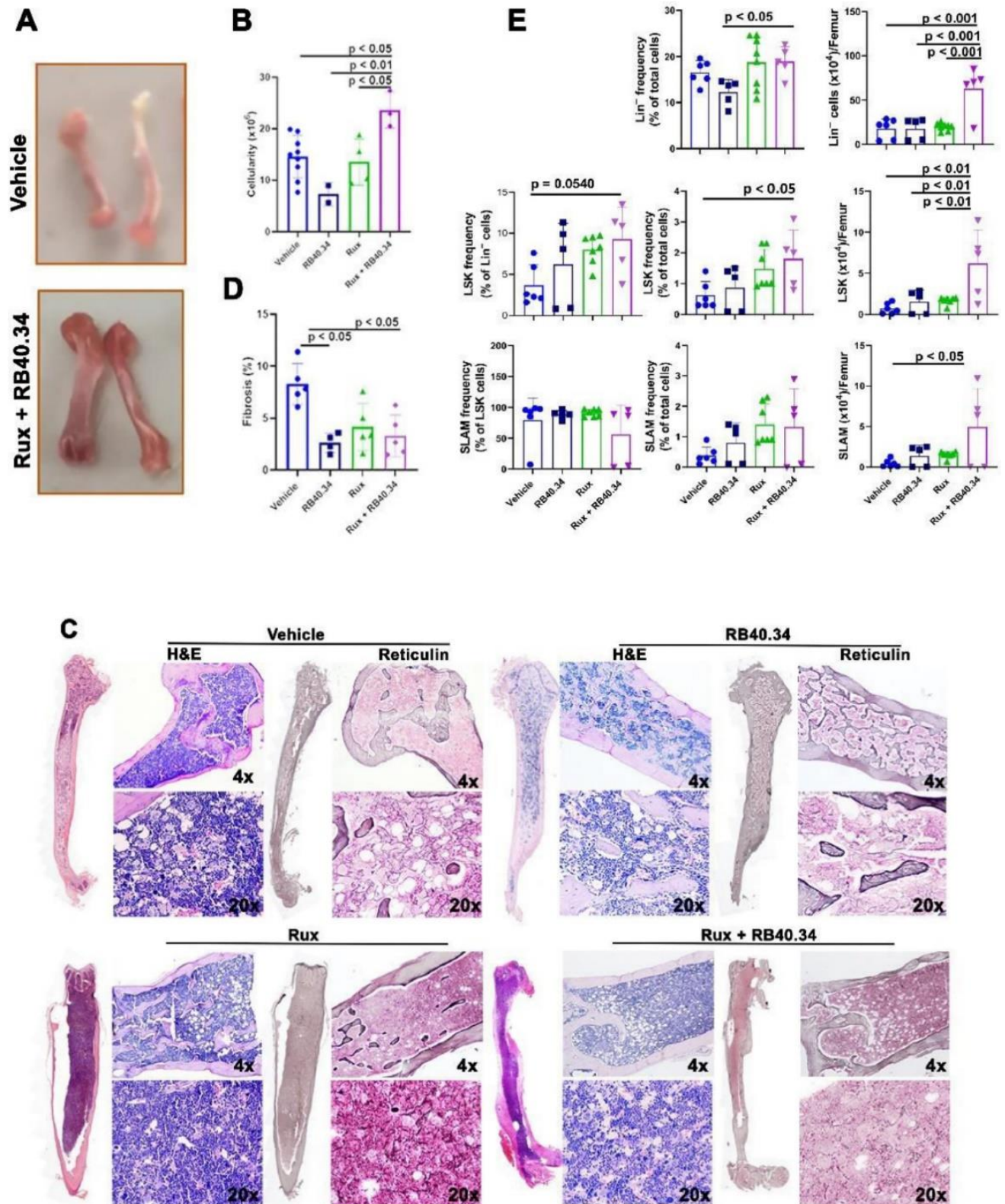


Figure 5. Treatment for 54 days with RB40.34 in combination with Rux increases the cellularity, reduces fibrosis, and restores hematopoiesis in the bone marrow (BM) of *Gata1^{low}* mice. **(A)** Photographs of the femur and tibia from representative mice treated for 54 days with vehicle and RB40.34 in combination with Rux, as indicated. **(B)** Number of cells per femur observed at day 54 in *Gata1^{low}* mice treated with vehicle, RB40.34, Rux, and the two drugs in combination. **(C)** Hematoxylin and eosin (H&E) and reticulिन staining of femurs of representative *Gata1^{low}* mice treated for 54 days with vehicle, RB40.34, Rux, and the two drugs in combination, as indicated. The femurs are presented as stack images (at 4X) and as representative sections at 4X and 20X magnification, as indicated. **(D)** Levels of fibrosis quantified by image analyses of the reticulिन staining of BM sections of *Gata1^{low}* mice treated for 54 days as indicated above. **(E)** Frequency and the total number of Lin⁻, LSK, and SLAM cells in the femur of *Gata1^{low}* mice treated with the various drug combinations. In **(B–E)**, results are presented as mean (\pm SD) and as values per individual mice (each symbol a mouse) and were analyzed using Tukey's multiple comparisons test. Statistically significant groups are indicated within the panels.

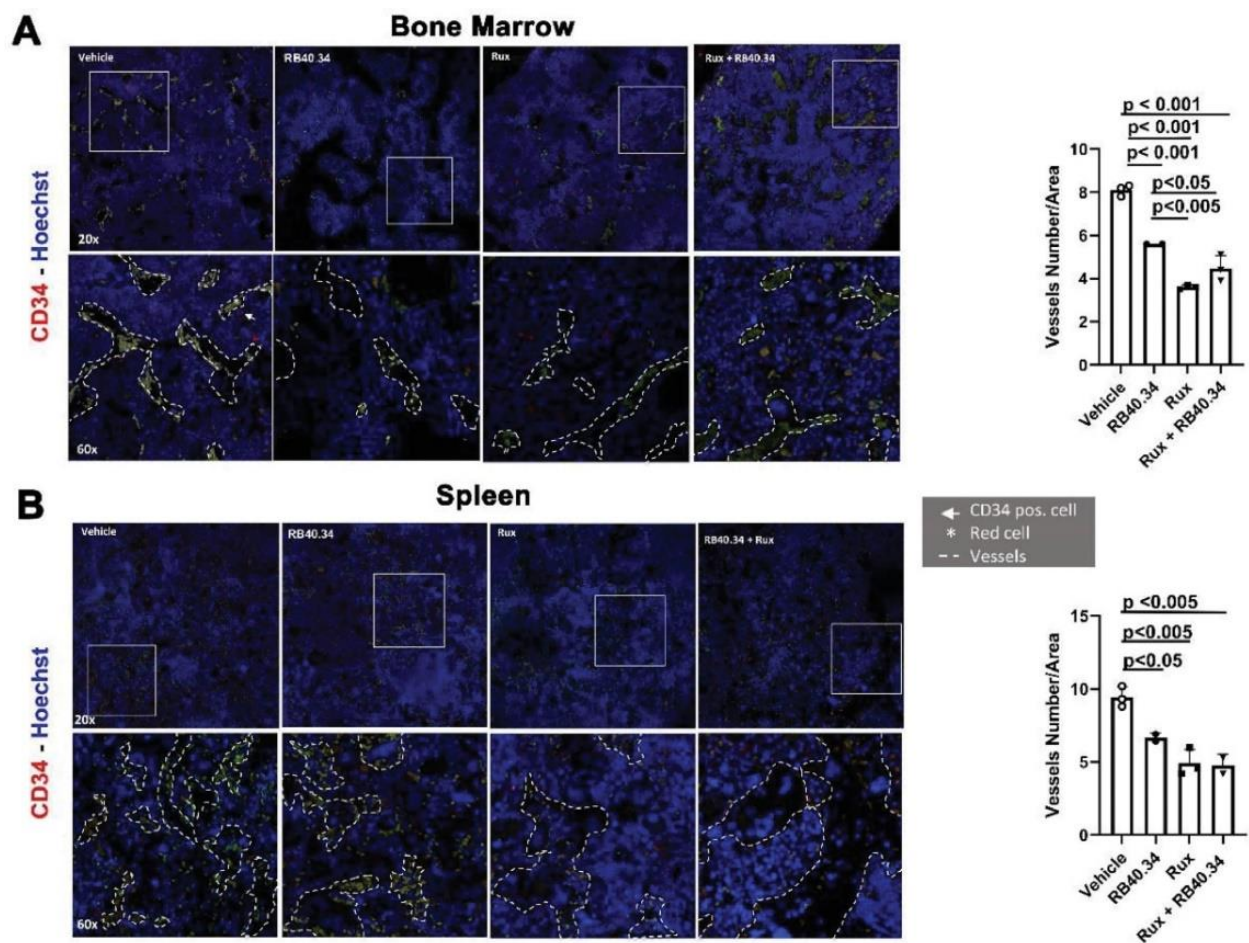


Figure 6. Treatment for 54 days with RB40.34 and Rux, alone and in combination, reduces the vessel density in the bone and spleen of *Gata1^{low}* mice. Confocal microscopy with CD34 and Hoechst (to counterstain the nuclei) of bone marrow **(A)** and spleen **(B)** sections of *Gata1^{low}* mice treated for 54 days with either vehicle or with RB40.34 and Rux alone and in combination. The panels in the first and third lanes are at 20X magnification, and the area depicted in the rectangles is shown at 60X in the corresponding panels in the second and third lanes. At 60X magnification, microvessels (dashed lines) are identified as structures surrounded by CD34⁺ cells (indicated by arrows) and containing red cells (autofluorescent cells not counterstained by Hoechst, asterisks). Quantitative results are shown on the right as mean (\pm SD) and as values per individual mice (each symbol a mouse). Statistical analysis was performed using Tukey's multiple comparisons test, and significant *p* values are indicated within the panels.

3.6 Treatment with RB40.34 in combination with Rux reduces fibrosis, extramedullary hematopoiesis and restores the architecture of the spleen from *Gata1^{low}* mice

Given the great relevance of JAK2 signaling in hematopoiesis (Perner et al., 2019), the observation that treatment with RB40.34 and Rux in combination greatly reduces the JAK2 content in the spleen suggest that this treatment decreases hematopoiesis in this organ. In agreement with this hypothesis, we observe marked reductions of fibrosis in spleen from *Gata1^{low}* mice treated with RB40.34 plus Rux for only 12 days (**Figure S7**). By day 54, a trend toward reduction in spleen size (both as weight, as ratio between spleen weight and body weight, and as cell numbers) is observed in the group treated with RB40.34 plus Rux (**Figure 7A-C**). Furthermore, a significant reduction in the total number of hematopoietic progenitor cells (Lin^{neg} cells) was observed at day 54 in the spleen from this group (**Figures 7D and S9**), supporting the hypothesis that RB40.34 and Rux in combination reduces extramedullary hematopoiesis in this organ.

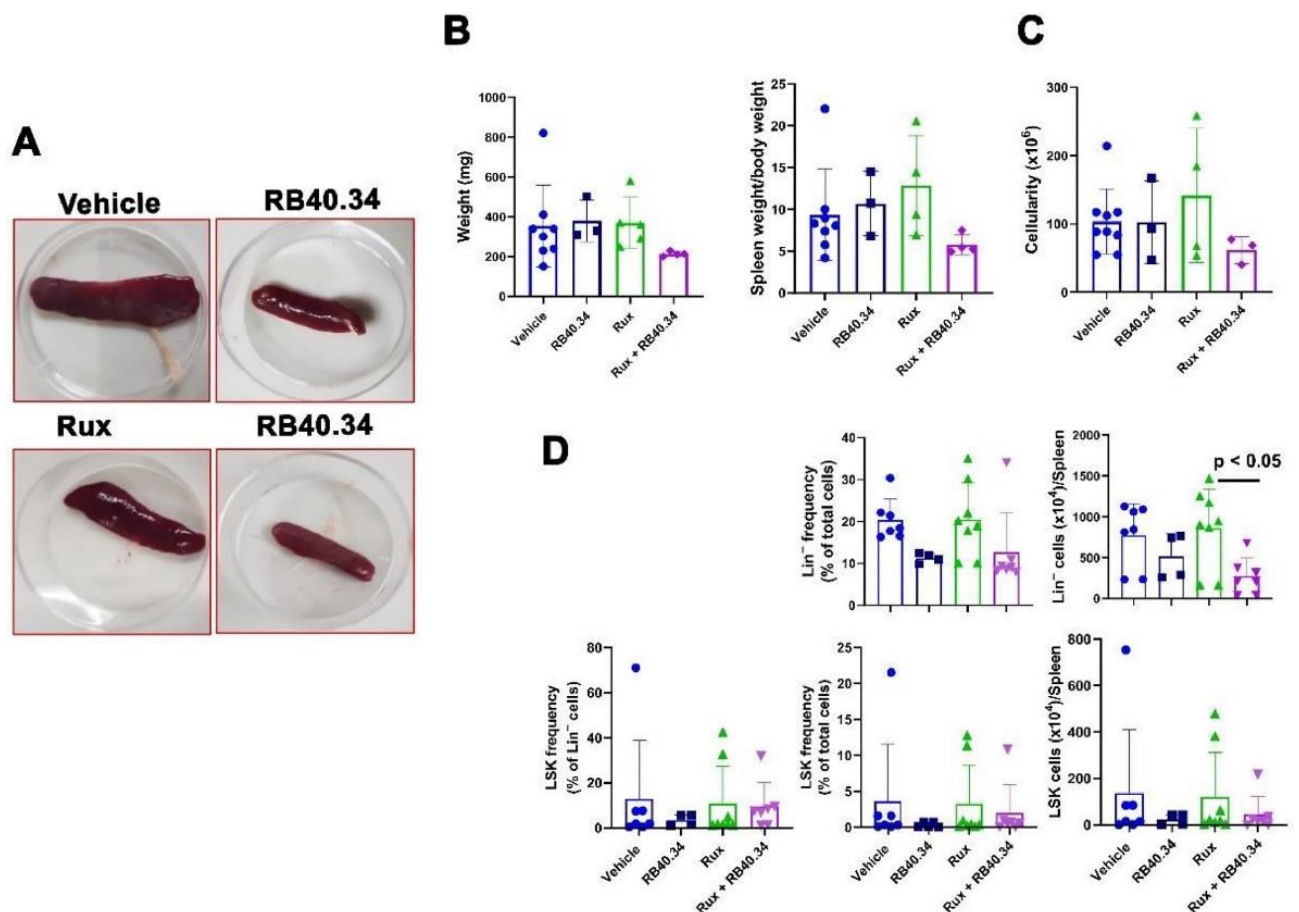
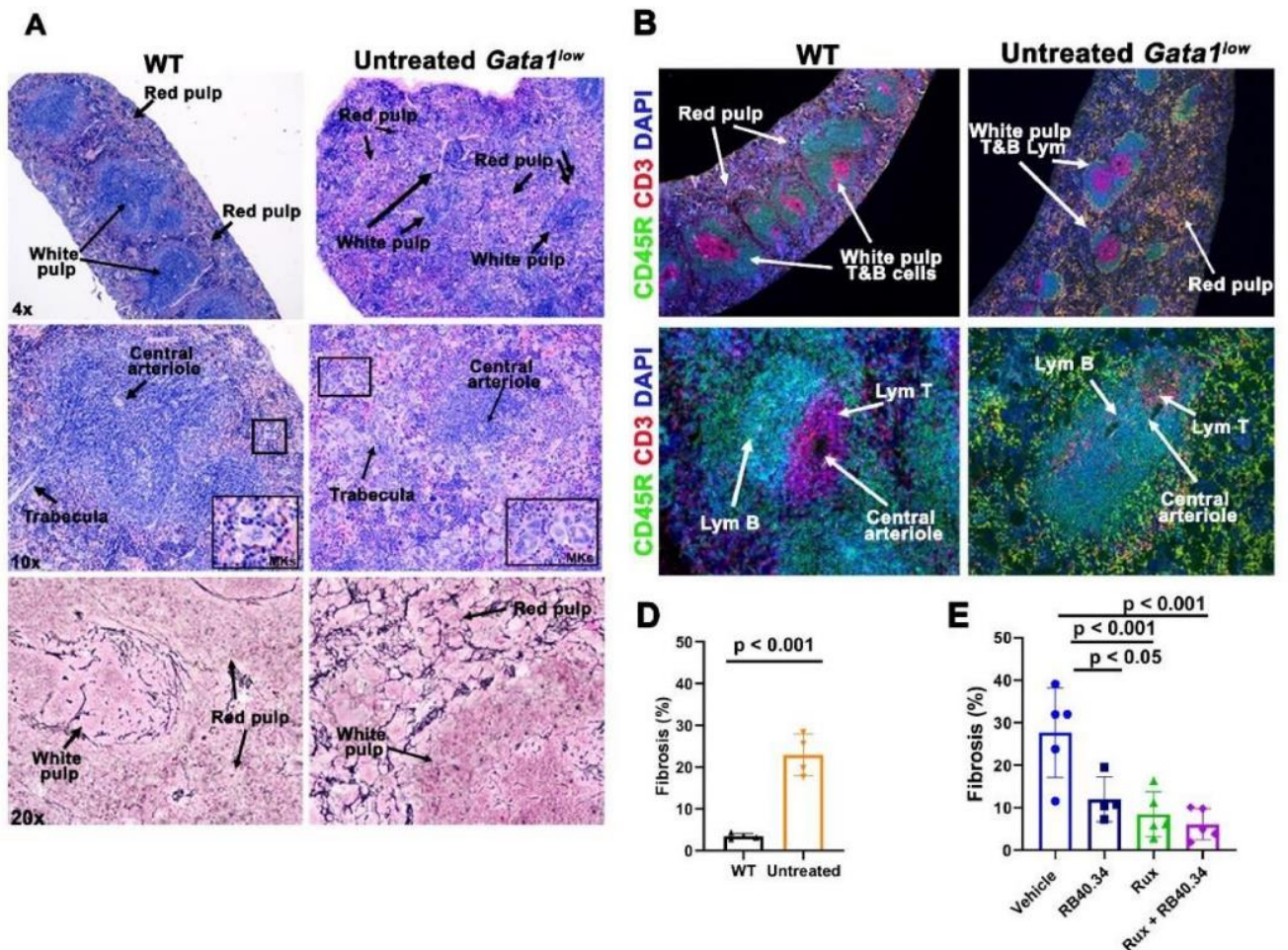


Figure 7. Treatment for 54 days with RB40.34 in combination with Rux decreases hematopoiesis of the spleen of *Gata1^{low}* mice. (A) Photographs of representative spleens treated for 54 days with the various drug combinations, as indicated. (B, C) Spleen size, as weight and ratio between spleen weight and body weight (B), and total cell numbers (C), of mice treated for 54 days with the various drug combinations. (D) Frequency and the total number of Lin⁻ and LSK cells in the spleen of *Gata1^{low}* mice treated with the various drug combinations. SLAM cells are not presented because they are almost 100% of the LSK cells detected in the spleen (**Supplementary Figure S9**). In (B–D), results are presented as mean (±SD) and as values per individual mice (each symbol a mouse). They were analyzed using Tukey's multiple comparisons test. Statistically significant groups are indicated within the panels.

The architecture of the spleen from *Gata1*^{low} mice is greatly altered by the fibrosis and by the underlying extramedullary hematopoiesis (**Figure 8A,B,D**). Significant reductions in fibrosis are observed in mice treated with RB40.34 alone, Rux alone and RB40.34 and Rux in combination, although the greater reductions are observed in mice treated with the combination (**Figure 8C,E**). As expected (Steiniger, 2015), CD45R/CD3 staining indicates that the architecture of the spleen from WT mice is characterized by the presence of large aggregates of lymphoid cells and a well-developed white pulp. Red blood cells are embedded in the reticular connective tissue which contains few megakaryocytes and supporting trabeculae. The T (CD3^{pos}, in red) and B (CD45R^{pos}, in green) lymphocytes are numerous and localized around the central arterioles: T lymphocytes form a sleeve around the central arteriole, the periarteriolar lymphoid sheath, while B cells are mainly localized in the outer region of the white pulp, defined the marginal zone. By contrast, the spleen from *Gata1*^{low} mice contains a hypoplastic white pulp and its periarteriolar lymphoid sheath contains a markedly reduced number of T cells. In addition, the red pulp appears disorganized by the presence of numerous MK and fibrosis (**Figure 8A-C**). Treatment of *Gata1*^{low} mice with RB40.34 and Rux in combination, and to a lesser extent by the two drugs as single agents, restores the normal architecture of the spleen with a great expansion of white pulp and a nearly normal organization of the periarteriolar lymphoid sheath and of the marginal zone (**Figure 8C**).



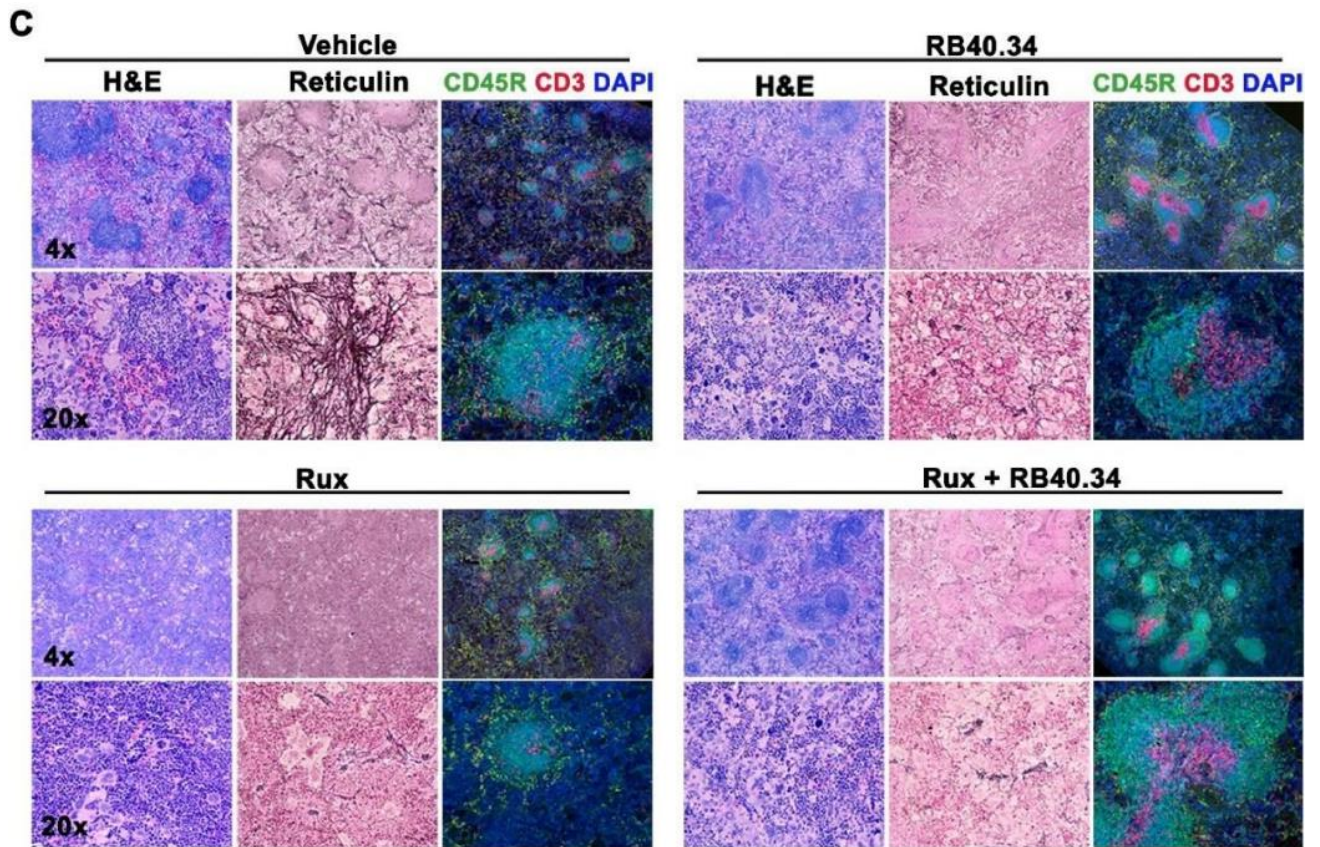


Figure 8. Treatment for 54 days with RB40.34 in combination with Rux decreases fibrosis and restores the architecture of the spleen of *Gata1*^{low} mice. **(A)** Hematoxylin and Eosin (H&E) and reticulin staining of spleen from representative 8- to 11-month-old WT and *Gata1*^{low} mice. WT spleens are characterized by the presence of large aggregates of lymphoid cells, well-developed white pulp, with the presence of RBCs embedded in reticular connective tissue containing few megakaryocytes (MKs) and supporting trabeculae. By contrast, *Gata1*^{low} spleen is characterized by hypoplastic white pulp and red pulp rich in MKs. Reticulin staining of the consecutive section indicates that fibrosis is localized mostly in the red pulp. Results are representative of those observed in at least three WT and three *Gata1*^{low} littermates, all of whom were 11 months old. **(B)** Double immunofluorescent analyses for CD3 (as a marker of T cells, red), CD45R (B220, as a marker for B cells, green), and DAPI (nuclei) of spleen sections from representative WT and *Gata1*^{low} mice, as indicated. The white pulp of the WT spleen contains numerous T and B lymphocytes, organized around central arterioles. T lymphocytes form a sleeve around the central arteriole, the periarteriolar lymphoid sheath, whereas B cells are mainly localized in the outer white pulp region, the marginal zone. In *Gata1*^{low} spleens, the white pulp is smaller than that in the WT organ and the periarteriolar lymphoid sheath contains a markedly reduced number of T cells. Magnification 4X, 10X, and 20X, as indicated. **(C)** H&E, reticulin staining, and triple staining with CD45R (green), CD3 (red), and DAPI (blue) of sections from the spleen of representative *Gata1*^{low} mice treated for 54 days with the various drug combinations, as indicated. Images are presented at 4X and 20X magnification. **(D)** Levels of fibrosis quantified by image analyses of the reticulin staining of spleen sections from untreated 8- to 11-month-old WT and *Gata1*^{low} littermates, as indicated. **(E)** Levels of fibrosis, quantified by image analyses of the reticulin staining, in spleen sections, of *Gata1*^{low} mice treated for 54 days, as indicated. In **(D, E)**, results are presented as mean (\pm SD) and as values per individual mice (each symbol a mouse) and were analyzed by *t*-test. Statistically significant groups are indicated within the panels.

3.7. RB40.34 in combination with Rux for 54 days improves MK maturation but does not decrease the MK content in the bone marrow and spleen from *Gata1*^{low} mice

The process of terminal megakaryocyte maturation involves a series of precursors that progressively acquire features of mature cells that release platelets (Campanelli et al., 2011; Sun et al., 2021). As these precursors progress along the maturation pathway, they express increased levels of CD41 and CD61 on their surface (Ghinassi et al., 2007; Sun et al., 2021). Therefore, flow cytometry analyses for CD41 and CD61 expression divides MK precursors into three classes: immature (CD41^{neg}CD61^{pos}), mature (CD41^{pos}CD61^{pos}) and very mature (CD41^{pos}CD61^{low}) while non-MK are negative for both markers. On the basis of this flow cytometry criteria, we determined whether the treatments rescued the defective MK maturation of *Gata1*^{low} mice (**Figure 9**). Since the BM of *Gata1*^{low} mice contains great number of MK (Vannucchi et al., 2002), it is not surprising that CD61^{pos} cells represent almost 30% of the total cells of BM and spleen from mutant mice (**Figure 9**). The total frequency of the CD61^{pos} cells in the BM and spleen from all the experimental groups remains high for all the duration of the treatments. By day 5 and 12, very few of the MK in the BM and spleen from *Gata1*^{low} mice in all the experimental groups had the very mature CD41b^{pos}CD61^{low} phenotype. The frequency of very mature CD41b^{pos}CD61^{low} MK is low and that of immature CD41b^{neg}CD61^{pos} MK high also in BM and spleen from mice treated with vehicle for 54 days. By contrast, by day 54, the frequency of MK with the very mature and immature phenotypes in the groups treated with RB40.34, Rux or RB40.34 and Rux in combination is, respectively, significantly greater and lower than in the vehicle group. These results suggest that the drugs, although ineffective in reducing the proliferation of the MK, are improving the cells maturation.

The abnormal maturation of MK from mouse models and MF patients includes localization of P-SEL on the DMS instead than in the α -granules (Thiele et al., 1997; Zetterberg et al., 2014; Zingariello et al., 2015). Since the DMS increases with maturation, the amount of PSEL exposed to the extracellular space also increases during this process. Therefore, the biotinylated RB40.34 which reach the BM should bind great numbers of *Gata1*^{low} MK and its binding should be greater as these cells mature. To assess whether the improved MK maturation induced by the treatments for 54 days included rescue of the altered cell surface expression of P-SEL, the binding of PE-Cy7-streptavidin to MK from the BM and spleen of mice treated for 5, 12 or 54 days was determined (**Figures 9A-C**). As expected, PE-Cy7- streptavidin binding is barely detected on BM and spleen cells from mice treated with either vehicle or Rux alone which had not received the antibody in any of the time points. The low levels PE-Cy7-streptavidin binding observed in these group probably represent background signals due to endogenously produced biotin and are not informative on the levels of P-SEL expressed by MK. By day 5 and 12, PE-Cy7-streptavidin binding is detected in cells both in the non-MK and in the MK gate. The binding of PE-Cy7-streptavidin to the non-MK cells is possibly related to the presence in this population of endothelial cells, also known to express P-SEL (Chagraoui et al., 2002).

By day 5 and 12, great numbers of MK from the BM and spleen of mice treated with RB40.34 alone or in combination with Rux bind PE-Cy7-streptavidin. As expected, the MFI of the binding increases in cells with a more mature phenotype, a reflection of the greater levels of P-SEL on the cell surface of *Gata1*^{low} MK as they mature. In addition, increases in MFI are also observed among MK of comparable maturation stage analyzed at day 5 and day 12, a possible reflection of increased bioavailability of the antibody in the microenvironment due to the reduction of fibrosis induced by the treatments. By contrast, PE-Cy7- streptavidin is found barely bound to MK from BM and spleen of mice treated with RB40.34 alone or in combination with Rux by day 54. These last results indicate that the improved MK maturation induced by these two drug combinations may include reduced localization of P-SEL on the DMS. By day 54, PE-Cy7- streptavidin binding is also barely detectable in the non-MK populations from mice treated with RB40.34 alone or in combination with Rux. Since the cells responsible for binding PE-Cy7-streptavidin in the non-MK population are probably endothelial cells and that P-SEL expression in endothelial cells is up-regulated by inflammation (Foreman et al., 1994), these data provide further support for the hypothesis that the treatments are reducing the inflammatory milieu of the BM and spleen from *Gata1*^{low} mice.

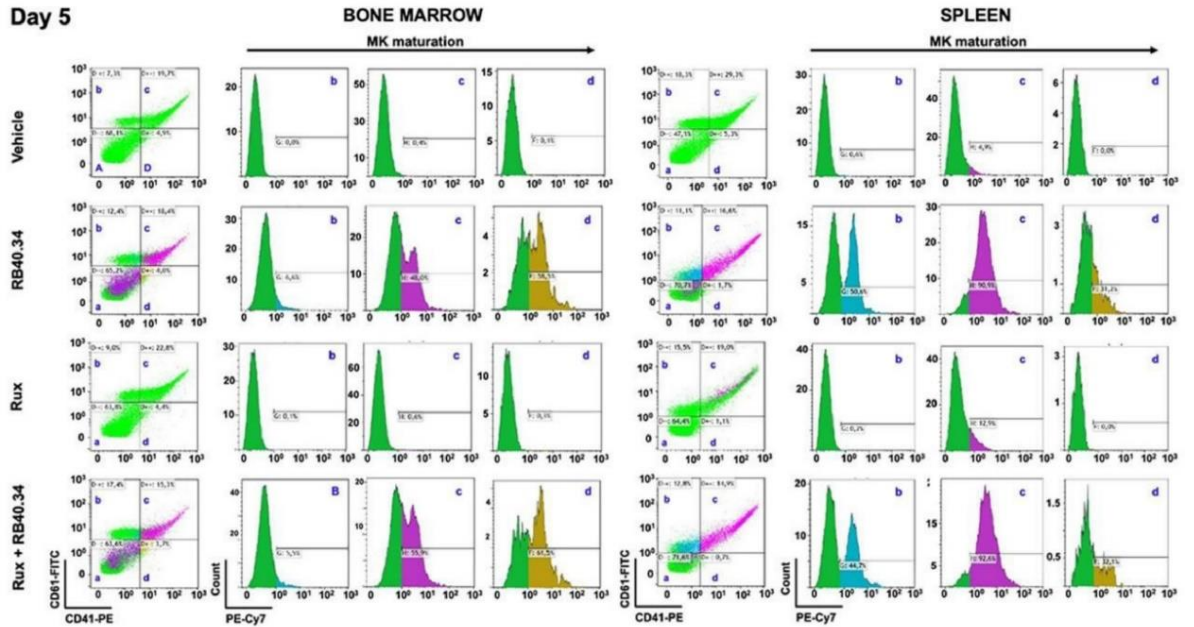
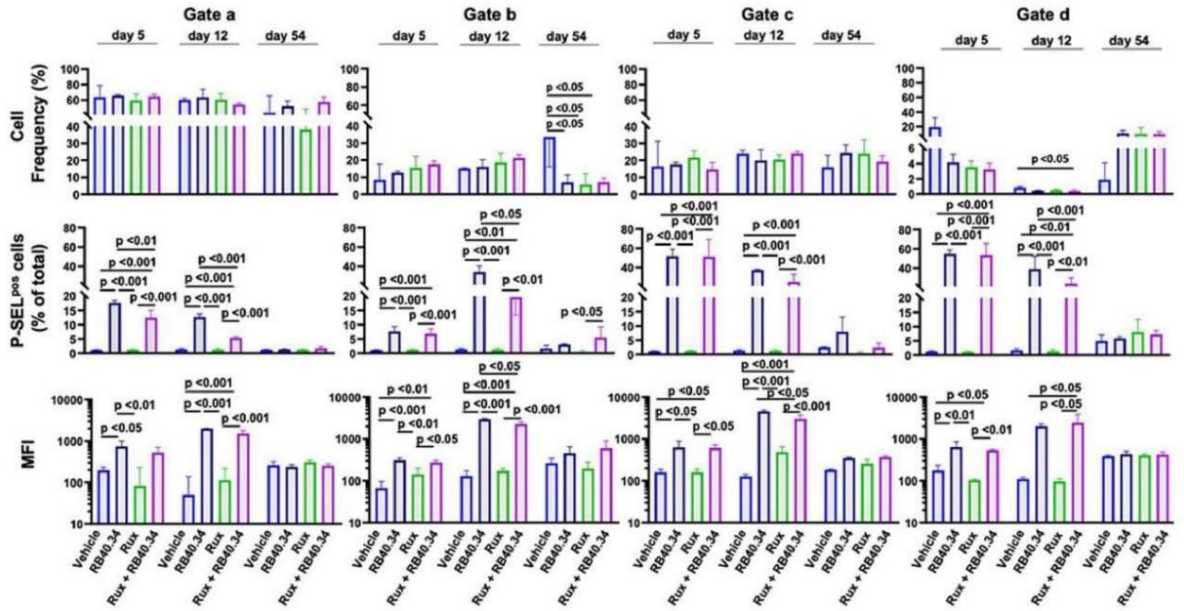
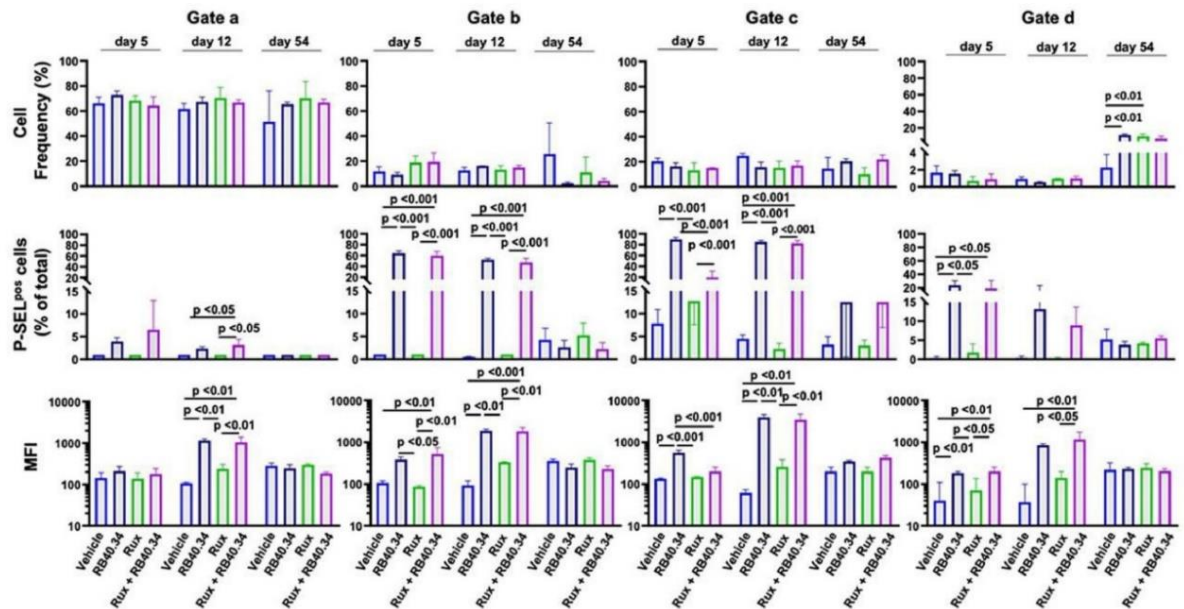
A**Day 5****B****C**

Figure 9. Treatment for 54 days with RB40.34 and Rux alone in combination improves the maturation profile of the megakaryocytes (MKs) from the bone marrow and spleen of *Gata1^{low}* mice. **(A)** Representative dot-plots and histograms of MKs from the bone marrow (left quadrant) and spleen (right quadrant) of one representative mouse from each experimental group treated for 5 days. MKs were labeled with CD41, CD61, and PE–Cy7–streptavidin. The a, b, c, and d gates identify non-MKs, immature MKs, mature MKs, and very mature MKs, respectively. The levels of APC–Cy7–streptavidin bound to the MKs at their different stages of maturation are presented by histograms. Because P-sel is abnormally expressed at high levels on the surface of *Gata1^{low}* MK, the APC–Cy7–streptavidin signal identifies the MK expressing P-sel, which has bound the biotinylated RB40.34 injected 5 hours earlier in the mice. **(B, C)** Frequency of cells in the non-MK (a), immature (b), mature (c), and very mature (d) MK gate (% of total cell number) and percentage and mean fluorescence intensity (MFI) of the events positive for PE–Cy7–streptavidin staining in each gate in the BM **(A)** and spleen **(B)** of *Gata1^{low}* mice treated for 5, 12, and 54 days with either vehicle or the different drug combinations, as indicated. Values were reported as means (\pm SD) of those detected in at least three mice per experimental group. Data were analyzed using Tukey's multiple comparisons and statistically significant differences among groups are indicated within the panels.

*3.8. Treatment with Rux increases the frequency of MK expressing detectable levels of GATA1 in the BM from *Gata1^{low}* mice*

The abnormal maturation of the MK which is thought to drive myelofibrosis in patients and mouse models is driven by defective content of GATA1 (Gilles et al., 2017; Malara et al., 2018; Vannucchi et al., 2005), the transcription factor which plays a pivotal role in supporting MK maturation (Crispino & Weiss, 2014; Malara et al., 2018). As expected, confocal microscopy analyses with antibodies against GATA1 and CD42b (as a marker of MK) indicated that the BM from *Gata1^{low}* mice contains great numbers of MK the nuclei of which are not stained by the GATA1 antibody (**Figure S10**). To generate insights on the possible mechanism(s) that rescues MK maturation in mice treated with RB40.34 and Rux, alone or in combination, we performed confocal microscopy analyses with the same antibodies of BM section from mice treated for 54 days with either vehicle, RB40.34 alone, Rux alone or the two drugs in combination (**Figure 10**). These analyses confirm the indications provided by flow cytometry (**Figure 9**) that none of the treatments affected the number of MK (as CD42b^{pos} cells) present in the BM, which remains high. As expected, very few of the MK from mice treated with vehicle contain GATA1. By contrast, a significant number of MK in the BM from mice treated with either RB40.34 or Rux alone contain detectable levels of GATA1 in their nuclei (**Figures 10 and S11**). It is surprising instead that GATA1 is not detected in MK in the BM from mice treated with RB40.34 and Rux in combination.

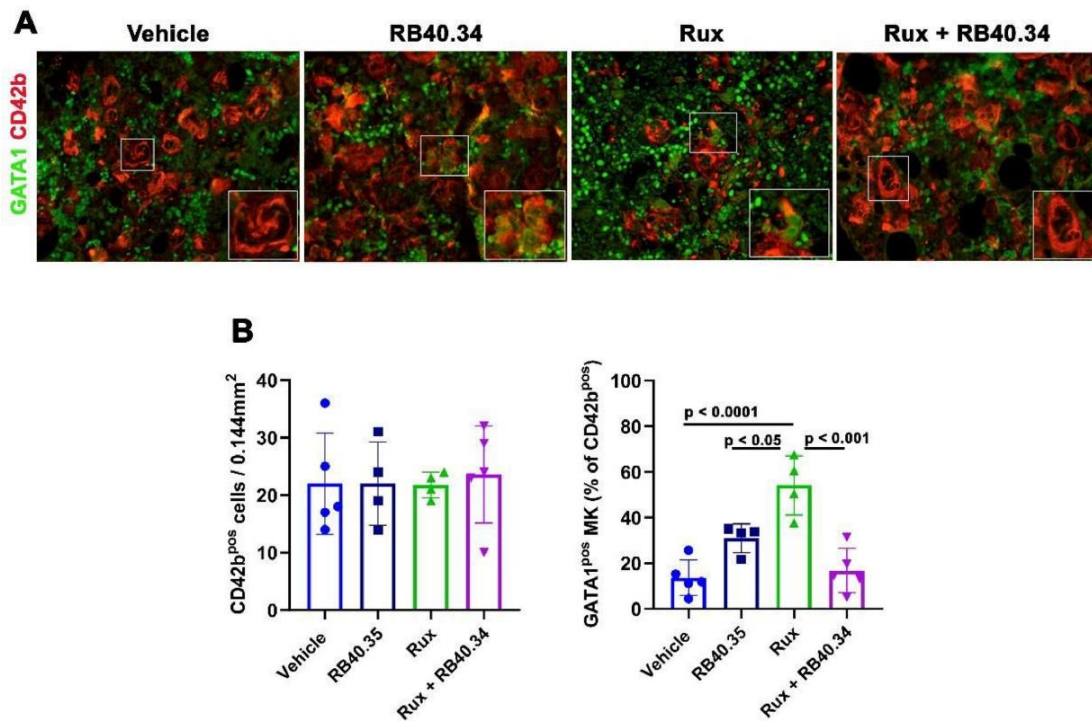


Figure 10. Treatment for 54 days with RB40.34 or Rux alone, but not in combination, increases the GATA1 content in the megakaryocytes (MKs) from the bone marrow (BM) of *Gata1*^{low} mice. **(A)** Merged GATA1 (FITCH-green) and CD42b (TRITCH-red, as a marker of MKs) images of the confocal microscopy analyses with the corresponding antibodies in BM sections from representative *Gata1*^{low} mice treated for 54 days with vehicle, RB40.34 alone, Rux alone, and the two drugs in combination, as indicated. The corresponding images acquired in the single channels, in the channel for DAPI (as an indication of the nuclear localization of GATA1), and in the bright field (to exclude autofluorescence) are presented in **Supplementary Figure S11**. Magnification 40X. **(B)** Frequency of MKs (CD42b-positive cells) and percentage of MK positive for GATA1 in BM sections of *Gata1*^{low} mice treated for 54 days, as indicated. Data are presented as mean (\pm SD) and as values in individual mice (each symbol a mouse). Results were analyzed using Tukey's multiple comparisons test and significant differences among groups are indicated within the panels.

3.9. Treatment with RB40.34 in combination with Rux reduces the TGF- β and CXCL1 content of the BM of *Gata1*^{low} mice

Increased bioavailability of the pro-inflammatory cytokines TGF- β and CXCL1, the murine equivalent of human IL-8 has been suggested to represent the driver for fibrosis and hematopoietic failure in BM of MF patients and mouse models (Dunbar et al., 2020; Emadi et al., 2005; Verachi et al., 2022). In previous studies we demonstrated that the cells responsible for increasing the bioavailability of these two cytokines in the BM (and spleen) from *Gata1*^{low} mice are the abnormal MK (Zingariello et al., 2022). To test whether treatment with RB40.34 in combination with Rux decreases the proinflammatory milieu of the BM microenvironment of *Gata1*^{low} mice, we performed histochemical evaluations with antibodies against TGF- β and CXCL1 of BM sections from *Gata1*^{low} mice treated for 54 days with either vehicle, RB4034 alone, Rux alone or the two drugs in combinations (**Figure 11**). As expected, the BM from *Gata1*^{low} mice treated with vehicle contains great levels of TGF- β and CXCL1. The levels of TGF β are significantly decreased by treatment with both Rux alone

or in combination with RB40.34 (**Figure 11A,B**). Morphological analyses of the cells which expressed TGF- β indicates that the reductions are mainly due to reduced numbers of MK expressing this factor (**Figure 11C**). CXCL1 instead is reduced only by RB40.34 in combination with Rux and the numbers of MK which express this factor remain high in all the groups (**Figure 11A-C**). Since in addition to MK, CXCL1 is expressed by many other cell types, we suggest that the two-drugs in combination reduce the pro-inflammatory milieu of *Gata1*^{low} mice by targeting not only the MK but also additional cells in the microenvironment.

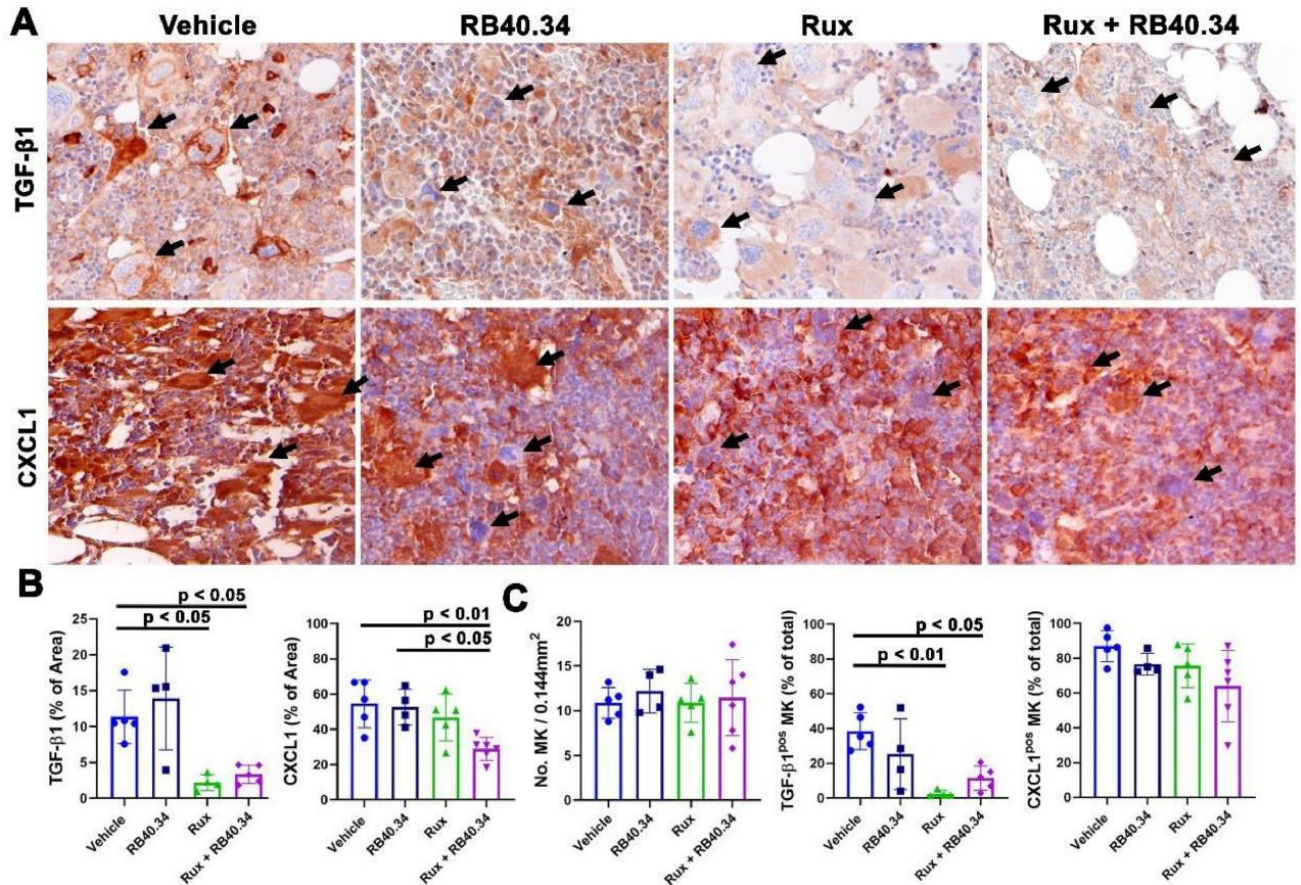


Figure 11. Treatment for 54 days with RB40.34 and Rux in combination decreases the TGF- β , mainly in the megakaryocytes (MKs), and CXCL1 content of bone marrow (BM) of *Gata1*^{low} mice. (A) BM sections from representative mice treated for 54 days with vehicle, RB40.34, Rux, and the two drugs in combination immune-stained for TGF- β 1 or CXCL1, as indicated. Representative MKs are indicated by arrows. Magnification 40X. (B) Quantification by computer-assisted imaging of the TGF- β 1 and CXCL1 content in the BM of *Gata1*^{low} mice treated for 54 days as indicated. (C) Frequency of MKs and percentage of MKs expressing high levels of TGF- β 1 and CXCL1 in BM sections of *Gata1*^{low} mice treated, as indicated. MKs were identified based on size (10 times greater than that of any other cell type in the section) and the polylobate morphology of their nuclei. In (B, C), data are presented as mean (\pm SD) and as values per individual mice (each symbol a different mouse) and were analyzed using Tukey's multiple comparisons test. Values statistically different are indicated within the panels.

4. Discussion

The hypomorphic *Gata1*^{low} mutation deletes only one of the three major hypersensitive sites which regulate the expression of the gene (McDevitt et al., 1997). After birth, the hematopoietic cells of these mice activate the expression of the gene from the two regulatory sites not affected by the

mutation so that the levels of Gata1 mRNA in the hematopoietic cells are overall normal (Migliaccio et al., 2009). However, the thrombocytopenia induced by the mutation activates the TPO/Mpl axis (Zingariello et al., 2017), which results in a RSP14 ribosomopathy, similar to that observed in MF patients (Gilles et al., 2017), which reduces the efficiency of the translation of Gata1 mRNA reducing the content of the protein. The mechanism(s) linking the TPO/Mpl axis to the RSP14 ribosomopathy in MF, and in animal models including *Gata1*^{low} mice, is still unknown. It has been suggested that it is represented by aurora kinases since their inhibition increase GATA1 in the MK while reducing fibrosis in animal models and in MF patients (Wen et al., 2025).

Although *Gata1*^{low} mice do not carry any of the MF driver mutations, are considered a bona fide animal model of MF because their HSC express an activated TPO/MPL axis, which may be drugged by JAK inhibitors, and a RSP14 ribosomopathy, which is responsible for low GATA1 content and altered MK maturation and P-SEL expression. In turn, altered P-SEL expression on the MK is responsible for the pathological cell interaction that increase the bioavailability of pro-inflammatory cytokines and drives fibrosis. Over the years we, and others (Corey et al., 2018; Kramer et al., 2020; Leiva et al., 2019), have extensively used *Gata1*^{low} mice as a tool to identify lesions which may be targeted to normalize their myelofibrosis phenotype. Based on previous observations indicating that deletion of P-sel prevents *Gata1*^{low} mice for developing myelofibrosis (Spangrude et al., 2016), we establish here whether inhibition of P-SEL, alone or in combination with Rux, may also normalize the phenotype of *Gata1*^{low} mice that have already established myelofibrosis. A summary of the results is presented in **Table S2**.

We first demonstrated that after short term-treatment, RB40.34 is bound to the platelets and the MK from the BM of *Gata1*^{low} mice, suggesting that the drug is retained in the circulation for at least 5h and that, in spite of fibrosis, reaches the BM of the animals. We also found that after 5 days, RB40.34 in combination with Rux normalizes non only the abnormal non-canonical TGF- β signals, which is a signature of a pro-fibrotic microenvironment, but also the abnormal canonical TGF- β signature, which indicates reduced hematopoiesis in the BM. These data suggests that after only 5 days the combination of RB40.34 and Rux is more effective than any of the two drugs alone in suppressing the cells responsible for fibrosis while reactivating hematopoiesis in the BM. The drug combination was also more effective than the two drugs as single agent in reducing JAK2 in the spleen from the mutant mice, suggesting that it is reducing extramedullary hematopoiesis in this organ.

Encouraged by these results, we analyzed the effects of long-term treatments with RB40.34 and Rux, alone or in combination, on the myelofibrotic phenotype expressed by *Gata1*^{low} mice using a vast range of clinically relevant end points. The results indicate that none of the treatments induce anemia nor rescue the thrombocytopenia of *Gata1*^{low} mice. However, treatment for 54 days with RB40.34 in combination with Rux, and to a less extent the two drugs alone, reduced anisocytosis, expression of P-SEL on MK, and probably on endothelial cells, and lymphocyte counts. Since the iron metabolism of

old *Gata1*^{low} mice is normal (Stefano Rivella, unpublished observation) and the mean corpuscular volume and Hb content of the RBC remain within normal values in all the treated mice (**Table S3**), it is unlikely that the high RDW detected in *Gata1*^{low} mice is a sign of impaired iron metabolism. Anisocytosis without raises in mean corpuscular volume is induced by pro-inflammatory cytokines in several benign and malignant disorders, including MF where it has been proposed as a marker that predict inferior survival (Corey et al., 2018). We hypothesize that the reduction in anisocytosis observed at day 54 in the RB40.34 alone or in combination with Rux groups reflects reductions in the proinflammatory cytokines TGF- β and/or CXCL1 that drives myelofibrosis in this model. Since TGF- β and CXCL1 are well known to affect directly (TGF- β) or indirectly (through neutrophil activation, CXCL1) lymphocyte counts (Bommireddy et al., 2003; Batle and Massagué, 2019; Mukaida, 2000; Palomino and Marti, 2015), this hypothesis is also consistent with the reduced lymphocyte counts observed by day 54 in the mice treated with the two drugs in combination. Reduction in microenvironment bioavailability of pro-inflammatory cytokines was directly tested by showing that RB40.34 and Rux in combination significantly reduces the TGF- β and CXCL1 content of the BM.

Finally, treatment for 54 days with RB40.34 in combination with Rux also reduced fibrosis in BM and spleen while improving effective hematopoiesis in BM and reducing extramedullary hematopoiesis restoring the architecture of the spleen.

Treatments for 54 days with RB40.34 and Rux, alone or in combination, were ineffective in reducing the proliferation of the MK which may be driven in our model, as well as in the patients, by the activated TPO/Mpl axis. They were, however, all effective in improving the maturation profile of the MK, including reducing the abnormally high level of cell surface expression of P-SEL and TGF- β content. RB40.34 and Rux alone were also effective in increasing the GATA1 content in a proportion of CD42b^{pos} MK. The mechanistic interpretation of these data is complicated by the recent single cell profiling indicating that murine (and human) BM contains four distinctive MK subpopulations, each one exerting a different function (Sun et al., 2021; Pariser et al., 2021; Wang et al., 2021; Yeung et al., 2020). The BM of adult mice and men contains at least three subpopulations: the platelet producing MK, the niche supportive MK, and the immune MK. Only platelet producing MK have the morphology of mature MK. Niche supportive MK and immune MK have instead the morphology of immature MK. In addition, by characterizing the MK subpopulations present in the embryos, Wang et al (Wang et al., 2021) identified a fourth subpopulation, which they defined niche-poised-MK that has an immature morphology and is characterized by high expression of extracellular matrix genes such as COL1A1, COL3A1, and COL6A2 and enrichment of the “response to TGF β signature”, which indicate that this subpopulation is sustained by TGF- β . Of interest for this paper, reduced GATA1 content blocks the maturation of platelet producing MK but not favors the maturation of the other three subpopulations (Pariser et al., 2021; Sun et al., 2021; Wang et al., 2021; Yeung et al., 2020). This new knowledge indicates that the nature of the immature *Gata1*^{low} MK found in great numbers in MF is presently not

known. Preliminary observations indicating that great numbers of the morphologically immature MKs in the BM from *Gata1*^{low} mice, as well as that of MF patients, express collagen (Abbonante et al., 2016; Malara et al., 2014) suggests that at least some of these MK are represented by niche poised MK the maturation of which is reactivated by TGF- β (Zingariello et al., 2013). It is, therefore, possible, that low levels of GATA1 drive the disease not only by retaining platelet forming MK immature (leading to the thrombocytopenia), but also by increasing the frequency of other megakaryocyte subtypes. According to this hypothesis, although RB40.34 and Rux in combination did not induce detectable increase in GATA1 content in MK (and did not increased platelet counts), it reduced the frequency of MK containing TGF- β , which may correspond to niche supporting MK. Reduced TGF- β bioavailability may have then limit the number of niche MK, which are sustained by this growth factors and are responsible for. On the other hand, Rux alone, which induced the greater increase of GATA1 in MK, also reduced the TGF- β containing MK but did not altered fibrosis, suggesting that the number of MK expressing collagen was not significantly affected. These data support the need of further studies, clearly outside the purpose of the current manuscript, to clarify the MK subpopulations which are altered in MF, which of them is responsible for the different traits of the myelofibrosis phenotype and how they are affected by RB40.34 and Rux alone or in combination.

In conclusion, these data provide pre-clinical evidence that treatment with the RB40.34 antibody in combination with Rux is more effective than the use of Rux alone for reverting the myelofibrotic trait in the *Gata1*^{low} mouse model and encourage clinical studies to validate the effects of Crizanlizumab, in combination with Rux, for the treatment of human PMF.

Conflict of interest. PV, FG, FM, MF, AV, GS and MZ declare no conflict. CW, AB and AP are employee of Novartis Pharmaceutical Corporation. ARM received research funds from Novartis Pharmaceutical Corporation.

Author contributions. PV, FG, FM, MF, FA and AV performed experiments and analyzed the data. PV and FG performed statistical analyses. GS reviewed all the histopathological determinations. ARM and MZ designed the study, interpreted the data and wrote the manuscript. CW, AB and AP revised the data and wrote the manuscript. All the authors read the manuscript and concur with its content.

Data Availability Statement. The individual data for each mouse are available on request. 8 Disclosure The content of the manuscript was presented as a poster at the 62rd ASH Annual Meeting & Exposition (Paola Verachi, Fabrizio Martelli, Maria Zingariello, Shalini Chaturvedi, Celine Wilke, Valerie Campello-Iddison, Anna Rita Migliaccio; Preclinical Rationale for the Use of Crizanlizumab (SEG101) in Myelofibrosis. Blood 2020; 136 (Supplement 1): 26–27. doi: <https://doi.org/10.1182/blood-2020-133896>). The data are unpublished and have not been submitted for publication to any other journal.

Funding. This study was supported by grants from the National Cancer Institute (P01-CA108671), the National Heart, Lung and Blood Institute (1R01-HL134684), Associazione Italiana Ricerca Cancro (AIRC, IG23525) and by Novartis Pharmaceutical Corporation.

Acknowledgments. The technical support of Mrs. Yvan Gilardi, Enrico Cardarelli and Andrea Giovannelli, of the Center for animal experimentation and well-being, Istituto Superiore di Sanità, Rome, Italy and the editorial assistance of Dr. Gisella Gaspari, Università Campus Biomedico, Rome, Italy, are gratefully acknowledged.

5. References

- Abbonante, V., Di Buduo, C.A., Gruppi, C., Malara, A., Gianelli, U., Celesti, G., Anselmo, A., Laghi, L., Vercellino, M., Visai, L., Iurlo, A., Moratti, R., Barosi, G., Rosti, V., Balduini, A. (2016). Thrombopoietin/TGF- β 1 Loop Regulates Megakaryocyte Extracellular Matrix Component Synthesis. *Stem Cells*, 34:1123–33. <https://doi.org/10.1002/stem.2285>.
- Ataga, K.I., Kutlar, A., Kanter, J., Liles, D., Cancado, R., Friedrisch, J., Guthrie, T.H., Knight-Madden, J., Alvarez, O.A., Gordeuk, V.R., Gualandro, S., Colella, M.P., Smith, W.R., Rollins, S.A., Stocker, J.W., Rother, R.P. (2017). Crizanlizumab for the Prevention of Pain Crises in Sickle Cell Disease. *New England Journal of Medicine*, 376:429–39. <https://doi.org/10.1056/NEJMoa1611770>.
- Barbui, T., Tefferi, A., Vannucchi, A.M., Passamonti, F., Silver, R.T., Hoffman, R., Verstovsek, S., Mesa, R., Kiladjan, J.J., Hehlmann, R., Reiter, A., Cervantes, F., Harrison, C., Mc Mullin, M.F., Hasselbalch, H.C., Koschmieder, S., Marchetti, M., Bacigalupo, A., Finazzi, G., Kroeger, N., Griesshammer, M., Birgegard, G., Barosi, G. (2018). Philadelphia chromosomenegative classical myeloproliferative neoplasms: revised management recommendations from European LeukemiaNet. *Leukemia*, 32:1057–69. <https://doi.org/10.1038/s41375-018-0077-1>.
- Battle, E., Massagué, J. (2019). Transforming growth factor- β signaling in immunity and cancer. *Immunity*, 50(4), 924–940. <https://doi.org/10.1016/j.immuni.2019.03.024>.
- Bommireddy, R., Saxena, V., Ormsby, I., Yin, M., Boivin, G.P., Babcock, G.F., Singh, R.R., Doetschman, T. (2003). TGF- β 1 regulates lymphocyte homeostasis by preventing activation and subsequent apoptosis of peripheral lymphocytes. *Journal of Immunology*, 170:4612–22. <https://doi.org/10.4049/jimmunol.170.9.4612>.
- Campanelli, R., Rosti, V., Villani, L., Castagno, M., Moretti, E., Bonetti, E., Bergamaschi, G., Balduini, A., Barosi, G., Massa, M. (2011). Evaluation of the bioactive and total transforming growth factor β 1 levels in primary myelofibrosis. *Cytokine*, 53(1), 100–106. <https://doi.org/10.1016/j.cyto.2010.07.427>.
- Centurione, L., Di Baldassarre, A., Zingariello, M., Bosco, D., Gatta, V., Rana, R.A., Langella, V., Di Virgilio, A., Vannucchi, A.M., Migliaccio, A.R. (2004). Increased and pathologic emperipolesis of neutrophils within megakaryocytes associated with marrow fibrosis in *Gata1*^{low} mice. *Blood*, 104(12), 3573–3580. <https://doi.org/10.1182/blood-2004-01-0193>.

- Ceglia, I., Dueck, A.C., Masiello, F., Martelli, F., He, W., Federici, G., Petricoin, E.F. 3rd, Zeuner, A., Iancu-Rubin, C., Weinberg, R., Hoffman, R., Mascarenhas, J., Migliaccio, A.R. (2016). Preclinical rationale for TGF- β inhibition as a therapeutic target for the treatment of myelofibrosis. *Experimental Hematology*, 44:1138-55. <https://doi.org/10.1016/j.exphem.2016.08.007>.
- Chagraoui, H., Komura, E., Tulliez, M., Giraudier, S., Vainchenker, W., Wendling, F. (2002). Prominent role of TGF- β 1 in thrombopoietin-induced myelofibrosis in mice. *Blood*, 100:3495–503. <https://doi.org/10.1182/blood-2002-04-1133>.
- Ciurea, S.O., Merchant, D., Mahmud, N., Ishii, T., Zhao, Y., Hu, W., Bruno, E., Barosi, G., Xu, M., Hoffman, R. (2007). Pivotal contributions of megakaryocytes to the biology of idiopathic myelofibrosis. *Blood*, 110:986–93. <https://doi.org/10.1182/blood-2006-12-064626>.
- Corey, S.J., Jha, J., McCart, E.A., Rittase, W.B., George, J., Mattapallil, J.J., Mehta, H., Ognoon, M., Bylicky, M.A., Summers, T.A., Day, R.M. (2018). Captopril mitigates splenomegaly and myelofibrosis in the *Gata1*^{low} murine model of myelofibrosis. *Journal of Cellular and Molecular Medicine*, 22:4274–82. <https://doi.org/10.1111/jcmm.13710>.
- Crispino, J.D., Weiss, M.J. (2014). Erythro-megakaryocytic transcription factors associated with hereditary anemia. *Blood*, 123:3080–8. <https://doi.org/10.1182/blood-2014-01-453167>.
- Dunbar, A.J., Rampal, R.K., Levine, R. (2020). Leukemia secondary to myeloproliferative neoplasms. *Blood*, 136:61–70. <https://doi.org/10.1182/blood.2019000943>.
- Emadi, S., Clay, D., Desterke, C., Guerton, B., Maquarre, E., Charpentier, A. (2005). IL-8 and its CXCR1 and CXCR2 receptors participate in the control of megakaryocytic proliferation, differentiation, and ploidy in myeloid metaplasia with myelofibrosis. *Blood*, 105, 464. <https://doi.org/10.1182/blood-2003-12-4415>.
- Embury, S.H., Matsui, N.M., Ramanujam, S., Mayadas, T.N., Noguchi, C.T., Diwan, B.A., Mohandas, N., Cheung, A.T. (2004). The contribution of endothelial cell P-selectin to the microvascular flow of mouse sickle erythrocytes in vivo. *Blood*, 104:3378–85. <https://doi.org/10.1182/blood-2004-02-0713>.
- Evangelista, V., Manarini, S., Sideri, R., Rotondo, S., Martelli, N., Piccoli, A., Totani, L., Piccardoni, P., Vestweber, D., de Gaetano, G., Cerletti, C. (1999). Platelet/polymorphonuclear leukocyte interaction: P-selectin triggers protein-tyrosine phosphorylation-dependent CD11b/CD18 adhesion: role of PSGL-1 as a signaling molecule. *Blood*, 93:876–85. <https://doi.org/10.1182/blood.V93.3.876>.
- Fletcher, K., Myant, N.B. (1960). Biotin in the Synthesis of Fatty Acid and Cholesterol by Mammalian Liver. *Nature*, 188:585. <https://doi.org/10.1038/188585a0>.
- Foreman, K.E., Vaporciyan, A.A., Bonish, B.K., Jones, M.L., Johnson, K.J., Glovsky, M.M., Eddy, S.M., Ward, P.A. (1994). C5a-induced expression of P-selectin in endothelial cells. *Journal of Clinical Investigation*, 94:1147–55. <https://doi.org/10.1172/JCI117430>.
- Garimella, R., Kacena, M.A., Tague, S.E., Wang, J., Horowitz, M.C., Anderson, H.C. (2007). Expression of bone morphogenetic proteins and their receptors in the bone marrow megakaryocytes of GATA-1^{low} mice: a

possible role in osteosclerosis. *Journal of Histochemistry & Cytochemistry*, 55:745–52. <https://doi.org/10.1369/jhc.6A7164.2007>.

Gastinne, T., Vigant, F., Lavenu-Bombled, C., Wagner-Ballon, O., Tulliez, M., Chagraoui, H., Villeval, J.L., Lacout, C., Perricaudet, M., Vainchenker, W., Benihoud, K., Giraudier, S. (2007). Adenoviral-mediated TGF- β 1 inhibition in a mouse model of myelofibrosis inhibit bone marrow fibrosis development. *Experimental Hematology*, 35:64–74. <https://doi.org/10.1016/j.exphem.2006.08.016>.

Gerds, A.T., Vannucchi, A.M., Passamonti, F., Kremyanskaya, M., Gotlib, J., Palmer, J.M., McCaul, K., Ribrag, V., Mead, A.J., Harrison, C., Mesa, R., Kiladjian, J.J., Barosi, G., Gerike, T.G., Shetty, J.K., Pariseau, J., Miranda, G., Schwickart, M., Giuseppi, A.C., Zhang, J., Backstrom, J.T., Verstovsek, S. (2020). Duration of response to luspatercept in patients (pts) requiring red blood cell (RBC) transfusions with myelofibrosis (MF) – updated data from the phase 2 ACE-536-MF-001 Study. *Blood*, 136 (Supplement 1): 47–48. <https://doi.org/10.1182/blood-2020-137265>.

Ghinassi, B., Sanchez, M., Martelli, F., Amabile, G., Vannucchi, A.M., Migliaccio, G., Orkin, S.H., Migliaccio, A.R. (2007). The hypomorphic *Gata1*^{low} mutation alters the proliferation/differentiation potential of the common megakaryocytic-erythroid progenitor. *Blood*, 109(4), 1460–1471. <https://doi.org/10.1182/blood-2006-07-030726>.

Gilles, L., Arslan, A.D., Marinaccio, C., Wen, Q.J., Arya, P., McNulty, M., Yang, Q., Zhao, J.C., Konstantinoff, K., Lasho, T., Pardanani, A., Stein, B., Plo, I., Sundaravel, S., Wickrema, A., Migliaccio, A., Gurbuxani, S., Vainchenker, W., Plataniias, L.C., Tefferi, A., Crispino, J.D. (2017). Downregulation of GATA1 drives impaired hematopoiesis in primary myelofibrosis. *Journal of Clinical Investigation*, 127(4), 1316–1320. <https://doi.org/10.1172/jci82905>.

Jeremy, W.Q., Yang, Q., Goldenson, B., Malinge, S., Lasho, T., Schneider, R.K., Breyfogle, L.J., Schultz, R., Gilles, L., Koppikar, P., Abdel-Wahab, O., Pardanani, A., Stein, B., Gurbuxani, S., Mullally, A., Levine, R.L., Tefferi, A., Crispino, J.D. (2015). Targeting megakaryocyte-induced fibrosis in myeloproliferative neoplasms by AURKA inhibition. *Nature Medicine*, 21:1473–80. <https://doi.org/10.1038/nm.3995>.

Kacena, M.A., Shivdasani, R.A., Wilson, K., Xi, Y., Troiano, N., Nazarian, A., Gundberg, C.M., Bouxsein, M.L., Lorenzo, J.A., Horowitz, M.C. (2004). Megakaryocyte-osteoblast interaction revealed in mice deficient in transcription factors GATA-1 and NF-E2. *Journal of Bone and Mineral Research*, 19(4), 652–660. <https://doi.org/10.1359/JBMR.0301254>.

Karagianni, A., Ravid, K. (2022). Myeloproliferative Disorders and its Effect on Bone Homeostasis: The Role of Megakaryocytes. *Blood*, 139, 3127–3137. <https://doi.org/10.1182/blood.2021011480>.

Kramer, F., Dervedde, J., Mezheyski, A., Tauber, R., Micke, P., Kappert, K. (2020). Platelet-derived growth factor receptor β activation and regulation in murine myelofibrosis. *Haematologica*, 105:2083–94. <https://doi.org/10.3324/haematol.2019.226332>.

- Leiva, O., Ng, S.K., Matsuura, S., Chitalia, V., Lucero, H., Findlay, A., Turner, C., Jarolimek, W., Ravid, K. (2019). Novel lysyl oxidase inhibitors attenuate hallmarks of primary myelofibrosis in mice. *International Journal of Hematology*, 110:699–708. <https://doi.org/10.1007/s12185-019-02751-6>.
- Li, L., Kim, J.H., Lu, W., Williams, D.M., Kim, J., Cope, L., Rampal, R.K., Koche, R.P., Xian, L., Luo, L.Z., Vasiljevic, M., Matson, D.R., Zhao, Z.J., Rogers, O., Stubbs, M.C., Reddy, K., Romero, A.R., Psaila, B., Spivak, J.L., Moliterno, A.R., Resar, L.M.S. (2022). HMGA1 chromatin regulators induce transcriptional networks involved in GATA2 and proliferation during MPN progression. *Blood*, 139:2797–815. <https://doi.org/10.1182/blood.2021013925>.
- Lucijanac, M., Pejisa, V., Jaksic, O., Mitrovic, Z., Tomasovic-Loncaric, C., Stoos-Veic, T., Prka, Z., Pirsic, M., Haris, V., Vasilj, T., Kusec, R. (2016). The degree of anisocytosis predicts survival in patients with primary myelofibrosis. *Acta Haematologica*, 136:98–100. <https://doi.org/10.1159/000445247>.
- Malara, A., Abbonante, V., Zingariello, M., Migliaccio, A., Balduini, A. (2018). Megakaryocyte contribution to bone marrow fibrosis: many arrows in the quiver. *Mediterranean Journal of Hematology and Infectious Diseases*, 10:e2018068. <https://doi.org/10.4084/MJHID.2018.068>
- Malara, A., Currao, M., Gruppi, C., Celesti, G., Viarengo, G., Buracchi, C., Laghi, L., Kaplan, D.L., Balduini, A. (2014). Megakaryocytes contribute to the bone marrow-matrix environment by expressing fibronectin, type IV collagen, and laminin. *Stem Cells*, 32(4), 926–937. <https://doi.org/10.1002/stem.1626>.
- Marcellino, B. K., Verstovsek, S., Mascarenhas, J. (2020). The myelodepletive phenotype in myelofibrosis: clinical relevance and therapeutic implication. *Clinical Lymphoma, Myeloma and Leukemia*, 1–7. <https://doi.org/doi:10.1016/j.clml.2020.01.008>.
- Martelli, F., Ghinassi, B., Panetta, B., Alfani, E., Gatta, V., Pancrazzi, A., Bogani, C., Vannucchi, A.M., Paoletti, F., Migliaccio, G., Migliaccio, A.R. (2005). Variegation of the phenotype induced by the *Gata1*^{low} mutation in mice of different genetic backgrounds. *Blood*, 106(13):4102-13. <https://doi.org/10.1182/blood-2005-03-1060>.
- Massagué, J., Blain, S.W., Lo, R.S. (2000). TGF β signaling in growth control, cancer, and heritable disorders. *Cell*, 103:295–309. [https://doi.org/10.1016/s0092-8674\(00\)00121-5](https://doi.org/10.1016/s0092-8674(00)00121-5).
- McDevitt, M.A., Fujiwara, Y., Shivdasani, R.A., Orkin, S.H. (1997). An upstream, DNase I hypersensitive region of the hematopoietic-expressed transcription factor GATA-1 gene confers developmental specificity in transgenic mice. *PNAS*, 94:7976–81. <https://doi.org/10.1073/pnas.94.15.7976>.
- Migliaccio, A.R., Martelli, F., Verrucci, M., Sanchez, M., Valeri, M., Migliaccio, G., Vannucchi, A.M., Zingariello, M., Di Baldassarre, A., Ghinassi, B., Rana, R.A., Van Hensbergen, Y., Fibbe, W.E. (2009). Gata1 expression driven by the alternative HS2 enhancer in the spleen rescues the hematopoietic failure induced by the hypomorphic *Gata1*^{low} mutation. *Blood*, 114(10), 2107–2120. <https://doi.org/10.1182/blood-2009-03-211680>.
- Moore, K.L., Stults, N.L., Diaz, S., Smith, D.F., Cummings, R.D., Varki, A., McEver, R.P. (1992). Identification of a specific glycoprotein ligand for P-selectin (CD62) on myeloid cells. *Journal of Cell Biology*, 118:445–56. <https://doi.org/10.1083/jcb.118.2.445>.

- Oguro, H., Ding, L., Morrison, S.J. (2013). SLAM family markers resolve functionally distinct subpopulations of hematopoietic stem cells and multipotent progenitors. *Cell Stem Cell*, 13:102–16. <https://doi.org/10.1016/j.stem.2013.05.014>.
- Palomino, D.C.T., Marti, L.C. (2015). Chemokines and immunity. *Einstein (São Paulo)*, 13:469–73. <https://doi.org/10.1590/S1679-45082015RB3438>.
- Pariser, D. N., Hilt, Z. T., Ture, S. K., Blick-Nitko, S. K., Looney, M. R., Cleary, S. J., Roman-Pagan, E., Saunders, J. 2nd, Georas, S.N., Veazey, J., Madere, F., Santos, L.T., Arne, A., Huynh, N.P., Livada, A.C., Guerrero-Martin, S.M., Lyons, C., Metcalf-Pate, K.A., McGrath, K.E., Palis, J., Morrell, C.N. (2021). Lung megakaryocytes are immune modulatory cells. *Journal of clinical investigation*, 131(1), e137377. <https://doi.org/10.1172/JCI137377>.
- Perner, F., Perner, C., Ernst, T., Heidel, F.H. (2019). Roles of JAK2 in aging, inflammation, hematopoiesis and malignant transformation. *Cells*, 8: 854-73. <https://doi.org/10.3390/cells8080854>.
- Schmitt, A., Jouault, H., Guichard, J., Wendling, F., Drouin, A., Cramer, E.M. (2000). Pathologic interaction between megakaryocytes and polymorphonuclear leukocytes in myelofibrosis. *Blood*, 96:1342–7. <https://doi.org/10.1182/blood.V96.4.1342.8>.
- Schneider, C.A., Rasband, W.S., Eliceiri, K.W. (2012). NIH Image to ImageJ: 25 years of image analysis. *Nature Methods*, 9:671–5. <https://doi.org/10.1038/nmeth.2089>.
- Spangrude, G.J., Lewandowski, D., Martelli, F., Marra, M., Zingariello, M., Sancillo, L., Rana, R.A., Migliaccio, A.R. (2016). P-Selectin Sustains Extramedullary Hematopoiesis in the *Gata1^{low}* Model of Myelofibrosis. *Stem Cells*, 34(1), 67–82. <https://doi.org/10.1002/stem.2229>.
- Stavnichuk, M., Komarova, S.V. (2022). Megakaryocyte-bone cell interactions: lessons from mouse models of experimental myelofibrosis and related disorders. *American Journal of Physiology-Cell Physiology*, 322:C177–84. <https://doi.org/10.1152/ajpcell.00328.2021>.
- Steiniger, B.S. (2015). Human spleen microanatomy: why mice do not suffice. *Immunology*, 145:334–46. <https://doi.org/10.1111/imm.12469>.
- Sun, S., Jin, C., Si, J., Lei, Y., Chen, K., Cui, Y., Liu, Z., Liu, J., Zhao, M., Zhang, X., Tang, F., Rondina, M.T., Li, Y., Wang, Q.F. (2021). Single-cell analysis of ploidy and the transcriptome reveals functional and spatial divergency in murine megakaryopoiesis. *Blood*, 138(14):1211-1224. <https://doi.org/10.1182/blood.2021010697>.
- Thiele, J., Lorenzen, J., Manich, B., Kvasnicka, H.M., Zirbes, T.K., Fischer, R. (1997). Apoptosis (programmed cell death) in idiopathic (primary) osteo-/myelofibrosis: naked nuclei in megakaryopoiesis reveal features of paraapoptosis. *Acta Haematologica*, 97:137–43. <https://doi.org/10.1159/000203671>.
- Vainchenker, W., Constantinescu, S.N. (2013). JAK/STAT signaling in hematological malignancies. *Oncogene*, 32:2601–13. <https://doi.org/10.1038/onc.2012.347>.

- Vannucchi, A.M., Bianchi, L., Cellai, C., Paoletti, F., Rana, R.A., Lorenzini, R., Migliaccio, G., Migliaccio, A.R. (2002). Development of myelofibrosis in mice genetically impaired for GATA-1 expression (*Gata1*^{low} mice). *Blood*, 100(4), 1123–1132. <https://doi.org/10.1182/blood-2002-06-1913>.
- Vannucchi, A. M., Pancrazzi, A., Guglielmelli, P., Di Lollo, S., Bogani, C., Baroni, G., Bianchi, L., Migliaccio, A.R., Bosi, A., Paoletti, F. (2005). Abnormalities of GATA-1 in megakaryocytes from patients with idiopathic myelofibrosis. *American Journal of Pathology*, 167(3), 849–858. [https://doi.org/10.1016/S0002-9440\(10\)62056-1](https://doi.org/10.1016/S0002-9440(10)62056-1).
- Varricchio, L., Iancu-Rubin, C., Upadhyaya, B., Zingariello, M., Martelli, F., Verachi, P., Clementelli, C., Denis, J.F., Rahman, A.H., Tremblay, G., Mascarenhas, J., Mesa, R. A., O’Connor-McCourt, M., Migliaccio, A.R., Hoffman, R. (2021). TGF- β 1 protein trap AVID200 beneficially affects hematopoiesis and bone marrow fibrosis in myelofibrosis. *JCI Insight*, 6(18). <https://doi.org/10.1172/jci.insight.145651>.
- Verachi, P., Gobbo, F., Martelli, F., Martinelli, A., Sarli, G., Dunbar, A., Levine, R.L., Hoffman, R., Massucci, M.T., Brandolini, L., Giorgio, C., Allegretti, M., Migliaccio, A.R. (2022). The CXCR1/CXCR2 inhibitor reparixin alters the development of myelofibrosis in the *Gata1*^{low} mice. *Frontiers in Oncology*, 12:853484- 98. <https://doi.org/10.3389/fonc.2022.853484>.
- Vyas, P., Ault, K., Jackson, C.W., Orkin, S.H., Shivdasani, R.A. (1999). Consequences of GATA-1 deficiency in megakaryocytes and platelets. *Blood*, 93, 2867–2875.
- Wang, H., He, J., Xu, C., Chen, X., Yang, H., Shi, S., Liu, C., Zeng, Y., Wu, D., Bai, Z., Wang, M., Wen, Y., Su, P., Xia, M., Huang, B., Ma, C., Bian, L., Lan, Y., Cheng, T., Shi, L., Liu, B., Zhou, J. (2021). Decoding human megakaryocyte development. *Cell Stem Cell*, 28(3), 535–549.e8. <https://doi.org/10.1016/j.stem.2020.11.006>.
- Woods, B., Chen, W., Chiu, S., Marinaccio, C., Fu, C., Gu, L., Bulic, M., Yang, Q., Zouak, A., Jia, S., Suraneni, P.K., Xu, K., Levine, R.L., Crispino, J.D., Wen, Q.J. (2019). Activation of JAK/STAT signaling in megakaryocytes sustains myeloproliferation in vivo. *Clinical Cancer Research*, 25:5901–12. <https://doi.org/10.1158/1078-0432.CCR-18-4089>.
- Zahr, A.A., Salama, M.E., Carreau, N., Tremblay, D., Verstovsek, S., Mesa, R., Hoffman, R., Mascarenhas, J. (2016). Bone marrow fibrosis in myelofibrosis: pathogenesis, prognosis and targeted strategies. *Haematologica*, 101(6), 660–671. <https://doi.org/10.3324/haematol.2015.141283>.
- Zetterberg, E., Verrucci, M., Martelli, F., Zingariello, M., Sancillo, L., D’Amore, E., Rana, R.A., Migliaccio, A.R. (2014). Abnormal P-selectin localization during megakaryocyte development determines thrombosis in the *Gata1*^{low} model of myelofibrosis. *Platelets*, 25:539–47. <https://doi.org/10.3109/09537104.2013.840720>.
- Zhang, Y., Lin, C.H.S., Kaushansky, K., Zhan, H. (2018). JAK2^{V617F} Megakaryocytes promote hematopoietic stem/progenitor cell expansion in mice through Thrombopoietin/MPL signaling. *Stem Cells*, 36:1676–84. <https://doi.org/10.1002/stem.2888>.
- Zingariello, M., Martelli, F., Ciaffoni, F., Masiello, F., Ghinassi, B., D’Amore, E., Massa, M., Barosi, G., Sancillo, L., Li, X., Goldberg, J. D., Rana, R. A., & Migliaccio, A. R. (2013). Characterization of the TGF- β 1

signaling abnormalities in the *Gata1*^{low} mouse model of myelofibrosis. *Blood*, 121(17), 3345–3363. <https://doi.org/10.1182/blood-2012-06-439661>.

Zingariello, M., Ruggeri, A., Martelli, F., Marra, M., Sancillo, L., Ceglia, I., Rana, R.A., Migliaccio, A.R. (2015). A novel interaction between megakaryocytes and activated fibrocytes increases TGF- β bioavailability in the *Gata1*^{low} mouse model of myelofibrosis. *American Journal of Blood Research*, 5(2), 34–61.

Zingariello, M., Sancillo, L., Martelli, F., Ciaffoni, F., Marra, M., Varricchio, L., Rana, R.A., Zhao, C., Crispino, J.D., Migliaccio, A.R. (2017). The thrombopoietin/MPL axis is activated in the *Gata1*^{low} mouse model of myelofibrosis and is associated with a defective RPS14 signature. *Blood Cancer Journal*, 7(6), 1–11. <https://doi.org/10.1038/bcj.2017.51>.

Zingariello, M., Verachi, P., Gobbo, F., Martelli, F., Falchi, M., Mazzarini, M., Valeri, M., Sarli, G., Marinaccio, C., Melo-Cardenas, J., Crispino, J.D., Migliaccio, A.R. (2022). Resident self-tissue of proinflammatory cytokines rather than their systemic levels correlates with development of myelofibrosis in *Gata1*^{low} mice. *Biomolecules*, 12: 234-60. <https://doi.org/10.3390/biom12020234>.

6. Supplementary Figures

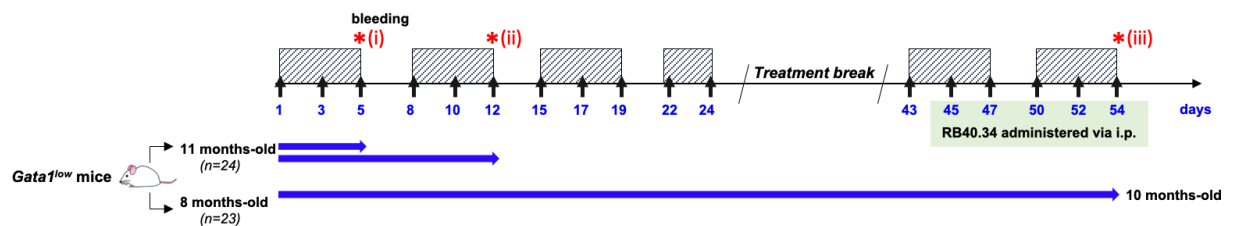
Treatment scheme

Group 1 (n=11): Vehicle (2% v/v DMSO in H₂O) 

Group 2 (n=12): mAb RB40.34 (30 μ g/mouse/day) by tail vein injection 

Group 3 (n=12): Ruxolitinib (45mg/Kg twice per day by gavage) 

Group 4 (n=12): mAb RB40.34 combined with Ruxolitinib  



* End points:

(i) **Day 5:** Body weight, blood parameters, presence of mAb RB40.34 on platelets, total BM cellularity (bones plus medulla), spleen cellularity and weight, presence of the mAb RB40.34 on MKs from BM and spleen; signaling studies: canonical (TGF- β receptor II, SMAD2/3 and pSMAD2/3) and non-canonical (p38, p-p38, ERK1/2 and pERK1/2) TGF- β signaling, JAK2 (JAK2 and STAT5) signaling.

(ii) **Day 12:** Blood parameters, body weight; total BM cellularity, spleen cellularity and weight, presence of mAb RB40.34 on MK from bone marrow and spleen; histological analyses: hematoxylin/Eosin on BM and spleen for overall cellular architecture; Gomori silver staining on BM and spleen; immunohistochemistry for TGF- β on BM.

(iii) **Day 54:** Overall survival, body weight, blood parameters, P-sel expression and response to thrombin of platelets; total BM cellularity (bones plus medulla), spleen weight, presence of the mAb RB40.34 on MK from BM and spleen; histological analyses: hematoxylin/Eosin on BM and spleen; Reticulin staining on BM and spleen; immunohistochemistry for TGF- β and CXCL1 on BM; immunofluorescence for GATA1 in megakaryocytes on BM; overall spleen architecture by confocal microscopy with CD3 and CD45R/B220.

Figure S1. Scheme of the treatments. The study involved 47 *Gata1*^{low} mice divided into two experimental groups. In the first experiment, 11-month-old *Gata1*^{low} mice ($n = 24$) were divided into four treatment groups. Three mice per group were treated for 5 days and sacrificed on day 5, whereas the other mice were treated for 7 additional days and sacrificed on day 12. In the second experiment, 8-month-old *Gata1*^{low} mice ($n = 23$) were divided into four groups and treated as described for 54 days with 2 weeks of break in between until they reached 10 months of age. Black arrows indicate the day of the administrations with the antibody RB40.34, whereas gray boxes indicate the cycles of treatment with Rux or vehicle. Red asterisks indicate the day when mice were sacrificed and their organs harvested for end-point evaluations (days 5 (i), 12 (ii), and 54 (iii), respectively). End points analyzed at each time point are also indicated. *BM*=bone marrow.

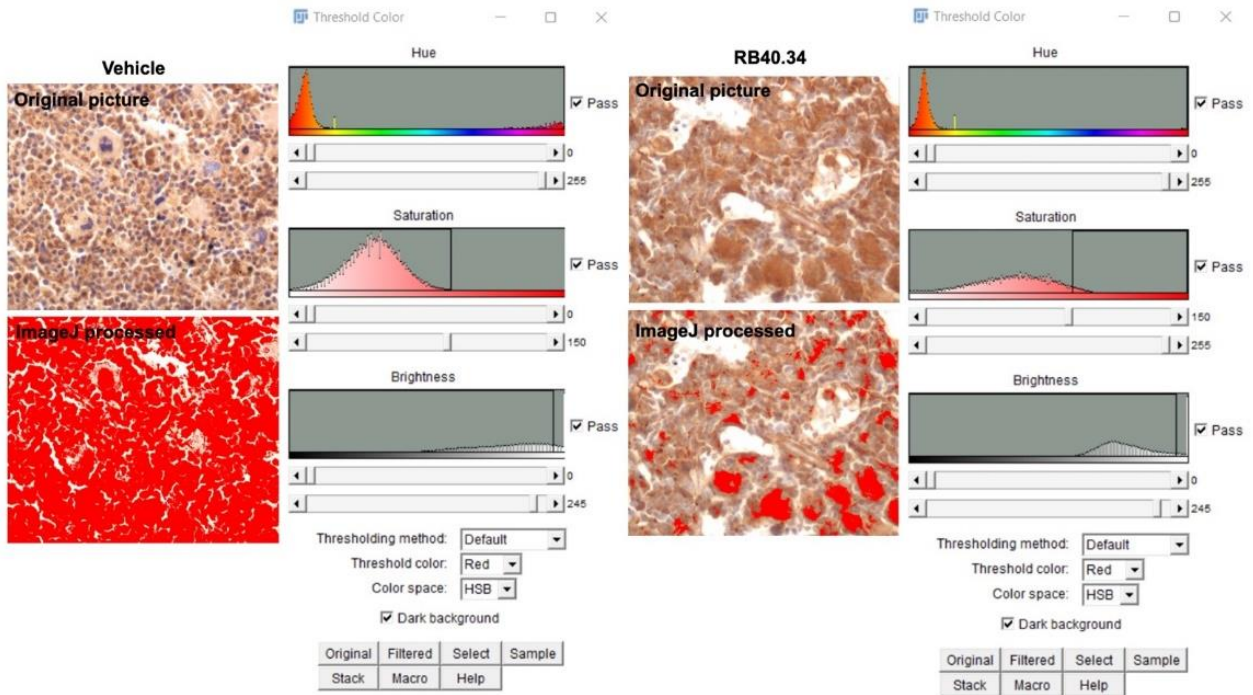


Figure S2. Computer-assisted image analysis used for assessing the binding of RB40.34 antibody to the megakaryocytes of the bone marrow of mice treated with RB40.34. Using ImageJ program, we first determined the level of the endogenous biotin signal above the background in the bone marrow sections from the vehicle group (saturation histogram). This level was considered as a threshold in the evaluation of the biotin signal in the RB40.34-treated mice. We then identified the areas of the bone marrow sections from the RB40.34-treated mice in which the biotin signal was greater than the threshold (brightness histogram) using ImageJ program, and had the computer artificially paint those areas in red. Magnification, 400X.

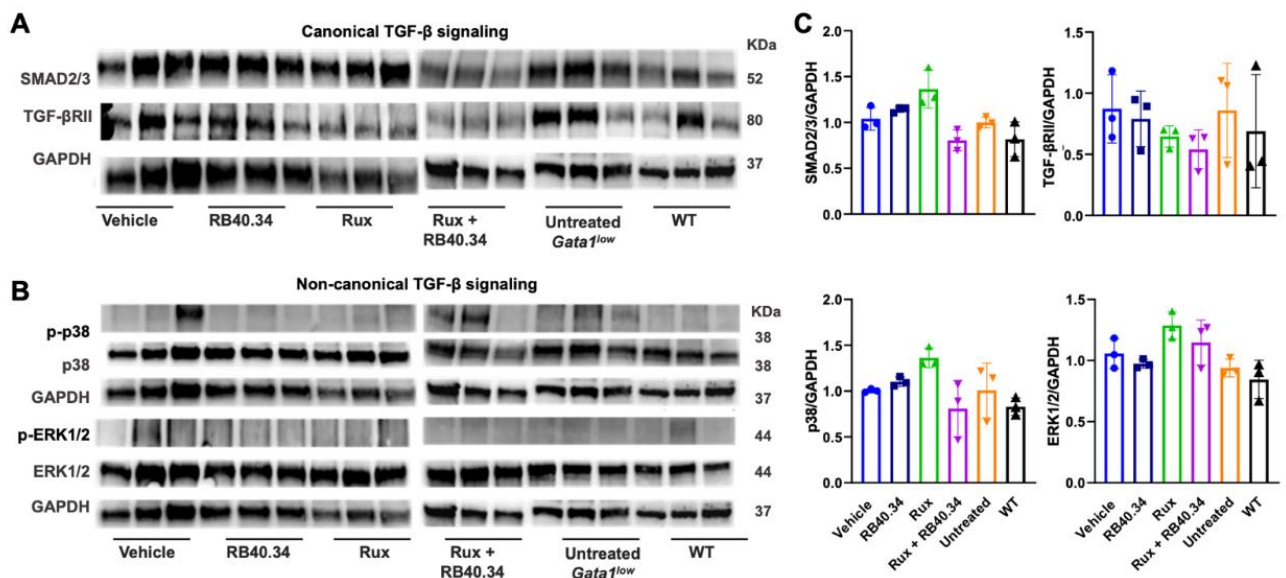


Figure S3. None of the treatments induced significant changes in canonical and noncanonical TGF- β signaling in the spleen of *Gata1*^{low} mice. (A,B) Original western blot determinations of the content of elements downstream to the canonical and noncanonical TGF- β signaling from the spleen of *Gata1*^{low} mice treated with vehicle, RB40.34, Rux, or the two drugs in combination, as indicated. Each line represents one mouse, with three mice per experimental group (in the same order as in Figure 2A, B). GAPDH was used as the loading control. (C) Levels of proteins analyzed in (A, B) normalized for the corresponding GAPDH levels. Values are presented as mean (\pm SD) of values observed with multiple mice and in individual

mice and were compared using Tukey's multiple comparison test. The data are not significantly different among groups. *GADPH*=glyceraldehyde-3-phosphate dehydrogenase *WT*=wild type.

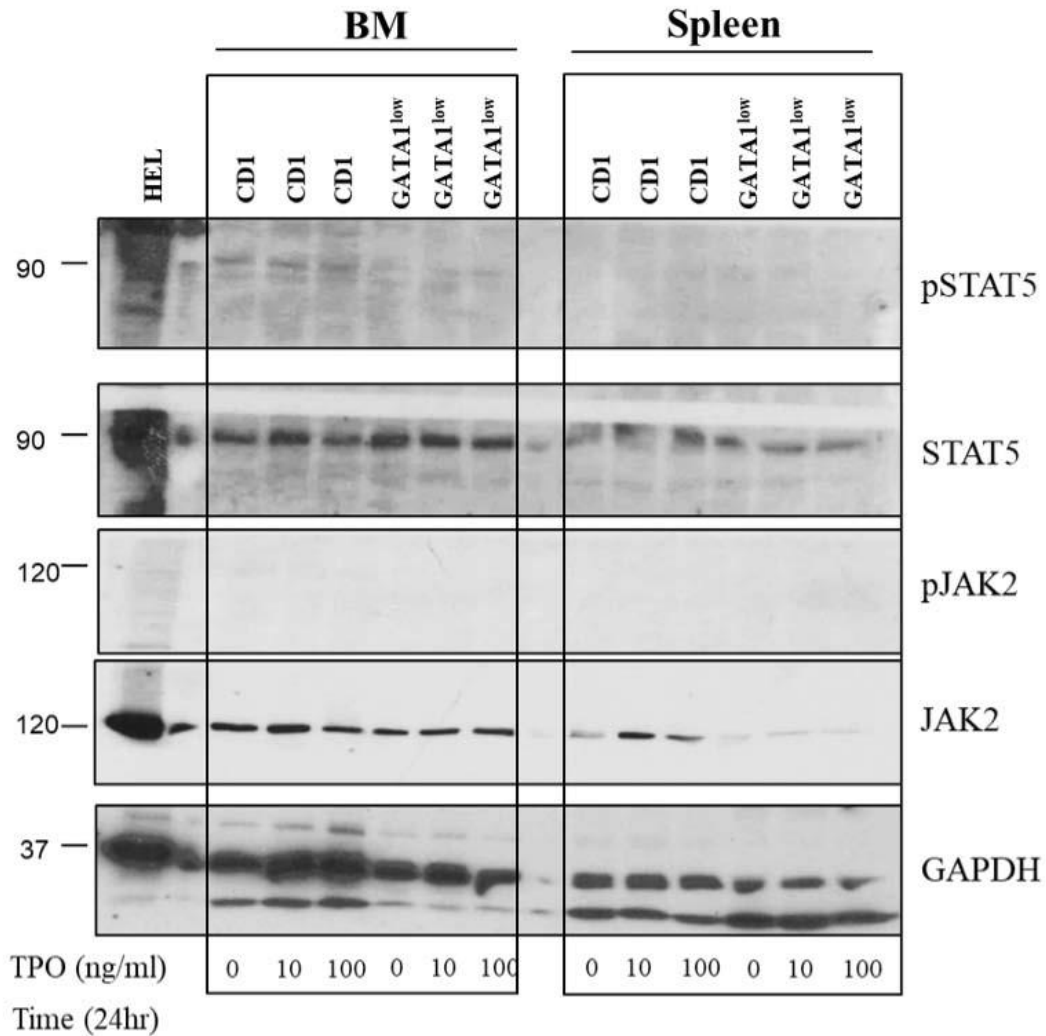


Figure S4. JAK2 and STA5 phosphorylation are barely detectable with thawed lysates of primary bone marrow cells from CD1 and *Gata1*^{low} mice even when these cells had been treated for 24 hours with 10 and 100 ng/mL of thrombopoietin. *TPO*=thrombopoietin.

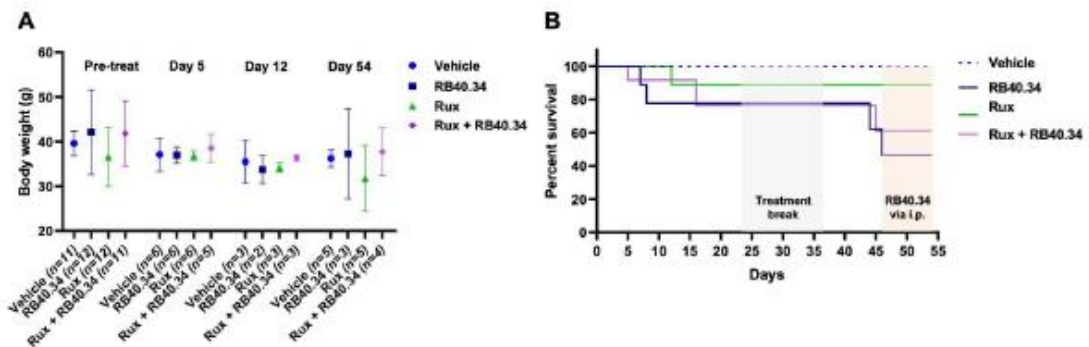


Figure S5. None of the drugs investigated induces significant changes in body weight and survival in *Gata1*^{low} mice treated for up to 54 days. **(A)** Body weight determinations of *Gata1*^{low} mice before (pretreat) and after treatment for 5, 12, and 54 days. Data are presented as mean (\pm SD) and are not statistically significant among groups using Tukey's multiple comparison test. The number of mice included in each group is indicated by *n*. **(B)** Kaplan–Meier survival curves of

Gata1^{low} mice treated with vehicle (dotted line, blue), RB40.34 alone (dark blue), Rux alone (green), or the two drugs in combination (lilac), as indicated. Mice sacrificed on days 5 ($n=12$) and 12 ($n=12$) were considered censored observations. The shaded vertical lines indicate the treatment break due to the holiday season and the change of RB40.34 administration from IV to IP, due to suspected mice intolerance to IV administration. The survival curves of the four groups are not statistically different by log-rank (Mantel–Cox) test.

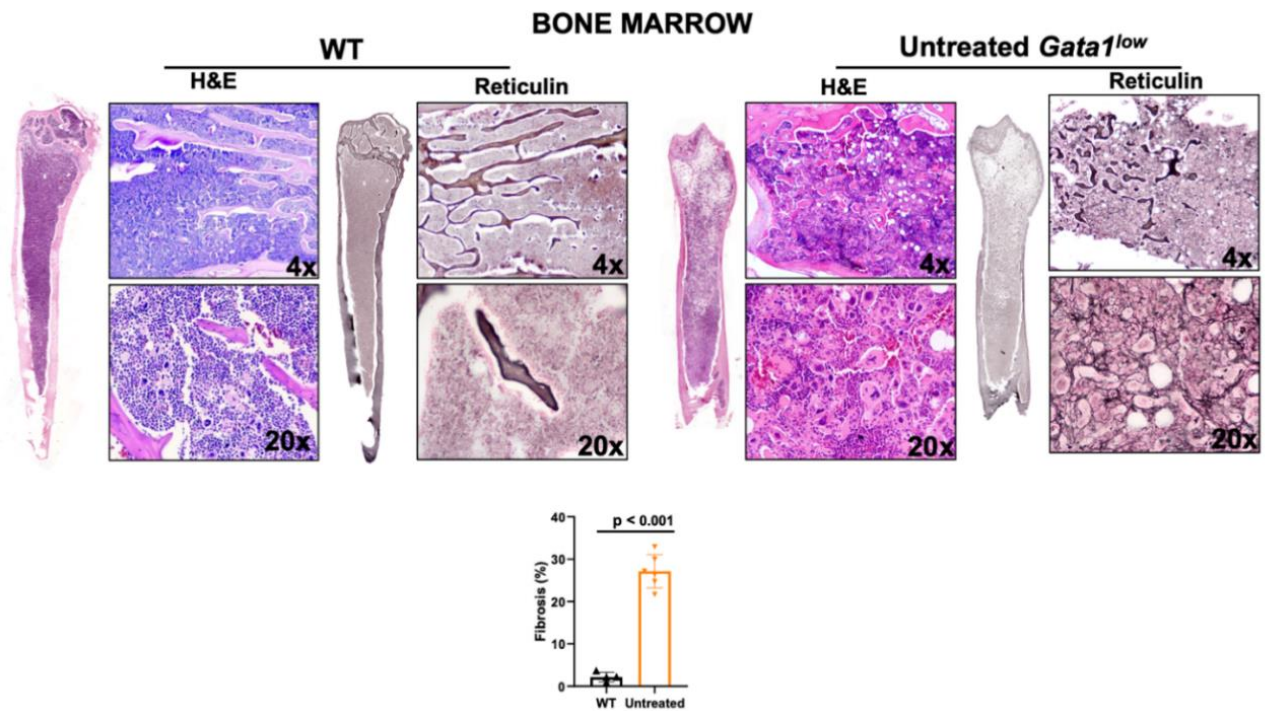


Figure S6. The femur of untreated *Gata1*^{low} mice contains fewer cells and greater levels of fibrosis than that of wild-type (WT) littermates. **(A)** Hematoxylin and eosin (H&E) and reticulin staining of sections from the femur of representative untreated 8-to 11-month-old *Gata1*^{low} and WT littermates, as indicated. The entire femur is presented as stack images (at 4×) and as detail at 4 × and 20 × magnification. **(B)** Levels of fibrosis quantified by image analyses of the reticulin staining of BM sections from untreated WT and *Gata1*^{low} littermates, as indicated. Results are presented as mean (±SD) and as values per individual mice (each symbol a mouse) and were analyzed by *t* test. The difference in the level of fibrosis between the two groups is statistically significant.

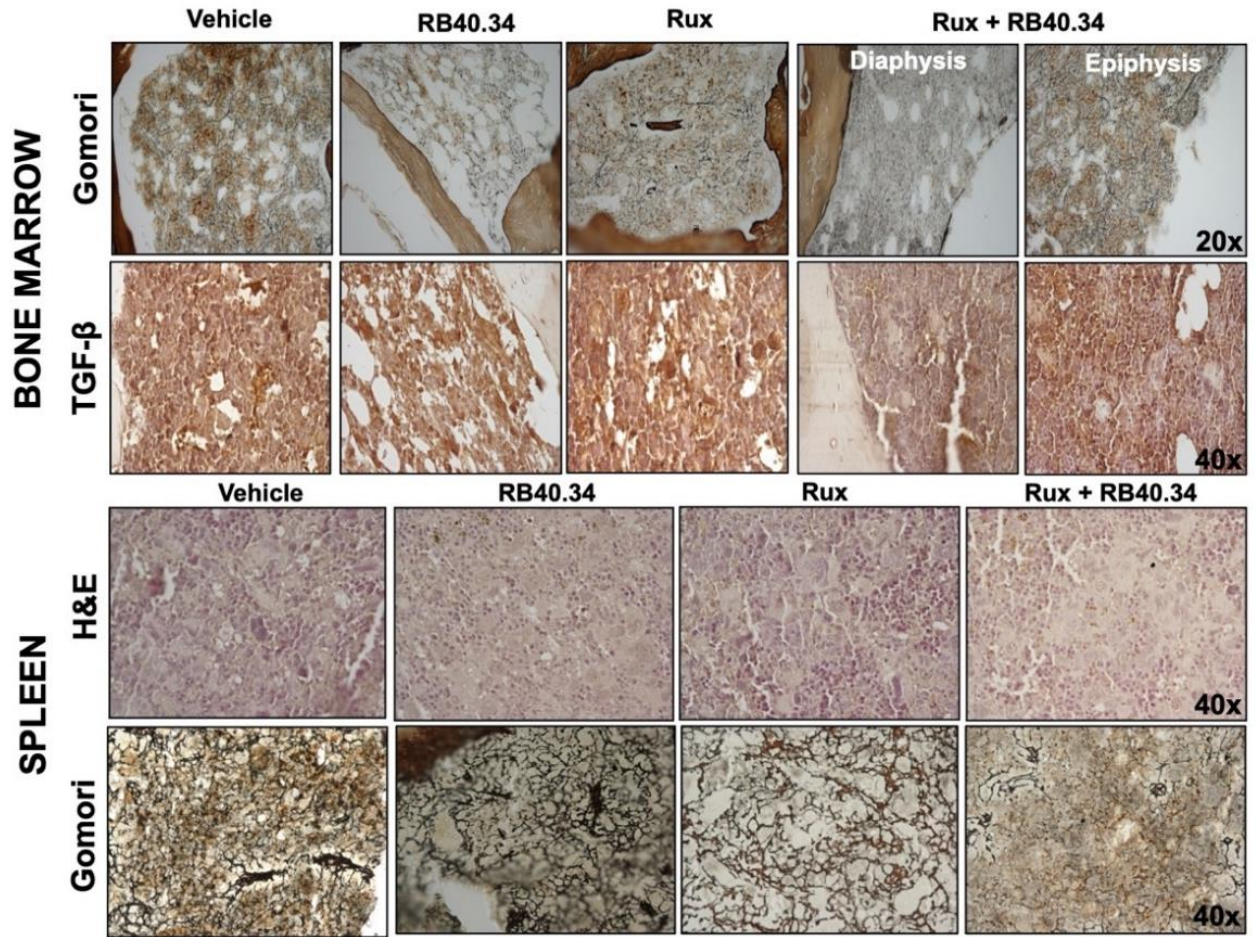


Figure S7. Treatment with RB40.34 in combination with Rux for 12 days reduced both fibrosis and TGF- β content only in the diaphysis of the femur and in the spleen of *Gata1*^{low} mice. Gomori and TGF- β immune-staining of sections from the femur and hematoxylin/eosin (H&E) and Gomori staining of sections from the spleen of representative *Gata1*^{low} mice treated for 12 days with either vehicle, RB40.34, Rux, or the two drugs in combination, as indicated. Original magnification 20X or 40X, as indicated.

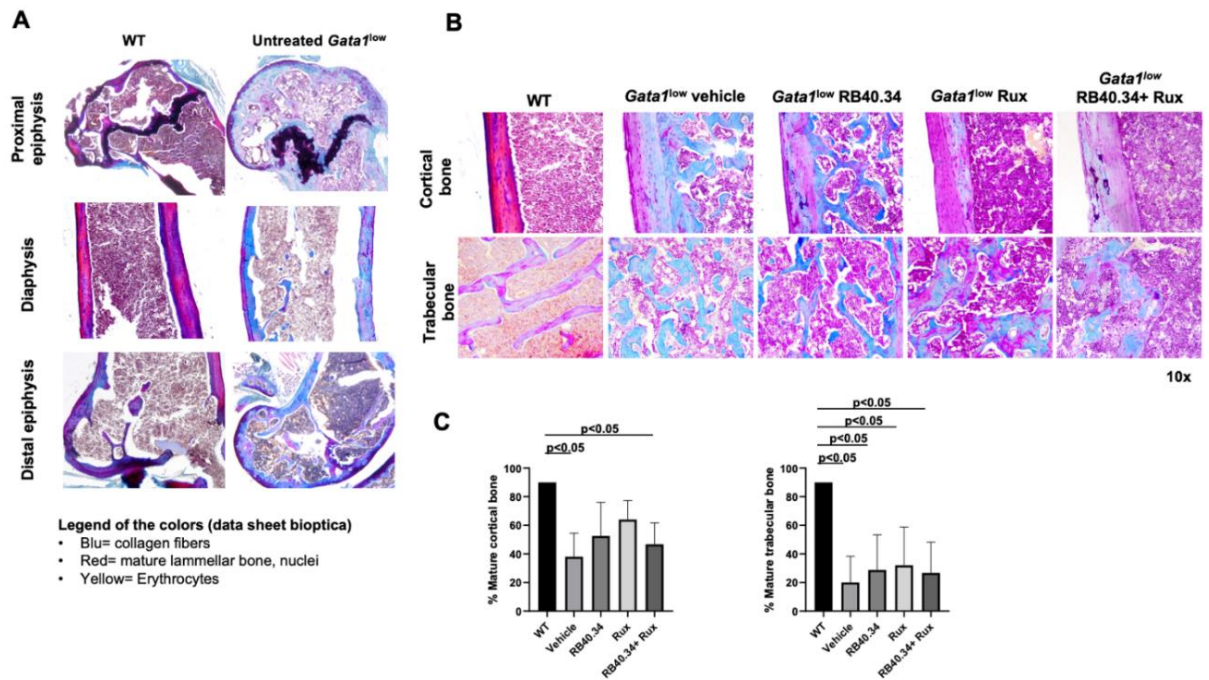


Figure S8. Treatment with Rux alone reduces osteopetrosis and improves the maturation of the cortical bone from the femur of *Gata1^{low}* mice. **(A)** Representative Mallory trichrome staining of the epiphysis and diaphysis of the femur from untreated 8- to 11-month-old WT and *Gata1^{low}* littermates. Original magnification 4X. **(B)** Mallory trichrome staining of the sections of the cortical and trabecular area of the femur of *Gata1^{low}* mice treated for 54 days with either vehicle, RB40.34, Rux, or RB40.34+Rux in combination, as indicated. Magnification 10X. **(C)** Quantification of the areas of mature bone of the cortex and the trabeculae of WT mice and *Gata1^{low}* mice treated for 54 days with either vehicle, RB40.34, Rux, or RB40.34+Rux in combinations. Data are presented as mean (\pm SD) and differences among groups were analyzed by analysis of variance. Values statistically different are presented within the panels.

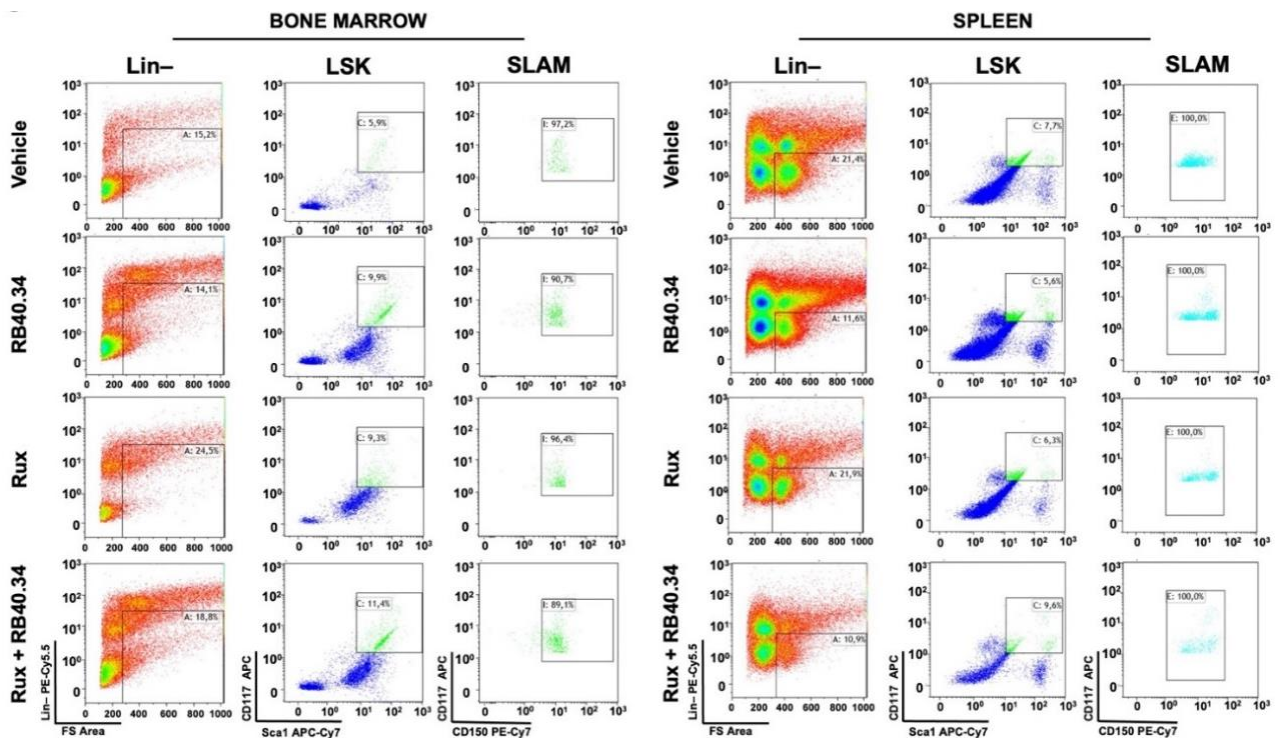


Figure S9. A representative sequence of gating used to identify the Lin-, LSK, and SLAM (CD150^{pos}/CD48^{neg} LSK) cells in bone marrow **(A)** and spleen **(B)** of *Gata1^{low}* mice treated for 54 days with either vehicle, RB40.34, Rux, or the two drugs in combination, as indicated.

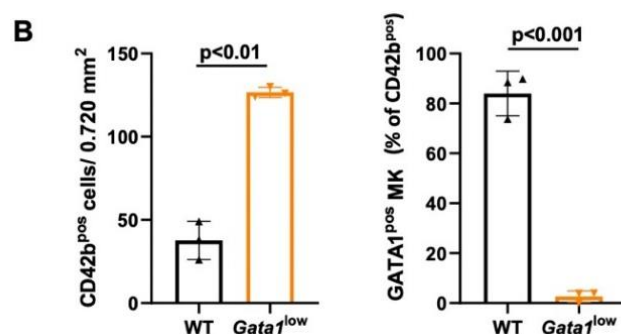
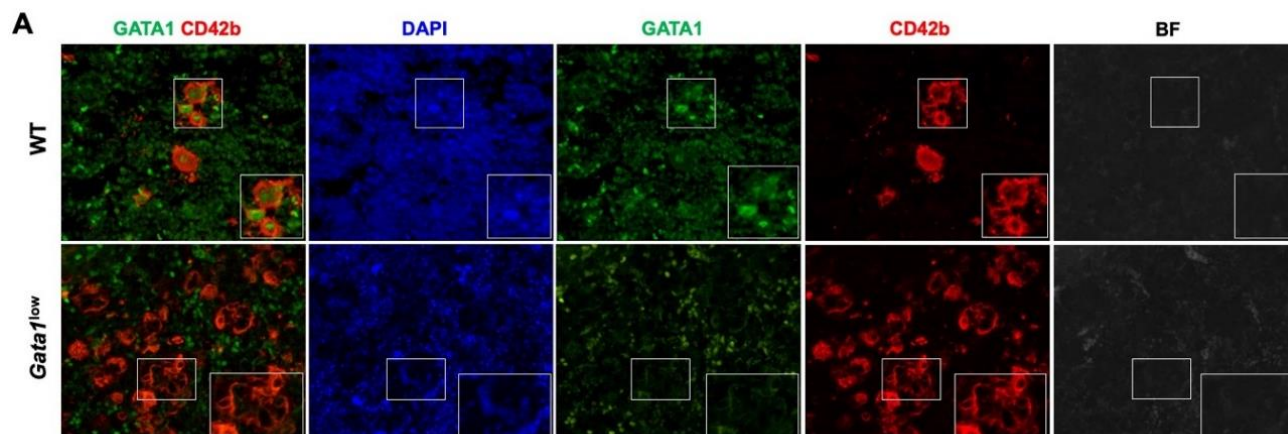


Figure S10. The bone marrow of *Gata1*^{low} mice contain great numbers of MK with barely detectable levels of GATA1. (A) Triple confocal microscopy analyses with antibodies against CD42b (as MK marker, red), GATA1 (in green), and counterstained with DAPI (blue) of BM sections from representative WT and *Gata1*^{low} littermates (one mouse each), as indicated. Images were acquired in the bright field channel (to evaluate autofluorescence), and in the red (555 nm), green (488 nm), and DAPI (405 nm) fields and are presented as single channels and in combination. (B) Frequency of CD42b^{pos} cells (MK) and CD42b^{pos} cells containing detectable levels of GATA1 in BM sections from multiple WT and *Gata1*^{low} littermates. Data are presented as mean (\pm SD) of values observed with three mice per experimental group and are compared by *t* test.

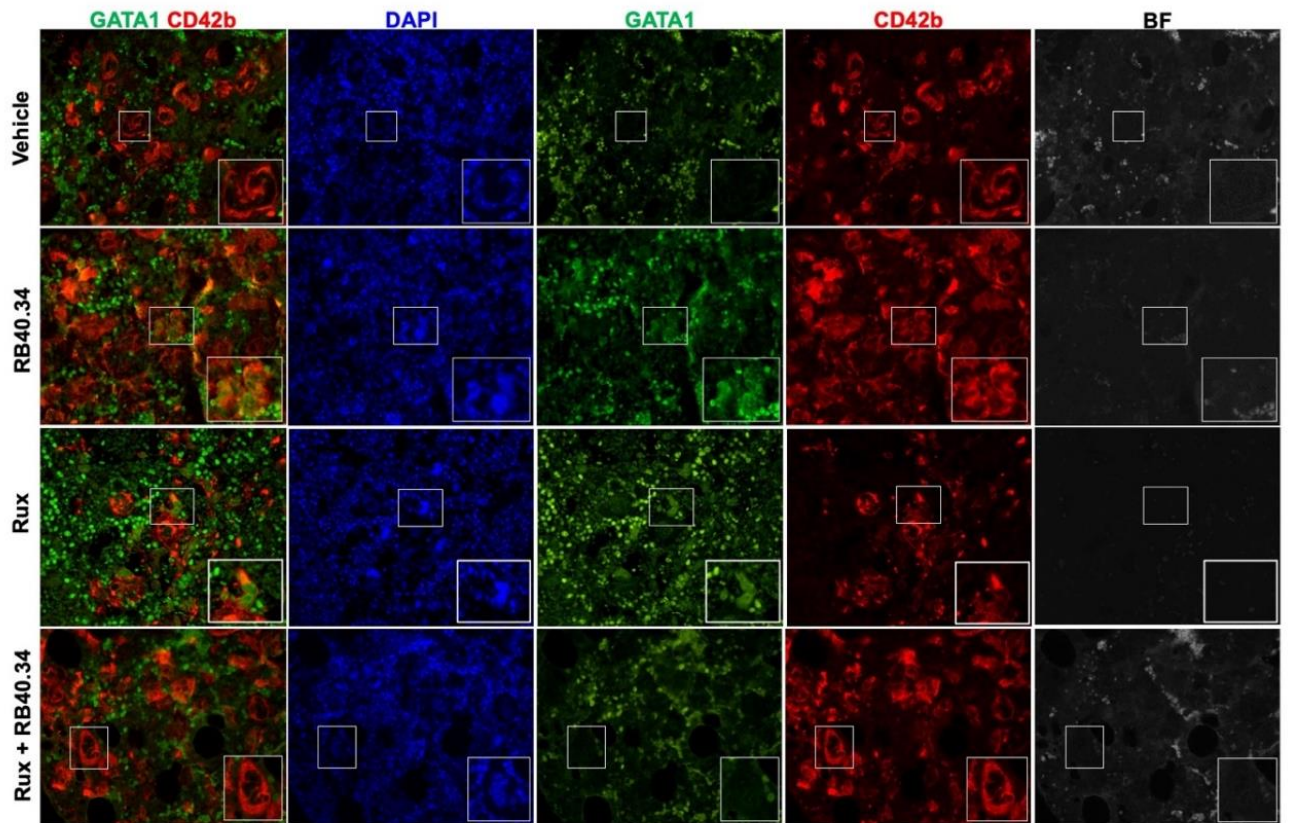


Figure S11. Treatment for 54 days with RB40.34 or Rux alone, but not in combination, increased the GATA1 content in MKs from the BM of *Gata1*^{low} mice. Triple immunofluorescence analyses with antibodies against GATA1 (FITCH-green), CD42b (TRITCH-red, as a marker of MKs), and DAPI (to identify the nuclei) of BM sections of representative *Gata1*^{low} mice treated for 54 days with either vehicle, RB40.34 alone, Rux alone, or the two drugs in combination, as indicated. The individual panels show images acquired in the bright field (an indication of autofluorescence from red blood cells) or in the DAPI, GATA1, and CD42b channels alone and in combination. See **Figure 10** for details.

Table S1. Summary table of deaths recorded in *Gatal*^{low} mice treated with vehicle, RB40.34, Rux, or the combination of drugs during the treatment period. In six out of eight cases (three mice treated with RB40.34 and three mice treated with the two drugs in combination), the cause of death remains unclear

Treatment	Recorded deaths	Days of treatment	Cause of death
Vehicle (n = 11)	0		
RB40.34 (n = 12)	4	7,8, 44, 46	Improper manipulation during the injection (n = 1); not established, found dead shortly after the venous injection (n = 3)
Rux (n = 12)	1	12	Suppressed for signs of suffering
Rux + RB40.34 (n = 12)	3	5, 16, 45	not established, found dead shortly after the venous injection (n = 3)

Table S2. Complete red blood cell values of *Gatal*^{low} mice 54 days posttreatment. Values among groups are not statistically significant by ANOVA multiple comparisons test

Treatment	Vehicle	RB40.34	Rux	Rux + RB40.34
RBC (10 ⁶ /μL)	6.12±0.74 ⁽⁵⁾	6.32±0.10 ⁽³⁾	5.47±0.74 ⁽⁵⁾	5.47±0.55 ⁽³⁾
Hgb (g/dL)	10.92±1.24 ⁽⁵⁾	11.27 ±0.15 ⁽³⁾	9.62±1.70 ⁽⁵⁾	9.60±0.61 ⁽³⁾
MCV (fL)	54.80±2.28 ⁽⁵⁾	52.97±1.19 ⁽³⁾	53.70±3.50 ⁽⁵⁾	53.40±3.22 ⁽³⁾
MCH (pg)	17.82±0.48 ⁽⁵⁾	17.80±0.52 ⁽³⁾	17.48±1.21 ⁽⁵⁾	17.53±0.67 ⁽³⁾
MCHC (g/dL)	32.58±0.87 ⁽⁵⁾	33.63±0.25 ⁽³⁾	32.58±0.30 ⁽⁵⁾	32.90±0.80 ⁽³⁾
CHCM (g/dL)	32.52±1.02 ⁽⁵⁾	31.17 ± 0.06 ⁽³⁾	32.30±0.16 ⁽⁵⁾	31.47±0.25 ⁽³⁾
MCHC/CHCM	1.00±0.00 ⁽⁵⁾	1.07 ± 0.06 ⁽³⁾	1.00 ± 0.00 ⁽⁵⁾	1.03 ± 0.06 ⁽³⁾
CH (pg)	16.66±1.03 ⁽⁵⁾	16.47±0.32 ⁽³⁾	16.64±1.00 ⁽⁵⁾	16.03±0.55 ⁽³⁾
CHDW (pg)	2.82±0.22 ⁽⁵⁾	2.83±0.06 ⁽³⁾	3.02±0.20 ⁽⁵⁾	2.93±0.32 ⁽³⁾
HDW (g/dL)	2.34±0.23 ⁽⁵⁾	2.50±0.00 ⁽³⁾	2.32±0.22 ⁽⁵⁾	2.53±0.06 ⁽³⁾

CH= hemoglobin content; CHCM=cell hemoglobin concentration mean; CHDW=cell hemoglobin distribution width; HDW=hemoglobin distribution width; Hgb=hemoglobin; MCH=mean cell hemoglobin; MCHC=mean cell hemoglobin concentration; MCV=mean cell volume; ⁽ⁿ⁾=Number of mice analyzed; RBC=red blood cells.

Table S3. Summary of the response of *Gata1*^{low} mice to the various treatments

End points		Treatment groups					
		Vehicle	RB40.34	Rux	RB.40.34 + Rux		
Blood	Day 5	Htc (%)	Normal	Normal	Normal	Normal	
		Platelets (10 ³ /μL)	Low	Low	Low	Low	
		Platelet binding to RB40.34	-	+	-	+	
	Day 54	Htc (%)	Normal	Normal	Normal	Normal	
		Anisocytosis	+	-	+	-	
		Platelets (10 ³ /μL)	Low	Low	Low	Low	
		WBCs (10 ³ /μL)	High	High	Normal	Normal	
		Lymphocytes (10 ³ /μL)	High	High	Normal	Normal	
	Bone Marrow	Day 5	Binding of RB40.34 to MKs	-	+	-	+
			Cellularity	Low	Low	Low	Low
TGF-β signaling			Activated	Activated	Activated	Normal	
Day 54		MK maturation	Immature	Mature	Mature	Mature	
		Cellularity	Low	Low	Low	Normal	
		Binding of RB40.34 to MK	?	-	?	-	
		Fibrosis	High	Low	High	Low	
		Hematopoiesis	Low	Low	Low	Improved	
		GATA1pos MKs	Few	Increased	Increased	Few	
		TGF-β/CXCL1	High	High	Low	Low	
		Neoangiogenesis	High	Reduced	Reduced	Reduced	
Osteopetrosis		High	High	Reduced	High		
Spleen		Day 5	Size	Enlarged	Enlarged	Enlarged	Enlarged
			Binding of RB40.34 to MKs	-	+	-	+
	JAK2 Signaling		Increased	Normal	Increased	Normal	
	Day 54	Size	Enlarged	Enlarged	Enlarged	Normal	
		Binding of RB40.34 to MKs	?	-	?	-	
		Fibrosis	High	Low	Low	Low	
		Hematopoiesis	High	High	High	Low	
		Architecture	Altered	Normal	Altered	Normal	
		Neoangiogenesis	High	Reduced	Reduced	Reduced	

Htc=Hematocrit; *MK*=megakaryocytes; *WBC*=white blood cell

3. General discussion and conclusions

Primary Myelofibrosis (PMF) is a chronic myeloproliferative neoplasm (MPN), belonging to the category of BCR-ABL negative MPNs (Marcellino et al., 2020). It is characterized by anemia, progressive splenomegaly, extra-medullary hematopoiesis, bone marrow (BM) fibrosis, leukemia progression and low survival (Harrison et al., 2020; Masarova et al., 2017). The best therapy currently available for myelofibrosis, includes treatment with the JAK inhibitor (Ruxolitinib), approved in 2011, which, however, only alleviates the symptoms of the disease (Cervantes & Pereira, 2017; Deininger et al., 2015; Iurlo & Cattaneo, 2017; Verstovsek, Gotlib, et al., 2017; Verstovsek, Mesa, et al., 2017).

Proinflammatory signaling is a hallmark feature of human cancer, including myelofibrosis (MF). Dysregulated inflammatory signaling contributes to fibrotic progression in MF; however, the individual cytokine mediators elicited by malignant MPN cells to promote collagen-producing fibrosis and disease evolution are yet to be fully elucidated (Mack, 2018). Previous studies have identified many cytokines whose plasma levels have increased in patients with PMF compared to healthy patients. Specifically, they contains greater levels of TGF- β (Campanelli et al., 2011), and interleukin-8 (IL-8) (Hoermann et al., 2012; Tefferi et al., 2011). These are produced by many different cells (Girbl et al., 2018; Hashimoto et al., 1996; Kaplanski et al., 1994; Martyré, 1995; Matsushima & Oppenheim, 1989; Takeuchi et al., 1999) and at high levels by the malignant megakaryocytes present in the bone marrow of MF patients (Dunbar et al., 2023; Zingariello et al., 2013b).

Mice carrying the hypomorphic *Gata1*^{low} mutation develop myelofibrosis and splenomegaly with age. In previous studies, megakaryocytic abnormalities similar to those observed in PMF patients were described in this mouse model, such as delayed maturation, low *Gata1* content and high expression of P-sel and TGF- β (Spangrude et al., 2016; Vannucchi et al., 2002; Vannucchi, Pancrazzi, et al., 2005; Zingariello et al., 2015).

In the **first study** (Zingariello et al., 2022), our aim was to investigate the relationship between serum levels of pro-inflammatory cytokines and their bioavailability in the bone marrow microenvironment in *Gata1*^{low} mice compared to wild-type littermates, and to identify the cell populations responsible for their increase and the consequences of their alterations. The mouse strain in which harbored the *Gata1*^{low} mutation is the CD1 mouse strain. These mice are known for their inflammation-associated diseases, such as amyloidosis, arteritis, nephropathy/glomerulonephritis, and multisite inflammation (Brayton et al., 2012), so it was not surprising to find the expression of serum levels of TGF- β 1, LCN2, and CXCL1, the murine

equivalent of human IL-8, higher than those expressed from the serum of C57BL6 mice or the DBA2 mice, which instead more rarely develop inflammatory diseases (Brayton et al., 2012). This finding, is important because inflammation has been considered for long time a key element in the development of MPNs, which are maintained by a continuous release of pro-inflammatory cytokines. In fact, MPNs are defined by a chronic inflammatory status contributing to microenvironmental transformation necessary for supporting tumor progression and severity of the disease (Longhitano et al., 2020; Mack, 2018). When comparing the serum levels of 32 inflammatory cytokines of pre-fibrotic and fibrotic *Gata1*^{low} mice with their wild-type littermates, we found a modest difference. However, by immunohistochemistry, the BM of *Gata1*^{low} mice contained higher levels of TGF- β 1, LCN-2, CXCL1 and its receptor (CXCR1) in the total area of the BM compared to WT. At the single-cell level, we observed increased expression of TGF- β 1, LCN-2, CXCL1 and its receptors CXCR1 and CXCR2 in malignant megakaryocytes compared with WT BM MKs. TGF- β 1 was also expressed, at comparable level to WT, by endothelial cells; LCN-2 by neutrophils; CXCL1 by endothelial cells, osteoblasts, and neutrophils; CXCR1 on endothelial cells, neutrophils, osteoblasts; CXCR2 was detectable on neutrophils, endothelial cells and osteoblasts. However, all cytokines and receptors were found to be highly expressed in the cytoplasm of malignant megakaryocytes compared to the corresponding WT. We also evaluated the numbers of endothelial cells, mesenchymal stem cells, osteoblasts, neutrophils and megakaryocytes in the bone marrow of *Gata1*^{low} and WT mice, and we observed higher numbers of all these categories of cells, except neutrophils, in the bone marrow of *Gata1*^{low} mice compared with those in the bone marrow of wild-type littermates. These results suggest that the increase in the bioavailability of these cytokines in the bone marrow microenvironment of mutant mice is due to both an increase in the number of cells expressing these cytokines, particularly megakaryocytes (in BM *Gata1*^{low} their number is 2-3 times higher) and an increase in the amount of these products at single cell level. These observations strengthen the hypothesis that malignant MKs play an important role in the development of myelofibrosis. Angiogenesis and neo-bone formation, typical features of myelofibrosis, are triggered by the interaction of cytokines such as TGF- β , VEGF and BMP-4 (Hankenson et al., 2015; Lin et al., 2015; Nguyen et al., 2013; Shen et al., 2009). In previous studies, it has been shown that *Gata1*^{low} mice exhibit high levels of VEGF (Vannucchi et al., 2005) and TGF- β (Zingariello et al., 2013) in the bone marrow. Moreover, in this work we have also demonstrated the presence of high levels of BMP4, especially in the megakaryocytes. In human and murine bone marrow, there are HSC niches that support hematopoiesis. In mice,

these are defined by their anatomical location (in the diaphysis or epiphysis of the femur), the type of blood vessels (sinusoids, arterioles, or transition zone vessels) they contain, and their proximity to the endosteal zone (Raaijmakers et al., 2010; Szade et al., 2018; Yang & de Haan, 2021). HSCs that repopulate the bone marrow in the long term are found in the outermost niches of the bone, within niches that head toward the central area of the marrow and harbor progressively more differentiated and eventually progenitor HSC cells (Lord, 1990). HSC niches may undergo remodeling during aging and inflammation, and these changes are presumed to account for the changes in HSC function observed with age (Ho & Méndez-Ferrer, 2020; Mitroulis et al., 2020). However, our knowledge of changes in the HSC niche with age in different strains is limited. In this study we found that in the bone marrow of old Wild-type mice, hematopoietic stem cells (HSCs) are localized in the epiphysis of the femur around adipocytes, whereas in that of *Gata1*^{low} mice, HSCs are localized in the diaphysis in areas of the marrow between bone trabeculae and vessels that contain large numbers of megakaryocytes. Therefore, it is possible that megakaryocytes within the cluster that phagocytize HSCs release growth factors (TGF- β , VEGF, and BMP-4), which, by inducing neoangiogenesis and bone formation, shape the *Gata1*^{low} BM microenvironment by increasing niches for short-term repopulation of HSCs and multilineage progenitor cells. These cells, however, are induced to apoptosis by the pro-inflammatory milieu of this microenvironment, resulting in hematopoietic failure. In conclusion, microenvironmental bioavailability of inflammatory cytokines in the BM, perhaps through remodeling of the HSC niche, plays a key role in the development of myelofibrosis in the *Gata1*^{low} mouse model.

On the basis of the previous data in which we demonstrated that megakaryocytes in the bone marrow of *Gata1*^{low} mice express not only high levels of TGF- β 1, but also high levels of CXCL1 and its receptors CXCR1 and CXCR2, the aim of the **second study** (Verachi et al., 2022) was to evaluate the efficacy of treatment with the drug Reparixin, that induce allosteric inhibition of CXCR1/2, in this mouse model. The results obtained showed that treatment with Reparixin in *Gata1*^{low} mice had a dose-dependent efficacy in reducing bone marrow and splenic fibrosis. Since CXCL1 and its receptors contribute to the control of megakaryocytic proliferation, differentiation, and ploidy in MF (Emadi et al., 2005), we evaluated whether inhibition of the CXCR1/R2 signaling might reduce the fibrosis by restoring the MKs abnormalities, including alteration in the pro-inflammatory cytokine content, observed in *Gata1*^{low} mice. We then assessed by immunohistochemistry, the expression of TGF- β 1, CXCL1 and its receptors (CXCR1/2) in the bone marrow of the treated mice. The treatment did not alter

the expression of CXCL1 or CXCR1/R2 receptors in the MKs from the BM of *Gata1*^{low} mice. This is consistent with the fact that allosteric modulation does not block the binding of the endogenous ligand to its receptors or alter its constitutive activity (Bertini et al., 2004). Since CXCR1/CXCR2 are also activated by other cytokines, such as CXCL6 and MIP2, we may not formally exclude that altered levels of these chemokines are also involved in the development of myelofibrosis in our model. We also showed that this treatment induced a decrease in TGF- β 1 content in the BM of *Gata1*^{low} mice. Since CXCL1 is known to induce neutrophil chemotaxis (Waugh & Wilson, 2008), it is possible that Reparixin, by decreasing the chemotaxis of neutrophils toward MKs, reduces their pathologic emperipolesis with these cells by reducing the amount of TGF- β that they release into the microenvironment, thereby reducing fibrosis.

GATA1 expression is required for terminal maturation of erythroid cells and megakaryocytes (Ling et al., 2018), therefore, its expression is believed to underlie the megakaryocyte defect in MF patients. Murine (and human) BM contains four distinctive MK subpopulations, each one exerting a different function (Pariser et al., 2021; Sun et al., 2021; Wang et al., 2021; Yeung et al., 2020) the platelet producing MK, the niche supportive MK, the immune MK and niche-poised-MK. The latter has an immature morphology and is characterized by high expression of extracellular matrix genes such as COL1A1, COL3A1, and COL6A2 and enrichment of the “response to TGF- β signature”. We then performed immunofluorescence analysis to see whether or not the treatment could induce the expression of Gata1 and Collagen III in the MK of the treated mice. We found that Reparixin treatment induced the expression of GATA1 and reduced the expression of Collagen III in megakaryocytes. The frequency of MKs expressing collagen III which were also positive for GATA1 was significantly greater in mice treated with Reparixin suggesting that Reparixin had specifically increased GATA1 content in niche-poised MKs, possibly hampering their pro-fibrotic functions. These data suggest that in the *Gata1*^{low} mouse model, Reparixin reduces fibrosis by reducing TGF- β 1 and Collagen III expression and increasing Gata1 in megakaryocytes. These results provide a preclinical rationale for further evaluation of this drug alone and in combination with the current drug.

In the **third study** (Verachi, Gobbo, Martelli, Falchi, et al., 2022), we aimed to test the hypothesis that pharmacological inhibition of P-selectin (P-SEL) with RB40.34, alone and in combination with Ruxolitinib, is effective in reversing the myelofibrotic phenotype expressed by *Gata1*^{low} mice. Fibrotic *Gata1*^{low} mice were treated with the monoclonal antibody RB40.34, alone and in combination with Ruxolitinib for 5, 12 and 54 days. We firstly decided to

investigate the effects of treatments on the BM and spleen signaling status of *Gata1*^{low} mice. To do so, we used a panel of antibodies targeting SMAD2/3 and TGF- β RII (canonical TGF- β signaling); p38, p-p38, ERK1/2 and p-ERK1/2 (non-canonical TGF- β signaling); and JAK2 and STAT5 (JAK/STAT signaling) for western-blot analysis. After 5 days of treatment with RB40.34 in combination with Ruxolitinib, the non-canonical TGF- β signaling, which is a signature of a pro-fibrotic microenvironment, and also the canonical TGF- β signature, which indicates impaired hematopoiesis in the bone marrow, were normalized. In addition, JAK2 in the spleen of mutant mice was also reduced, suggesting that it is reducing extramedullary hematopoiesis in this organ. These data indicate that treatment for only 5 days with the combination Rux+RB03.34 induces detectable biochemical changes in the bone marrow and spleen of *Gata1*^{low} mice. We also analyzed the effects of long-term (54 days) treatments with RB40.34 and Ruxolitinib, alone or in combination, on the myelofibrotic phenotype expressed by *Gata1*^{low} mice. None of the treatments induced anemia or rescued thrombocytopenia in these mice. However, treatment for 54 days with RB40.34 in combination with Rux reduced anisocytosis and P-SEL expression on megakaryocytes. Anisocytosis without increased mean corpuscular volume is induced by pro-inflammatory cytokines in several benign and malignant diseases, including MF, where it has been proposed as a predictive marker of inferior survival (Corey et al., 2018). At days 5 and 12 of treatment, bone marrow fibrosis and cellularity were mostly unchanged. At day 54, the femur of mice in the RB40.36+ Rux group contained significantly more cells than those in the vehicle group and showed reduced fibrosis in the bone marrow. Conversely, single treatment with RB40.34 significantly reduced fibrosis but did not increase BM cellularity while, as previously reported (Zingariello et al., 2017) treatment with Rux alone does not increase BM cellularity and does not reduce fibrosis in *Gata1*^{low} mice. The reason why, unlike our data, Rux is effective in reducing fibrosis in the JAK2^{V617F} driven mouse model (Li et al., 2022) is unclear and deserves to be further investigated. We also investigated by immunofluorescence whether neoangiogenesis, a very common feature in MF (Vannucchi et al., 2002), was reduced with pharmacological treatment. Indeed, at day 54, the vessel density of all treatment groups was significantly lower than that of vehicle. We found that treatment with the combination of RB40.34 and Rux significantly reduces JAK2 content in the spleen, suggesting that, since JAK2 signaling is very important in hematopoiesis (Perner et al., 2019), this treatment reduces hematopoiesis in this organ. In accord with this hypothesis, we observe a marked reduction in fibrosis and a significant reduction in the total number of hematopoietic progenitor cells in the spleens of *Gata1*^{low} mice treated with RB40.34 and Rux, supporting the

hypothesis that RB40.34 and Rux in combination reduce extramedullary hematopoiesis in this organ. In addition, this treatment restores spleen architecture that is distorted in *Gata1*^{low} mice. The presence of high levels of pro-inflammatory cytokines, such as TGF- β and CXCL1, the murine equivalent of human IL-8, is a trigger of fibrosis and hematopoietic failure in the BM of MF patients and in mouse models (Dunbar et al., 2023; Emadi et al., 2005; Verachi, Gobbo, Martelli, Martinelli, et al., 2022). In the first study, we have shown that the cells responsible for the increased bioavailability of these two cytokines in the BM (and spleen) of *Gata1*^{low} mice are the abnormal MKs (Zingariello et al., 2022). Based on the assumption that the reduction in anisocytosis observed at day 54 in the RB40.34 groups alone or in combination with Rux reflects the reduction in pro-inflammatory cytokines TGF- β and/or CXCL1 that drive myelofibrosis in this model, we performed histochemical evaluations with antibodies against TGF- β and CXCL1 in the BM of the treated mice. Our results show that in mice treated for 54 days with the combination of RB40,34 and Rux, there was a decrease in TGF- β and CXCL1 content. The maturation process of terminal megakaryocytes involves a series of precursors that progressively acquire the characteristics of mature platelet cells, which express increased levels of CD41 and CD61 on their surface (Sun et al., 2021). We then performed flow cytometry analysis for the expression of CD41 and CD61 and observed that treatment for 54 days with RB40.34 and Rux alone or in combination improved the maturation profile of megakaryocytes (MKs) in the bone marrow and spleen of *Gata1*^{low} mice. *Gata1* expression is a sign of megakaryocyte maturation (Ling et al., 2018). Therefore, we performed immunofluorescence analysis to see whether or not treatments could induce its expression. In partial agreement with the flow cytometry results, we found that a significant number of MKs in the BM of mice treated with RB40.34 or Rux alone contain detectable levels of GATA1 in their nuclei. Conversely, it is surprising that GATA1 is not detected in the MKs in the BM of mice treated with RB40.34 and Rux in combination. However, analysis of the number of megakaryocytes in the bone marrow showed that none of the treatments were effective in reducing the number of these cells in the bone marrow. These results provide preclinical evidence that treatment with an antibody against P-selectin in combination with Ruxolitinib may be more effective than treatment with Ruxolitinib alone in patients with PMF.

These studies provide new information on the proinflammatory milieu of the bone marrow microenvironment in the *Gata1*^{low} mouse model of PMF, and the effects on fibrosis and cytokine expression of treatment with an inhibitor of CXCL1 (Reparixin) and P-selectin (RB40.34), alone or in combination with Ruxolitinib.

The two groups of treatments (P-sel inhibitor in combination or not with the JAK inhibitor and CXCR1/2 inhibitor) influence the reduction of bone marrow fibrosis by modulating different effects by acting on cellularity, on the maturation of MKs and platelet production. However, the contribution given to these phenomena with the different therapeutic strategies is different.

The most significant reduction in bone marrow fibrosis was recorded with Reparixin (20 days) which induced a significant reduction in TGF- β 1 (37 days). However, it did not influence the cellularity of the femurs. It should be noted that the lack of effect on the marrow cellularity is not necessarily an indication that the treatments has not restored haemopoiesis. In fact, in our experiments, cellularity was quantified as a whole, also considering osteoblasts and endothelial cells, whose numbers are increased in myelofibrosis. Therefore, with our strategy, the treatment-induced increase in hematopoietic cells in the femur can be masked by any reductions in osteogenesis and vessel formation induced at the same time by the treatments.

P-selectin inhibition in combination with Ruxolitinib also proved to be very effective in reducing the myelofibrotic trait in this animal model acting on the reduction of the expression of TGF- β 1 and CXCL1, and it was the most effective treatment in reducing weight, cellularity and fibrosis in the spleen. In addition, the treatment with Ruxolitinib alone reduce fibrosis mainly by acting on the reduction of TGF- β 1, thus influencing the microenvironment with the effect of restoring cellularity. These findings are consistent with those from clinical trials with Ruxolitinib indicating that the drug is effective in reducing splenomegaly in patients with myelofibrosis but has limited effects on bone marrow fibrosis. Interestingly, as in our animal model, in JAK2^{V617} mice Ruxolitinib effectively reduced bone marrow fibrosis when used in combination with hemideficiency of an epigenetic modifier (HMGA1 gene) that reduces the proinflammatory environment (Li et al., 2022).

Among the treatments, the GATA1 content in megakaryocytes was increased by RB40.34 alone, Ruxolitinib and Reparixin. Among these treatments, the one that most increased the number of megakaryocytes with high GATA1 content was Ruxolitinib. The morphology, however, of the megakaryocytes remained immature in all the cases, explaining why any of these treatments increased the number of platelets in the blood.

In summary, the results presented in this thesis demonstrate that CXCL1 and TGF- β 1 are expressed at higher than normal levels in the microenvironment of the bone marrow of *Gata1*^{low} mice, particularly in megakaryocytes. Furthermore, we demonstrate the similarity but also the diversity of the efficacy of P-selectin, JAK2 and CXCR1/2 inhibitors in reducing the

myelofibrotic phenotype of *Gata1*^{low} mice. All treatments appear to reduce fibrosis by decreasing TGF- β 1.

In conclusion, these data provide preclinical evidence that treatment with Reparixin and RB40.34 antibody in combination with Ruxolitinib are effective in reversing the myelofibrotic trait in the *Gata1*^{low} mouse model and encourage clinical trials to validate the effects of these compounds for the treatment of human PMF.

4. References

Bertini, R., Allegretti, M., Bizzarri, C., Moriconi, A., Locati, M., Zampella, G., Cervellera, M.N., Di Cioccio, V., Cesta, M.C., Galliera, E., Martinez, F.O., Di Bitondo, R., Troiani, G., Sabbatini, V., D'Anniballe, G., Anacardio, R., Cutrin, J.C., Cavalieri, B., Mainiero, F., Strippoli, R., Villa, P., Di Girolamo, M., Martin, F., Gentile, M., Santoni, A., Corda, D., Poli, G., Mantovani, A., Ghezzi, P., Colotta, F. (2004). Noncompetitive allosteric inhibitors of the inflammatory chemokine receptors CXCR1 and CXCR2: Prevention of reperfusion injury. *PNAS*, 101(32), 11791–11796. <https://doi.org/10.1073/pnas.0402090101>.

Brayton, C.F., Treuting, P.M., Ward, J.M. (2012). Pathobiology of aging mice and GEM. *Veterinary Pathology*, 49(1), 85–105. <https://doi.org/10.1177/0300985811430696>.

Campanelli, R., Rosti, V., Villani, L., Castagno, M., Moretti, E., Bonetti, E., Bergamaschi, G., Balduini, A., Barosi, G., Massa, M. (2011). Evaluation of the bioactive and total transforming growth factor β 1 levels in primary myelofibrosis. *Cytokine*, 53(1), 100–106. <https://doi.org/10.1016/j.cyto.2010.07.427>.

Cervantes, F., Pereira, A. (2017). Does ruxolitinib prolong the survival of patients with myelofibrosis? *Blood*, 129(7), 832–837. <https://doi.org/10.1182/blood-2016-11-731604>.

Corey, S.J., Jha, J., McCart, E.A., Rittase, W.B., George, J., Mattapallil, J.J., Mehta, H., Ognoon, M., Bylicky, M.A., Summers, T.A., Day, R.M. (2018). Captopril mitigates splenomegaly and myelofibrosis in the *Gata1*^{low} murine model of myelofibrosis. *Journal of Cellular and Molecular Medicine*, 22(9), 4274–4282. <https://doi.org/10.1111/jcmm.13710>.

Deininger, M., Radich, J., Burn, T. C., Huber, R., Paranagama, D., Verstovsek, S. (2015). The effect of long-term ruxolitinib treatment on JAK2^{V617F} allele burden in patients with myelofibrosis. *Blood*, 126(13), 1551–1554. <https://doi.org/10.1182/blood-2015-03-635235>.

Dunbar, A. J., Kim, D., Lu, M., Farina, M., Bowman, R. L., Yang, J. L., Park, Y., Karzai, A., Xiao, W., Zaroogian, Z., O'Connor, K., Mowla, S., Gobbo, F., Verachi, P., Martelli, F., Sarli, G., Xia, L., Elmansy, N., Kleppe, M., Chen, Z., Xiao, Y., McGovern, E., Snyder, J., Krishnan, A., Hill, C., Cordner, K., Zouak, A., Salama, M.E., Yohai, J., Tucker, E., Chen, J., Zhou, J., McConnell, T., Migliaccio, A.R., Koche, R., Rampal, R., Fan, R., Levine, R.L., Hoffman, R. (2023). CXCL8/CXCR2 signaling mediates bone

marrow fibrosis and is a therapeutic target in myelofibrosis. *Blood*, 141(20), 2508–2519. <https://doi.org/10.1182/blood.2022015418>.

Emadi, S., Clay, D., Desterke, C., Guerton, B., Maquarre, E., Jasmin, C. (2005). IL-8 and its CXCR1 and CXCR2 receptors participate in the control of megakaryocytic proliferation, differentiation, and ploidy in myeloid metaplasia with myelofibrosis. *Blood*, 105(2), 464–473. <https://doi.org/10.1182/blood-2003-12-4415>.

Girbl, T., Lenn, T., Perez, L., Rolas, L., Barkaway, A., Thiriote, A., del Fresno, C., Lynam, E., Hub, E., Thelen, M., Graham, G., Alon, R., Sancho, D., Von Andrian, U.H., Voisin, M.B., Rot, A., Nourshargh, S. (2018). Distinct compartmentalization of the chemokines CXCL1 and CXCL2 and the atypical receptor ACKR1 determine discrete stages of neutrophil diapedesis. *Immunity*, 49(6), 1062–1076.e6. <https://doi.org/10.1016/j.immuni.2018.09.018>.

Hankenson, K.D., Gagne, K., Shaughnessy, M. (2015). Extracellular signaling molecules to promote fracture healing and bone regeneration. *Advanced Drug Delivery Reviews*, 94, 3–12. <https://doi.org/10.1016/j.addr.2015.09.008>.

Harrison, C.N., Schaap, N., Mesa, R.A., Harrison, C.N. (2020). Management of myelofibrosis after ruxolitinib failure. *Annals of Hematology*, 16, 1–13.

Hashimoto, S., Yoda, M., Yamada, M., Yanai, N., Kawashima, T., Motoyoshi, K. (1996). Macrophage colony-stimulating factor induces interleukin-8 production in human monocytes. *Experimental Hematology*, 24(2), 123–128. <http://europepmc.org/abstract/MED/8641333>.

Ho, Y.H., Méndez-Ferrer, S. (2020). Microenvironmental contributions to hematopoietic stem cell aging. *Haematologica*, 105(1), 38–46. <https://doi.org/10.3324/haematol.2018.211334>.

Hoermann, G., Cerny-Reiterer, S., Herrmann, H., Blatt, K., Bilban, M., Gisslinger, H., Gisslinger, B., Müllauer, L., Kralovics, R., Mannhalter, C., Valent, P., Mayerhofer, M. (2012). Identification of oncostatin M as a JAK2^{V617F}-dependent amplifier of cytokine production and bone marrow remodeling in myeloproliferative neoplasms. *The FASEB Journal*, 26(2), 894–906. <https://doi.org/10.1096/fj.11-193078>.

Iurlo, A., Cattaneo, D. (2017). Treatment of myelofibrosis: old and new strategies. *Clinical Medicine Insights: Blood Disorders*, 10, 1–10. <https://doi.org/10.1177/1179545X17695233>.

Kaplanski, G., Farnarier, C., Kaplanski, S., Porat, R., Shapiro, L., Bongrand, P., Dinarello, C.A. (1994). Interleukin-1 induces interleukin-8 secretion from endothelial cells by a juxtacrine mechanism. *Blood*, 84(12), 4242–4248. <http://europepmc.org/abstract/MED/7994038>.

Li, L., Kim, J.H., Lu, W., Williams, D.M., Kim, J., Cope, L., Rampal, R.K., Koche, R.P., Xian, L., Luo, L.Z., Vasiljevic, M., Matson, D.R., Zhao, Z.J., Rogers, O., Stubbs, M.C., Reddy, K., Romero, A.R.,

- Psaila, B., Spivak, J.L., Moliterno, A.R., Resar, L.M.S. (2022). HMGA1 chromatin regulators induce transcriptional networks involved in GATA2 and proliferation during MPN progression. *Blood*, 139:2797–815. <https://doi.org/10.1182/blood.2021013925>.
- Lin, S., Xie, J., Gong, T., Shi, S., Zhang, T., Fu, N., Ye, L., Wang, M., Lin, Y. (2015). TGF β signalling pathway regulates angiogenesis by endothelial cells, in an adipose-derived stromal cell/endothelial cell co-culture 3D gel model. *Cell Proliferation*, 48(6), 729–737. <https://doi.org/10.1111/cpr.12222>.
- Ling, T., Crispino, J.D., Zingariello, M., Martelli, F., Migliaccio, A.R. (2018). GATA1 insufficiencies in primary myelofibrosis and other hematopoietic disorders: consequences for therapy. *Expert Review of Hematology*, 11(3), 169–184. <https://doi.org/10.1080/17474086.2018.1436965>.
- Longhitano, L., Li Volti, G., Giallongo, C., Spampinato, M., Barbagallo, I., Di Rosa, M., Romano, A., Avola, R., Tibullo, D., Palumbo, G.A. (2020). The Role of Inflammation and Inflammasome in Myeloproliferative Disease. *Journal of Clinical Medicine*, 9(8), 2334. <https://doi.org/10.3390/jcm9082334>.
- Lord, B.I. (1990). The architecture of bone marrow cell populations. *The International Journal of Cell Cloning*, 8(5), 317–331. <https://doi.org/10.1002/stem.5530080501>.
- Mack, M. (2018). Inflammation and fibrosis. *Matrix Biology: Journal of the International Society for Matrix Biology*, 68–69, 106–121. <https://doi.org/10.1016/j.matbio.2017.11.010>.
- Marcellino, B.K., Verstovsek, S., Mascarenhas, J. (2020). The myelodepletive phenotype in myelofibrosis: clinical relevance and therapeutic implication. *Clinical Lymphoma, Myeloma and Leukemia*, 1–7. <https://doi.org/doi:10.1016/j.clml.2020.01.008>.
- Martyré, M.C. (1995). TGF- β and megakaryocytes in the pathogenesis of myelofibrosis in myeloproliferative disorders. *Leukemia & Lymphoma*, 20(1–2), 39–44. <https://doi.org/10.3109/10428199509054751>.
- Masarova, L., Bose, P., Daver, N., Pemmaraju, N., Newberry, K.J., Cortes, J., Kantarjian, H.M., Verstovsek, S. (2017). Patients with post-essential thrombocythemia and post-polycythemia vera differ from patients with primary myelofibrosis. *Leukemia Research*, 59, 110–116. <https://doi.org/10.1016/j.leukres.2017.06.001>.
- Matsushima, K., Oppenheim, J.J. (1989). Interleukin-8 and MCAF: novel inflammatory cytokines inducible by IL1 and TNF. *Cytokine*, 1(1), 2–13. [https://doi.org/https://doi.org/10.1016/1043-4666\(89\)91043-0](https://doi.org/https://doi.org/10.1016/1043-4666(89)91043-0).
- Mitroulis, I., Kalafati, L., Bornhäuser, M., Hajishengallis, G., Chavakis, T. (2020). Regulation of the bone marrow niche by inflammation. *Frontiers in Immunology*, 11, 1540. <https://doi.org/10.3389/fimmu.2020.01540>.

- Nguyen, J., Tang, S.Y., Nguyen, D., Alliston, T. (2013). Load regulates bone formation and Sclerostin expression through a TGF β -dependent mechanism. *PloS One*, 8(1), e53813. <https://doi.org/10.1371/journal.pone.0053813>.
- Pariser, D. N., Hilt, Z. T., Ture, S. K., Blick-Nitko, S. K., Looney, M. R., Cleary, S. J., Roman-Pagan, E., Saunders, J. 2nd, Georas, S.N., Veazey, J., Madere, F., Santos, L.T., Arne, A., Huynh, N.P., Livada, A.C., Guerrero-Martin, S.M., Lyons, C., Metcalf-Pate, K.A., McGrath, K.E., Palis, J., Morrell, C.N. (2021). Lung megakaryocytes are immune modulatory cells. *Journal of clinical investigation*, 131(1), e137377. <https://doi.org/10.1172/JCI137377>.
- Perner, F., Perner, C., Ernst, T., Heidel, F.H. (2019). Roles of JAK2 in aging, inflammation, hematopoiesis and malignant transformation. *Cells*, 8(8), 854. <https://doi.org/10.3390/cells8080854>.
- Raaijmakers, M.H., Mukherjee, S., Guo, S., Zhang, S., Kobayashi, T., Schoonmaker, J.A., Ebert, B.L., Al-Shahrour, F., Hasserjian, R.P., Scadden, E.O., Aung, Z., Matza, M., Merckenschlager, M., Lin, C., Rommens, J.M., Scadden, D.T. (2010). Bone progenitor dysfunction induces myelodysplasia and secondary leukaemia. *Nature*, 464(7290), 852–857. <https://doi.org/10.1038/nature08851>.
- Shen, Q., Zhu, S., Hu, J., Geng, N., Zou, S. (2009). Recombinant human bone morphogenetic protein-4 (BMP-4)-stimulated cell differentiation and bone formation within the expanding calvarial suture in rats. *The Journal of Craniofacial Surgery*, 20(5), 1561–1565. <https://doi.org/10.1097/SCS.0b013e3181b09cc1>.
- Spangrude, G.J., Lewandowski, D., Martelli, F., Marra, M., Zingariello, M., Sancillo, L., Rana, R.A., Migliaccio, A.R. (2016). P-Selectin sustains extramedullary hematopoiesis in the *Gata1*^{low} model of myelofibrosis. *Stem Cells*, 34(1), 67–82. <https://doi.org/10.1002/stem.2229>.
- Sun, S., Jin, C., Si, J., Lei, Y., Chen, K., Cui, Y., Liu, Z., Liu, J., Zhao, M., Zhang, X., Tang, F., Rondina, M.T., Li, Y., Wang, Q. (2021). Single-cell analysis of ploidy and the transcriptome reveals functional and spatial divergency in murine megakaryopoiesis. *Blood*, 138(14), 1211–1224. <https://doi.org/10.1182/blood.2021010697>.
- Szade, K., Gulati, G.S., Chan, C.K.F., Kao, K.S., Miyanishi, M., Marjon, K.D., Sinha, R., George, B.M., Chen, J.Y., Weissman, I.L. (2018). Where hematopoietic stem cells live: the bone marrow niche. *Antioxidants & Redox Signaling*, 29(2), 191–204. <https://doi.org/10.1089/ars.2017.7419>.
- Takeuchi, K., Higuchi, T., Yamashita, T., Koike, K. (1999). Chemokine production by human megakaryocytes derived from cd34-positive cord blood cells. *Cytokine*, 11(6), 424–434. <https://doi.org/https://doi.org/10.1006/cyto.1998.0455>.
- Tefferi, A., Vaidya, R., Caramazza, D., Finke, C., Lasho, T., Pardanani, A. (2011). Circulating interleukin (IL)-8, IL-2R, IL-12, and IL-15 levels are independently prognostic in primary

myelofibrosis: a comprehensive cytokine profiling study. *Journal of Clinical Oncology*, 29(10), 1356–1363. <https://doi.org/10.1200/JCO.2010.32.9490>.

Vannucchi, A.M., Bianchi, L., Cellai, C., Paoletti, F., Rana, R.A., Lorenzini, R., Migliaccio, G., Migliaccio, A.R. (2002). Development of myelofibrosis in mice genetically impaired for GATA-1 expression (*Gata1^{low}* mice). *Blood*, 100(4), 1123–1132. <https://doi.org/10.1182/blood-2002-06-1913>.

Vannucchi, A.M., Bianchi, L., Paoletti, F., Pancrazzi, A., Torre, E., Nishikawa, M., Zingariello, M., Di Baldassarre, A., Rana, R.A., Lorenzini, R., Alfani, E., Migliaccio, G., Migliaccio, A.R. (2005). A pathobiologic pathway linking thrombopoietin, GATA-1, and TGF- β 1 in the development of myelofibrosis. *Blood*, 105(9), 3493–3501. <https://doi.org/10.1182/blood-2004-04-1320>.

Vannucchi, A.M., Pancrazzi, A., Guglielmelli, P., Di Lollo, S., Bogani, C., Baroni, G., Bianchi, L., Migliaccio, A.R., Bosi, A., Paoletti, F. (2005). Abnormalities of GATA-1 in megakaryocytes from patients with idiopathic myelofibrosis. *American Journal of Pathology*, 167(3), 849–858. [https://doi.org/10.1016/S0002-9440\(10\)62056-1](https://doi.org/10.1016/S0002-9440(10)62056-1).

Verachi, P., Gobbo, F., Martelli, F., Falchi, M., di Virgilio, A., Sarli, G., Wilke, C., Bruederle, A., Prahallad, A., Arciprete, F., Zingariello, M., Migliaccio, A. (2022). Preclinical studies on the use of a P-selectin-blocking monoclonal antibody to halt progression of myelofibrosis in the *Gata1^{low}* mouse model. *Experimental Hematology*. <https://doi.org/10.1016/j.exphem.2022.09.004>.

Verachi, P., Gobbo, F., Martelli, F., Martinelli, A., Sarli, G., Dunbar, A., Levine, R., Hoffman, R., Massucci, M., Brandolini, L., Giorgio, C., Allegretti, M., Migliaccio, A. (2022). The CXCR1/CXCR2 inhibitor reparixin alters the development of myelofibrosis in the *Gata1^{low}* mice. *Frontiers in Oncology*, 12. <https://doi.org/10.3389/fonc.2022.853484>.

Verstovsek, S., Gotlib, J., Mesa, R.A., Vannucchi, A.M., Kiladjan, J.J., Cervantes, F., Harrison, C.N., Paquette, R., Sun, W., Naim, A., Langmuir, P., Dong, T., Gopalakrishna, P., Gupta, V. (2017). Long-term survival in patients treated with ruxolitinib for myelofibrosis: COMFORT-I and -II pooled analyses. *Journal of Hematology & Oncology*, 10(1), 156. <https://doi.org/10.1186/s13045-017-0527-7>.

Verstovsek, S., Mesa, R.A., Gotlib, J., Gupta, V., DiPersio, J., Catalano, J.V., Deininger, M.W., Miller, C.B., Silver, R.T., Talpaz, M., Winton, E.F., Harvey, J.H., Arcasoy, M.O., Hexner, E.O., Lyons, R.M., Paquette, R., Raza, A., Jones, M., Kornacki, D., Sun, K., Kantarjian, H. (2017). Long-term treatment with ruxolitinib for patients with myelofibrosis: 5-year update from the randomized, double-blind, placebo-controlled, phase 3 COMFORT-I trial. *Journal of Hematology & Oncology*, 10(1):55. <https://doi.org/10.1186/s13045-017-0417-z>.

Wang, H., He, J., Xu, C., Chen, X., Yang, H., Shi, S., Liu, C., Zeng, Y., Wu, D., Bai, Z., Wang, M., Wen, Y., Su, P., Xia, M., Huang, B., Ma, C., Bian, L., Lan, Y., Cheng, T., Shi, L., Liu, B., Zhou, J.

- (2021). Decoding human megakaryocyte development. *Cell Stem Cell*, 28(3), 535–549.e8. <https://doi.org/10.1016/j.stem.2020.11.006>.
- Waugh, D.J.J., Wilson, C. (2008). the interleukin-8 pathway in cancer. *Clinical Cancer Research*, 8(21), 6735–6742. <https://doi.org/10.1158/1078-0432.CCR-07-4843>.
- Yang, D., De Haan, G. (2021). Inflammation and aging of hematopoietic stem cells in their niche. *Cells*, 10(8), 1849. <https://doi.org/10.3390/cells10081849>.
- Yeung, A.K., Villacorta-Martin, C., Hon, S., Rock, J.R., Murphy, G.J. (2020). Lung megakaryocytes display distinct transcriptional and phenotypic properties. *Blood Advances*, 4(24), 6204–6217. <https://doi.org/10.1182/bloodadvances.2020002843>.
- Zingariello, M., Martelli, F., Ciaffoni, F., Masiello, F., Ghinassi, B., D'Amore, E., Massa, M., Barosi, G., Sancillo, L., Li, X., Goldberg, J.D., Rana, R. A., Migliaccio, A.R. (2013). Characterization of the TGF-beta1 signaling abnormalities in the *Gata1*^{low} mouse model of myelofibrosis. *Blood*, 121(17), 3345–3363. <https://doi.org/10.1182/blood-2012-06-439661>.
- Zingariello, M., Ruggeri, A., Martelli, F., Marra, M., Sancillo, L., Ceglia, I., Rana, R.A., Migliaccio, A. R. (2015). A novel interaction between megakaryocytes and activated fibrocytes increases TGF-β bioavailability in the *Gata1*^{low} mouse model of myelofibrosis. *American Journal of Blood Research*, 5(2), 34–61. <http://www.ncbi.nlm.nih.gov/pubmed/27069753>.
- Zingariello, M., Sancillo, L., Martelli, F., Ciaffoni, F., Marra, M., Varricchio, L., Rana, R.A., Zhao, C., Crispino, J.D., Migliaccio, A.R. (2017). The thrombopoietin/MPL axis is activated in the *Gata1*^{low} mouse model of myelofibrosis and is associated with a defective RPS14 signature. *Blood Cancer Journal*, 7(6), 572. <https://doi.org/10.1038/bcj.2017.51>.
- Zingariello, M., Verachi, P., Gobbo, F., Martelli, F., Falchi, M., Mazzarini, M., Valeri, M., Sarli, G., Marinaccio, C., Melo-Cardenas, J., Crispino, J.D., Migliaccio, A.R. (2022). Resident self-tissue of proinflammatory cytokines rather than their systemic levels correlates with development of myelofibrosis in *Gata1*^{low} mice. *Biomolecules*, 12(2). <https://doi.org/10.3390/biom12020234>.

List of acronyms

Abi-1, Abelson's Interactor 1
ASXL1, Additional sex comb-like
b-FGF, Basic fibroblast growth factor
BM, Bone marrow
BMP-4, Bone morphogenetic protein 4
BMT, Bone marrow transplant
CALR, Calreticulin
CBC, Cell blood counts
CCL2, C-C motif chemokine 2
CLP, common lymphoid progenitor
CMP, common myeloid progenitor
Col III, Collagen type III
COL1A1, Collagen type I alpha 1 chain
COL3A1, Collagen type III alpha 1 chain
COL6A2, Collagen type VI alpha 2 chain
CXCL1, C-X-C Motif Chemokine Ligand 1
CXCL2, C-X-C Motif Chemokine Ligand 2
CXCL3, C-X-C Motif Chemokine Ligand 3
CXCL4, C-X-C Motif Chemokine Ligand 4
CXCL5, C-X-C Motif Chemokine Ligand 5
CXCL6, C-X-C Motif Chemokine Ligand 6
CXCL7, C-X-C Motif Chemokine Ligand 7
CXCL8, C-X-C Motif Chemokine Ligand 8
CXCR1, C-X-C Motif Chemokine Receptor 1
CXCR2, C-X-C Motif Chemokine Receptor 2
DMS, Demarcation membrane system
DNMT3A, DNA methyl transferase 3
ECM, Extracellular matrix
ECs, Endothelial cells
EPO, Erythropoietin
ERK1/2, Extracellular signal-Related Kinase 1/2
ES, Embryonic stem

ESI, Electrospray ionization
ET, Essential thrombocythemia
EZH2, Enhancer of zeste homolog 2
GFP, Green fluorescent protein
GM-CSF, Granulocyte-macrophage colony-stimulating factor
GMP, Granulocyte/macrophage progenitor
H&E, Hematoxylin and eosin
HMGA1, High Mobility Group AT-Hook 1
HPLC, High-performance liquid chromatography
HSC, Hematopoietic stem cell
HSPC, Hematopoietic stem and progenitor cells
Htc, Hematocrit
IDH1/2, Isocitrate dehydrogenase 1/2
IFN γ , Interferon gamma
IL10, Interleukin 10
IL13, Interleukin 13
IL15, Interleukin 15
IL17, Interleukin 17
IL1-a, Interleukin 1 alpha
IL1- β , Interleukin 1 beta
IL2, Interleukin 2
IL3, Interleukin 3
IL4, Interleukin 4
IL5, Interleukin 5
IL6, Interleukin 6
IL7, Interleukin 7
IL8, Interleukin 8
IL9, Interleukin 9
IP10, Interferon gamma-induced protein 10
JAK2, Janus kinase 2
LCN2, lipocalin-2
LIF, Leukemia inhibitory factor
LIX, LPS-induced CXC chemokine

LOX, Lysyl oxidase
LSK, (Lin)⁻Sca-1⁺c-Kit⁺
MAPK, Mitogen-activated protein kinase
MCP1, Monocyte chemoattractant protein-1
M-CSF, Macrophage-stimulating factor
MEP, Megakaryocyte erythrocyte progenitor
MF, Myelofibrosis
MIG, B lymphocyte antigen receptors
MIP1a, Macrophage inflammatory protein-1 alpha
MIP1b, Macrophage inflammatory protein-1 beta
MIP-2, Macrophage inflammatory protein-2
MKs, Megakaryocytes
MMP, Matrix metalloproteinase
MPK, Megakaryocyte progenitors
MPL, Myeloproliferative leukaemia virus oncogene (thrombopoietin receptor)
MPNs, Myeloproliferative neoplasms
MPP9, Metalloproteinase 9
MSCs, Mesenchymal stem cells
Neu, Neutrophils
NF- κ B, Nuclear factor kappa-light-chain-enhancer of activated B cells
OBCs, Osteoblasts
OPG, Osteoprotegerin
PDGF, Platelet derived growth factor
PDX, Primary patient-derived cells
PF4, Platelet factor 4
PI3K, Phosphoinositol kinase 3
Plts, Platelets
PMF, Primary myelofibrosis
P-sel, P-selectin
PSGL-1, P-selectin glycoprotein ligand-1
PV, Polycythemia vera
RBC, Red blood cell
RDW distribution width

Rux, Ruxolitinib
SLAM, Signaling lymphocytic activation molecule
Src, Proto-oncogene tyrosine-protein kinase
SRSF2, Serine arginine splicing factor 2
STAT, Signal transducer and activation of transcription
TGF- β , Transforming growth factor β
TGF- β RII, Transforming growth factor, beta receptor II
TIMP, Tissue inhibitors of matrix metalloproteinase
TNF, Tumor necrosis factor
TNFa, Tumour necrosis factor- alpha
TPO, Thrombopoietin
U2AF1, U2 small nuclear RNA auxiliary factor 1
VEGF, Vascular endothelial growth factor
WBC, White blood cells
WT, Wild-type